



**UNIVERSIDADE FEDERAL DO CEARÁ**  
**CENTRO DE CIÊNCIAS**  
**DEPARTAMENTO DE QUÍMICA ORGÂNICA E INORGÂNICA**  
**PROGRAMA DE PÓS-GRADUAÇÃO EM QUÍMICA**

**ÁLISON BATISTA DA SILVA**

**NOVOS COMPOSTOS COM PROPRIEDADES ANTIBIÓTICAS DE *Salinispora arenicola*, UMA BACTÉRIA ASSOCIADA AO SEDIMENTO MARINHO DO ARQUIPÉLAGO DE SÃO PEDRO E SÃO PAULO**

**FORTALEZA**

**2021**

ÁLISON BATISTA DA SILVA

NOVOS COMPOSTOS COM PROPRIEDADES ANTIBIÓTICAS DE *Salinispora arenicola*, UMA BACTÉRIA ASSOCIADA AO SEDIMENTO MARINHO DO ARQUIPÉLAGO DE SÃO PEDRO E SÃO PAULO

Tese apresentada ao Programa de Pós-Graduação em Química da Universidade Federal do Ceará como requisito parcial à obtenção do título de Doutor em Química.  
Área de concentração: Química Orgânica.

Orientadora: Prof<sup>a</sup>. Dra. Otília Deusdênia  
Loiola Pessoa.

FORTALEZA

2021

Dados Internacionais de Catalogação na Publicação  
Universidade Federal do Ceará  
Biblioteca Universitária

Gerada automaticamente pelo módulo Catalog, mediante os dados fornecidos pelo(a) autor(a)

---

- S584n Silva, Álison Batista da.  
Novos compostos com propriedades antibióticas de *Salinispora arenicola*, uma bactéria associada ao sedimento marinho do Arquipélago de São Pedro e São Paulo / Álison Batista da Silva. – 2021.  
193 f. : il. color.
- Tese (doutorado) – Universidade Federal do Ceará, Centro de Ciências, Programa de Pós-Graduação em Química, Fortaleza, 2021.  
Orientação: Profa. Dra. Otilia Deusdênia Loiola Pessoa.
1. Bactéria marinha. 2. *Salinispora arenicola*. 3. Aminonaftoquinonas. 4. Rifamicinas. 5. Atividade antimicrobiana. I. Título.

CDD 540

---

ÁLISON BATISTA DA SILVA

NOVOS COMPOSTOS COM PROPRIEDADES ANTIBIÓTICAS DE *Salinispora arenicola*, UMA BACTÉRIA ASSOCIADA AO SEDIMENTO MARINHO DO ARQUIPÉLAGO DE SÃO PEDRO E SÃO PAULO

Tese apresentada ao Programa de Pós-Graduação em Química da Universidade Federal do Ceará como requisito parcial à obtenção do título de Doutor em Química.  
Área de concentração: Química Orgânica.

Aprovada em: 29/07/2021

BANCA EXAMINADORA

---

Prof<sup>ª</sup>. Dra. Otilia Deusdênia Loiola Pessoa (Orientadora)  
Universidade Federal do Ceará (UFC)

---

Prof<sup>ª</sup>. Dra. Mary Anne Sousa Lima  
Universidade Federal do Ceará (UFC)

---

Prof<sup>ª</sup>. Dra. Maria da Conceição Ferreira de Oliveira  
Universidade Federal do Ceará (UFC)

---

Prof<sup>ª</sup>. Dra. Alessandra Leda Valverde  
Universidade Federal Fluminense (UFF)

---

Prof<sup>ª</sup>. Dra. Miriam de Barcellos Falkenberg  
Universidade Federal de Santa Catarina (UFSC)

---

Prof<sup>ª</sup>. Dra. Letícia Veras Costa Lotufo  
Universidade de São Paulo (USP)

A Deus, por me proporcionar força e vontade de vencer na vida.

Aos meus pais, irmãos e professores por participarem dessa conquista.

## AGRADECIMENTOS

Primeiramente a Deus, por sempre me acompanhar, iluminando os meus passos ao longo de minha vida e por sempre me guiar pelo melhor caminho.

À minha família, em especial à minha irmã Ana Cristina e seu esposo Júnior, por terem me aceitado em sua casa, cuidando de mim como próprio filho. Agradeço pela preocupação, ajuda, cuidado e carinho.

À minha orientadora, Professora Dra. Oflia Deusdenia L. Pessoa pelo exemplo de dedicação ao trabalho e orientação. Obrigado pelos ensinamentos e pela confiança.

Ao Prof. Dr. Diego V. Wilke e ao Dr. Elthon G. Ferreira pela parceria no desenvolvimento deste trabalho, principalmente no cultivo, identificação da bactéria estudada.

Ao Prof. Dr. Edilberto R. Silveira, por conceder a realização dos espectros de RMN e me tornar operador do CENAUREMN.

Ao Dr. Kirley Canuto, por permitir a utilização da estrutura da EMBRAPA para obtenção dos espectros de RMN e EM.

Ao Prof. Dr. José Delano B. Marinho Monteiro Filho pela parceria no desenvolvimento deste trabalho, principalmente na realização da atividade antimicrobiana.

Aos professores do curso de Pós-graduação em química (UFC), pela contribuição em meu aprendizado.

Aos operadores do CENAUREM, IV e EM pelos espectros obtidos.

Aos amigos da família LAFIPLAM, Chaguinha, Patrícia, Luana, João Paulo, Fábio, Taynara, Herbert, Kaline e Késya pela amizade, convívio e pelos momentos de descontração no laboratório.

O presente trabalho foi realizado com apoio da Coordenação de Aperfeiçoamento de Pessoal de Nível Superior - Brasil (CAPES) - Código de Financiamento 001.

A todos que de alguma forma contribuíram, direta ou indiretamente para a realização desse trabalho, meu muito obrigado.

“A ciência não é acumulação de fatos, mas  
resolução de mistérios.” (Matt Ridley)

## RESUMO

Este trabalho descreve a investigação química do extrato em acetato de etila (AcOEt) da bactéria *Salinispora arenicola* isolada a partir de sedimentos marinhos coletados no Arquipélago de São Pedro e São Paulo (ASPSP), visando o isolamento e a elucidação estrutural de novos compostos bioativos. A investigação química resultou no isolamento de treze novos compostos: cinco aminonaftoquinonas denominadas de salinaftoquinonas A-E (**SA-1** a **SA-5**), dois derivados do *N*-metil-2-oxindol nomeados de 3-hidroxi-6-metoxi-3-(2-oxo-propil)-*N*-metil-2-oxindol (**SA-6**) e 5-cloro-3-hidroxi-6-metoxi-3-(2-oxo-propil)-*N*-metil-2-oxindol (**SA-7**), um tetracetídeo denominado de 3-hidroxi-5-(1-hidroxi-1-fenilpropan-2-il)-2-metilpiran-2-ona (**SA-8**), além de cinco rifamicinas designadas de salinirrifamicinas A-E (**SA-9** a **SA-13**). Para fracionamento e isolamento dos compostos foram utilizadas técnicas cromatográficas como extração em fase sólida (*SPE*-C18), Sephadex LH-20 e cromatografia líquida de alta eficiência (CLAE). A determinação estrutural dos compostos isolados foi realizada através de técnicas espectroscópicas tais como ressonância magnética de  $^1\text{H}$  e  $^{13}\text{C}$  (RMN  $^1\text{H}$  e  $^{13}\text{C}$ , 1D e 2D), espectrometria de massas (EM), análise de difração de raios-X monocristal e por fim, comparação com dados da literatura para compostos análogos. Os compostos isolados de *S. arenicola* foram submetidos a testes antibacterianos utilizando cepas de *Staphylococcus aureus* incluindo uma cepa resistente à meticilina, *Enterococcus faecalis*, também incluindo uma cepa resistente à vancomicina, e *Escherichia coli*. As salinirrifamicinas **SA-9**, **SA-10**, **SA-11** e **SA-13** mostram potente atividade contra *S. aureus* e *E. faecalis* com valores de CIM variando entre 0,02 a 3,1  $\mu\text{g/mL}$ . Salinirrifamicina A (**SA-9**), o primeiro exemplo natural de rifamicina com um sistema tetracíclico 5/6/6/6 fundido com piridina isolado de *Salinispora*, revelou uma atividade (CIM de 0,02  $\mu\text{g/mL}$ ) semelhante à rifampicina usada como controle positivo (CIM 0,03  $\mu\text{g/mL}$ ), enquanto a salinaftoquinona B (**SA-2**) mostrou moderada atividade contra *S. aureus* e *E. faecalis* com valores de CIM variando entre 15,6-125,0  $\mu\text{g/mL}$ .

**Palavras-chave:** bactéria marinha; *Salinispora arenicola*; aminonaftoquinonas; rifamicinas; atividade antimicrobiana.



## ABSTRACT

This work describes the chemical investigation of the ethyl acetate extract (EtOAc) obtained from a bacterial strain identified as *Salinispora arenicola*, which was isolated from marine sediments collected in the Saint Peter and Saint Paul Archipelago-Brazil (ASPSP), aiming at the isolation of new bioactive compounds. The chemical investigation resulted in the isolation of thirteen new compounds: five aminonaphthoquinones designated as salinaphthoquinones A-E (**SA-1** to **SA-5**), two *N*-methyl-2-oxindole derivatives 3-hydroxy-6-methoxy-3-(2-oxo-propyl)-*N*-methyl-2-oxindole (**SA-6**) and 5-chloro-3-hydroxy-6-methoxy-3-(2-oxo-propyl)-*N*-methyl-2-oxindole (**SA-7**), a tetraketide named 3-hydroxy-5-(1-hydroxy-1-phenylpropan-2-yl)-2-methyl-pyran-2-one (**SA-8**), besides five rifamycin derivatives designated as salinirifamycins A-E (**SA-9** to **SA-13**). All isolated compounds were subjected to antibacterial assays against *Staphylococcus aureus*, including a methicillin-resistant strain, *Enterococcus faecalis*, also including a vancomycin-resistant strain and *Escherichia coli*. Salinirifamycins **SA-9**, **SA-10**, **SA-11**, and **SA-13** showed potent activity against *S. aureus* and *E. faecalis* with MIC values ranging from 0.02 through 3.1 µg/mL. Salinirifamycin A (**SA-9**), the first example of rifamycin bearing a natural tetracyclic 5/6/6/6 pyridine-fused system isolated from *Salinispora*, revealed an activity (MIC of 0.02 µg/mL) similar to rifampicin (MIC 0.03 µg/mL), used as positive control. Regarding the other compounds, only Salinaphthoquinone B (**SA-2**) exhibited satisfactory activity (MIC 15.6-125.0 µg / mL) against both *S. aureus* and *E. faecalis*.

**Keywords:** marine bacteria; *Salinispora arenicola*; aminonaphthoquinones; rifamycins; antimicrobial activity.

## LISTA DE FIGURAS

Figura 1	– Ilustração do número de fármacos (micromoléculas) aprovados pelo FDA entre 1998 a 2017.....	16
Figura 2	– Primeiros compostos biativos de origem marinha.....	17
Figura 3	– Estruturas das rifamicinas de uso clínico.....	21
Figura 4	– Vista panorâmica do Arquipélago de São Pedro e São Paulo (ASPSP), litoral de Pernambuco-Brasil, com destaque para a estação científica ECASPSP.....	24
Figura 5	– Mapa mostrando a Zona Econômica Exclusiva Brasileira.....	25
Figura 6	– Culturas de cepas de <i>S. tropica</i> , <i>S. pacifica</i> e <i>arenicola</i> , respectivamente.....	26
Figura 7	– Cromatograma da subfração AB4 observada na faixa de 210-400 nm.....	38
Figura 8	– Cromatograma da mistura AB4P1 observada na faixa de 210-400 nm.....	38
Figura 9	– Cromatograma da subfração AC4 observada na faixa de 350-600 nm.....	39
Figura 10	– Cromatograma da subfração AD5 observada na faixa de 350-600 nm.....	40
Figura 11	– Cromatograma da subfração AB3 observada na faixa de 210-400 nm.....	41
Figura 12	– Cromatograma da subfração AD2 observada na faixa de 210-400 nm.....	41
Figura 13	– Cromatograma da subfração B2 observada na faixa de 350-600 nm.....	42
Figura 14	– Estruturas dos metabólitos isolados do extrato em AcOEt produzido por <i>S. arenicola</i> .....	189

## LISTA DE TABELAS

Tabela 1	– Medicamentos de origem marinha aprovados para o tratamento do câncer...	18
Tabela 2	– Fármacos isolados de microrganismos em fase de teste clínicos para o tratamento do câncer.....	19
Tabela 3	– Concentração inibitória mínima (CIM) do extrato em AcOEt e frações frente as cepas de <i>Staphylococcus aureus</i> .....	22
Tabela 4	– Exemplos de compostos relatados a partir de espécies do gênero <i>Salinispora</i> .....	27
Tabela 5	– Fracionamento cromatográfico do extrato em AcOEt de <i>S. arenicola</i> .....	36
Tabela 6	– Fracionamento cromatográfico da fração A .....	36
Tabela 7	– Fracionamento cromatográfico da fração AB.....	37
Tabela 8	– Fracionamento cromatográfico da fração AC.....	38
Tabela 9	– Fracionamento cromatográfico da fração AD.....	40
Tabela 10	– Fracionamento cromatográfico da fração B.....	42

## LISTA DE ABREVIATURAS E SIGLAS

CCD	Cromatografia em Camada Delgada
CIM	Concentração Inibitória Mínima
CLAE	Cromatografia Líquida de Alta Eficiência
COSY	Correlation Spectroscopy
DEPT	Distortionless Enhancement by Polarization Transfer
EM	Espectrometria de Massa
EM-ESI	Espectrometria de Massa com Ionização por Eletrospray
HMBC	Heteronuclear Multiple Bond Correlation
IV	Infravermelho
RMN <sup>1</sup> H	Ressonância Magnética Nuclear de Hidrogênio
SPE	Solid Phase Extraction
UV	Ultravioleta

## LISTA DE SÍMBOLOS

%	Porcentagem
Hz	Hertz
$J$	Constante de Acoplamento
$[\alpha]_D^{22}$	Rotação Óptica
®	Marca Registrada

## SUMÁRIO

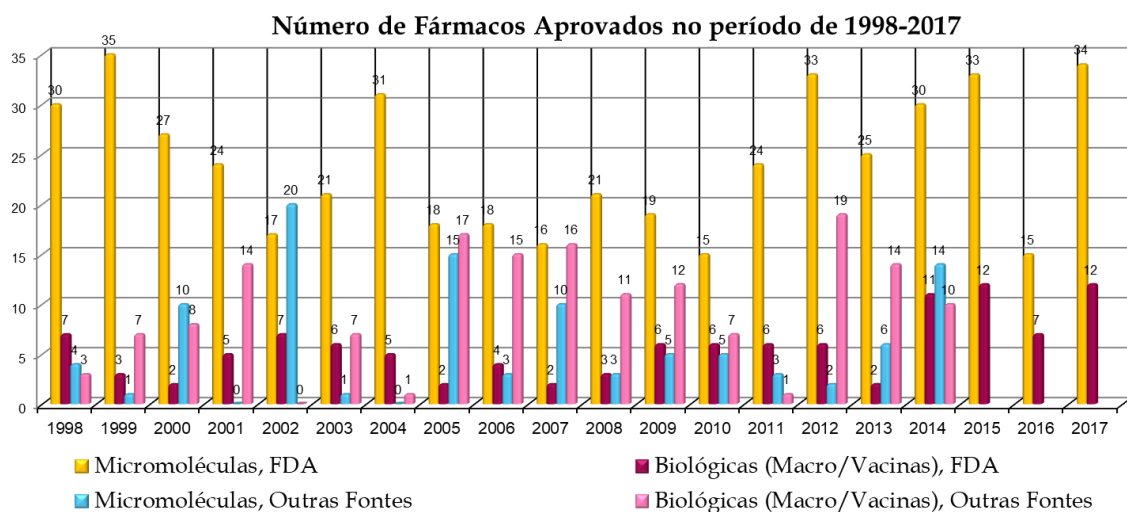
1	INTRODUÇÃO.....	16
1.1	Objetivos.....	23
1.1.1	<i>Objetivo geral</i> .....	23
1.1.2	<i>Objetivos específicos</i> .....	23
2	CONSIDERAÇÕES GERAIS.....	24
2.1	O Arquipélago de São Pedro e São Paulo (ASPSP).....	24
2.2	O gênero <i>Salinispora</i> .....	26
3	PROCEDIMENTOS EXPERIMENTAIS.....	31
3.1	Métodos cromatográficos.....	31
3.1.1	<i>Cromatografia de adsorção</i> .....	31
3.1.2	<i>Cromatografia de exclusão molecular</i> .....	31
3.1.3	<i>Cromatografia líquida de alta eficiência (CLAE)</i> .....	31
3.1.4	<i>Extração em fase sólida (SPE)</i> .....	32
3.2	Métodos Físicos.....	32
3.2.1	<i>Ponto de fusão</i> .....	32
3.2.2	<i>Rotação óptica</i> .....	32
3.3	Métodos Espectrométricos.....	32
3.3.1	<i>Espectrometria de massas (EM)</i> .....	32
3.3.2	<i>Espectroscopia de ressonância magnética nuclear (RMN)</i> .....	32
3.3.3	<i>Espectroscopia de Difração de raios-X</i> .....	33
3.4	Estudo dos microrganismos.....	33
3.4.1	<i>Coleta do material</i> .....	33
3.4.2	<i>Isolamento dos microrganismos</i> .....	34
3.4.3	<i>Purificação, cultivo e criopreservação dos microrganismos</i> .....	34
3.4.4	<i>Obtenção dos extratos em pequena escala</i> .....	34
3.4.5	<i>Crescimento em larga escala da cepa em estudo</i> .....	35
3.4.6	<i>Identificação molecular da cepa BRA-213</i> .....	35
3.4.7	<i>Fracionamento cromatográfico do extrato em AcOEt da bactéria <i>Salinispora arenicola</i></i> .....	35
3.5	Ensaio de atividade Antimicrobiana <i>in vitro</i> .....	43
4	RESULTADOS E DISCUSSÃO.....	44

<b>4.1</b>	<b>Capítulo 1.....</b>	<b>47</b>
<b>4.2</b>	<b>Capítulo 2.....</b>	<b>85</b>
<b>4.3</b>	<b>Capítulo 3.....</b>	<b>117</b>
<b>4.4</b>	<b>Capítulo 4.....</b>	<b>147</b>
<b>5</b>	<b>CONSIDERAÇÕES FINAIS.....</b>	<b>188</b>
	<b>REFERÊNCIAS.....</b>	<b>190</b>

## 1 INTRODUÇÃO

A reputação terapêutica dos produtos naturais (PNs) botânicos é milenar e indiscutível. Baseados em conhecimentos empíricos repassados através de gerações, os PNs vegetais passaram a constituir a base de inúmeros sistemas de medicina tradicional em todo o mundo, bem como de gestão de saúde pública de governos. Com a evolução do conhecimento e da ciência, as plantas não somente continuaram com o papel de protagonistas, como passaram a ser objetos de incessantes estudos pela busca de isolamento de seus princípios ativos e descoberta de novos compostos bioativos. Seguindo esta tendência, laboratórios de pesquisas e indústrias farmacêuticas têm explorados os extratos vegetais com vistas ao isolamento de compostos bioativos com atividades específicas, seguras e eficazes, contribuindo de forma significativa com o desenvolvimento da ciência e da produção de novos fármacos, bem como fonte de inspiração para o design de novos medicamentos. Até o final de 2013, a Food and Drug Administration (FDA) havia aprovado 547 fármacos, incluindo produtos derivados de PNs (PATRIDGE *et al.*, 2016). Nos últimos 20 anos, do total de fármacos aprovados cerca de 50 % são PN, ou são derivados destes, ou foram inspirados nestes (Figura 1). Na área do câncer, o percentual aumenta para aproximadamente 74 % (RAO *et al.*, 2019, CRAGG; NEWMAN, 2016 e 2020).

**Figura 1:** Ilustração do número de fármacos (micromoléculas) aprovados pelo FDA entre 1998 a 2017.



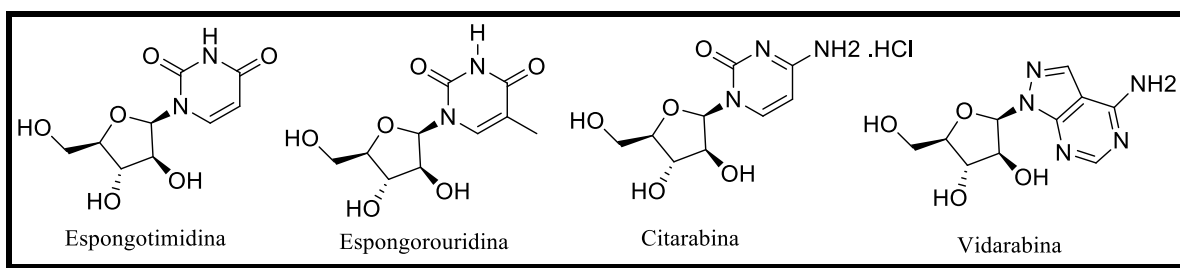
Fonte: Adaptado de NEWMAN E CRAGG, 2016 e 2020.



De maneira semelhante aos PNs de origem vegetal, os PNs marinhos passaram a ser objetos de estudos. Note-se que ao contrário do que acontece com os organismos terrestres, os organismos marinhos têm procurado se adaptar às condições ambientais extremas, como: altas pressões, altas concentrações de sal, baixos níveis de nutrientes, baixas temperaturas, luz escassa e baixo teor de oxigênio. Assim, os organismos marinhos desenvolveram estratégias de sobrevivência e adaptação culminando na produção de extraordinária diversidade química (ABDELMOHSEN *et al.*, 2017).

Os primeiros compostos bioativos de origem marinha foram a espongotimidina e a espongotimidina, ambos isolados da esponja *Cryptotheca crypta* (Figura 2), os quais foram aprovados pelo FDA em 1969 e 1976, respectivamente, levando ao desenvolvimento de Ara-A (vidarabina, um agente antiviral) e Ara-C (citarabina, um agente anti-leucêmico) (CHIN *et al.*, 2006).

**Figura 2:** Primeiros compostos bioativos de origem marinha.



Fonte: Próprio autor

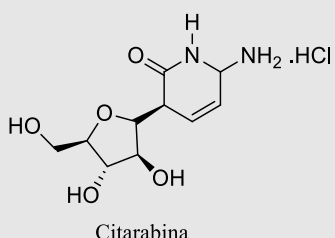
Contudo, os organismos marinhos somente começaram a ser intensivamente estudados a partir da década de 70, fruto do esforço pluridisciplinar de pesquisadores de áreas como, biologia, química, bioquímica, ecologia e farmacologia (JIMÉNEZ, 2018; ABDELMOHSEN *et al.*, 2017). Como resultado destas ações conjuntas, os organismos marinhos passaram a ser reconhecidos como verdadeiras fábricas vivas de novos compostos, de estruturas únicas e complexas, além de altamente funcionalizadas, inclusive halogenadas (raramente isolados de plantas). Como consequência, inúmeros metabólitos secundários de origem marinha passaram a ser avaliados como candidatos a novos fármacos, muitos deles encontrando-se em estágio pré-clínico ou clínico de desenvolvimento.

Os PNs marinhos têm se mostrado relevantes na área oncológica, por exemplo, já inclui 04 medicamentos aprovados e 18 agentes em testes clínicos, 06 dos quais estão em desenvolvimento (Tabela 1), oferecendo novas esperanças para o tratamento de pacientes afetados por tipos de câncer anteriormente intratáveis (PEREIRA *et al.*, 2019).

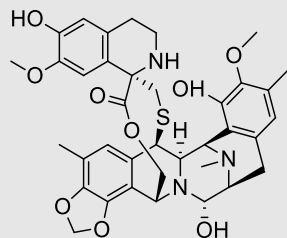
**Tabela 1.** Medicamentos de origem marinha aprovados para tratamento do câncer.

Nome do composto (nome de mercado)	Protótipo (Fonte)	Câncer
Citarabina (Cytosar-U®; DepoCyt®)	Espongotimidina (Esponja)	Leucemia; Meningite linfocitária
Trabectedina (Yondelis®)	Trabectedina (Tunicato)	Sarcoma de tecido mole; câncer de ovarino
Mesilato de eribulina (Halaven®)	Halicondrina B (Esponja)	Câncer de mama metastático; Lipossarcoma avançado
Brentuximabe vedotina (Adcetris®)	Dolastatina 10 (Molusco/Cianobactéria)	Linfoma de Hodgkin

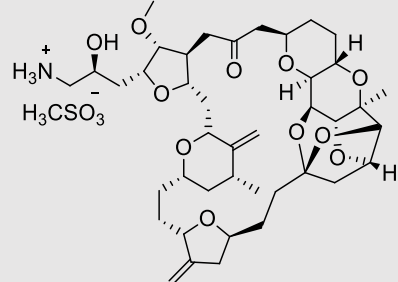
  



Citarabina

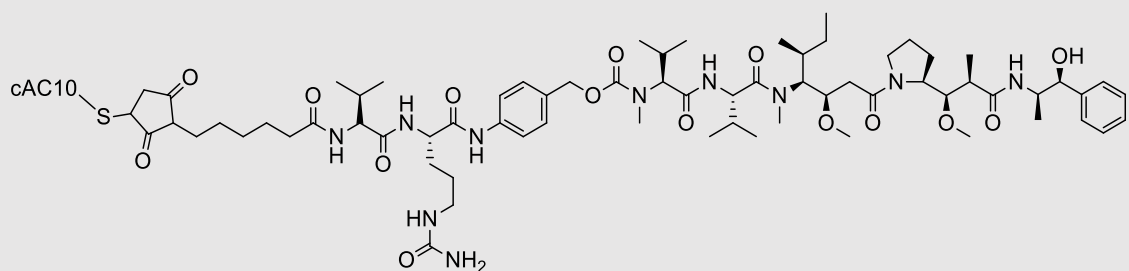


Trabectedina



Mesilato de eribulina



Brentuximabe vedotina

Fonte: Próprio autor

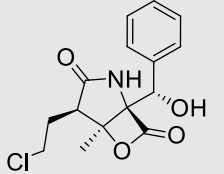
Apesar dos bons resultados, é fato que a obtenção de invertebrados marinhos em quantidades para suprir as quantidades necessárias para todos os estudos biológicos é muito difícil. Contudo, a química de produtos naturais marinhos tem sido incrementada com a investigação de microrganismos associados, os quais mostram uma alta percentagem de metabólitos secundários com atividades diversas, sobretudo citotóxica e antibiótica. Some-se a isto, a facilidade de cultivo e produção destes (WAITES *et al.*, 2001).

Como resultado dos estudos envolvendo os microrganismos, também já existem vários compostos em fase de testes clínicos. Um exemplo é a salinosporamida A, produzida pelo actinomiceto marinho *Salinispora tropica*, uma bactéria encontrada em sedimentos do

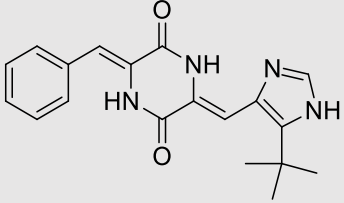
fundo do oceano (FENICAL; JENSEN, 2006). Salinosporamida A (NPI-0052), denominada de marizomibe, mostra alta eficácia contra mieloma múltiplo recidivado e outros tipos de tumores sólidos (Tabela 2). Este composto, apesar de ter sido denominado medicamento órfão pela FDA dos EUA e pela Agência Europeia de Medicamentos (EMA), tem sido investigado como um dos inibidores da proteassoma de segunda geração, garantindo um melhor tratamento a pacientes com câncer (MA; DIAO, 2015). Outro composto em desenvolvimento é a plinabulina NPI-2358 (Tabela 2), um análogo sintético da dicetopiperazina halimida (NPI-2350), a qual foi obtida por meio da fermentação de um fungo encontrado no oceano (*Aspergillus* sp.). A plinabulina é uma molécula com efeitos imunológicos e atividade anticâncer que tem potencial para ser uma alternativa segura, econômica e conveniente para tratar a neutropenia induzida por quimioterapia, com muito menos dor óssea e um perfil de segurança mais favorável (TONRA *et al.*, 2020; PEREIRA *et al.*, 2019).

**Tabela 2.** Fármacos isolados de microrganismos em fase de testes clínicos para o tratamento de câncer.

Nome do composto (nome de mercado)	Protótipo (Fonte)	Câncer
Salinosporamida A (Marizomibe®)	Salinosporamida A (Bactéria)	Glioblastoma
Plinabulina	Halimida (Fungo)	câncer de pulmão de células não pequenas; neutropenia induzida por quimioterapia



Salinosporamida A



Plinabulina (NPI2358)

Fonte: Próprio autor

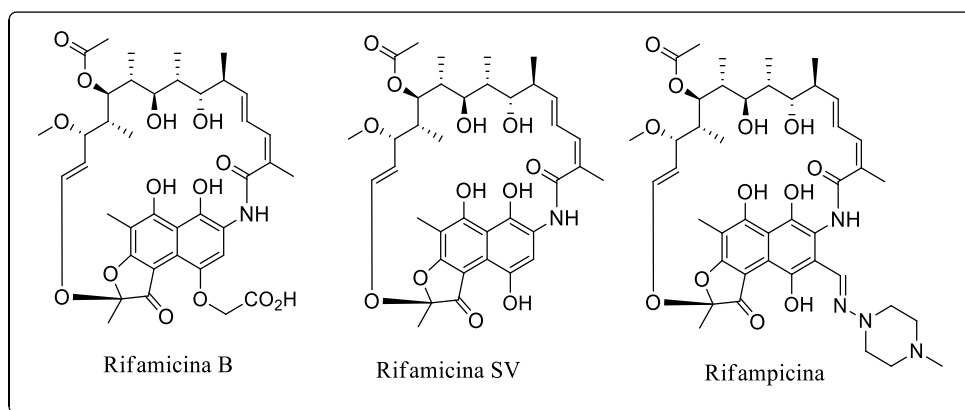
A evolução, a resistência ou o surgimento de novas doenças têm aumentado o interesse pela descoberta de novos compostos que possam vir a ser utilizados como medicamentos, com ação mais eficiente, seletiva e com menos efeitos adversos. Um dos maiores desafios que a medicina enfrenta atualmente é o aumento generalizado da resistência aos antibióticos por patógenos que causam infecções graves a humanos devido ao uso indiscriminado ou incorreto destes (MEREDITH *et al.*, 2015).

De acordo com dados da Organização Mundial da Saúde (OMS), as doenças infecciosas causadas por bactérias, como por exemplo a tuberculose, são umas das principais causas de morte no mundo e o combate das mesmas tem sido um desafio para a humanidade desde a antiguidade até os dias de hoje (WHO, 2020). Muitos dos antibióticos em uso clínico são produtos naturais isolados a partir de microrganismos marinhos, sendo estes uma fonte para a descoberta e desenvolvimento de novos agentes antimicrobianos de importância terapêutica como as rifamicinas (MOLONEY, 2016; WILLIAMS *et al.*, 2017).

Rifamicinas são compostos macrocíclicos de estruturas complexas e altamente funcionalizados. Devido ao grande número de derivados e análogos disponíveis, as rifamicinas têm sido amplamente utilizadas na eliminação de bactérias patogênicas que se tornaram resistentes aos antibióticos comumente utilizados. Em geral, as rifamicinas inibem o crescimento de muitas bactérias, tanto Gram-positivas quanto Gram-negativas (ARISTOFF *et al.*, 2010). Estes compostos foram primeiramente isolados em 1957, a partir de um processo de fermentação da bactéria *Streptomyces mediterranei* (hoje conhecida como *Amycolatopsis rifamycinica*) (BALA *et al.*, 2004).

A rifamicina B foi o primeiro composto desta classe disponibilizada comercialmente, para o combate da tuberculose. Após o descobrimento da rifamicina B, a precursora de vários outros derivados, um significativo número de outras rifamicinas com elevada ação antibiótica e de uso clínico foram descobertas. A rifampicina (um derivado semissintético da rifamicina SV) em associação com a isoniazida é muito utilizada para o tratamento da tuberculose, devido seu amplo espectro antibiótico e sua grande biodisponibilidade oral (BADHAN; GITTINS; AL ZABIT, 2019). Outro exemplo se trata da rifamicina SV (rifocina) um antibiótico tópico utilizado no tratamento de infecções em superfícies externas do corpo causadas por microrganismos (Figura 3) (LUPI; FERRARI, 1962).

Fica, portanto, evidente que os microrganismos marinhos surgiram como uma fonte promissora para a descoberta de novos metabólitos secundários bioativos (FENICAL; JENSEN, 2006; MOLINSKI *et al.*, 2009; JENSEN; MOORE; FENICAL, 2015). Destaca-se que os oceanos representam um ambiente de microbiologia altamente diversificado e complexo, com abundâncias estimadas em  $10^6$  microrganismos/mL de água do mar e  $10^9$ /cm<sup>3</sup> de sedimento (FENICAL; JENSEN, 2006).

**Figura 3:** Estruturas das rifamicinas de uso clínico.

Fonte: Próprio autor

Detentor de um litoral com cerca de 8.500 km de extensão, os mares brasileiros representam um grande potencial para a descoberta de substâncias de interesse médico e farmacológico. A exemplo deste, segue o Nordeste do Brasil, composto por nove Estados, sendo todos eles banhados pelas águas do oceano atlântico. Some-se a isto, a existências de vários parques e reservas biológicas situados nos mares desta região, como, os Parques Nacionais Marinhos de Fernando de Noronha (Pernambuco), Abrolhos (Bahia) e Pedra da Risca do Meio (Ceará), além da reserva biológica Atol das Rocas (Rio Grande do Norte) e Arquipélago de São Pedro e São Paulo (Pernambuco). Neste imenso cenário, onde a biodiversidade marinha do nordeste do Brasil ainda permanece praticamente desconhecida, a investigação química e do potencial farmacológico das espécies que habitam o litoral nordestino tem sido objeto de estudos do nosso grupo de pesquisa. Inicialmente, os esforços foram concentrados em invertebrados marinhos, posteriormente em microrganismos (bactérias) e algas.

Neste contexto, o Arquipélago de São Pedro e São Paulo (ASPS) merece especial atenção por ser um dos pontos mais remotos do oceano Atlântico com uma grande biodiversidade ainda pouco explorada. Vale a pena mencionar que pouquíssimos estudos foram relatados na área de química de produtos naturais (BAUERMEISTER *et al.*, 2018), incluindo os de nosso grupo de pesquisa (SILVA *et al.*, 2017; FERREIRA *et al.*, 2016).

Como parte do meu projeto de mestrado, no Programa de Pós-graduação em Química da Universidade Federal do Ceará, desenvolvi pesquisas investigando extratos de bactérias associadas ao sedimento do ASPSP (FERREIRA *et al.*, 2016). Entre as várias cepas bacterianas isoladas, uma foi identificada como *Salinispora arenicola* (BRA-213), cujo extrato

mostrou potente ação antimicrobiana (0,06 µg/mL) contra a cepa *Staphylococcus aureus* resistente à metilicina (Tabela 3).

**Tabela 3.** Concentração inibitória mínima (CIM) do extrato em AcOEt e frações frente as cepas de *Staphylococcus aureus*.

<b>Código</b>	<b><i>S. aureus</i> ATCC 29213</b>	<b><i>S. aureus</i> ATCC 43300 (MRSA)</b>
<b>BRA-213A</b>	0,12 µg/mL	0,06 µg/mL
<b>BRA-213A-A</b>	0,12 µg/mL	0,12 µg/mL
<b>BRA-213A-B</b>	0,12 µg/mL	0,24 µg/mL
<b>BRA-213A-C</b>	0,24 µg/mL	0,12 µg/mL
<b>Rifampicina*</b>	0,03 µg/mL	0,03 µg/mL

\*Controle positivo.

Fonte: Próprio autor

Dando continuidade ao projeto de pesquisa, neste trabalho descreve-se o estudo químico e biológico do extrato em AcOEt da bactéria marinha *Salinispora arenicola* (BRA213) concentrando-se na identificação, isolamento, caracterização e avaliação do potencial antimicrobiano dos seus metabólitos secundários, em particular no isolamento de rifamicinas.

## 1.1 Objetivos

### 1.1.1 Objetivo geral

Investigar o extrato em AcOEt da bactéria marinha *S. arenicola* recuperada de sedimentos marinhos coletados no Arquipélago de São Pedro e São Paulo, com vistas ao isolamento e caracterização química de seus metabólitos secundários, bem como avaliar possíveis atividades biológicas.

### 1.1.2 Objetivos específicos

- Dar continuidade ao primeiro estudo químico da cepa microbiana *Salinispora arenicola* recuperada de sedimentos brasileiro;
- Isolar novos metabólitos secundários, particularmente, rifamicinas;
- Isolar novas classes de compostos;
- Avaliar a atividade antimicrobiana frente a cepas de bactérias Gram-positivas [(*Staphylococcus aureus*, *Staphylococcus aureus* resistente à meticilina (MRSA), *Enterococcus faecalis* e *Enterococcus faecalis* resistente à vancomicina (VRE)] e Gram-negativa (*Escherichia coli*).

## 2 CONSIDERAÇÕES GERAIS

### 2.1 O Arquipélago de São Pedro e São Paulo (ASPSP)

O ASPSP é formado por um conjunto de pequenas ilhas rochosas medindo aproximadamente 17.000 m<sup>2</sup> de área emersa, situado próximo à linha do Equador, no hemisfério Norte (00°56' N; 29°21' W). Distante 1.010 Km de Natal – RN, é considerado o território do Brasil mais próximo do continente Africano. Apesar de não ser habitável, devido a ocorrência de abalos sísmicos e ausência de água doce e vegetação, foi na ilha de Belmonte (maior ilha dentre aquelas que compõem o ASPSP) que foi erguida a Estação Científica ECASPSP, que fica situada 18 metros acima do nível do mar (Figura 4).

**Figura 4-** Vista panorâmica do Arquipélago de São Pedro e São Paulo (ASPSP), litoral de Pernambuco-Brasil, com destaque para a estação científica ECASPSP.



Fonte: Adaptado de Marinha do Brasil

Desde julho de 1996, o governo brasileiro tem mantido o Programa Arquipélago de São Pedro e São Paulo (PRO-ARQUIPÉLAGO) com o objetivo de garantir direitos permanentes de habitação no remoto território ASPSP expandindo sua área econômica exclusiva para 4,5 milhões de Km<sup>2</sup>, a chamada Amazônia azul (Figura 5). Entretanto, devido as condições inóspitas, sua habitação tem sido direcionada a pesquisadores vinculados a projetos científicos previamente selecionados em áreas tais como: geologia, geofísica, meteorologia, oceanografia, sismografia, recursos pesqueiros e biologia (VASKE-JR *et al.*,



2010). Neste contexto, vale ressaltar que o material biológico que resultou neste trabalho, foi originário do sedimento coletado em uma das expedições apoiada pelo projeto PRO-ARQUIPÉLAGO.

**Figura 5-** Mapa mostrando a Zona Econômica Exclusiva Brasileira.



Fonte: Adaptado de Marinha do Brasil

### 2.2.2 O gênero *Salinispora*

A primeira espécie de actinomiceto que originou o gênero *Salinispora* foi isolada pela primeira vez por Jensen e colaboradores em 1991, a partir de fragmento da região das Bahamas, tendo sido inicialmente identificado por ferramentas taxonômicas tradicionais como sendo uma espécie do gênero *Micromonospora*, o qual pertence à família *Micromonosporaceae* (JENSEN; WIGHT; FENICAL, 1991).

Posteriormente, com base em estudos de filogenia molecular e usando sequenciamento do gene 16S ADNr, foi demonstrado que tal actinomiceto diferia de todas as espécies, até então, identificadas no gênero *Micromonospora*. Assim, foi proposto, para este actinomiceto, um novo gênero que foi nomeado primeiramente como *Salinospira*, mas que foi posteriormente renomeado para *Salinispora* (MINCER *et al.*, 2002).

O taxon *Salinispora*, um grupo de actinomicetos exclusivamente marinho, foi formalmente descrito em 2005 por Maldonado e colaboradores, sendo que até meados de 2020, eram descritas apenas as espécies *S. tropica*, *S. pacifica* e *S. arenicola* (Figura 6) para esse gênero (MALDONADO *et al.*, 2005; JENSEN *et al.*, 2007), porém, ainda neste mesmo ano, seis novas espécies foram registradas: *Salinispora cortesiana* sp. nov., *Salinispora fenicalii* sp. nov., *Salinispora goodfellowii* sp. nov., *Salinispora mooreana* sp. nov., *Salinispora oceanensis* sp. nov. e *Salinispora vitiensis* sp. nov., (ROMÁN-PONCE *et al.*, 2020).

**Figura 6-** Culturas de cepas de *S. tropica*, *S. pacifica* e *arenicola*, respectivamente.



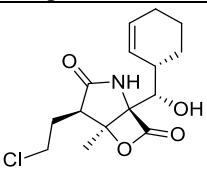
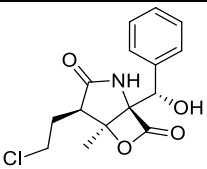
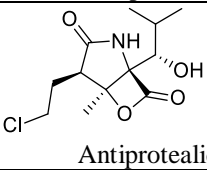
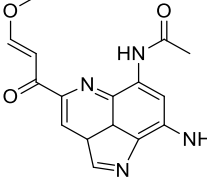
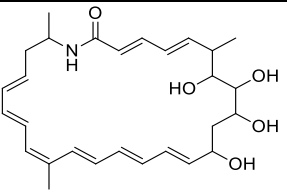
Fonte: (Jensen, <https://atlas.actino.jp/>).

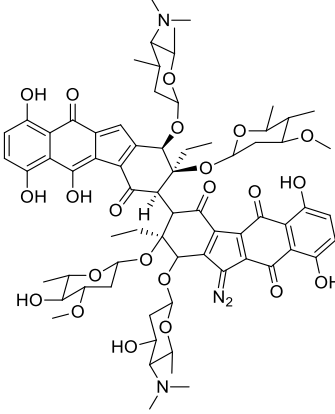
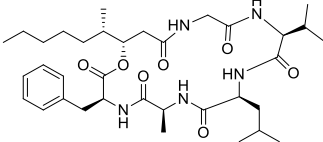
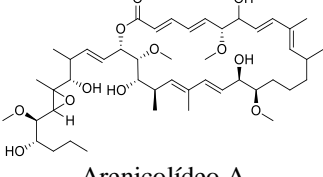
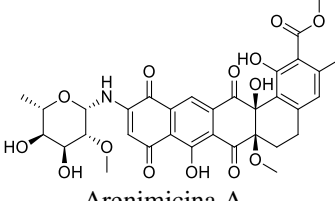
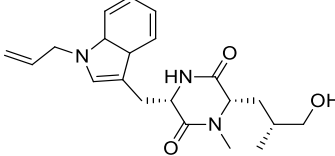
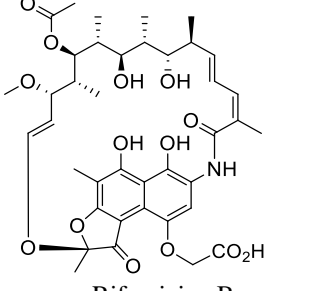
Vale ressaltar que *Salinispora* spp. são mais frequentemente relatadas a partir de sedimentos marinhos das regiões oceânicas tropicais e subtropicais (MINCER *et al.*, 2002), mas também foram relatadas associadas à ascídeas, algas marinhas e esponjas marinhas (HE *et al.*, 2001; JENSEN *et al.*, 2005; KIM *et al.*, 2006; SINGH *et al.*, 2014).

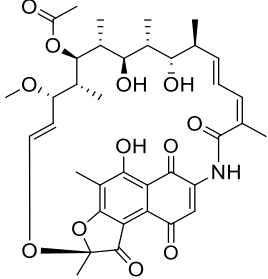
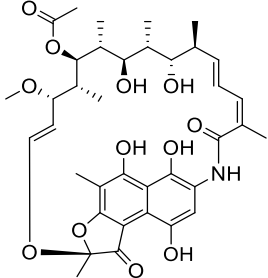
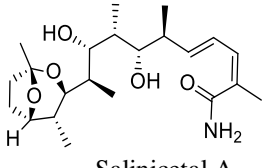
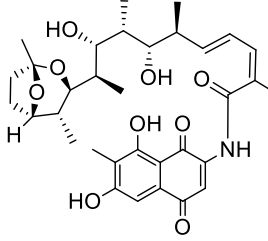
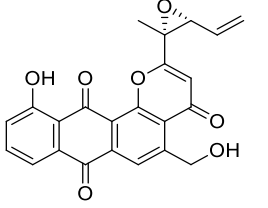
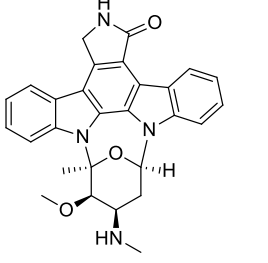
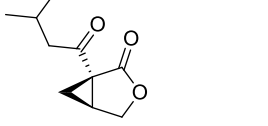
Devido à capacidade de produzir metabólitos secundários biologicamente ativos, as cepas de *Salinispora* foram investigadas intensivamente (JENSEN; MOORE; FENICAL,

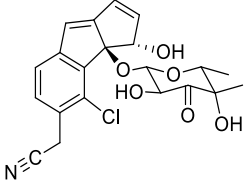
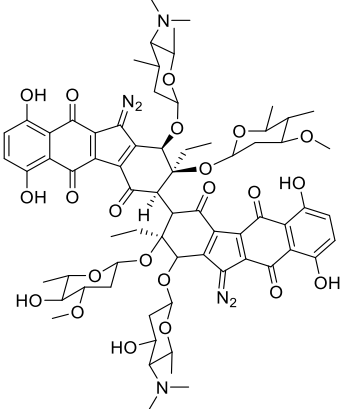
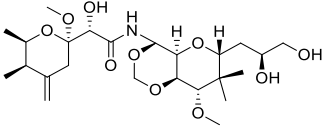
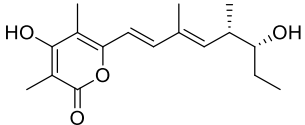
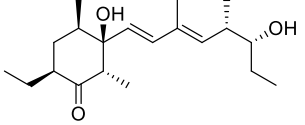
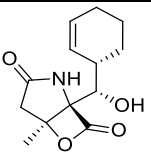
2015). Como resultado, dezenas de compostos estruturalmente diversos e sem precedentes foram isolados de espécies de *Salinispora* como as salinosporamidas, saliniquinonas, salinicetais, arenamidas, salinipironas e pacificanonas (FELING *et al.*, 2003; WILLIAMS *et al.*, 2007; OH *et al.*, 2008; ASOLKAR *et al.*, 2009; MURPHY *et al.*, 2010). Muitos destes compostos exibem atividades interessantes e relevantes como antimicrobiana, anticâncer, antimalárica e imunossupressora, mas o principal interesse está focado na descoberta de agentes anticâncer como as salinosporamidas (WILLIAMS *et al.*, 2005; PRUDHOMME *et al.*, 2008; ASOLKAR *et al.*, 2010; MIYANAGA *et al.*, 2011). Alguns exemplos de compostos isolados de espécies do gênero *Salinispora* estão ilustrados a seguir com destaque para a classe, espécie produtora, bem como as principais atividades relatadas para cada composto (Tabela 4).

**Tabela 4.** Exemplos de compostos relatados a partir de espécies do gênero *Salinispora*.

Composto	Classe	Espécie	Atividade	Referência
 <p>Salinosporamida A</p>	$\beta$ -lactonas	<i>S. tropica</i>	Citotóxica; Antimalárica	FELING <i>et al.</i> , 2003;  PRUDHOMME <i>et al.</i> , 2008
 <p>Salinosporamida X4</p>	$\beta$ -lactonas	<i>S. tropica</i>	Citotóxica	NETT <i>et al.</i> , 2009
 <p>Antiprotealideo</p>	$\beta$ -lactonas	<i>S. tropica</i>	Citotóxica	MANAM <i>et al.</i> , 2009
 <p>Linfostina</p>	Alcaloides	<i>S. tropica</i> <i>S. arenicola</i> <i>S. pacifica</i>	Citotóxica	MIYANAGA <i>et al.</i> , 2011
 <p>Salinilactama A</p>	Macrolactama	<i>S. tropica</i>	-	SCHULTZ <i>et al.</i> , 2008

 <p>Lomaiviticina C</p>	Quinonas	<i>S. tropica</i> <i>S. pacifica</i>	Citotóxica	KERSTEN <i>et al.</i> , 2013;  WOO <i>et al.</i> , 2018
 <p>Arenamida A</p>	Peptídeos	<i>S. arenicola</i>	Anti-inflamatória	ASOLKAR <i>et al.</i> , 2009
 <p>Arenicolídeo A</p>	Macrolactonas	<i>S. arenicola</i>	Citotóxica	WILLIAMS <i>et al.</i> , 2007
 <p>Arenimicina A</p>	Quinonas	<i>S. arenicola</i>	Antibacteriana	ASOLKAR <i>et al.</i> , 2010
 <p>Ciclomarazina A</p>	Dietopiperazinas	<i>S. arenicola</i>	Antibacteriana	SCHULTZ <i>et al.</i> , 2008
 <p>Rifamicina B</p>	Ansamicinas	<i>S. arenicola</i>	Antibacteriana	BOSE <i>et al.</i> , 2015

 <p>Rifamicina S</p>	Ansamicinas	<i>S. arenicola</i>	Antibacteriana	BOSE <i>et al.</i> , 2015
 <p>Rifamicina SV</p>	Ansamicinas	<i>S. arenicola</i>	Antibacteriana	WILSON <i>et al.</i> , 2010
 <p>Salinicetala A</p>	Policetídeos	<i>S. arenicola</i>	Citotóxica	WILLIAMNS <i>et al.</i> , 2007
 <p>Salinisporamicina</p>	Quinonas	<i>S. arenicola</i>	Antibacteriana	MATSUDA <i>et al.</i> , 2009
 <p>Saliniquinona A</p>	Antraquinonas	<i>S. arenicola</i>	Citotóxica	MURPHY <i>et al.</i> , 2010
 <p>Estaurosporina</p>	Alcaloide	<i>S. arenicola</i>	Citotóxica	FREEL <i>et al.</i> , 2011
 <p>Salinilactona A</p>	$\gamma$ -lactonas	<i>S. arenicola</i>	Antibacteriana	SCHLAWIS <i>et al.</i> , 2018

 <p>Cianosporasídeo A</p>	Policetídeos	<i>S. pacifica</i>	Citotóxica	OH <i>et al.</i> , 2008
 <p>Lomaiviticina A</p>	Quinonas	<i>S. pacifica</i>	Citotóxica	WOO <i>et al.</i> , 2018
 <p>Micalamida</p>	Policetídeos	<i>S. pacifica</i>	Antiviral; Imunossupressora	ÖZAKIN AND İNCE, 2019; MOSEY AND FLOREANCIG, 2012
 <p>Salinipirona A</p>	Policetídeos	<i>S. pacifica</i>	-	OH <i>et al.</i> , 2008
 <p>Pacificanona A</p>	Policetídeos	<i>S. pacifica</i>	-	OH <i>et al.</i> , 2008
 <p>Salinosporamida K</p>	$\beta$ -lactonas	<i>S. pacifica</i>	Citotóxica	EUSTAQUIO <i>et al.</i> , 2011

### 3. PROCEDIMENTOS EXPERIMENTAIS

#### 3.1 Métodos cromatográficos

##### 3.1.1 Cromatografia de adsorção

A análise em coluna cromatográfica foi realizada empregando gel de sílica 60 da Merck<sup>®</sup> ou da Vetec<sup>®</sup> [Ø 70-230 µm] em coluna de vidro. O comprimento e o diâmetro das colunas variaram de acordo com as alíquotas das amostras e as quantidades de gel de sílica utilizadas. Para a análise em cromatografia em camada delgada (CCD) utilizou-se cromatoplasmas de alumínio cobertas com gel de sílica 60 [Ø 5-40 µm] F<sub>254</sub> – Merck<sup>®</sup> (espessura de 0,2 mm).

A revelação das substâncias nas placas foi realizada através de exposição à lâmpada ultravioleta da marca Spectroline<sup>®</sup> modelo CM-10 em dois comprimentos de onda (254 e 365 nm) e pulverização com solução de vanilina em HClO<sub>4</sub> 0,75 M/EtOH (1:1), seguido de aquecimento (100 °C) em chapa elétrica até sua completa revelação. Os eluentes utilizados foram: hexano, acetona, acetato de etila (AcOEt) e metanol (MeOH), puros ou combinados em proporções crescentes de polaridade. Os solventes P.A. utilizados na eluição foram das marcas Vetec<sup>®</sup> e Synth<sup>®</sup>.

##### 3.1.2 Cromatografia de exclusão molecular

Os fracionamentos por cromatografia de exclusão molecular foram efetuados em gel de dextrana Sephadex LH-20 da marca Pharmacia Fine Chemicals, utilizando MeOH como fase móvel.

##### 3.1.3 Cromatografia líquida de alta eficiência (CLAE)

As análises por CLAE foram realizadas empregando um aparelho da marca SHIMADZU, modelo UFLC, equipado com detector UV-Vis com arranjo de diodos (SPD-M20A) e um sistema de bomba ternário. As separações foram feitas em colunas semi-preparativas C18 (10 mm x 250 mm, 5 µm), Fenil-hexil (10 mm x 250 mm, 5 µm) e Sílica (10 mm x 250 mm, 5 µm) da marca Phenomenex<sup>®</sup> e uma coluna analítica quiral OD-H (4,6 x 150 mm, 5µm) da marca CHIRALCEL<sup>®</sup> todas mantidas em um forno termostático a 35°C.

Os solventes empregados grau HPLC (acetonitrila, hexano, acetona) e H<sub>2</sub>O deionizada (Milli-Q) foram adequadamente filtrados através de membranas de nylon com poros de 0,45 µm (Milipore). As amostras foram dissolvidas nas fases móveis empregadas em cada análise e filtradas através de membranas de politetrafluoretileno com poros de 0,45 µm (Whatman).

### **3.1.4 Extração em fase sólida (SPE)**

As extrações em fase sólida foram realizadas em cartuchos de fase reversa (Strata C18-E, 20g /60 mL, 55  $\mu$ m, 70  $\text{Å}$ ) da Phenomenex<sup>®</sup>. O uso dos cartuchos foi precedido por ativação do adsorvente com metanol, seguida de acondicionamento com água deionizada (Milli-Q), utilizando alíquotas equivalentes a três vezes o volume do cartucho.

## **3.2 Métodos Físicos**

### **3.2.1 Ponto de Fusão**

Os pontos de fusão dos compostos cristalinos isolados foram obtidos em aparelho digital Microquímica MQAPF-302, pertencente ao Departamento de Química Orgânica e Inorgânica da Universidade Federal do Ceará. As determinações foram realizadas com uma velocidade de aquecimento 1  $^{\circ}\text{C}/\text{min}$  e não foram corrigidos.

### **3.2.2 Rotação óptica**

As rotações ópticas foram obtidas em polarímetro digital da Jasco Brasil P2000, pertencente ao Departamento de Química Orgânica e Inorgânica da Universidade Federal do Ceará à temperatura de 22  $^{\circ}\text{C}$ . O solvente utilizado foi MeOH em cubeta de 2,5 mm de diâmetro e 100 mm de comprimento.

## **3.3 Métodos Espectrométricos**

### **3.3.1 Espectrometria de massas (EM)**

Os espectros de massas de alta resolução foram obtidos no Laboratório Multiusuário de Química de Produtos Naturais na Embrapa Agroindústria Tropical utilizando um espectrômetro Acquity UPLC acoplado a um sistema quadrupolo/TOF equipado com fonte de ionização por *electrospray* (IES), sendo as *scans* adquiridas no modo positivo.

### **3.3.2 Espectroscopia de ressonância magnética nuclear (RMN)**

Os espectros de ressonância magnética nuclear de  $^{13}\text{C}$  e  $^1\text{H}$  (uni e bidimensionais) foram obtidos em espectrômetros Bruker<sup>®</sup> modelo DRX-500 e DPX-300 equipados com sonda de 5mm no Centro Nordestino de Aplicação e Uso da Ressonância Magnética Nuclear (CENAUREMN) pertencente à Universidade Federal do Ceará. Também foi utilizado um espectrômetro Agilent, modelo DD2, operando na frequência de 600 MHz, este pertencente ao Laboratório Multiusuário de Química de Produtos Naturais da Embrapa Agroindústria Tropical.



Os solventes deuterados utilizados na dissolução das amostras e obtenção dos espectros foram clorofórmio, metanol e dimetilsulfóxido, todos produzidos por Cambridge Isotope Laboratories.

Os deslocamentos químicos ( $\delta$ ) foram expressos em partes por milhão (ppm) e referenciados nos espectros de RMN  $^1\text{H}$  pelo sinal de hidrogênio pertencente à fração não deuterada dos solventes: clorofórmio ( $\delta_{\text{H}}$  7,27), metanol ( $\delta_{\text{H}}$  3,31) e dimetilsulfóxido ( $\delta_{\text{H}}$  2,50) e para os espectros RMN  $^{13}\text{C}$  pelos picos de carbono-13 dos solventes: clorofórmio ( $\delta_{\text{C}}$  77,23) metanol ( $\delta_{\text{C}}$  49,15) e dimetilsulfóxido ( $\delta_{\text{C}}$  39,51).

As multiplicidades das absorções foram indicadas segundo a convenção: s (simpleto), sl (singleto largo), d (duplete), dd (duplo duplete), dq (duplo quarteto) t (tripleto) e m (multiplete).

O padrão de hidrogenação dos carbonos foi determinado através da utilização das técnicas  $^{13}\text{C}$ -DEPT 135°,  $^{13}\text{C}$ -APT e HSQC-editado, e expressado segundo a convenção: C (carbono não hidrogenado), CH (carbono metínico),  $\text{CH}_2$  (carbono metilênico) e  $\text{CH}_3$  (carbono metílico).

### ***3.3.3 Espectroscopia de Difração de Raios-X***

As análises de difração de raios-X foram realizadas em um difratômetro de monocristal da marca Bruker® modelo D8 Venture equipado com gerador de radiação de molibdênio e cobre pertencente ao Laboratório de Cristalografia Estrutural da Universidade Federal do Ceará. Os cristais das amostras foram preparados através da lenta evaporação do solvente (acetona ou MeOH) em refrigerador por um período entre 1 a 2 semanas.

## **3.4 Estudo dos microrganismos**

### ***3.4.1 Coleta do material***

As amostras de sedimentos foram coletadas em duas expedições realizadas em fevereiro e novembro de 2011 nas ilhas Boca da Enseada, Enseada e Cabeça de Tartaruga, pertencentes ao ASPSP. Os sedimentos foram coletados em porções de 20 g e, armazenados em sacos estéreis de 7,5 x 18,5 centímetros (Whirl-Park, Nasco) à temperatura de 20 °C para o transporte. A coleta foi realizada pelo Prof. Dr. Tito Monteiro da Cruz Lotufo, hoje pertencente ao Instituto Oceanográfico da Universidade de São Paulo, através de mergulho com SCUBA nos pontos do ASPSP citados acima.

### **3.4.2 Isolamento dos microrganismos**

Todo o material coletado foi processado *in situ* na Estação Científica do Arquipélago São Pedro e São Paulo (ECASPSP), e processados novamente após a chegada ao Laboratório de Ecotoxicologia Marinha pertencente ao Instituto de Ciências do Mar da Universidade Federal do Ceará. Ao chegar ao laboratório, as amostras de sedimento coletadas foram processadas em um ambiente estéril em fluxo laminar.

As colônias foram selecionadas através de observações macroscópicas das placas de cultura e por suas características fenotípicas (cor, brilho, forma, textura, etc). As colônias foram recuperadas utilizando palitos de madeira estéreis, em seguida repicadas para uma nova placa de petri com meio de cultura sólido (A1) composto por água do mar/água destilada 75 % (v/v), 2 % peptona, 10 % de amido, 4 % extrato de levedura e 18 % de ágar.

### **3.4.3 Purificação, cultivo e criopreservação dos microrganismos**

A purificação das linhagens de microrganismos foi realizada por meio de repiques sucessivos, pela técnica de esgotamento por estrias. Quando as cepas encontravam-se totalmente puras, eram inoculadas em meio de cultura líquido (A1) onde cresciam por 7 dias, sob agitação em agitadores orbitais com rotação de 200 rpm e temperatura de  $28 \pm 2$  °C. Após este período, uma alíquota de 12,5 mL do fermentado biológico foi diluído com uma solução de glicerol 50 % (v/v) na proporção de 1:1 e homogeneizado, em seguida essa solução do fermentado foi alíquotada em tubos criogênicos e congelada a -80 °C e catalogadas no banco de microrganismos do Laboratório de Ecotoxicologia Marinha, os quais foram denominados de BRA, seguidas da numeração ordenada no banco (FERREIRA *et al.*, 2016).

### **3.4.4 Obtenção dos extratos em pequena escala**

Para a obtenção dos fermentados biológicos em pequena escala, as culturas puras foram inoculadas em erlenmeyers de 500 mL contendo aproximadamente 100 mL de meio de cultura líquido (A1), e mantidos em agitação de 200 rpm à temperatura de  $28 \pm 2$  °C durante o período de 7 a 14 dias. Após esse período, foi adicionado aos erlenmeyers 100 mL de AcOEt, e mantendo-se sob agitação de 200 rpm, por 1 hora e depois o caldo de cultura foi submetido a um procedimento de separação líquido-líquido em funil de decantação. Após esses processos, os extratos líquidos obtidos foram secos em evaporador rotativo, para a obtenção do extrato bruto (FERREIRA *et al.*, 2016).

### **3.4.5 Crescimento em larga escala da cepa BRA-213**

O crescimento em larga escala da estirpe BRA-213, foi realizado em frascos de erlenmeyers de 2 L, usando um volume 0,5 L de meio A1 suplementado com carbonato de cálcio 0,5 g/L [CaCO<sub>3</sub>] e 5 g/L das soluções de sulfato de ferro (III) [Fe<sub>2</sub>(SO<sub>4</sub>)<sub>3</sub>] e brometo de potássio (KBr).

A cepa BRA-213 foi cultivada em 20 L de meio de cultura suplementado (A1) durante um período de 14 dias, temperatura de 28 °C e sob agitação de 200 rpm. No segundo dia de crescimento, foram adicionados 10 g da resina Amberlite® XAD 16 (Sigma) ao fermentado biológico. Após o período de crescimento, a resina foi separada da biomassa e extraída com 2 L de acetona PA, onde a fase orgânica foi evaporada da fase aquosa em um evaporador rotativo. A fase aquosa foi então submetida a uma extração líquido-líquido em funil de decantação com 2 L de AcOEt para obtenção do extrato bruto (9,0 g).

### **3.4.6 Identificação molecular da cepa em estudo**

A cepa selecionada foi identificada com base na sequência do gene 16S RNAr e análise no banco genético utilizando-se o programa *Basic Local Alignment Search Tool* (BLAST). A busca no BLAST alinha as sequências de 16S RNAr obtidas numa base de dados de sequências conhecidas a fim de encontrar o pareamento taxonômico mais aproximado. Este programa encontra-se disponível na página do Centro Nacional para Informações em Biotecnologia dos Estados Unidos (National Center for Biotechnology Information) através do endereço <http://www.ncbi.nlm.nih.gov/BLAST>.

Após a análise no banco genético (BLAST), a cepa BRA-213 foi agrupada com maior similaridade ao gênero *Salinispora*. A maior semelhança em pares observada para o gênero *Salinispora* (> 99%) foi com a espécie *Salinispora arenicola*.

### **3.4.7 Fracionamento cromatográfico do extrato em AcOEt da bactéria *Salinispora arenicola***

O extrato bruto BRA-213 (9,0 g) foi dividido em porções de 1,0 g, sendo cada alíquota dissolvida em 2 mL de uma mistura composta por MeOH/H<sub>2</sub>O 7:3 (v/v) e adicionada a um cartucho *SPE-C18*, já ativado e equilibrado com a fase móvel. Nesse processo uma parte não solubilizou e foi denominado de resíduo insolúvel (RI). O cartucho foi eluído com as misturas dos solventes H<sub>2</sub>O e MeOH, como indicado na tabela 5. Foram geradas 3 frações de aproximadamente 200 mL cada.

**Tabela 5-** Fracionamento cromatográfico do extrato em AcOEt de *Salinispora arenicola*.

<b>Eluente</b>	<b>Fração</b>	<b>Massa (g)</b>	<b>Rendimento (%)</b>
MeOH/H <sub>2</sub> O (7:3)	A	5,0	55,5
MeOH/H <sub>2</sub> O (4:1)	B	1,1	12,2
MeOH/H <sub>2</sub> O (1:0)	C	1,3	14,5
-	RI	1,0	11,1
<b>TOTAL</b>	-	<b>8,4</b>	<b>93,3</b>

Fonte: Próprio autor.

A fração A (5,0 g) também foi dividida em porções de 1,0 g e cada alíquota foi dissolvida em 2 mL de uma mistura composta por MeOH/H<sub>2</sub>O 3:7 (v/v) e adicionada a um cartucho *SPE-C18*. O cartucho foi eluído com as misturas dos solventes H<sub>2</sub>O e MeOH, gerando 7 frações (AA-AG) de 200 mL cada como indicado na tabela 6.

**Tabela 6-** Fracionamento cromatográfico da fração A.

<b>Eluente</b>	<b>Fração</b>	<b>Massa (g)</b>	<b>Rendimento (%)</b>
MeOH/H <sub>2</sub> O (3:7)	AA	1,20	24,0
MeOH/H <sub>2</sub> O (2:3)	AB	0,66	13,2
MeOH/H <sub>2</sub> O (1:1)	AC	0,61	12,2
MeOH/H <sub>2</sub> O (3:2)	AD	0,91	18,2
MeOH/H <sub>2</sub> O (7:3)	AE	0,60	12,0
MeOH/H <sub>2</sub> O (4:1)	AF	0,70	14,0
MeOH/H <sub>2</sub> O (1:0)	AG	0,18	3,6
<b>TOTAL</b>		<b>4,86</b>	<b>97,2</b>

Fonte: Próprio autor.

A fração AB (660,0 mg) foi dissolvida em 1 mL de MeOH e separada por cromatografia em Sephadex LH-20 (10 g em coluna de 1,0 cm de diâmetro), resultando em 41 frações com aproximadamente 5 mL cada. Essas frações foram monitoradas por CCD e reveladas com vanilina, resultando em 5 frações nomeadas de AB1-AB5, conforme mostrado na tabela 7.

A subfração AB4 (32,0 mg) foi purificada por CLAE, utilizando-se uma coluna semipreparativa de fase reversa C-18. Essa amostra foi dissolvida em 3 mL de CH<sub>3</sub>CN/H<sub>2</sub>O 1:1

(v/v), sendo utilizado 200  $\mu$ L da mesma em cada análise. A coleta foi realizada usando um método gradiente composto por  $\text{CH}_3\text{CN}/\text{H}_2\text{O}$  (0,1 % TFA) variando de 50 a 100 % de  $\text{CH}_3\text{CN}$  em 30 minutos, com um fluxo de 3,0 mL/min. O cromatograma mostrou dois picos registrados com  $R_t = 5,5$  min (pico 1) e  $R_t = 6,6$  min (pico 2) (Figura 7), os quais foram coletados e após secos, forneceram 8,0 mg de uma mistura codificada de AB4P1 e 3,8 mg de um sólido cristalino incolor em formas de agulhas denominado de 3-hidroxi-5-(1-hidroxi-1-fenilpropan-2-il)-2-metil-piran-2-ona (**SA-8**).

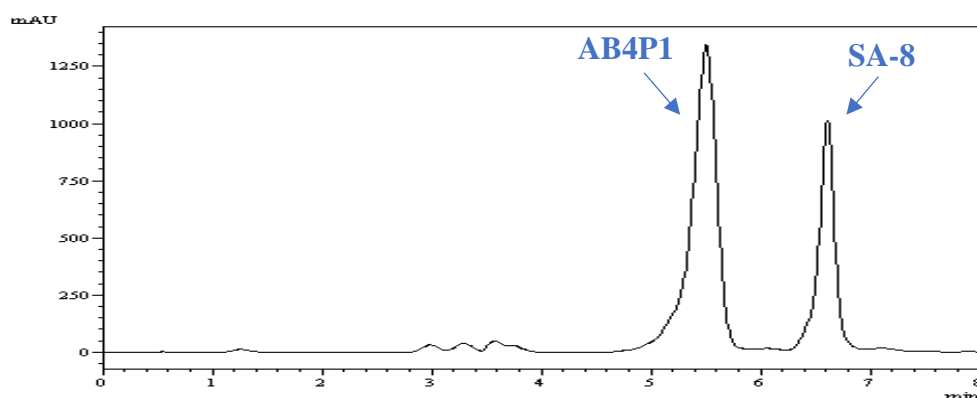
A mistura AB4P1 (8,0 mg) foi submetida a cromatografia CLAE, usando uma coluna semipreparativa de fase reversa fenil-hexil. Essa amostra foi dissolvida em 1,0 mL de  $\text{CH}_3\text{CN}/\text{H}_2\text{O}$  1:1 (v/v), sendo utilizado 100  $\mu$ L dessa solução em cada análise. Foi utilizado como fase móvel um gradiente composto por  $\text{CH}_3\text{CN}/\text{H}_2\text{O}$  (0,1 % TFA) variando de 40 a 70 % de  $\text{CH}_3\text{CN}$  em 30 minutos, com um fluxo de 3,0 mL/min. O cromatograma mostrou dois picos bem definidos com um tempo total de corrida de 11,0 min (Figura 8), os quais foram coletados. O pico 1 com  $R_t = 8,2$  min, após seco forneceu 2,0 mg de uma resina amarela denominada de 3-hidroxi-6-metoxi-3-(2-oxo-propil)-*N*-metil-2-oxindol (**SA-6**), enquanto o pico 2 com  $R_t = 10,5$  min, forneceu 1,0 mg de um sólido amarelo cristalino denominado de 5-cloro-3-hidroxi-6-metoxi-3-(2-oxo-propil)-*N*-metil-2-oxindol (**SA-7**).

**Tabela 7**-Fracionamento cromatográfico da fração AB.

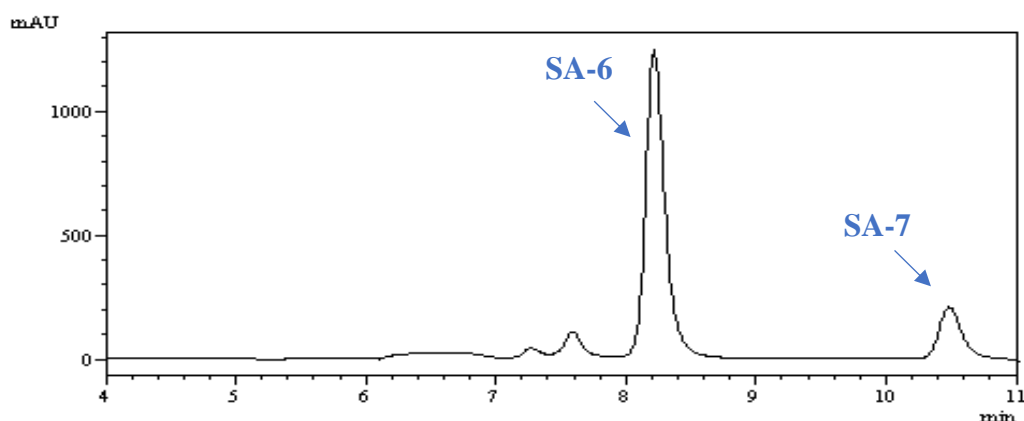
Frações reunidas	Fração	Massa (mg)	Rendimento (%)
1-17	AB1	122,8	18,6
18-25	AB2	215,0	32,6
26-31	AB3	120,7	18,3
33-39	AB4	32,0	4,8
40-41	AB5	126,2	19,1
<b>TOTAL</b>		<b>616,7</b>	<b>93,4</b>

Fonte: Próprio autor.

A fração AC (610 mg) foi dissolvida em 1mL de MeOH e submetida à cromatografia em Sephadex LH-20 (10 g em coluna de 1,0 cm de diâmetro), resultando em 44 frações com aproximadamente 5 mL. As frações foram monitoradas por CCD e reveladas com vanilina, possibilitando a reunião em frações nomeadas de AC1-AC4 e o isolamento de 12,5 mg de um sólido vermelho amorfo denominado de Salinaftoquinona A (**SA-1**), conforme mostrado na tabela 8.

**Figura 7-** Cromatograma da subfração AB4 observada na faixa de 210-400 nm.

Fonte: Próprio autor.

**Figura 8-** Cromatograma da mistura AB4P1 observada na faixa de 210-400 nm.

Fonte: Próprio autor.

**Tabela 8-** Fracionamento cromatográfico da fração AC.

Frações reunidas	Fração	Massa (mg)	Rendimento (%)
1-8	AC1	86,4	14,2
9-19	AC2	136,0	22,3
20-27	AC3	228,7	37,5
28-35	AC4	90,0	14,7
36-44	<b>SA-1</b>	12,5	2,0
<b>TOTAL</b>		<b>553,6</b>	<b>90,7</b>

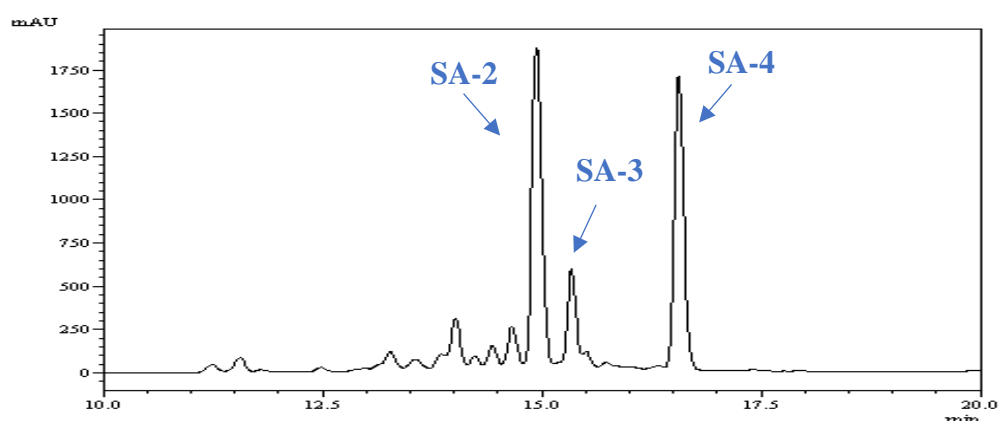
Fonte: Próprio autor.

A subfração AC4 (90,0 mg) foi purificada por CLAE, injetando-se alíquotas de 200  $\mu$ L da amostra dissolvida em 10 mL de uma mistura de hexano/acetona 1:1 (v/v). A separação foi realizada utilizando-se uma coluna semipreparativa de Sílica, usando como fase móvel um

gradiente composto por hexano/acetona variando de 10 a 100 % de acetona em 30 minutos, com um fluxo de 3,0 mL/min.

Foram coletados três picos com tempo de retenção de 14,9 min (pico 1), 15,3 min (pico 2), 16,6 min (pico 3), com tempo total de corrida de 20 minutos (Figura 9). O pico 1 forneceu 8,0 mg de um sólido laranja cristalino denominado de Salinaftoquinona B (SA-2). O pico 2 forneceu 1,0 mg de um sólido laranja amorfo denominado de Salinaftoquinona C (SA-3), enquanto o pico 3 forneceu 5,0 mg de um sólido vermelho cristalino denominado de Salinaftoquinona D (SA-4).

**Figura 9**-Cromatograma da subfração AC4 observada na faixa de 350-600 nm.



Fonte: Próprio autor.

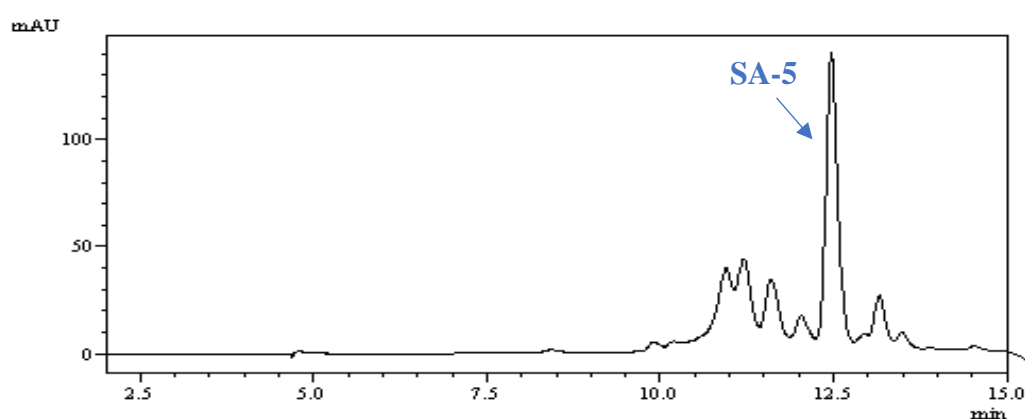
A fração AD (910,0 mg) foi dissolvida em 1,5 mL de MeOH e separada por cromatografia em Sephadex LH-20 (10 g em coluna de 1,0 cm de diâmetro), resultando em 45 frações com aproximadamente 5 mL cada. Essas frações foram monitoradas por CCD e reveladas com vanilina, resultando em 5 frações nomeadas de AD1-AD5 (tabela 9).

A subfração AD5 (20,0 mg) foi submetida à cromatografia CLAE, usando uma coluna semipreparativa de Sílica. Essa amostra foi dissolvida em 2,0 mL de hexano/acetona 1:1 (v/v), sendo utilizado 200  $\mu$ L dessa solução em cada análise, usando como fase móvel um gradiente composto por hexano/acetona variando de 30 a 100 % de acetona em 20 minutos, com um fluxo de 3,0 mL/min. Foi coletado um pico com  $R_t = 12,5$  min (Figura 10) que após seco, forneceu 2,0 mg de um sólido laranja cristalino denominado de Salinaftoquinona E (SA-5).

**Tabela 9**-Fracionamento cromatográfico da fração AD.

Frações reunidas	Fração	Massa (mg)	Rendimento (%)
1-6	AD1	70,4	7,7
7-20	AD2	118,0	13,0
21-27	AD3	253,4	27,8
28-32	AD4	341,2	37,5
33-45	AD5	20,0	2,2
<b>TOTAL</b>		<b>803,0</b>	<b>88,2</b>

Fonte: Próprio autor.

**Figura 10**-Cromatograma da subfração AD5 observada na faixa de 350-600 nm.

Fonte: Próprio autor.

A subfração AB3 (120,7 mg) foi purificada por CLAE, utilizando-se uma coluna semipreparativa de fase reversa C-18. Essa amostra foi dissolvida em 4 mL de CH<sub>3</sub>CN/H<sub>2</sub>O 1:1 (v/v), sendo utilizado 200 µL da mesma em cada análise. A coleta foi realizada usando um método gradiente composto por CH<sub>3</sub>CN/H<sub>2</sub>O (0,1% TFA) variando de 50 a 80 % de CH<sub>3</sub>CN em 30 minutos, com um fluxo de 3,0 mL/min.

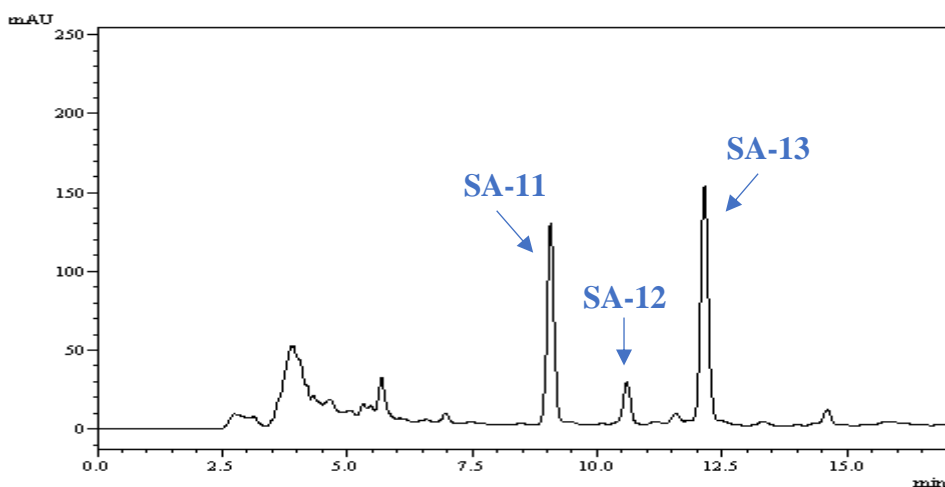
Foram coletados três picos com tempo de retenção de 9,2 min (pico 1), 10,6 min (pico 2), 12,3 min (pico 3), com tempo total de corrida de 20 minutos (Figura 11). O pico 1 forneceu 3,0 mg de um sólido amarelo denominado de Salinirrifamicina C (**SA-11**). O pico 2 forneceu 0,6 mg de um sólido amarelo denominado de Salinirrifamicina D (**SA-12**), enquanto o pico 3 forneceu 2,5 mg de um sólido amarelo denominado de Salinirrifamicina E (**SA-13**).

A subfração AD2 (118,0 mg) foi submetida à cromatografia CLAE, usando uma coluna semipreparativa de fase reversa C-18 usando o mesmo método descrito pra subfração



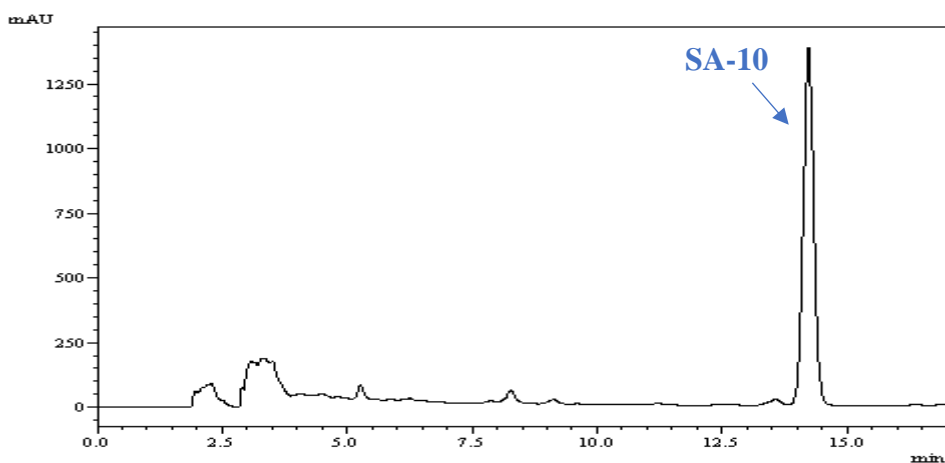
AB3 acima. Foi coletado um pico com  $R_t = 14,3$  min (Figura 12) que após seco, forneceu 15,0 mg de um sólido amarelo denominado de Salinirrifamicina B (SA-10).

**Figura 11**-Cromatograma da subfração AB3 observada na faixa de 210-400 nm.



Fonte: Próprio autor.

**Figura 12**-Cromatograma da subfração AD2 observada na faixa de 210-400 nm.



Fonte: Próprio autor.

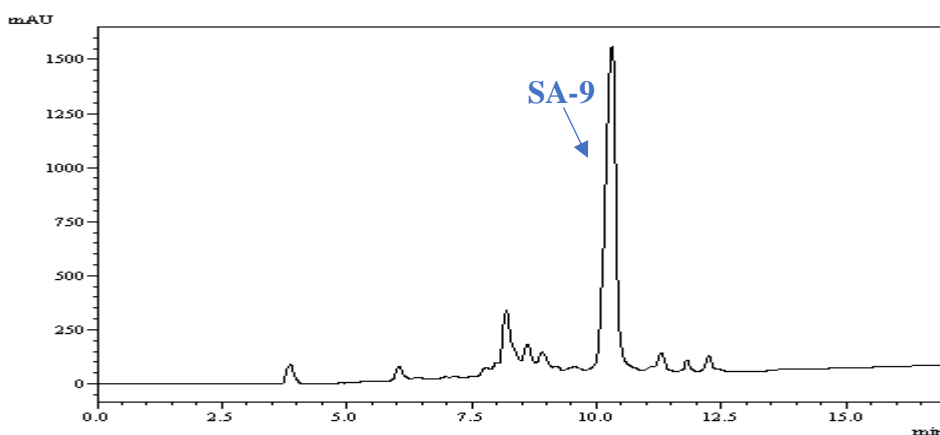
A fração B (1,1 g) foi dissolvida em 2 mL de MeOH e separada por cromatografia em Sephadex LH-20 (10 g em coluna de 1,0 cm de diâmetro), resultando em 52 frações com aproximadamente 5 mL cada. Essas frações foram monitoradas por CCD e reveladas com vanilina, resultando em 6 frações nomeadas de AD1-AD6 (tabela 10).

**Tabela 10**-Fracionamento cromatográfico da fração B.

Frações	Fração	Massa (mg)	Rendimento (%)
1-6	B1	101,4	9,2
7-20	B2	55,0	5,0
21-25	B3	234,7	21,3
26-35	B4	350,8	31,9
36-45	B5	185,6	16,9
46-52	B6	123,3	11,2
<b>TOTAL</b>	<b>-</b>	<b>950,8</b>	<b>95,5</b>

Fonte: Próprio autor.

A subfração B2 (55,0 mg) foi submetida à cromatografia CLAE, usando uma coluna semipreparativa de Sílica. Essa amostra foi dissolvida em 2,0 mL de hexano/acetona 1:1 (v/v), sendo utilizado 200 µL dessa solução em cada análise, usando como fase móvel um gradiente composto por hexano/acetona variando de 30 a 100 % de acetona em 20 minutos, com um fluxo de 3,0 mL/min. Foi coletado um pico com  $R_t = 10,3$  min (Figura 13) que após seco, forneceu 1,5 mg de um sólido vermelho denominado de Salinaftoquinona A (**SA-9**).

**Figura 13**-Cromatograma da subfração B2 observada na faixa de 350-600 nm.

### **3.5 Ensaio de atividade Antimicrobiana in vitro**

Para avaliar a atividade antibacteriana das substâncias isoladas, foram utilizadas quatro cepas de bactérias Gram-positivas: *Staphylococcus aureus* (ATCC 29213), *Staphylococcus aureus* resistente à meticilina (ATCC 43300, MRSA), *Enterococcus faecalis* (ATCC 29212) e *Enterococcus faecalis* resistente à vancomicina (ATCC 51212, VRE), e uma cepa Gram-negativa: *Escherichia coli* (ATCC 25922 ). Os testes foram realizados pelo Prof. Dr. José Delano B. Marinho Monteiro Filho no laboratório de microbiologia da Universidade Federal do Piauí.

Para os experimentos, as linhagens foram previamente semeadas em placas de Petri contendo ágar Mueller Hinton (Difco <sup>TM</sup>), as quais foram incubadas por 24 horas a temperatura de  $35 \pm 2$  ° C, sob condições aeróbicas. Após esse período, as colônias isoladas foram coletadas e suspensas em solução salina estéril NaCl 0,85 % (p/v). Esta suspensão foi então usada para se obter o inóculo bacteriano em meio de cultura Mueller Hinton Broth -MHB (Difco <sup>TM</sup>) com uma concentração bacteriana final de  $5 \times 10^5$  UFC/mL. O método utilizado foi a microdiluição em caldo em placa de 96 poços, na qual as concentrações inibitórias mínimas (CIMs) das substâncias foram determinadas de acordo com o Instituto de Padrões de Laboratório Clínico (2015).

## 4 RESULTADOS E DISCUSSÃO

Em acordo com os objetivos e a metodologia descrita previamente, iniciou-se o projeto de pesquisa com a investigação química do extrato em AcOEt de *S. arenicola* usando diferentes métodos cromatográficos de separação, incluindo extração em fase sólida (SPE), cromatografia de exclusão molecular (Sephadex LH-20) e cromatografia líquida de alta eficiência (CLAE).

Com isto, fruto de um minucioso trabalho químico e com a colaboração interdisciplinar/multidisciplinar foram isolados e caracterizados treze novos compostos (Figura 14), cujas estruturas foram determinadas por meio de técnicas espectroscópicas/espectrométricas (IV, UV, EM, RMN  $^1\text{H}$  e  $^{13}\text{C}$ ), incluindo difração de raios-X. Além disto, para o composto Salinirrifamicin A, foram realizados cálculos teóricos visando certificar de forma inequívoca as atribuições de deslocamentos químicos e determinação da estereoquímica relativa. Aliado a esses resultados, foi também investigada a atividade antimicrobiana dos compostos isolados frente a cepas de bactérias Gram-positivas [(*Staphylococcus aureus*, *Staphylococcus aureus* resistente à metilina (MRSA), *Enterococcus faecalis* e *Enterococcus faecalis* resistente à vancomicina (VRE)] e Gram-negativa (*Escherichia coli*). Os resultados obtidos nesta tese foram compilados em formato de artigos que estão incluídos nesta seção de resultados e discussão como capítulos 1, 2, 3 e 4.

Os resultados apresentados no Capítulo 1 culminaram na publicação de um artigo na revista *Journal Natural Products* com título: “Antibacterial Salinaphthoquinones from a Strain of the Bacterium *Salinispora arenicola* Recovered from the Marine Sediments of St. Peter and St. Paul-Archipelago, Brazil” *J. Nat. Prod.*, 2019, 82, 1831–1838. Doi:10.1021/acs.jnatprod.9b00062. Os dados apresentados no Capítulo 2 resultaram na publicação de um artigo na revista *Fitoterapia* com título: “4-Hydroxy-pyran-2-one and 3-hydroxy-*N*-methyl-2-oxindole derivatives of *Salinispora arenicola* from Brazilian marine sediments” *Fitoterapia.*, 2019, 138, 104357–104361. Doi:10.1016/j.fitote.2019.104357. Os resultados apresentados no capítulo 3 com título: “Salinirifamicin A, a Natural Pyridine-Rifamicin from the Marine Actinomycete *Salinispora arenicola*” e capítulo 4 com título: “Salinirifamicins B–E: Further Rifamicin S Derivatives from the Marine Actinomycete *Salinispora arenicola*” encontram-se em revisão para submissão em revistas especializadas da área de produtos naturais.

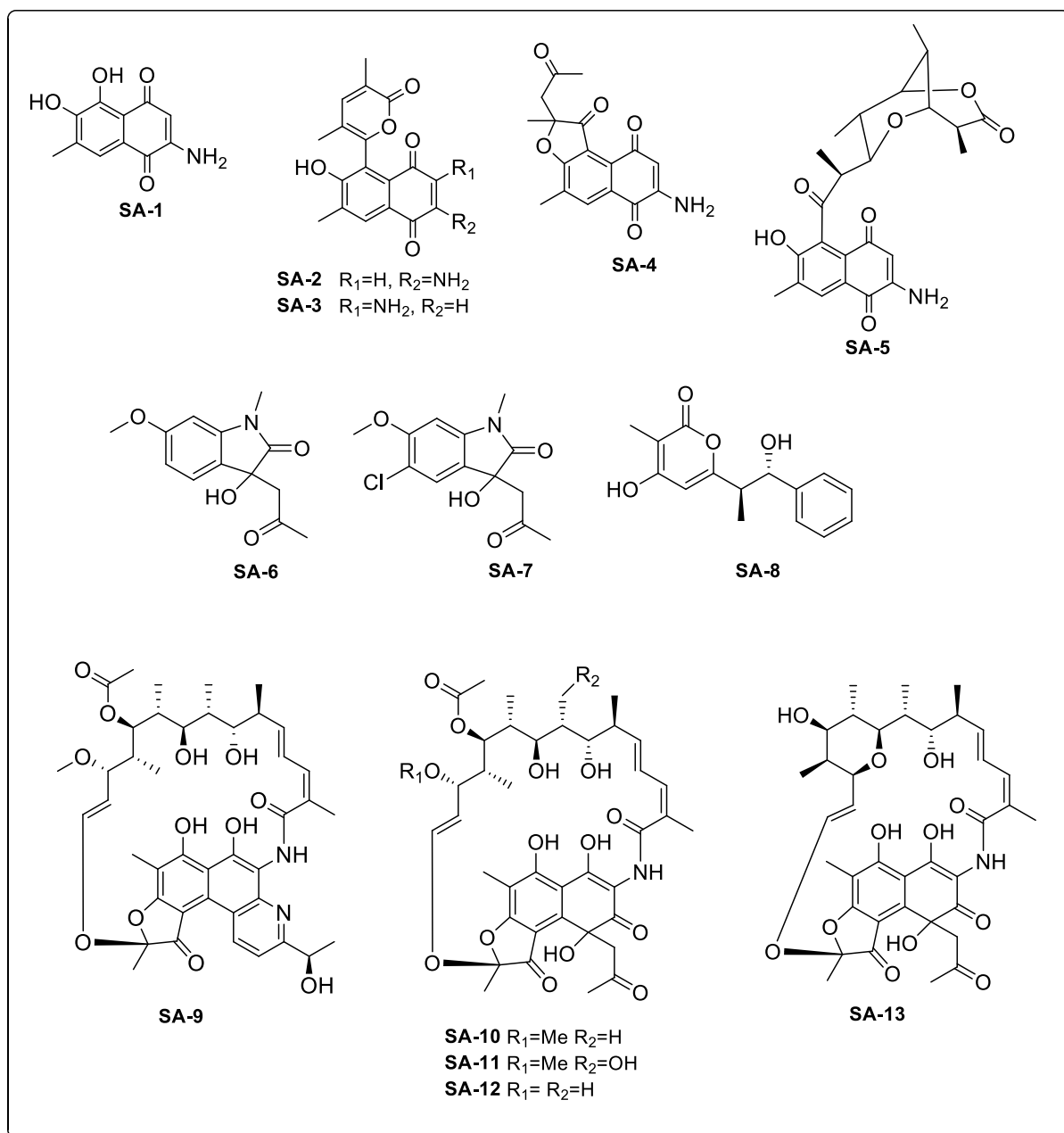
Dentre os treze compostos, foram isolados aminonafquinonas (SA-1–SA-5), *N*-metil-2-oxindóis (SA-6 e SA-7), derivados de 4-hidroxi-pirona-2-onas (SA-8), e rifamicinas (SA-9–SA-13).

Naftoquinonas são uma grande classe de compostos naturais produzidos por plantas superiores, bactérias e fungos (BABULA *et al.*, 2009; QIU, *et al.*, 2018). Por outro lado, poucos exemplos relacionados ao isolamento de aminonaftoquinonas são descritos (POLONIK *et al.*, 2011). Vale mencionar que aminonaftoquinonas constituem uma unidade estrutural essencial de vários macrolídeos naturais de importância biológica como as rifamicinas (ZHANG, *et al.*, 2017). Entretanto, apesar do grande número de rifamicinas relatadas, naturais ou sintéticas, o grupo amino está principalmente na posição C-2 do núcleo quinona, exceto pelos compostos 3-amino-27-desmetoxi-27-hidroxi-rifamicina S e 3-amino-rifamicina S, previamente isolado de culturas de *Micromonospora* sp. (WILLIAMS, *et al.*, 2017).

Vale ressaltar que derivados naturais 3-hidroxi-2-oxindóis foram isolados de várias fontes naturais, incluindo plantas (KAGATA *et al.*, 2006), microrganismos (PENG *et al.*, 2013) e invertebrados marinhos (KAMANO, *et al.*, 1995). Entretanto, este é o primeiro relato desta classe de *Salinispora*, adicionando ao gênero, mais uma classe de interesse farmacológica já que propriedades anticâncer, anti-HIV e neuroprotetoras, são descritas para esta classe de compostos naturais os quais que tem inspirado inúmeras sínteses orgânicas com vistas a descoberta de novas drogas (PEDDIBHOTA, 2009; MOGHADDAM; JALAL; ZERAATKAR, 2018).

Quanto às rifamicinas, já existem relatos de identificação destas a partir do gênero *Salinispora*, como por exemplo: as rifamicinas B e S (KIM, *et al.*, 2020). Porém, apesar da grande contribuição e revolução na área de antibióticos, pouca atenção tem sido dada a esses compostos em espécies de *Salinispora*, sendo estes apenas identificados. Este trabalho mostra o primeiro isolamento de novas rifamicinas de *Salinispora*, contribuindo para o reconhecimento desse gênero como modelo para descoberta de novos metabólitos secundários.

**Figura 14**-Novos compostos isolados de *S. arenicola*.



Fonte: Próprio autor.

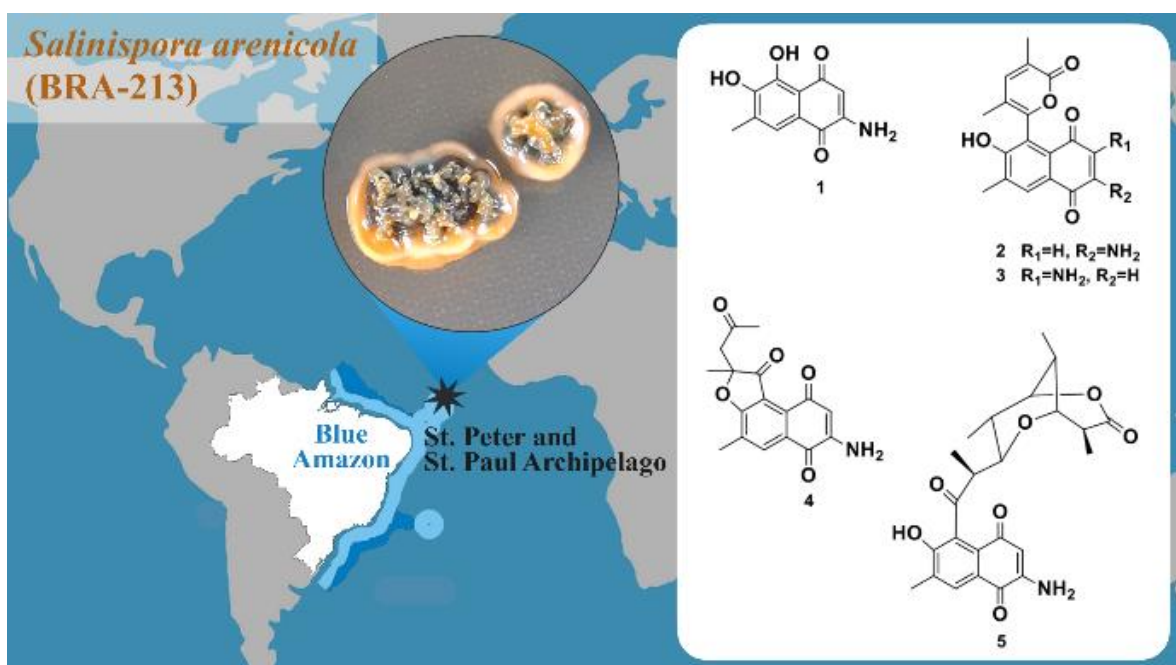
4.1

# Capítulo 1

---

**Antibacterial Salinaphthoquinones from a Strain of the Bacterium *Salinispora arenicola* Recovered from the Marine Sediments of St. Peter and St. Paul-Archipelago, Brazil**

---



## **Antibacterial Salinaphthoquinones from a Strain of the Bacterium *Salinispora arenicola* Recovered from the Marine Sediments of St. Peter and St. Paul-Archipelago, Brazil**

Alison B. da Silva,<sup>†</sup> Edilberto R. Silveira,<sup>†</sup> Diego V. Wilke,<sup>‡</sup> Elhton G. Ferreira,<sup>‡</sup> Leticia V. Costa-Lotufo,<sup>§</sup> Maria Conceição M. Torres,<sup>†</sup> Alejandro Pedro Ayala,<sup>⊥</sup> Wendell S. Costa,<sup>||</sup> Kirley M. Canuto,<sup>∇</sup> Alyne R. de Araújo-Nobre,<sup>°</sup> Ana Jérсия Araújo,<sup>°</sup> José Delano B. Marinho Filho,<sup>°</sup> and Otilia Deusdenia L. Pessoa<sup>\*,†</sup>

<sup>†</sup>*Departamento de Química Orgânica e Inorgânica, Universidade Federal do Ceará, 60.021-970, Fortaleza-CE, Brazil*

<sup>‡</sup>*Núcleo de Pesquisa e Desenvolvimento de Medicamentos, Universidade Federal do Ceará, 60.430-275, Fortaleza-CE, Brazil*

<sup>§</sup>*Departamento de Farmacologia, Universidade de São Paulo, 05508-900, São Paulo-SP, Brazil*

<sup>⊥</sup>*Departamento de Física, Universidade Federal do Ceará, 60.440-970, Fortaleza-CE, Brazil*

<sup>||</sup>*Departamento de Farmácia, Universidade Federal do Ceará, 60.430-170, Fortaleza-CE, Brazil*

<sup>∇</sup>*Embrapa Agroindústria Tropical, 60.511-110, Fortaleza-CE, Brazil*

<sup>°</sup>*Núcleo de Pesquisa em Biodiversidade e Biotecnologia, Universidade Federal do Piauí, 64202-020, Parnaíba-PI, Brazil*



**ABSTRACT:** Salinaphthoquinones A–E (**1–5**) were isolated from a marine *Salinispora arenicola* strain, recovered from sediments of the St. Peter and St. Paul Archipelago, Brazil. The structures of the compounds were elucidated using a combination of spectroscopic (NMR, IR, HRESIMS) data, including single-crystal X-ray diffraction analysis. A plausible biosynthetic pathway for **1–5** is proposed. Compounds **1** to **4** displayed moderated activity against *Staphylococcus aureus* and *Enterococcus faecalis* with MIC values of 125 to 16 µg/mL.

## INTRODUCTION

Marine microorganisms, in particular the actinomycetes, are known as a highly promising source of unusual and new active compounds, many of which exhibit relevant roles in cellular mechanisms or as key sub-structures in the design of new drugs.<sup>1</sup> The taxon *Salinispora*, a group of exclusively marine actinomycetes, was formally described in 2005.<sup>2</sup> So far, only the species *S. tropica*, *S. pacifica*, and *S. arenicola* have been described for this genus.<sup>3</sup> It is worth noting that *Salinispora* spp. are most frequently reported from marine sediments, but, they have also been reported as associated microorganisms of ascidians,<sup>4</sup> marine algae,<sup>5</sup> and marine sponges.<sup>6–8</sup> Due to the ability to produce biologically active secondary metabolites, *Salinispora* strains have been investigated intensively with a main focus on the discovery of anticancer agents like the salinosporamides.<sup>9</sup> The Brazilian seas are poorly explored from the chemical standpoint, however, these sites can represent great potential for the discovery of new biologically important chemical entities. The northeast Brazil coastline, bathed by the Atlantic Ocean, houses several parks and biological reserves including the Saint Peter and Saint Paul Archipelago (SPSPA), a remote group of 15 small islets and rocks.<sup>10</sup> A previous study concerning *Salinispora* strains recovered from different sites including sediments from the SPSPA described their interesting and somewhat unique metabolic profiles.<sup>11</sup> As part of our ongoing research trying to find active natural products from marine microorganisms, we have investigated the EtOAc extract of *S. arenicola* (BRA-213). In this study, the isolation of five new aminonaphthoquinones (**1–5**), along with their antibiotic effects is described.

## RESULTS AND DISCUSSION

HPLC analysis of the MeOH/H<sub>2</sub>O (7:3) fraction, obtained from fractionation on a C18 cartridge of the EtOAc extract of *S. arenicola* revealed a series of compounds which exhibited unusual and similar UV-PDA ( $\lambda$  211, 260, 327 and 429 nm) profiles. Selection and purification of these peaks afford the compounds **2–5**, while **1** was isolated by Sephadex LH-

20 chromatography. The structures of **1–5**, designed as salinaphthoquinones A–E (Figure 1), were established based on detailed interpretation of their MS and NMR spectroscopic data, and by single-crystal X-ray diffraction analyses.

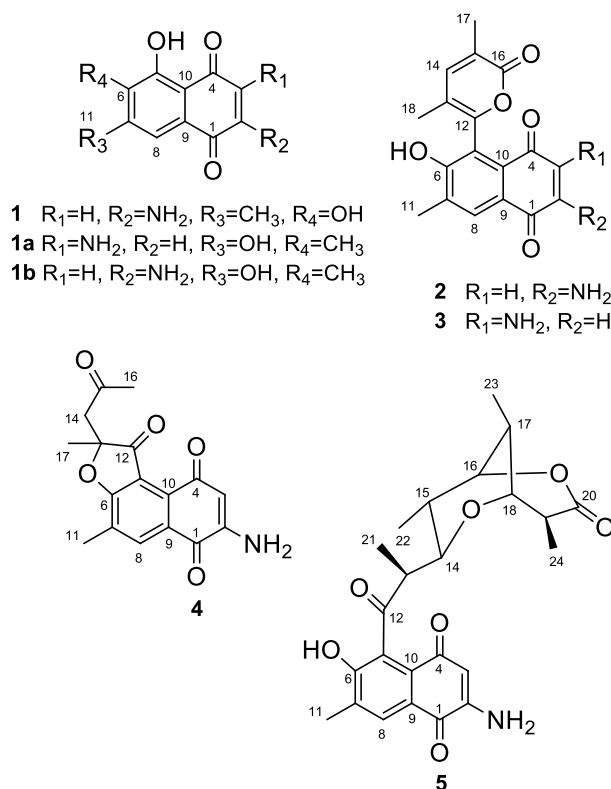


**Figure 1.** Chemical structures of compounds **1–5**.

Salinaphthoquinone A (**1**), an amorphous red powder, had its molecular formula assigned as  $C_{11}H_9NO_4$  based on the  $[M + H]^+$  ion peak at  $m/z$  220.0612 obtained by HRESIMS. Its  $^1H$  NMR spectrum exhibited signals for two hydroxy groups at  $\delta_H$  13.85 (s) and 10.27 (br s), and amino protons at  $\delta_H$  7.87 (br s) and 7.28 (br s). In addition, it displayed three singlets at  $\delta_H$  7.34, 5.67 and 2.18, which in the HSQC spectrum showed correlations with the carbon signals at  $\delta_C$  122.5 (C-8), 100.1 (C-3) and 16.1 (Me-11), respectively. The  $^{13}C$  NMR spectrum showed 11 carbon signals corresponding to one methyl, two  $sp^2$  methines, and eight  $sp^2$  non-hydrogenated carbons according to the DEPT and HSQC spectra. In addition to the chemical shifts above-mentioned, the carbon signals at  $\delta_C$  188.6 (C-4), 179.6 (C-1) and 152.8 (C-2), including the eight degrees of unsaturation required by the molecular formula, were compatible with an amino-1,4-naphthoquinone core. In fact, the above data were similar to those of 2- and 3-amino-5,7-dihydroxy-6-methyl-1,4-naphthoquinones (**1a** and **1b**) previously synthesized by Moody and co-workers.<sup>12</sup> Comparing the  $^1H$  and  $^{13}C$  NMR data of **1** (Table 1), with those of

the above-mentioned compounds led to the suggestion that **1** was indeed a 3-aminonaphthoquinone bearing two hydroxy groups and one methyl group. Interestingly, the chemical shifts values related to the dihydroxylated aromatic ring changed noticeably. For instance, the chemical shifts for the Me-11 in **1a** ( $\delta_C$  8.2) and **1b** ( $\delta_C$  8.7) appear more shielded than for **1** ( $\delta_C$  16.1), whereas the hydroxylated carbons (**1a**:  $\delta_C$  163.9 and 162.2 and **1b**:  $\delta_C$  160.9 and 160.2) were deshielded relative to the same carbons of **1** (152.1 and 148.8). These data supported the evidence that the hydroxy groups were *ortho*-positioned in **1**, while the methyl group was *ortho* just to one hydroxy group. HMBC correlations (Figure 2) of the proton at  $\delta_H$  2.18 (Me-11) with both carbon signals at  $\delta_C$  152.1 (C-6) and 122.5 (C-8) as well as the proton at  $\delta_H$  7.34 (H-8) with the carbons at  $\delta_C$  179.6 (C-1) and 113.5 (C-10) support the structure of **1** as a new 2-aminonaphthoquinone.

Salinaphthoquinone B (**2**), as orange crystals, had its molecular formula  $C_{18}H_{15}NO_5$  deduced from the  $[M + H]^+$  at  $m/z$  326.1029 as observed by HRESIMS. Analyses of the  $^1H$  and  $^{13}C$  NMR data showed a 2-amino-7-methyl-1,4-naphthoquinone moiety similar to **1**, however, bearing a dimethyl  $\alpha,\beta,\gamma,\delta$ -conjugated  $\delta$ -lactone at C-5 (Table 1). A methyl group ( $\delta_H/\delta_C$  2.03/16.1) was positioned at the  $\alpha$ -carbon of the lactone carboxyl by the HMBC correlations of it with the carbon signals at  $\delta_C$  163.6 (C-16), 121.9 (C-15) and 144.1 (C-14). A second methyl ( $\delta_H/\delta_C$  1.60/14.6) was positioned at the  $\gamma$ -carbon as inferred from its correlations with the carbon signals at  $\delta_C$  152.1 (C-12), 111.9 (C-13) and 144.1 (C-14) (Figure 2). The unequivocal structure of **2** was confirmed by a single-crystal X-ray diffraction analysis (Figure 3, Table S1). Based on the aforementioned data the complete structure of **2** was also established as a further new 2-aminonaphthoquinone derivative.

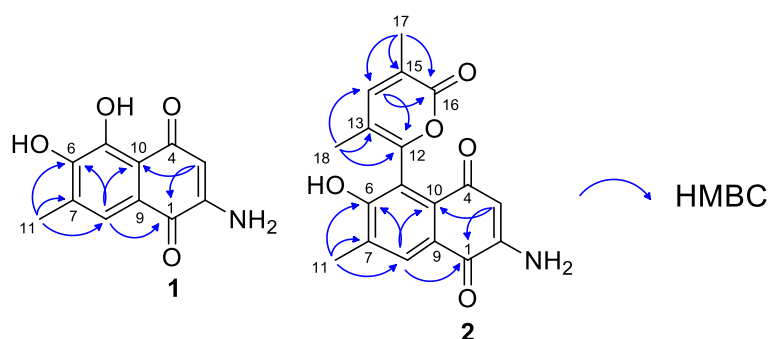


**Figure 2.** Key HMBC correlations of compounds **1** and **2**.

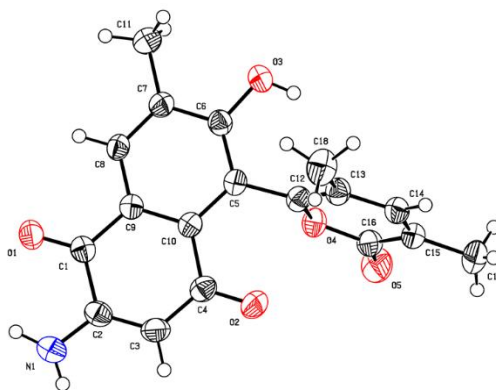


**Figure 3.** Asymmetric unit of the crystalline structure of compound **2**.

Salinaphthoquinone C (**3**), was isolated as an orange amorphous powder. Its molecular formula was also assigned as  $C_{18}H_{15}NO_5$  based on the  $[M + H]^+$  ion peak at  $m/z$  326.1031 in the HRESIMS spectrum. As can be seen from Table 1, its  $^1H$  NMR spectrum was almost identical to that of **2** however the  $^{13}C$  NMR data for the aminonaphthoquinone nucleus were clearly different. Although some chemical shifts were missing, the HMBC spectrum displayed signals for two carbonyls at  $\delta_C$  181.8 and 181.5 ppm. Key HMBC correlations of the benzene proton at  $\delta_H$  7.83 (s, H-8) with the carbons at  $\delta_C$  181.5 (C-1), 157.6 (C-6) and 127.8 (C-10), and the quinoid proton at  $\delta_H$  5.67 (s, H-2) with the carbons at  $\delta_C$  181.8 (C-4) and 125.7 (C-9) were in agreement with the structure of a 1,4-naphthoquinone bearing an amino group at C-3 (Figure 4), different from compounds **1** and **2**. The complete  $^1H$  and  $^{13}C$  NMR chemical shifts of **3** were assigned by a combination of the HSQC and HMBC experiments, and comparison with previously reported data for amino-1,4-naphthoquinones.<sup>12</sup> Thus, the structure of **3** was proposed as the 3-aminonaphthoquinone isomer of **2**.

Salinaphthoquinone D (**4**), was isolated as red crystals. Its molecular formula  $C_{17}H_{15}NO_5$ , which requires 11 degrees of unsaturation, was established by HRESIMS. The  $^1H$  NMR spectrum exhibited signals for an amino-1,4-naphthoquinone nucleus as observed for **1**. In addition, it also displayed a signal for deshielded methylene protons at  $\delta_H$  3.33 (H<sub>2</sub>-14), as well as signals at  $\delta_H$  2.04 (s, H<sub>3</sub>-16) and 1.33 (s, H<sub>3</sub>-17) corresponding to two extra methyl groups. The  $^{13}C$  NMR spectrum showed resonances for 17 carbons which were characterized through DEPT and HSQC spectra, as three methyls, one methylene, two  $sp^2$  methines, and 11  $sp^2$  non-hydrogenated carbons (Table 2). The chemical shifts at  $\delta_C$  204.1 (C-15), 197.6 (C-12), 173.7 (C-6), 87.1 (C-13), 49.9 (C-14), and 29.6 (C-16) were attributed to a C-5/C-6 fused dihydrofuran-3-one moiety bearing a methyl and a 2-oxo-propyl as substituents. The HMBC spectrum revealed that those two substituents were  $\alpha$ -positioned to the carbonyl C-12 due to the

long-range correlations of the methylene protons at  $\delta_{\text{H}}$  3.33 (H<sub>2</sub>-14) with both carbonyl carbons at  $\delta_{\text{C}}$  204.1 (C-15) and 197.6 (C-12) as well as of the methyl protons at  $\delta_{\text{H}}$  1.33 (Me-17) with  $\delta_{\text{C}}$  197.6 (C-12), 87.1 (C-13) and 49.9 (C-14) as depicted in Figure 4. In addition, the structure of **4** was confirmed by X-ray diffraction analysis (Figure 5, Table S1), as another new 2-aminonaphthoquinone. Despite the specific rotation  $[\alpha]_{\text{D}}^{22} + 25.6$  (*c* 0.13, MeOH) observed for compound **4**, by no reasoning, after the crystallization procedure in MeOH to obtain the single-crystal for X-ray diffraction analysis, what took two weeks, after the space group determination a racemic mixture was characterized.

**Table 1.** <sup>1</sup>H (500 MHz) and <sup>13</sup>C (125 MHz) NMR Data Assignments for Compounds 1–3 ( $\delta$  in ppm) in DMSO-*d*<sub>6</sub>.

No.	<b>1</b>		<b>2</b>		<b>3<sup>a</sup></b>	
	$\delta_{\text{C}}$ , type	$\delta_{\text{H}}$	$\delta_{\text{C}}$ , type	$\delta_{\text{H}}$	$\delta_{\text{C}}$ , type	$\delta_{\text{H}}$
1	179.6, C		180.7, C		181.5, C	
2	152.8, C		149.4, C		100.7, CH	5.67 s
3	100.1, CH	5.67 s	102.6, CH	5.60 s	nd	
4	188.6, C		181.7, C		181.8, C	
5	148.8, C		123.1, C		nd	
6	152.1, C		159.5, C		157.6, C	
7	128.1, C		129.4, C		133.1, C	
8	122.5, CH	7.34 s	130.4, CH	7.90 s	129.3, CH	7.83 s
9	120.8, C		117.7, C		125.7, C	
10	113.5, C		131.4, C		127.8, C	
11	16.1, CH <sub>3</sub>	2.18 s	16.6, CH <sub>3</sub>	2.31 s	16.9, CH <sub>3</sub>	2.31 s
12			152.1, C		151.9, C	
13			111.9, C		112.5, C	
14			144.1, CH	7.30 s	144.0, CH	7.35 s
15			121.9, C		122.5, C	
16			163.6, C		163.7, C	
17			16.1, CH <sub>3</sub>	2.03 s	15.9, CH <sub>3</sub>	2.05 s
18			14.6, CH <sub>3</sub>	1.60 s	14.6, CH <sub>3</sub>	1.65 s
NH-2		7.28 br s/ 7.87 br s		7.04 br s		
NH-3						7.00 br s
HO-5		13.85 s				
HO-6		10.27 br s		10.11 br s		

nd: not detected; <sup>a</sup><sup>13</sup>C value was determined by analysis of 2D spectra.

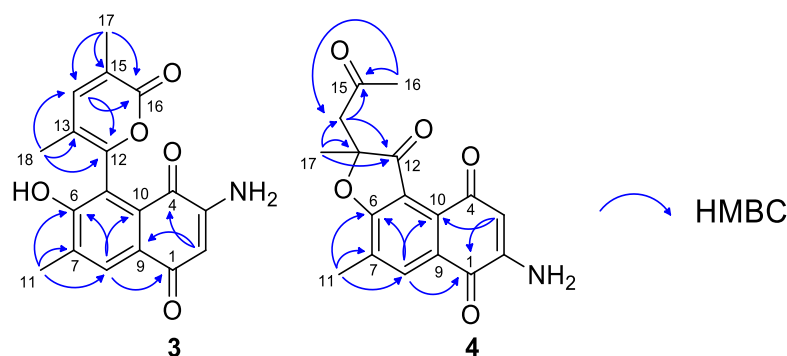


**Figure 4.** Key HMBC correlations of compounds **3** and **4**.

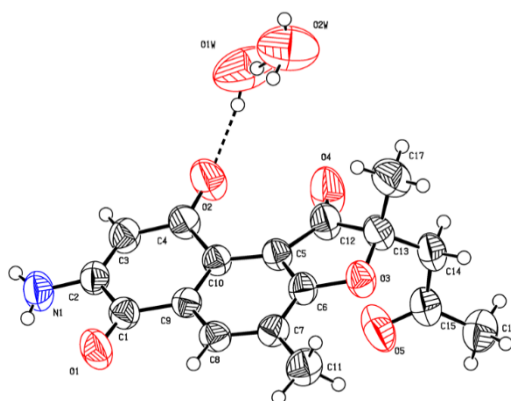


**Figure 5.** Asymmetric unit of the crystalline structure of compound **4**.

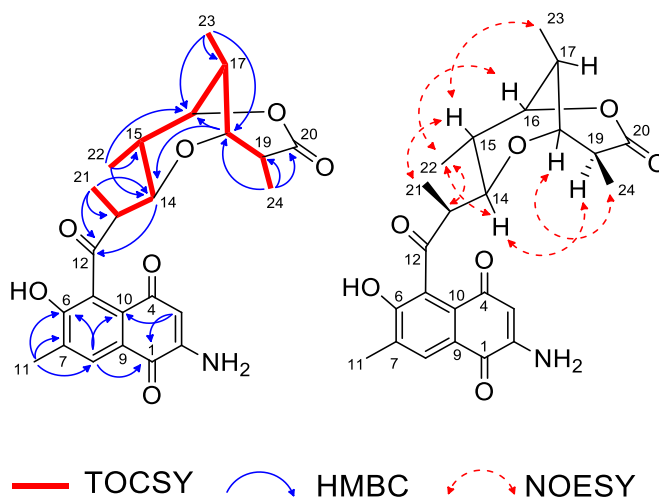
Salinaphthoquinone E (**5**), red crystals, had its molecular formula assigned as  $C_{24}H_{27}NO_7$  by HRESIMS. Comparison of its  $^1H$  and  $^{13}C$  NMR data with those of **2** suggested it as a 2-amino-7-methyl-1,4-naphthoquinone moiety. In addition, signals were observed for seven methine protons, three of them attached to oxygenated carbons at  $\delta_H$  4.28 (br s, H-16), 3.43 (br s, H-18) and 3.36 (m, H-14), and four methyl doublets at  $\delta_H$  1.19 (d,  $J = 7.0$  Hz, H-21), 1.08 (d,  $J = 7.6$  Hz, H-24), 1.05 (d,  $J = 7.3$  Hz, H-23) and 0.63 (d,  $J = 6.6$  Hz, H-22). The TOCSY spectrum clearly showed a sequence of scalar couplings for the spin system Me-21 (C-13) through Me-24(C-19) as depicted in Figure 6. Comparison of the  $^1H$  NMR and MS data of **5** with those reported for a structurally related intermediate of the polyketide rifamycin (SY7), previously isolated from *Amycolatopsis mediterranei* N/813 (rifamycin B producer)<sup>13,14</sup> showed that these compounds are isomers. The  $^{13}C$  NMR spectrum showed 24 carbons, whose hydrogenation pattern was determined through the HSQC spectrum (Table 2). Comparison of the  $^{13}C$  NMR data of these compounds revealed as the main difference the absence of the C-13/C-14 double bond in **5**. Interestingly, the HMBC correlation exhibited by the proton signal at  $\delta_H$  3.43 (br s, H-18) with the lactone carbonyl at  $\delta_C$  172.9 (C-20) and the oxymethine

carbon at  $\delta_C$  70.2 (C-14) indicated cyclization between the oxygen atom at C-18 with C-14, easily justified by the nucleophilic addition of the HO-18 on the  $\beta$ -methine carbon of the  $\alpha,\beta$ -unsaturated carbonyl system of the above SY7 derivative as shown in Scheme 1. The relative configuration of **5** was assigned by single-crystal X-ray diffraction (Figure 7, Table S1) and the NOESY spectrum which displayed correlations for the Me-22 ( $\delta_H$  0.63, d,  $J = 6.6$  Hz) with the  $\alpha$ -positioned protons H-16 ( $\delta_H$  4.28, brs), H-14 ( $\delta_H$  3.36, m), and H-13 ( $\delta_H$  2.89, q,  $J = 7.0$  Hz), as well as between the H-18 ( $\delta_H$  3.43, brs) and Me-24 ( $\delta_H$  1.08, d,  $J = 7.6$  Hz) giving evidences for the  $\beta$ -orientation of the methyls 21, 23 and 24 (Figure 4). Despite the determination of the X-ray data, using a Cu radiation source, the quality of the crystal was not sufficient to determine the absolute configuration. Based on the aforementioned data the structure of **5** was established as a 2-aminonaphthoquinone bearing a cyclic polyketide side chain. Interestingly, a detailed analysis of the NMR spectra of **5** (recorded in DMSO at 25 °C) shows double resonances (ratio of 2:1) for the cyclic polyketide chain indicating the occurrence of atropisomers due to the hindered rotation around C-5/C-12 bond.<sup>13</sup>

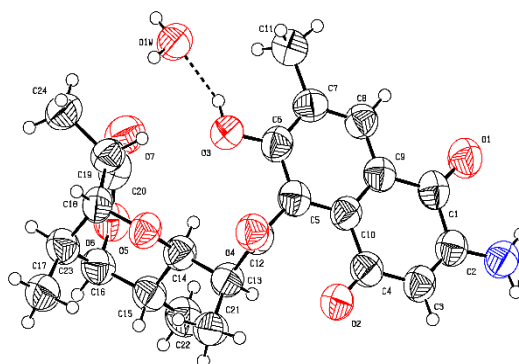
Naphthoquinones represent a large class of natural compounds produced by various plants, bacteria and fungi.<sup>15,16</sup> Comparatively, just a few examples of  $\alpha$ -aminonaphthoquinones are described.<sup>17</sup> The aminonaphthoquinone moiety constitutes an essential framework of several natural macrolides like the rifamycins.<sup>18</sup> Despite the large number of rifamycins reported, either natural or synthetic, the amino group is mostly found at the C-2 position of the naphthoquinone nucleus. Naturally occurring 3-aminonaphthoquinones, although rare, have been reported previously.<sup>19,20</sup> This can explain the presence, in this case, of compound **3** (3-amino) among compounds **1**, **2**, **4** and **5**.

In accordance with previously published works,<sup>14,21-26</sup> a reasonable biosynthetic pathway for compounds **1** through **5**, all possessing a 2- or 3-aminonaphthoquinone backbone, was suggested based on already well-established biosyntheses of similar compounds like the rifamycins,<sup>27</sup> naphthomycins,<sup>28</sup> and hygrocins<sup>29</sup>. Thus, the aminonaphthoquinone nucleus is biogenetically derived from 3-amino-5-hydroxybenzoic acid (AHBA) as the starter unit coupled with methyl malonyl-CoA and malonyl-CoA-derived moieties.<sup>14,21</sup> Compound **1** could be easily obtained after decarboxylation and dehydration followed by oxidation. To build **2-4** two additional methyl malonyl-CoA extenders are necessary, while for compound **5** four units of methyl malonyl-CoA are needed. After this, a sequence of typical reactions such as dehydration, reduction, oxidation, decarboxylation, cyclization, and isomerization could afford compounds **2-5**. Indeed, SY5 and SY7, isolated by Floss et al., were incorporated to Scheme

1, in order to explain the biogenetic formation of compounds **2–4** from the former, and compound **5** from the latter.<sup>14</sup>



**Figure 6.** Key TOCSY, HMBC and NOESY correlations of compound **5**.

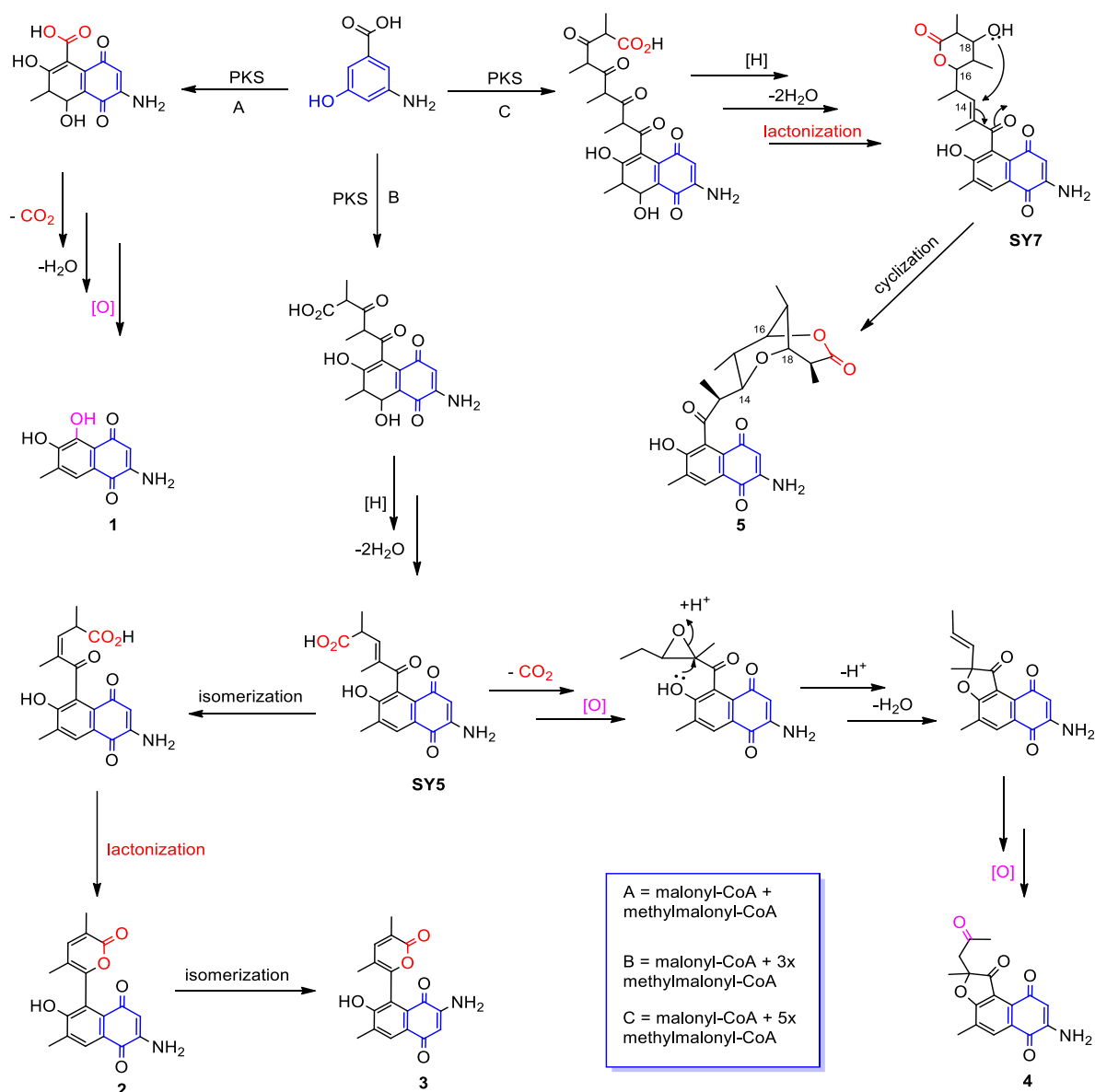


**Figure 7.** Asymmetric unit of the crystalline structure of compound **5**.

The antibacterial activities of compounds **1** to **5** were evaluated against *Enterococcus faecalis* and *Escherichia coli* (Table 3) bacterial strains. Compounds **2** and **4** were found to inhibit *S. aureus* and *E. faecalis* with MICs values of 125 to 31, and 125 to 16  $\mu\text{g/mL}$ , respectively. Compounds **1** and **3** were susceptible only against *E. faecalis*, whereas **5** was inactive.

In conclusion, compounds **1–5** are 2- or 3-amino-1,4-naphthoquinones, however, they have the important core present in several biologically important natural products such as rifamycins,<sup>30</sup> salinisporamycin,<sup>31</sup> and a Cdc25A inhibitor.<sup>19</sup>



**Scheme 1.** Plausible Biogenetic Pathways for Salinaphthoquinones A–E (1–5).

## EXPERIMENTAL SECTION

### General Experimental Procedures.

Melting points were recorded on a digital Microquimica MQAPF-302 apparatus and were uncorrected. Optical rotations were measured using a JASCO P-2000 digital polarimeter. Ultraviolet–visible (UV–vis) were acquired on a SHIMADZU 2600 UV-vis spectrophotometer. IR spectra were recorded using a Perkin-Elmer Spectrum 100 FTIR spectrometer equipped with universal attenuated total reflectance accessory (UATR) in the range from 4000 to 600 cm<sup>-1</sup>. NMR spectra were obtained either on a Bruker Avance DRX-500 or Avance DPX-300 spectrometers. High resolution electrospray ionization mass spectra

(HRESIMS) were acquired using on an Acquity Xevo UPLC-QTOF-MS system from Waters. Sephadex LH-20 (Pharmacia) and SPE cartridges C18 (20g/60 mL; Strata, Phenomenex) were used for the chromatographic fractionations. HPLC analyses were carried out using a UFLC (SHIMADZU) system equipped with an SPD-M20A diode array UV-Vis detector, a Phenomenex Silica column, 5  $\mu\text{m}$  (10.0 x 250 mm).

**Table 2.**  $^1\text{H}$  and  $^{13}\text{C}$  NMR Data Assignments for Compounds **4** and **5** ( $\delta$  in ppm) in  $\text{DMSO-}d_6$ .

No.	<b>4<sup>a</sup></b>		<b>5<sup>b</sup></b>	
	$\delta_{\text{C}}$ , type	$\delta_{\text{H}}$	$\delta_{\text{C}}$ , type	$\delta_{\text{H}}$ ( <i>J</i> in Hz)
1	180.5, C		180.2, C	
2	148.6, C		150.5, C	
3	103.0, CH	5.73 s	101.2, CH	5.62 s
4	180.8, C		182.2, C	
5	125.5, C		122.1, C	
6	173.7, C		158.7, C <sup>c</sup>	
7	126.7, C		129.1, C	
8	134.2, CH	8.11 s	129.3, CH	7.77 s
9	117.2, C		116.4, C	
10	132.3, C		131.0, C	
11	14.2, CH <sub>3</sub>	2.29 s	16.4, CH <sub>3</sub>	2.26 s
12	197.6, C		205.1, C	
13	87.1, C		46.4, CH	2.89 q (7.0)
14	49.9, CH <sub>2</sub>	3.33 ovl	70.2, CH	3.36 m ovl
15	204.1, C		29.5, CH	2.12 m
16	29.6, CH <sub>3</sub>	2.04 s	81.3, CH	4.28 br s
17	22.4, CH <sub>3</sub>	1.33 s	29.0, CH	1.95 m
18			74.4, CH	3.43 br s ovl
19			39.0, CH	2.20 d (7.6)
20			172.9, C	
21			8.5, CH <sub>3</sub>	1.19 d (7.0)
22			13.7, CH <sub>3</sub>	0.63 d (6.6)
23			13.2, CH <sub>3</sub>	1.05 d (7.3)
24			17.4, CH <sub>3</sub>	1.08 d (7.6)
NH-2		7.01 br s		7.24 br s

ovl: overlap with H<sub>2</sub>O; <sup>a</sup> 500 MHz ( $^1\text{H}$ ) and 125 MHz ( $^{13}\text{C}$ ); <sup>b</sup> 300 MHz ( $^1\text{H}$ ) and 75 MHz ( $^{13}\text{C}$ ); <sup>c</sup>  $^{13}\text{C}$  value was determined by analysis of 2D spectra.

**Table 3. Minimum Inhibitory Concentrations (MICs,  $\mu\text{g/mL}$ ) of Compounds 1–5.**

Compound	<i>S. aureus</i> (ATCC 29213)	<i>S. aureus</i> (ATCC 43300, MRSA)	<i>E. faecalis</i> (ATCC 29219)	<i>E. faecalis</i> (ATCC 51212, VRE)	<i>E. coli</i> (ATCC 25922)
<b>1</b>	<i>a</i>	<i>a</i>	16	<i>a</i>	<i>a</i>
<b>2</b>	31	62	16	125	<i>a</i>
<b>3</b>	<i>a</i>	<i>a</i>	125	<i>a</i>	<i>b</i>
<b>4</b>	125	125	125	125	<i>b</i>
<b>5</b>	<i>a</i>	<i>a</i>	<i>a</i>	<i>a</i>	<i>b</i>

<sup>a</sup> No activity in the tested concentrations. Rifampicin showed MIC  $\leq 0.03 \mu\text{g/mL}$  for Gram-positive strains.

<sup>b</sup> Not evaluated

### Bacterial Material.

The bacterial strain BRA-213 was identified as *Salinispora arenicola* by Bauermeister et al.,<sup>11</sup> (deposited in GenBank with an accession number MH910695). A voucher strain is preserved at the Laboratory of Marine Bioprospection and Biotechnology, Universidade Federal do Ceará, Brazil. The bacteria strain was isolated on solid A1 media [18 g agar, 10 g starch, 4 g yeast extract, and 2 g peptone dissolved in 1 L of artificial seawater Red Sea Fish Pharm Ltd (40.0 g/L)] from a marine sediment collected around SPSPA, Pernambuco, Brazil at a depth of 16 m (N 0°55', W 29°38') in November 2011.

### Fermentation.

Colonies of the strain BRA-213 were inoculated into Erlenmeyer flasks (2 L) containing 500 mL of A1 media (10 g soluble starch, 4 g yeast extract and 2 g peptone in 1 L of artificial seawater, supplemented with calcium carbonate (0.5 g/L  $\text{CaCO}_3$ ), 5 mL of solutions of iron (III) sulfate (8 g/L  $\text{Fe}_2(\text{SO}_4)_3$ ) and potassium bromide (20 g/L KBr). Sterile Amberlite XAD-16 resin (10 g) was added to each flask on day 2. The culture flasks were shaken at 200 rpm at 28 °C for 14 days.

### Extraction and Isolation.

The whole fermentation broth (20 L) was filtered through cloth to separate the resin from the supernatant. The resin was then extracted with acetone (2 L), which was posteriorly removed under vacuum, while the residual aqueous phase was extracted with ethyl acetate (3 x 500 mL). The resulting EtOAc fraction was vacuum dried and yielding an organic extract (9.0 g), which was fractionated on a C18 cartridge by elution with MeOH/H<sub>2</sub>O (7:3; 4:1 and 1:0) to give three fractions (A-C). Fraction A (5.0 g) was chromatographed using a C18 cartridge and

elution with MeOH/H<sub>2</sub>O (3:7; 2:3; 1:1; 3:2; 7:3; 4:1 and 1:0) to give seven fractions (AA-AG). The fraction AC (610 mg) was chromatographed over a Sephadex LH-20 column, using also MeOH as eluent, to give four subfractions (AC1-AC4) and to afford the pure compound **1** (12.5 mg). Subfraction AC4 (90.0 mg) was directly purified by semipreparative HPLC (hexane/acetone, 10-100 %, 20 min, flow rate of 3.0 mL/min) to give compounds **2** (8.0 mg,  $t_R$  = 14.9 min), **3** (1.0 mg,  $t_R$  = 15.3 min) and **4** (5.0 mg,  $t_R$  = 16.6 min). The fraction AD (910 mg) was chromatographed over a Sephadex LH-20 column, using MeOH as eluent, to give five subfractions (AD1-AD5). Subfraction AD5 (20.0 mg) was directly purified by semipreparative HPLC (hexane/acetone, 30-100 %, 20 min, flow rate of 3.0 mL/min) to give compound **5** (2.0 mg,  $t_R$  = 12.5 min).

### Physical and spectroscopic data of 1–5.

*Salinaphthoquinone A (1)*: amorphous red powder; UV (MeOH)  $\lambda_{\max}$  (log  $\epsilon$ ) 210 (3.54), 261 (3.44), 329 (3.26), 433 (3.04) nm; IR ( $\nu_{\max}$ ) 3452, 3403, 3191, 2922, 2853, 1619, 1597, 1474, 1429, 1323, 1260, 1052, 843, 729 cm<sup>-1</sup>; <sup>1</sup>H and <sup>13</sup>C NMR data, Table 1; HRESIMS  $m/z$  220.0612 [M + H]<sup>+</sup> (calcd for C<sub>11</sub>H<sub>10</sub>NO<sub>4</sub>, 220.0604).

*Salinaphthoquinone B (2)*: orange crystals; mp 235–236 °C; UV (MeOH)  $\lambda_{\max}$  (log  $\epsilon$ ) 217 (4.04), 280 (3.99), 321 (3.98), 459 (2.83) nm; IR ( $\nu_{\max}$ ) 3436, 3323, 2924, 2857, 1680, 1620, 1567, 1335, 1289, 1184, 964, 843, 760 cm<sup>-1</sup>; <sup>1</sup>H and <sup>13</sup>C NMR data, Table 1; HRESIMS  $m/z$  326.1029 [M + H]<sup>+</sup> (calcd for C<sub>18</sub>H<sub>16</sub>NO<sub>5</sub>, 326.1023).

*Salinaphthoquinone C (3)*: amorphous orange powder; UV (MeOH)  $\lambda_{\max}$  (log  $\epsilon$ ) 216 (4.20), 280 (4.16), 321 (4.11), 460 (3.00) nm; IR ( $\nu_{\max}$ ) 3432, 3324, 2925, 2849, 1694, 1624, 1567, 1366, 1250, 1096, 961, 843, 760 cm<sup>-1</sup>; <sup>1</sup>H and <sup>13</sup>C NMR data, Table 1; HRESIMS  $m/z$  326.1031 [M + H]<sup>+</sup> (calcd for C<sub>18</sub>H<sub>16</sub>NO<sub>5</sub>, 326.1023).

*Salinaphthoquinone D (4)*: red crystals; mp 134–135 °C;  $[\alpha]_D^{22} + 25.6$  (c 0.13, MeOH); UV (MeOH)  $\lambda_{\max}$  (log  $\epsilon$ ) 225 (4.40), 286 (4.17), 322 (4.18), 469 (3.14) nm; IR ( $\nu_{\max}$ ) 3444, 3222, 2926, 2849, 1715, 1618, 1574, 1322, 1182, 1090, 962, 815, 744 cm<sup>-1</sup>; <sup>1</sup>H and <sup>13</sup>C NMR data, Table 2; HRESIMS  $m/z$  314.1029 [M + H]<sup>+</sup> (calcd for C<sub>17</sub>H<sub>16</sub>NO<sub>5</sub>, 314.1023).

*Salinaphthoquinone E (5)*: orange crystals; mp 140–141 °C  $[\alpha]_D^{22} - 26.1$  (c 0.10, MeOH); UV (MeOH)  $\lambda_{\max}$  (log  $\epsilon$ ) 210 (4.32), 279 (4.16), 319 (4.01), 458 (3.05) nm; IR ( $\nu_{\max}$ ) 3436, 3325, 2935, 2881, 1712, 1618, 1570, 1330, 1273, 1188, 999, 854, 731 cm<sup>-1</sup>; <sup>1</sup>H and <sup>13</sup>C NMR data, Table 2; HRESIMS  $m/z$  442.1866 [M + H]<sup>+</sup> (calcd for C<sub>24</sub>H<sub>28</sub>NO<sub>7</sub>, 442.1860).

### X-ray Crystallographic Analyses of Compounds 2, 4 and 5.

The single-crystal X-ray intensity data of compounds **2**, **4** and **5** were measured on a Bruker D8 Venture equipped with a microfocus Mo generator ( $\lambda K\alpha = 0.71073 \text{ \AA}$ ) or a microfocus Cu generator ( $\lambda K\alpha = 1.54178 \text{ \AA}$ ) and a Photon II CMOS detector. Data collection on compounds **2** and **4** were performed with Mo radiation, whereas data collection on compound **5** was performed with Cu radiation. The frames were integrated with the Bruker SAINT software package (v8.34A)<sup>32</sup> using a narrow-frame algorithm. The final cell parameters for each crystal were based upon the refinement of the XYZ-centroids of some reflections. Data were corrected for absorption effects using the Multi-Scan method. The structure was solved using Olex2,<sup>33</sup> with the ShelXT<sup>34</sup> structure solution program using Charge Flipping or Direct Methods and refined with the ShelXL<sup>35</sup> refinement package using Least Squares minimization. Olex2 was also used to prepare the crystallographic information file (CIF). The program ORTEP-III (version 1.0.3)<sup>36</sup> was used to prepare the artwork representations for publication.

*X-ray Crystallography Analysis of Salinaphthoquinone B (2):* Orange prism crystals of compound **2** were obtained from a MeOH solution after slow evaporation in a refrigerator for 2 weeks.  $C_{18}H_{15}NO_5$ ,  $M_r = 325.31 \text{ g mol}^{-1}$ ; size  $0.836 \times 0.276 \times 0.084 \text{ mm}$ ; monoclinic, space group  $P2_1/c$ ,  $a = 13.8289(6) \text{ \AA}$ ,  $b = 6.8772(3) \text{ \AA}$ ,  $c = 16.9481(7) \text{ \AA}$ ,  $\alpha = 90^\circ$ ,  $\beta = 108.007(2)^\circ$ ,  $\gamma = 90^\circ$ ;  $V = 1532.88(11) \text{ \AA}^3$ ,  $Z = 4$ ,  $\rho_{\text{calc}} = 1.410 \text{ g cm}^{-3}$ ,  $\mu (\text{Mo } K\alpha) = 0.71073 \text{ cm}^{-1}$ , multi-scan,  $trans_{\text{min}} = 0.5176$ ,  $trans_{\text{max}} = 0.7461$ ,  $F(000) = 680.0$ . The total number of reflections was 23 319 ( $-18 \leq h \leq 18$ ,  $-9 \leq k \leq 9$ ,  $-22 \leq l \leq 22$ ) measured in the range  $5.054^\circ \leq \Theta \leq 56.56^\circ$ , completeness  $\Theta_{\text{max}} = 100.0\%$ , 3 792 unique ( $R_{\text{int}} = 0.0380$ ,  $R_{\text{sigma}} = 0.0242$ ) which were used in all calculations; Final indices:  $R_{\text{obs}} = 0.0444$ ,  $wR_{2\text{obs}} = 0.1285$  [ $I \geq 2\sigma(I)$ ];  $R_{\text{all}} = 0.0624$ ,  $wR_{2\text{all}} = 0.1285$  [all data], GOOF = 1.072, largest difference peak and hole  $0.21/-0.25 \text{ e \AA}^{-3}$ .

*X-ray Crystallography Analysis of Salinaphthoquinone D (4):* Red irregular crystals of compound **4** were obtained from a MeOH solution after slow evaporation in a refrigerator for 2 weeks. It was found that compound **4** crystallizes with two molecules of  $H_2O$ , as a hydrate. Refinement also showed that compound **4** crystallizes as a racemic mixture.  $C_{17}H_{19}NO_7$ ,  $M_r = 349.33 \text{ g mol}^{-1}$ ; size  $0.249 \times 0.218 \times 0.160 \text{ mm}$ ; triclinic, space group  $P\bar{1}$ ,  $a = 7.5548(16) \text{ \AA}$ ,  $b = 9.708(2) \text{ \AA}$ ,  $c = 13.168(2) \text{ \AA}$ ,  $\alpha = 104.560(6)^\circ$ ,  $\beta = 100.175(7)^\circ$ ,  $\gamma = 107.218(7)^\circ$ ;  $V = 859.3(3) \text{ \AA}^3$ ,  $Z = 2$ ,  $\rho_{\text{calc}} = 1.350 \text{ g cm}^{-3}$ ,  $\mu (\text{Mo } K\alpha) = 0.106 \text{ mm}^{-1}$ , multi-scan,  $trans_{\text{min}} = 0.491$ ,  $trans_{\text{max}} = 0.746$ ,  $F(000) = 368.0$ . The total number of reflections was 36 379 ( $-9 \leq h \leq 9$ ,  $-12 \leq k \leq 12$ ,  $-17 \leq l \leq 17$ ) measured in the range  $5.866^\circ \leq \Theta \leq 54.966^\circ$ , completeness  $\Theta_{\text{max}} = 100.0\%$ , 3 947 unique ( $R_{\text{int}} = 0.0984$ ,  $R_{\text{sigma}} = 0.0514$ ) which were used in all calculations; Final indices:

$R_{1\text{obs}} = 0.0612$ ,  $wR_{2\text{obs}} = 0.1605$  [ $I \geq 2\sigma(I)$ ];  $R_{1\text{all}} = 0.1296$ ,  $wR_{2\text{all}} = 0.2015$  [all data], GOOF = 1.032, largest difference peak and hole 0.28/-0.32 e  $\text{\AA}^{-3}$ .

*X-ray Crystallography Analysis of Salinaphthoquinone E (5)*: Orange prism crystals of compound **5** were obtained from a MeOH solution after slow evaporation in a refrigerator for 2 weeks. Compound **5** crystallizes with one molecules of H<sub>2</sub>O, as a hydrate. C<sub>24</sub>H<sub>29</sub>NO<sub>8</sub>,  $M_r = 459.48$  g mol<sup>-1</sup>; size 0.148 × 0.111 × 0.058 mm; orthorhombic, space group  $P2_12_12_1$ ,  $a = 8.6893(3)$   $\text{\AA}$ ,  $b = 15.2942(6)$   $\text{\AA}$ ,  $c = 16.9431(6)$   $\text{\AA}$ ,  $\alpha = 90^\circ$ ,  $\beta = 90^\circ$ ,  $\gamma = 90^\circ$ ;  $V = 2251.67(14)$   $\text{\AA}^3$ ,  $Z = 4$ ,  $\rho_{\text{calc}} = 1.355$  g cm<sup>-3</sup>,  $\mu$  (Cu K $\alpha$ ) = 0.849 mm<sup>-1</sup>, multi-scan,  $\text{trans}_{\text{min}} = 0.464$ ,  $\text{trans}_{\text{max}} = 0.753$ ,  $F(000) = 976.0$ . The total number of reflections was 43 312 ( $-10 \leq h \leq 10$ ,  $-18 \leq k \leq 16$ ,  $-20 \leq l \leq 20$ ) measured in the range  $7.788^\circ \leq 2\theta \leq 136.452^\circ$ , completeness  $\Theta_{\text{max}} = 99\%$ , 4073 unique ( $R_{\text{int}} = 0.1241$ ,  $R_{\text{sigma}} = 0.0679$ ) which were used in all calculations; Final indices:  $R_{1\text{obs}} = 0.0715$ ,  $wR_{2\text{obs}} = 0.1876$  [ $I \geq 2\sigma(I)$ ];  $R_{1\text{all}} = 0.1298$ ,  $wR_{2\text{all}} = 0.2318$  [all data], GOOF = 1.045, Flack parameter = 0.3(4), largest difference peak and hole 0.19/-0.23 e  $\text{\AA}^{-3}$ .

The Crystallographic data for compounds **2**, **4** and **5** have been submitted to the Cambridge Crystallographic Data Center as supplementary publication no. CCDC 1847810, 1872395 and 1885988, respectively. Copies of the data are available online free of charge at <http://www.ccdc.cam.ac.uk> (or from CCDC, 12 Union Road, Cambridge CB2 1EZ, e-mail: [deposit@ccdc.cam.ac.uk](mailto:deposit@ccdc.cam.ac.uk), fax: +44-1223-336033).

### Antimicrobial Assay.

To evaluate the antibacterial activities of the isolated substances, four strains of Gram-positive bacteria were used: *Staphylococcus aureus* (ATCC 29213), Methicillin-Resistant *Staphylococcus aureus* (ATCC 43300, MRSA), *Enterococcus faecalis* (ATCC 29212) and Vancomycin-Resistant *Enterococcus faecalis* (ATCC 51212, VRE), and one Gram-negative strain: *Escherichia coli* (ATCC 25922), from the culture collection stored in the microbiology laboratory of the Universidade Federal do Piauí, Brazil. For the experiments, the strains were previously seeded in Petri dishes containing Mueller Hinton agar (Difco), which were incubated for 24 h at temperature of  $35 \pm 2^\circ\text{C}$ , under aerobic conditions. After this time, isolated colonies were collected and suspended in sterile saline solution (NaCl 0.85% (w/v)). This suspension was then used to obtain the bacterial inoculum in Mueller Hinton Broth -MHB (Difco) with final bacterial concentration of  $5 \times 10^5$  CFU/mL. The method used was broth microdilution in a 96-well plate, in which the minimum inhibitory concentrations (MICs) of the substances was determined according to CLSI (2015).<sup>37</sup> Therefore, bacteria were exposed to a

two-fold serial dilution of the compounds **1–5**. Rifampicin was used as positive control. The microplates were incubated under the same conditions cited above and the MIC was determined after observation of the absence of bacterial growth in the culture medium.

## ASSOCIATED CONTENT

### Supporting Information

The Supporting Information is available free of charge on the ACS publications website at DOI: 10.1021/acs.jnatprod.9b00062.

HRESIMS, UV and NMR data of compounds **1–5** (PDF)

X-ray crystallographic files of compounds **2** (CIF), **4** (CIF) and **5** (CIF)

## AUTHOR INFORMATION

### Corresponding Author

\*Phone: +55-85-33669441. E-mail: [otilialoiola@gmail.com](mailto:otilialoiola@gmail.com)

### Notes

The authors declare no competing financial interest.

## ACKNOWLEDGMENTS

The authors are grateful to Secretaria da Comissão Interministerial dos Recursos do Mar (SECIRM) for providing all the logistic support disposed to the scientific expedition, as part of the Program PROARQUIPELAGO. This work was financially supported by CNPq (No. 420454/2016-0 and 309060/2016-8), CAPES/FUNCAP (No. 88887.113263/2015-01), INCT BioNat (No. 465637/2014-0) and FAPESP (2015/17177-6 and 2014/50926-0).

## REFERENCES

- (1) Zotchev, S. B. *J. Biotechnol.* **2012**, *158*, 168–175.
- (2) Maldonado, L. A.; Fenical, W.; Jensen, P. R.; Kauffman, C. A.; Mincer, T. J.; Ward, A. C.; Bull, A. T.; Goodfellow, M. *Int. J. Syst. Evol. Microbiol.* **2005**, *55*, 1759–1766.
- (3) Jensen, P. R.; Williams, P. G.; Oh, D. C.; Zeigler, L.; Fenical, W. *Appl. Environ. Microbiol.* **2007**, *73*, 1146–1152.
- (4) He, H.; Ding, W. D.; Bernan, V. S.; Richardson, A. D.; Ireland, C. M.; Greenstein, M.; Ellestad, G. A.; Carter, G. T. *J. Am. Chem. Soc.* **2001**, *123*, 5362–5363.
- (5) Jensen, P. R.; Gontang, E.; Mafnas, C.; Mincer, T. J.; Fenical, W. *Environ. Microbiol.* **2005**,

7, 1039–1048.

(6) Kim, T. K.; Hewavitharana, A. K.; Nicholas, P.; Fuerst, J. a; Shaw, P. N. *Appl. Environ. Microbiol.* **2006**, *72*, 2118–2125.

(7) Izumi, H.; Gauthier, M. E. A.; Degnan, B. M.; Ng, Y. K.; Hewavitharana, A. K.; Shaw, P. N.; Fuerst, J. A. *FEMS Microbiol. Lett.* **2010**, *313*, 33–40.

(8) Singh, S.; Prasad, P.; Subramani, R.; Aalbersberg, W. *Asian Pac. J. Trop. Biomed.* **2014**, *4*, 825–831.

(9) Feling, R. H.; Buchanan, G. O.; Mincer, T. J.; Kauffman, C. A.; Jensen, P. R.; Fenical, W. *Angew. Chemie - Int. Ed.* **2003**, *42*, 355–357.

(10) Vieira, L.; Farrapeira, C.; Amaral, F.; Lira, S. *Cah. Biol. Mar.* **2012**, *53*, 159–167.

(11) Bauermeister, A.; Velasco-Alzate, K.; Dias, T.; Macedo, H.; Ferreira, E. G.; Jimenez, P. C.; Lotufo, T. M. C.; Lopes, N. P.; Gaudêncio, S. P.; Costa-Lotufo, L. V. *Front Microbiol.* **2018**, *9*, 3021.

(12) Nawrat, C. C.; Lewis, W.; Moody, C. J. *J. Org. Chem.* **2011**, *76*, 7872–7881.

(13) Stratmann. A.; Toupet. C.; Schilling. W.; Traber. R.; Oberer. L.; Schupp. T. *Microbiology* **1999**, *145*, 3365–3375.

(14) Yu, T-W.; Shen, Y.; Doi-Katayama, Y.; Tang, L.; Park, C.; Moore, B. S.; Hutchinson, C. R.; Floss, H. G. *Proc. Natl. Acad. Sci.* **1999**, *96*, 9051–9056.

(15) Babula, P.; Adam, V.; Havel, L.; Kizek, R. *Curr. Pharm. Anal.* **2009**, *5*, 47–68.

(16) Qiu, H. Y.; Wang, P. F.; Lin, H. Y.; Tang, C. Y.; Zhu, H. L.; Yang, Y. H. *Chem. Biol. Drug Des.* **2018**, *91*, 681–690.

(17) Polonik, N. S.; Polonik, S. G.; Denisenko, V. A.; Moiseenko, O. P. *Synthesis* **2011**, *20*, 3350–3358.

(18) Zhang, J.; Li, S.; Wu, X.; Guo, Z.; Lu, C.; Shen, Y. *Org. Lett.* **2017**, *19*, 2442–2445.

(19) Kulanthaivel, P.; Perun, T. J.; Belvo, M. D.; Strobel, R. J.; Paul, D. C.; Williams, D. C. *J. Antibiot.* **1999**, *52*, 256–262.

(20) Williams, D. E.; Dalisay, D. S.; Chen, J.; Polishchuck, E. A.; Patrick, B. O.; Narula, G.; Ko, M.; Av-Gay, Y.; Li, H.; Magarvey, N.; Andersen, R. J. *Org. Lett.* **2017**, *19*, 766–769.

(21) Dewick, P.M. *Medicinal Natural Products: a biosynthetic approach*. 2th ed. UK, 2002.

(22) Floss. H.G. *J. Nat. Prod.* **2006**, *69*, 158–169.

(23) Wilson. M.C.; Gulder, T.A.M.; Mahmud, T.; Moore, B. S. *J. Am. Chem. Soc.* **2010**, *132*, 12757–12765.

(24) Bułyszko, I.; Dräger, G.; Klenge, A.; Kirschning, A. *Chem. Eur. J.* **2015**, *21*, 19231–19242.



- (25) Kang, Q.; Shen, Y.; Bai, L. *Nat. Prod. Rep.* **2012**, *29*, 243-263.
- (26) Feng, Y.; Liu, J.; Carrasco, Y. P.; McMillan, J. B.; Brabander, J. K. *J. Am. Chem. Soc.* **2016**, *138*, 7130-7142.
- (27) August, P. R.; Tang, L.; Yoon, Y. J.; Ning, S.; Muller, R.; Yu, T. W.; Taylor, M.; Hoffmann, D.; Kim, C. G.; Zhang, X. H.; Hutchinson, C. R.; Floss, H. G. *Chem. Biol.* **1998**, *5*, 69-79.
- (28) Wu, Y.; Kang, Q.; Shen, Y.; Su, W.; Bai, L. *Mol. Biosyst.* **2011**, *7*, 2459-2469.
- (29) Li, S.; Wang, H.; Li, Y.; Deng, J.; Lu, C.; Shen, Y.; Shen, Y. *ChemBioChem* **2014**, *15*, 94-102.
- (30) Kigonde, E. M.; Wasuna, A.; Warner, D. F.; Chibale, K. *Bioorganic Med. Chem.* **2014**, *22*, 4453-4461.
- (31) Matsuda, S.; Adachi, K.; Matsuo, Y.; Nukina, M.; Shizuri, Y. *J. Antibiot.* **2009**, *62*, 519-526.
- (32) Bruker, SAINT, version 8.34A. *Bruker AXS Inc.* **2012**, Madison, Wisconsin, USA.
- (33) Dolomanov, O.V.; Bourhis, L. J.; Gildea, R. J.; Howard, J. A. K.; Puschmann, H. *J Appl Crystallogr.* **2009**, *42*, 339-341.
- (34) Sheldrick, G.M. *Acta Crystallogr. C Struct Chem*, **2015**, *71*, 6-8.
- (35) Sheldrick, G.M. *Acta Crystallogr. A*, **2008**, *64*, 112-122.
- (36) Burnett, M.N., Johnson, C.K., ORTEP-III: Oak Ridge Thermal Ellipsoid Plot Program for crystal structure illustrations. United States: N. p., **1996**.
- (37) CLSI - Clinical Laboratory Standards Institute (2015) Approved standard M07-A10. Wayne, Pa.

## SUPPORTING INFORMATION

### Table of Contents

- Table S1.** Hydrogen bonds for compounds **2**, **4** and **5**
- Figure S1.**  $^1\text{H}$  NMR (500 MHz) spectrum of **1** in  $\text{DMSO-}d_6$
- Figure S2.**  $^{13}\text{C}$  NMR (125 MHz) spectrum of **1** in  $\text{DMSO-}d_6$
- Figure S3.** DEPT  $135^\circ$  NMR (125 MHz) spectrum of **1** in  $\text{DMSO-}d_6$
- Figure S4.** HSQC NMR spectrum of **1** in  $\text{DMSO-}d_6$
- Figure S5.** HMBC NMR spectrum of **1** in  $\text{DMSO-}d_6$
- Figure S6.** HRESIMS spectrum of **1**
- Figure S7.** UV spectrum of **1**
- Figure S8.**  $^1\text{H}$  NMR (500 MHz) spectrum of **2** in  $\text{DMSO-}d_6$
- Figure S9.**  $^{13}\text{C}$  NMR (125 MHz) spectrum of **2** in  $\text{DMSO-}d_6$
- Figure S10.** DEPT  $135^\circ$  NMR (125 MHz) spectrum of **2** in  $\text{DMSO-}d_6$
- Figure S11.** HSQC NMR spectrum of **2** in  $\text{DMSO-}d_6$
- Figure S12.** HMBC NMR spectrum of **2** in  $\text{DMSO-}d_6$
- Figure S13.** HRESIMS spectrum of **2**
- Figure S14.** UV spectrum of **2**
- Figure S15.**  $^1\text{H}$  NMR (500 MHz) spectrum of **3** in  $\text{DMSO-}d_6$
- Figure S16.** HSQC NMR spectrum of **3** in  $\text{DMSO-}d_6$
- Figure S17.** HMBC NMR spectrum of **3** in  $\text{DMSO-}d_6$
- Figure S18.** HRESIMS spectrum of **3**
- Figure S19.** UV spectrum of **3**
- Figure S20.**  $^1\text{H}$  NMR (500 MHz) spectrum of **4** in  $\text{DMSO-}d_6$
- Figure S21.**  $^{13}\text{C}$  NMR (125 MHz) spectrum of **4** in  $\text{DMSO-}d_6$
- Figure S22.** DEPT  $135^\circ$  NMR (125 MHz) spectrum of **4** in  $\text{DMSO-}d_6$
- Figure S23.** HSQC NMR spectrum of **4** in  $\text{DMSO-}d_6$
- Figure S24.** HMBC NMR spectrum of **4** in  $\text{DMSO-}d_6$
- Figure S25.** HRESIMS spectrum of **4**
- Figure S26.** UV spectrum of **4**
- Figure S27.**  $^1\text{H}$  NMR (300 MHz) spectrum of **5** in  $\text{DMSO-}d_6$
- Figure S28.**  $^{13}\text{C}$  NMR (75 MHz) spectrum of **5** in  $\text{DMSO-}d_6$
- Figure S29.** TOCSY NMR spectrum of **5** in  $\text{DMSO-}d_6$

**Figure S30.** HSQC NMR spectrum of **5** in DMSO-*d*<sub>6</sub>

**Figure S31.** HMBC NMR spectrum of **5** in DMSO-*d*<sub>6</sub>

**Figure S32.** NOESY NMR spectrum of **5** in DMSO-*d*<sub>6</sub>

**Figure S33.** HRESIMS spectrum of **5**

**Figure S34.** UV spectrum of **5**

**Table S1**– Hydrogen bonds for compounds **2**, **4** and **5**.

<b>Compound 2</b>					
Donor-H...Acceptor	Type	D...H(Å)	H...A(Å)	D...A(Å)	D-H...A(°)
N1--H1A..O2		0.82	2.07	2.868(2)	163
N1--H1B..O1	Intra	0.91(2)	2.23(2)	2.646(2)	107.2(18)
O3--H3..O5		0.82	2.02	2.7174(19)	142
<b>Compound 4</b>					
Donor-H...Acceptor	Type	D...H(Å)	H...A(Å)	D...A(Å)	D-H...A(°)
O1W--H1WA..O2		0.85	2.03	2.849(5)	163
N1--H1A..O1	Intra	0.79(4)	2.26(4)	2.658(4)	112(3)
N1--H1A..O5		0.79(4)	2.30(4)	3.033(4)	153(4)
N1--H1B..O1W		0.89(5)	2.01(5)	2.881(5)	168(4)
O1W--H1WB..O2W		0.85	1.93	2.765(6)	167
O2W--H2WA..O1		0.85	2.07	2.885(5)	160
O2W--H2WB..O2		0.85	2.44	3.211(5)	150
O2W--H2WB..O4		0.85	2.43	3.085(5)	134
C16--H16B..O4		0.96	2.58	3.337(5)	136
C17--H17A..O1		0.96	2.57	3.520(4)	168
<b>Compound 5</b>					
Donor-H...Acceptor	Type	D...H(Å)	H...A(Å)	D...A(Å)	D-H...A(°)
O1W--H1WA..O2		0.87	1.89	2.758(7)	176
N1--H1A..O4		0.88	2.18	2.973(9)	150
N1--H1B..O1	Intra	0.88	2.32	2.664(10)	104
O1W--H1WB..O7		0.87	2.02	2.873(8)	165
O3--H3..O1W		0.84	1.92	2.599(7)	137
C3--H3A..O4		0.95	2.48	3.241(9)	137
C13--H13..O2	Intra	1.00	2.51	2.863(9)	101
C19--H19..O3	Intra	1.00	2.38	3.327(10)	158
C21--H21C..O5	Intra	0.98	2.56	2.958(10)	104

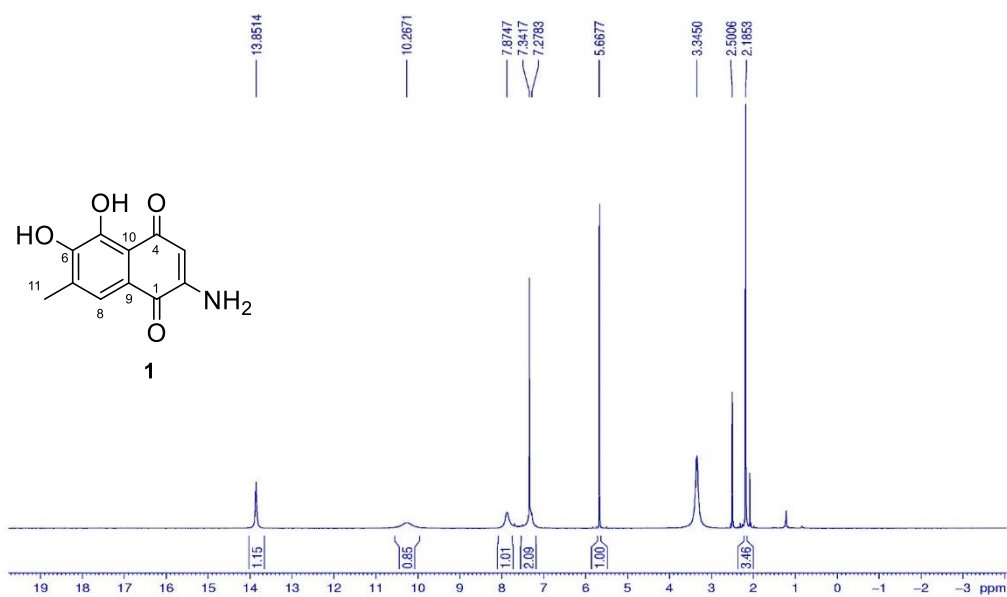


**Figure S1.**  $^1\text{H}$  NMR (500 MHz) spectrum of **1** in  $\text{DMSO-}d_6$ .

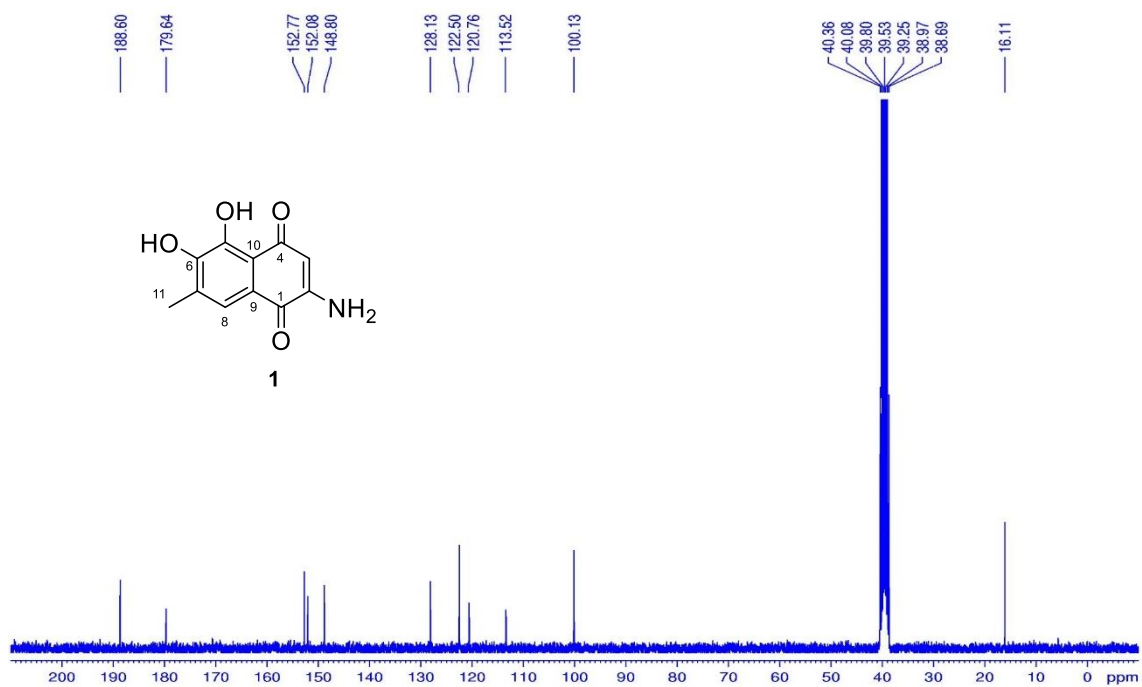


**Figure S2.**  $^{13}\text{C}$  NMR (125 MHz) spectrum of **1** in  $\text{DMSO-}d_6$ .

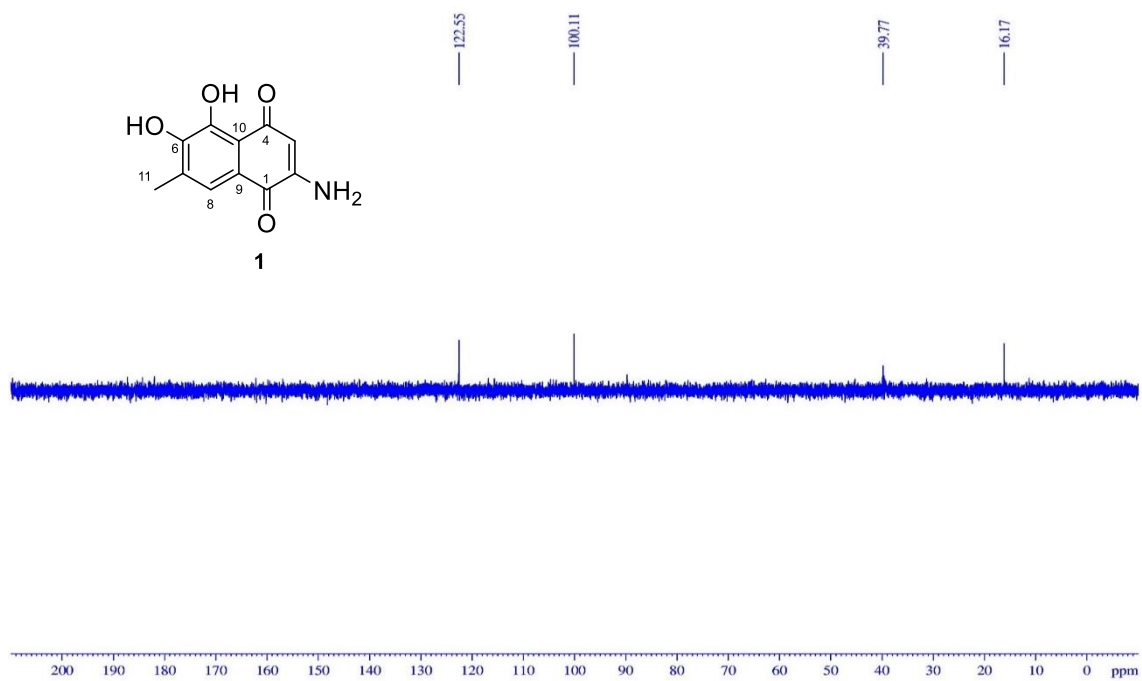


**Figure S3.** DEPT 135° NMR (125 MHz) spectrum of **1** in DMSO-*d*<sub>6</sub>.

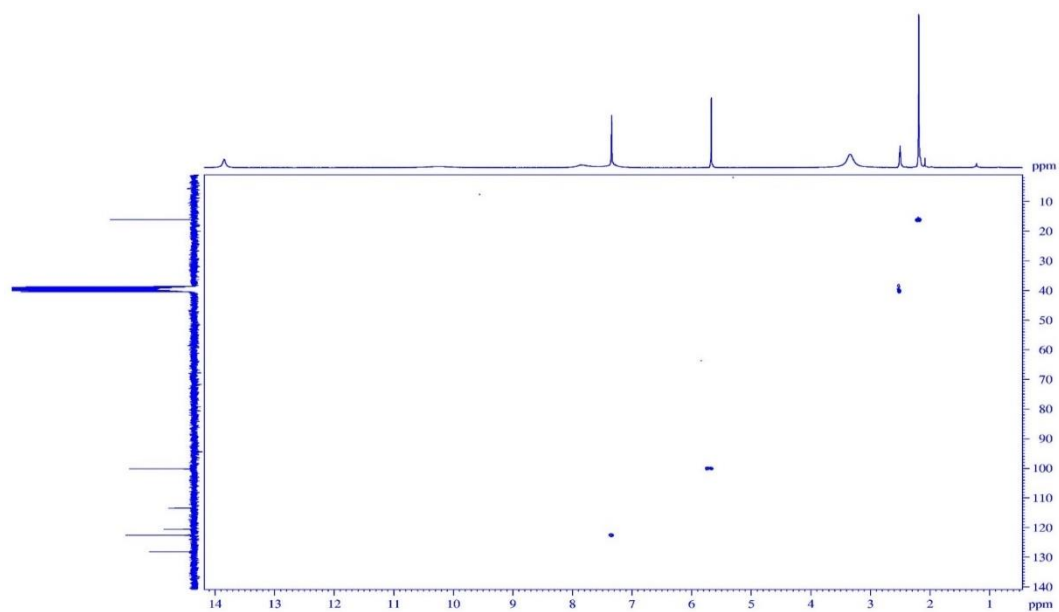


**Figure S4.** HSQC NMR spectrum of **1** in DMSO-*d*<sub>6</sub>.

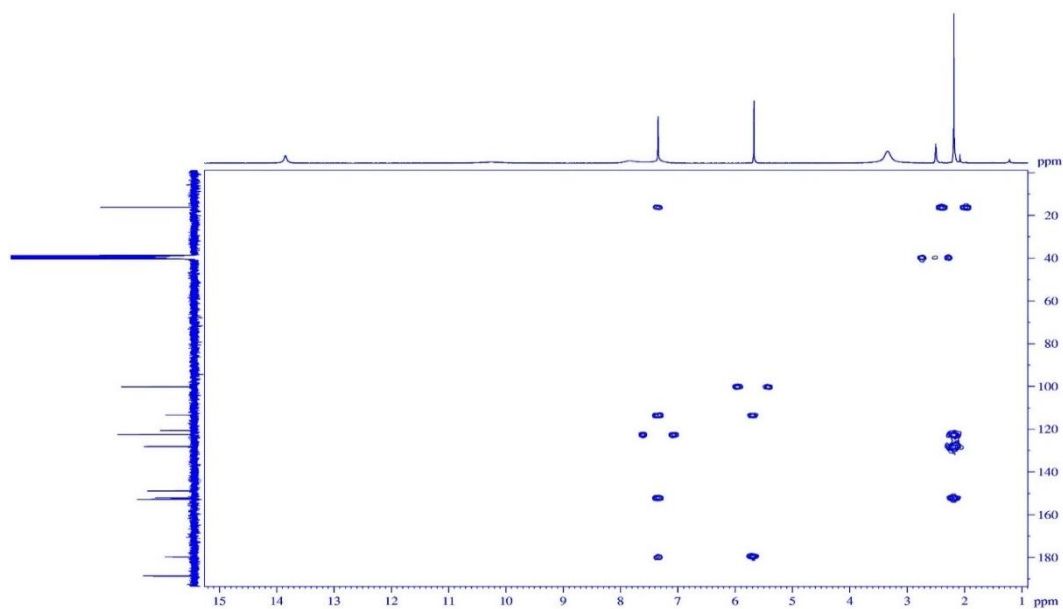


**Figure S5.** HMBC NMR spectrum of **1** in DMSO-*d*<sub>6</sub>.

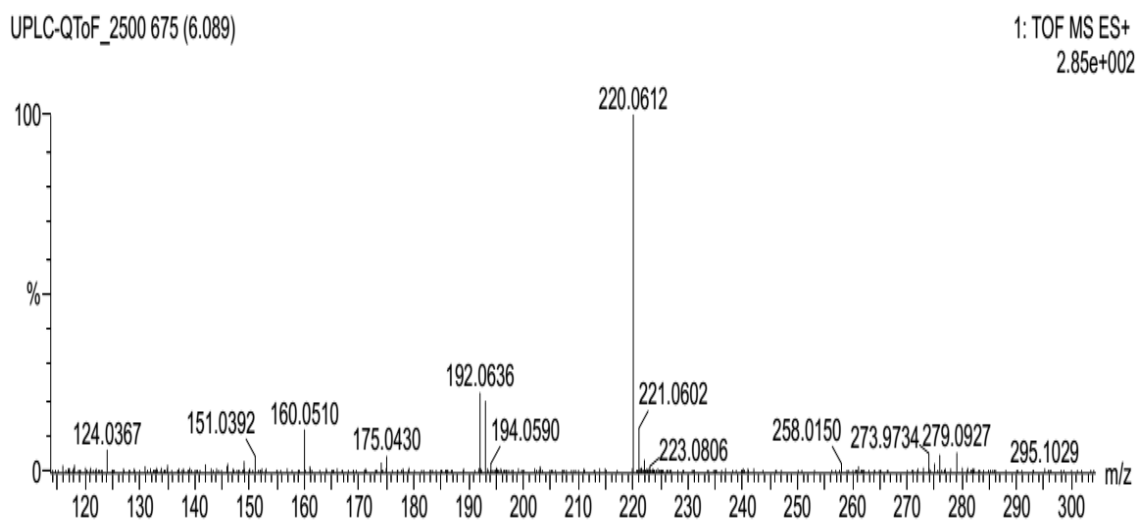


**Figure S6.** HRESIMS spectrum of **1**.

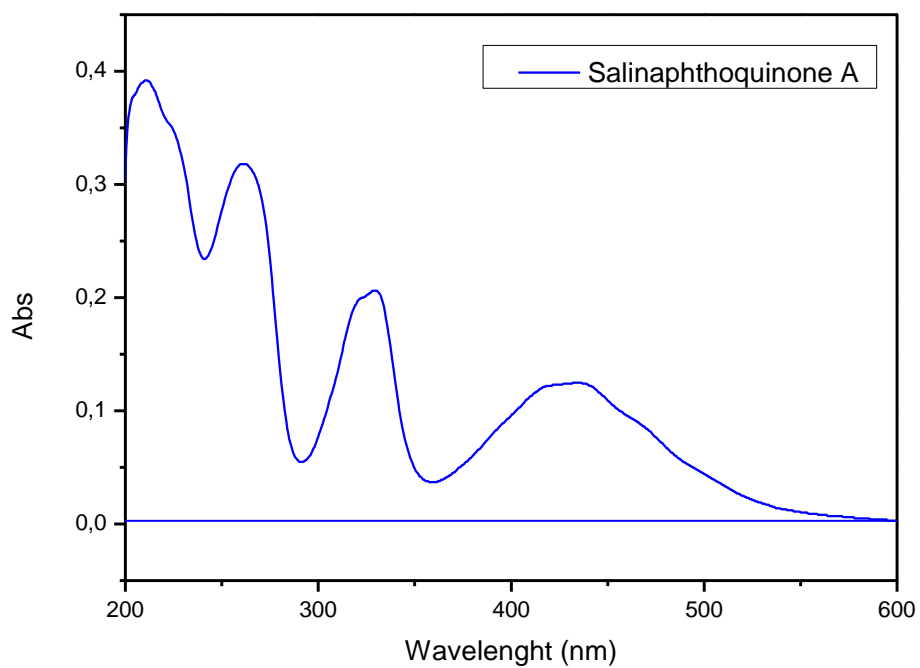


Figure S7. UV spectrum of **1**.

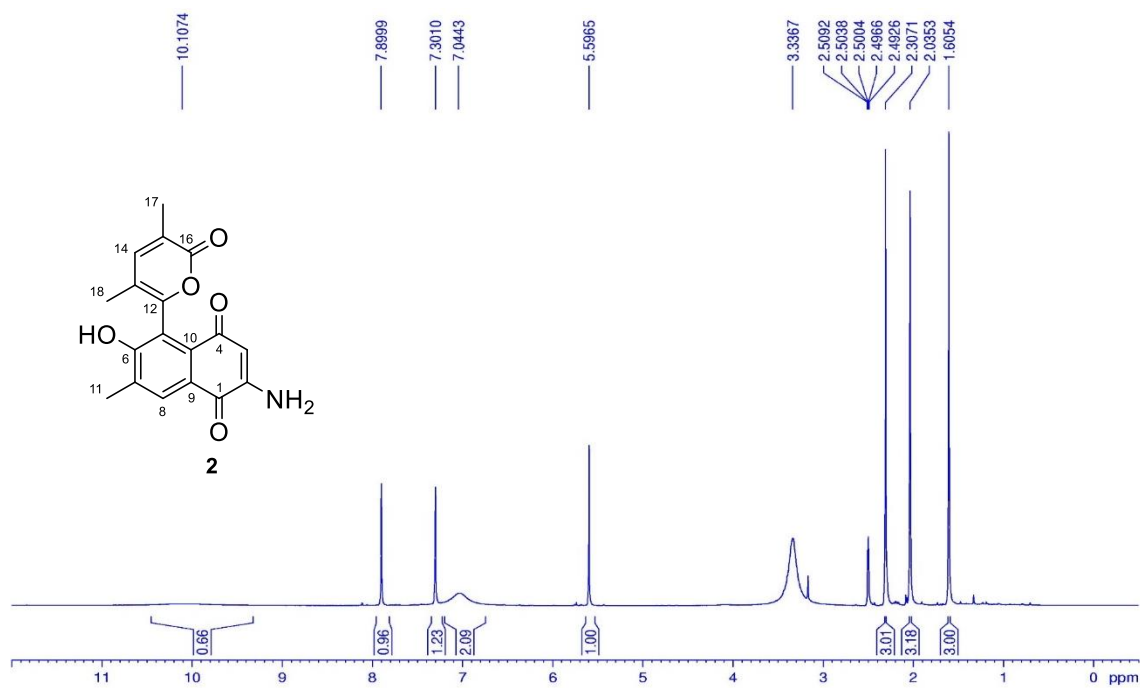
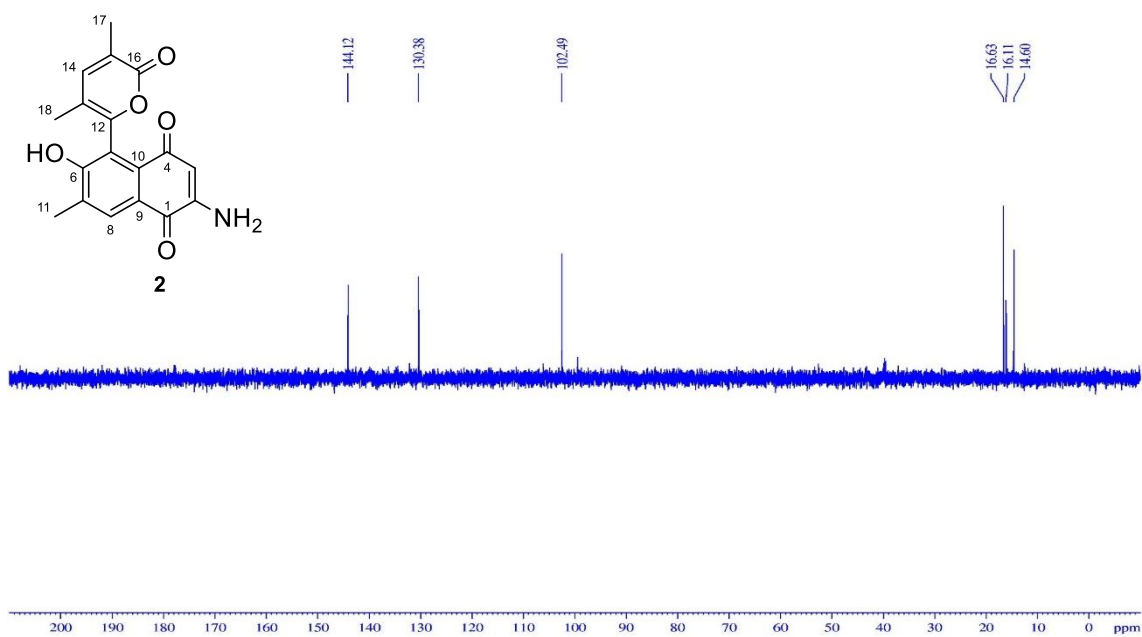
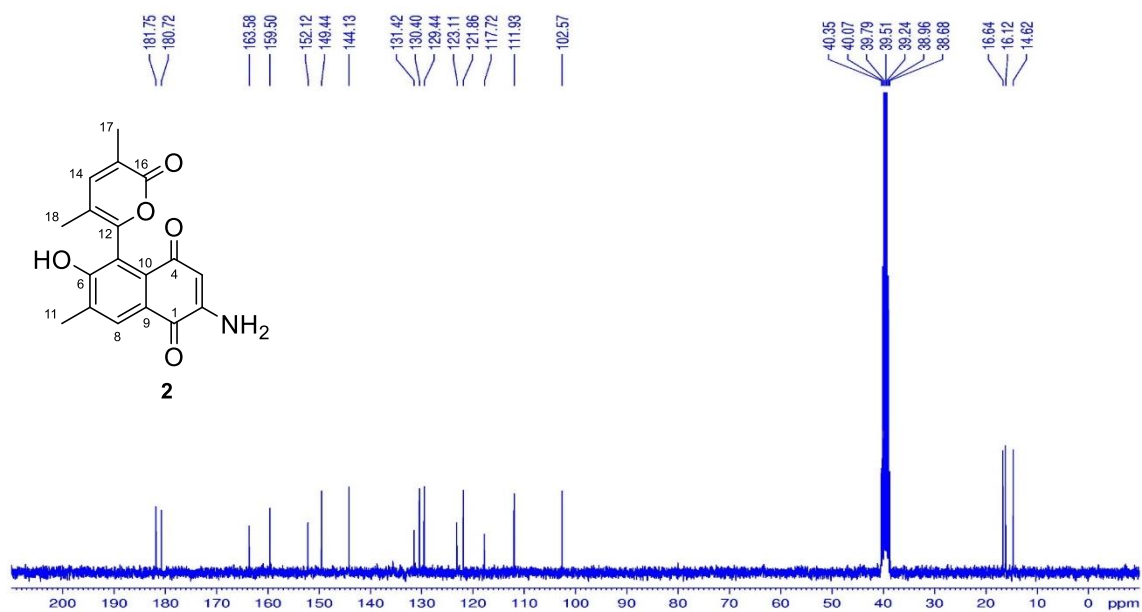
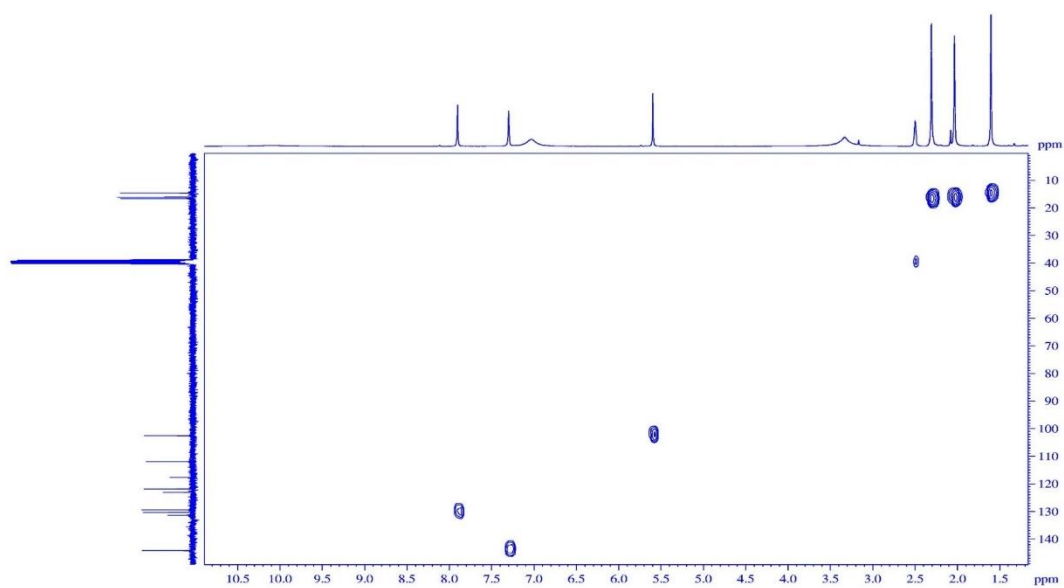


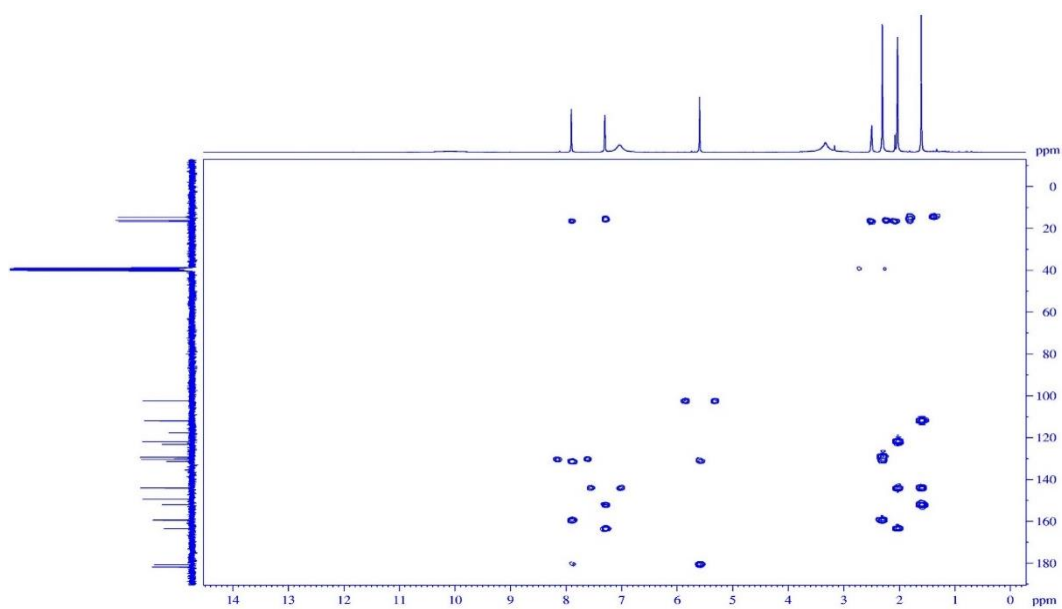
Figure S8. <sup>1</sup>H NMR (500 MHz) spectrum of **2** in DMSO-*d*<sub>6</sub>.



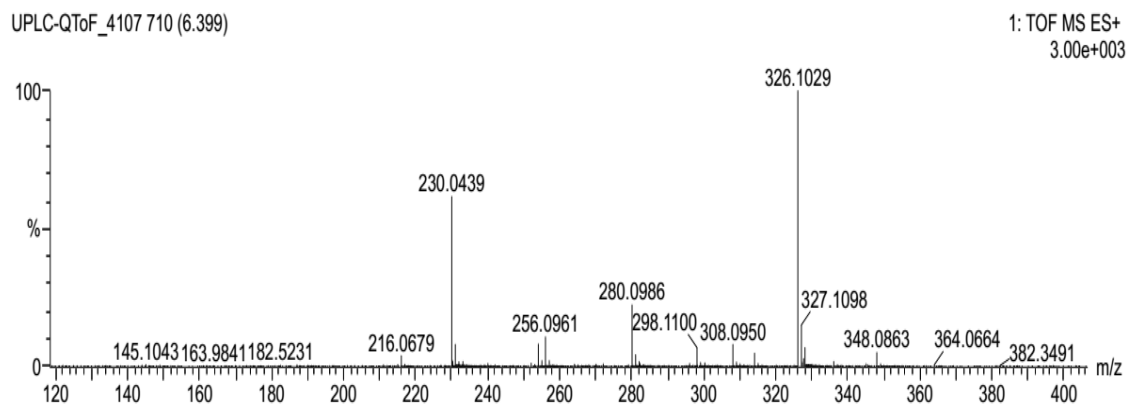




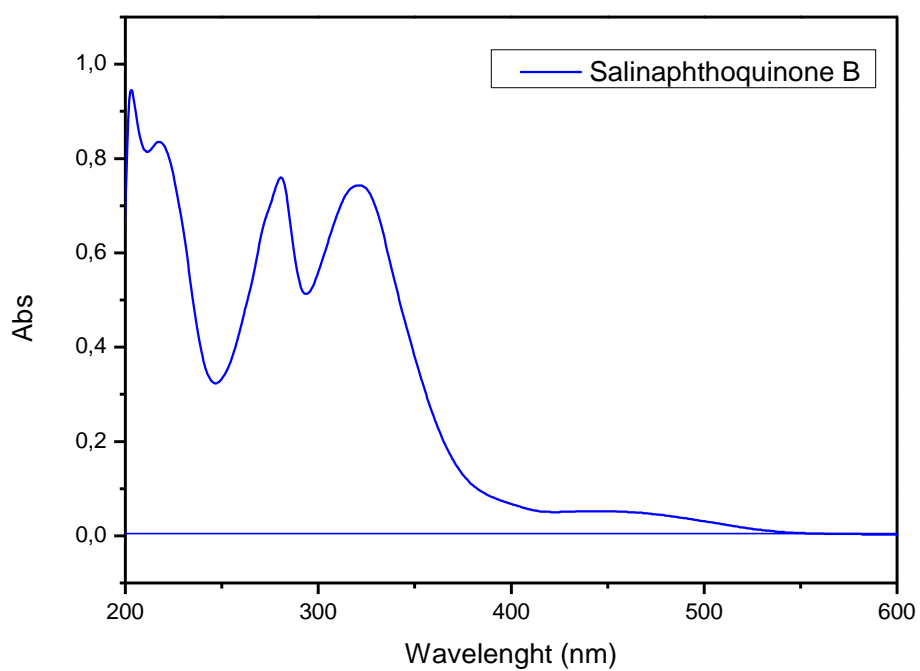
**Figure S11.** HSQC NMR spectrum of **2** in DMSO- $d_6$ .



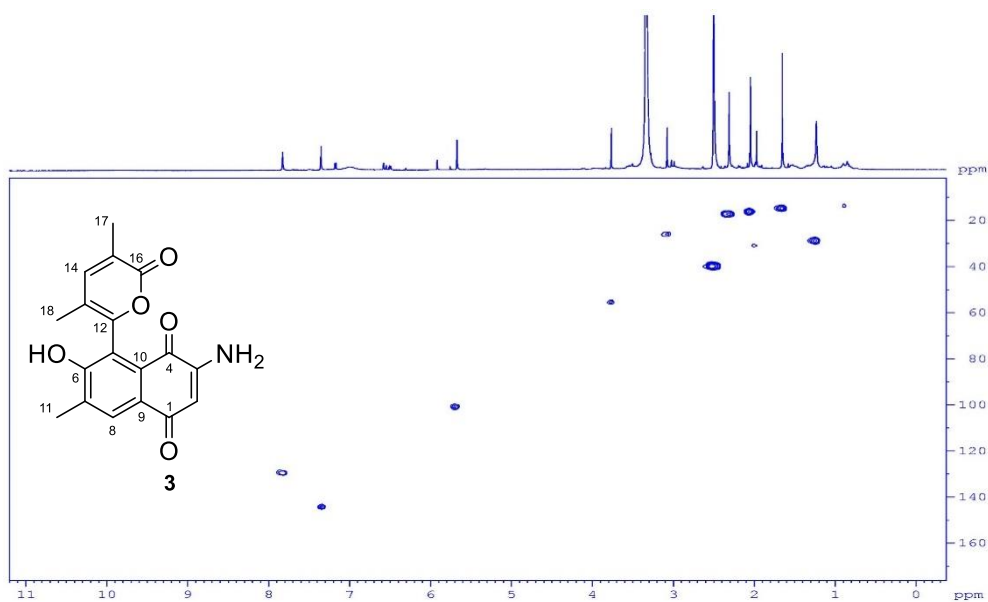
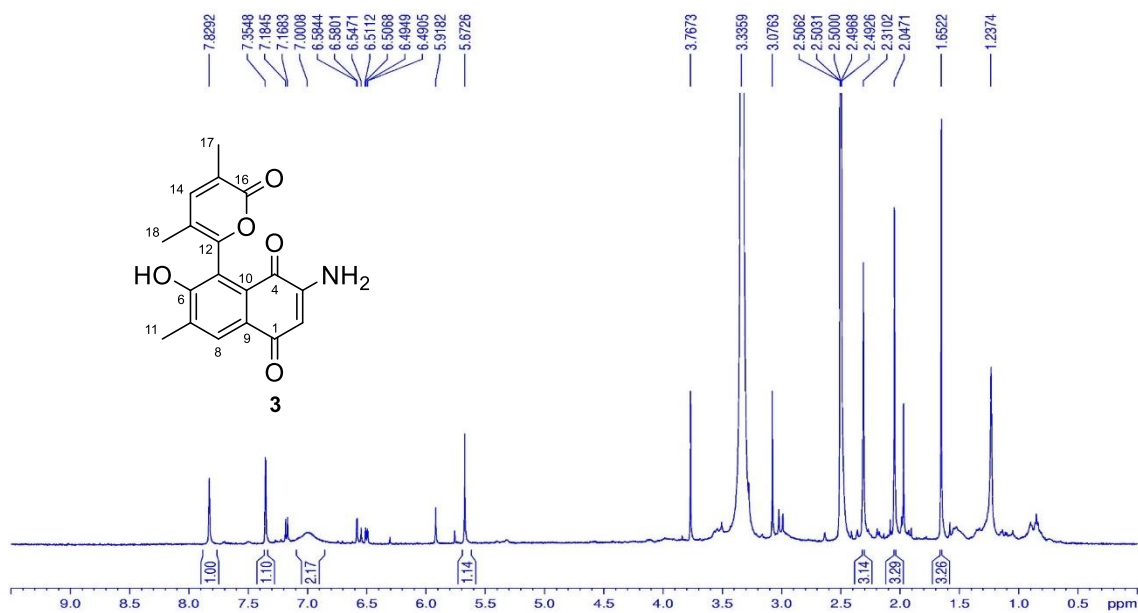
**Figure S12.** HMBC NMR spectrum of **2** in DMSO- $d_6$ .



**Figure S13.** HRESIMS spectrum of **2**.



**Figure S14.** UV spectrum of **2**.



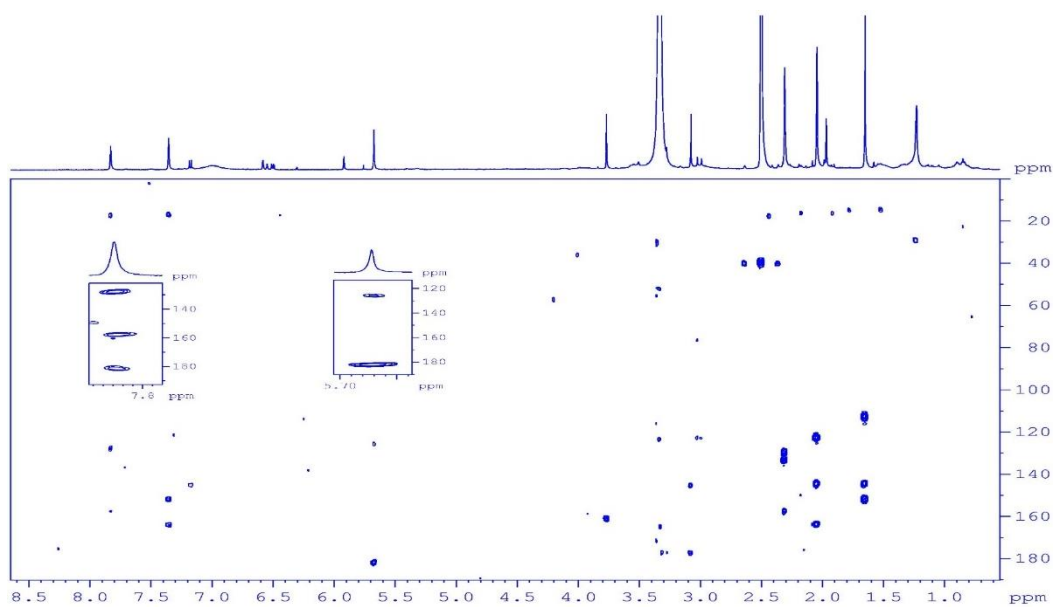


**Figure S17.** HMBC NMR spectrum of **3** in DMSO-*d*<sub>6</sub>.

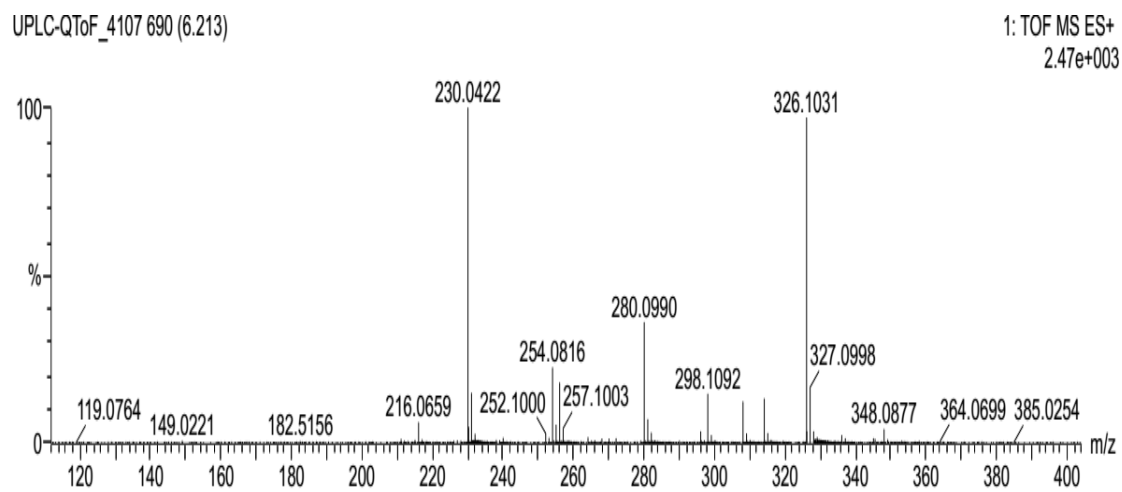


**Figure S18.** HRESIMS spectrum of **3**.

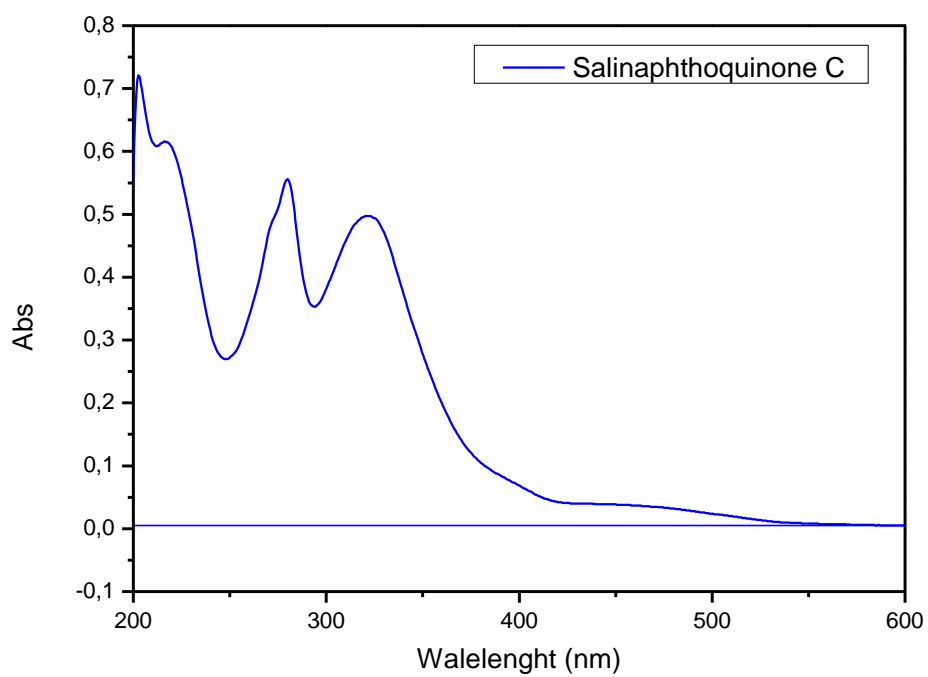


Figure S19. UV spectrum of **3**.

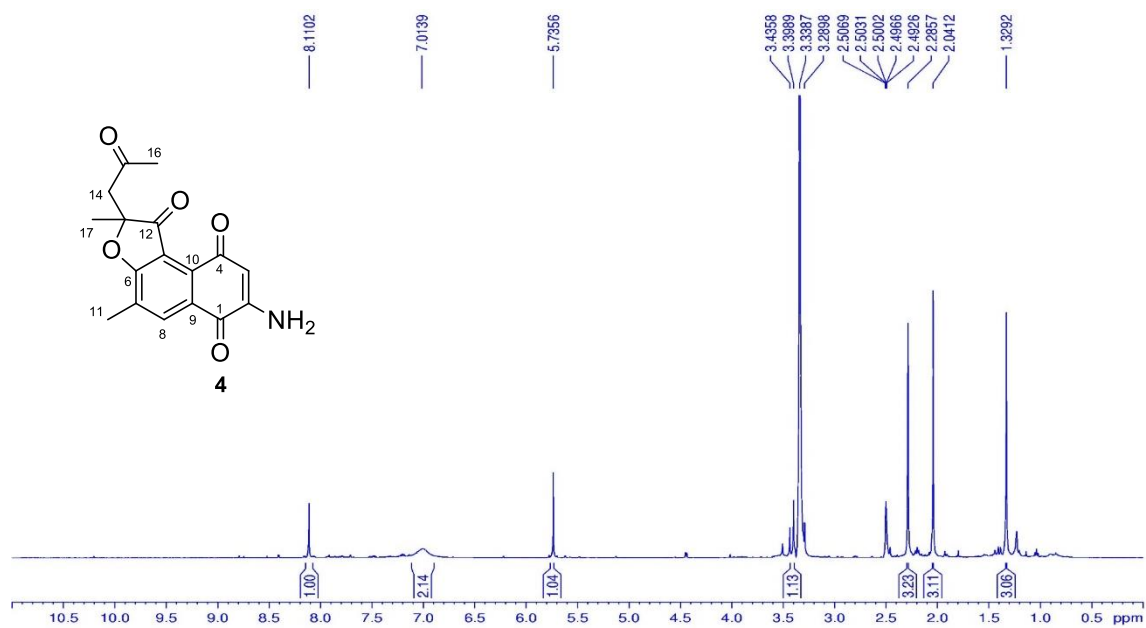
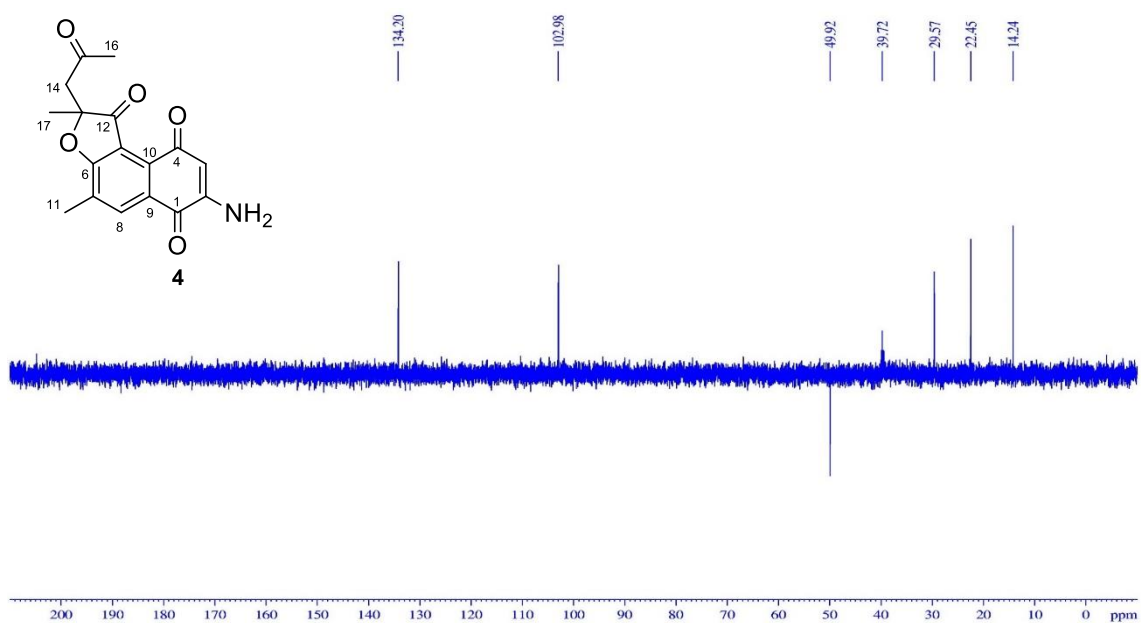
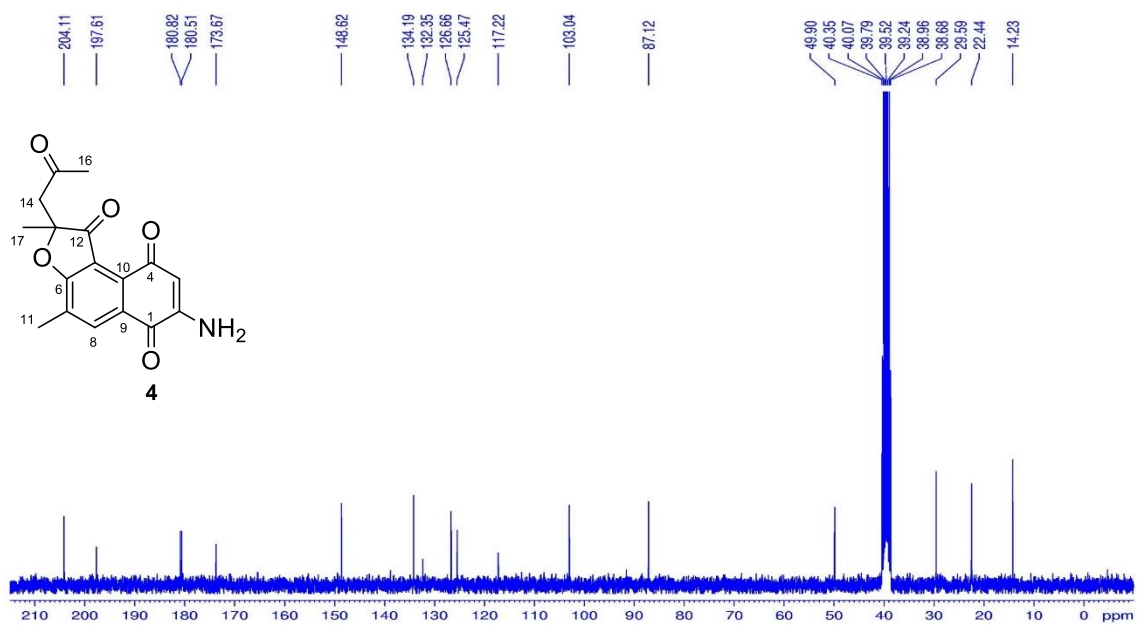
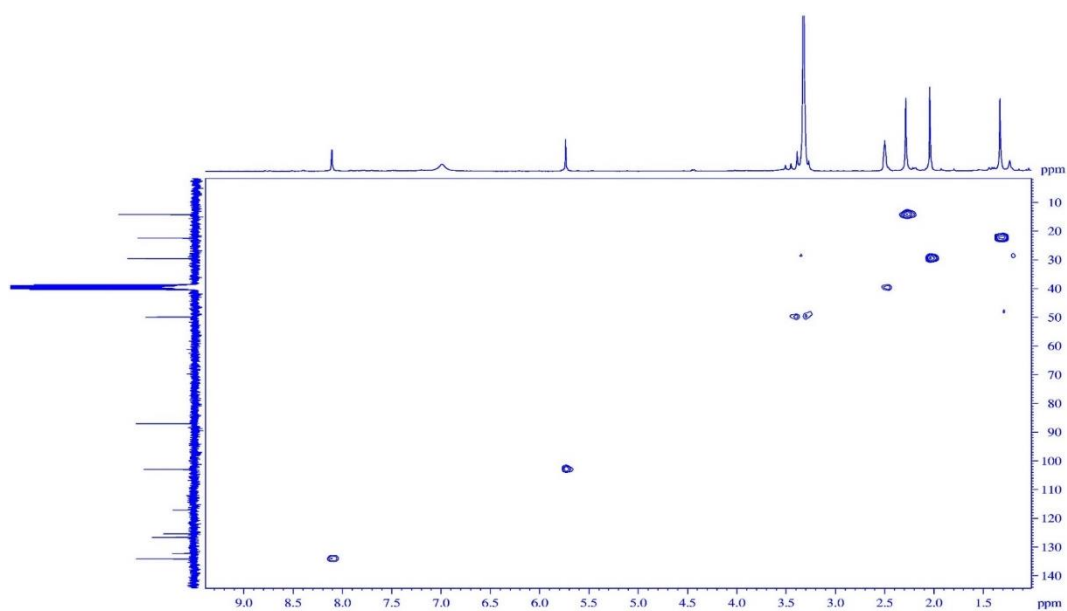
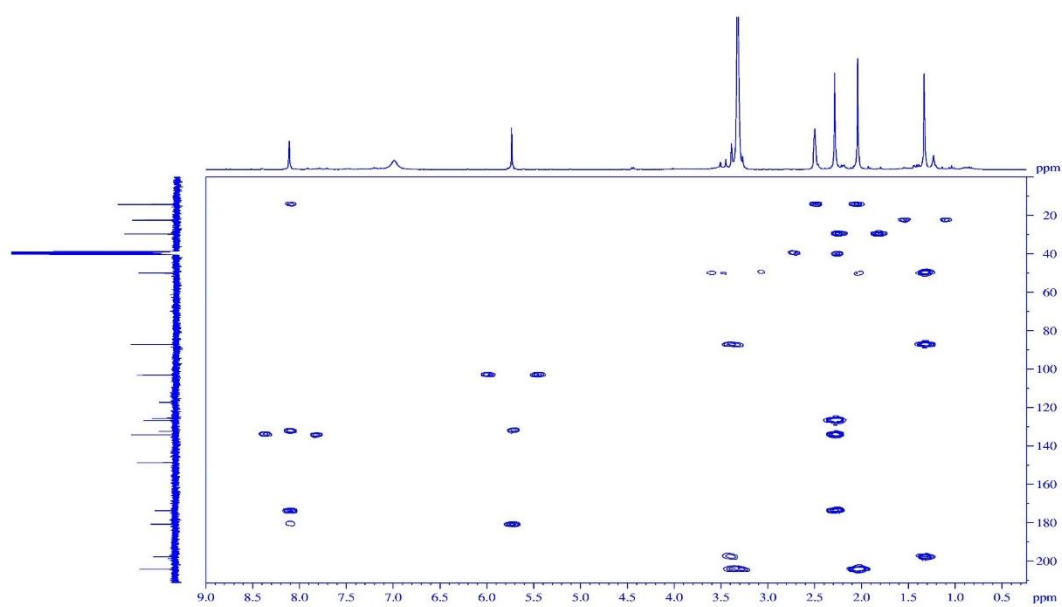


Figure S20. <sup>1</sup>H NMR (500 MHz) spectrum of **4** in DMSO-*d*<sub>6</sub>.





**Figure S23.** HSQC NMR spectrum of **4** in DMSO- $d_6$ .



**Figure S24.** HMBC NMR spectrum of **4** in DMSO- $d_6$ .

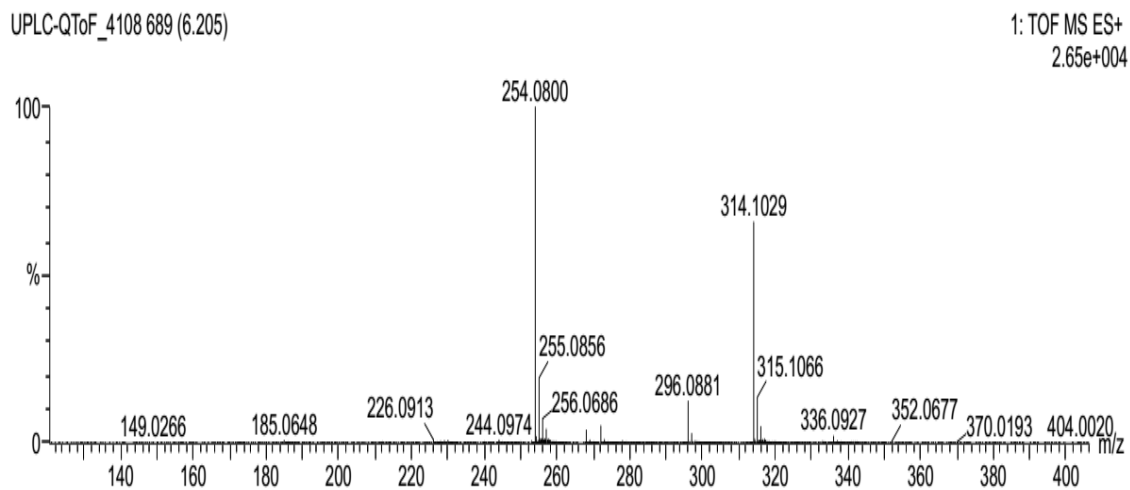


**Figure S25.** HRESIMS spectrum of **4**.

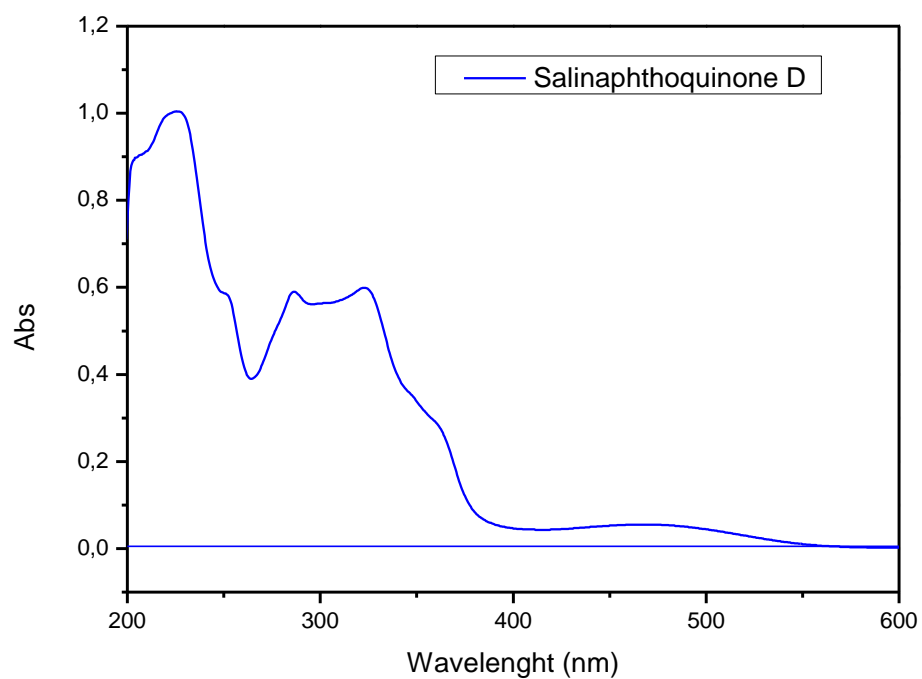


**Figure S26.** UV spectrum of **4**.



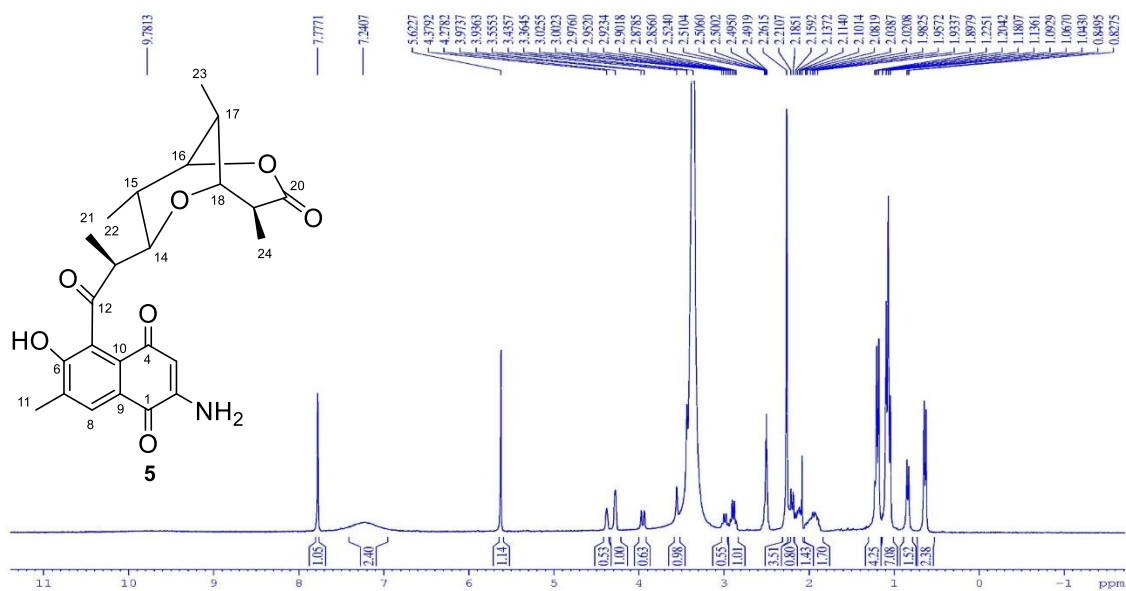


Figure S27.  $^1\text{H}$  NMR (300 MHz) spectrum of **5** in  $\text{DMSO-}d_6$ .

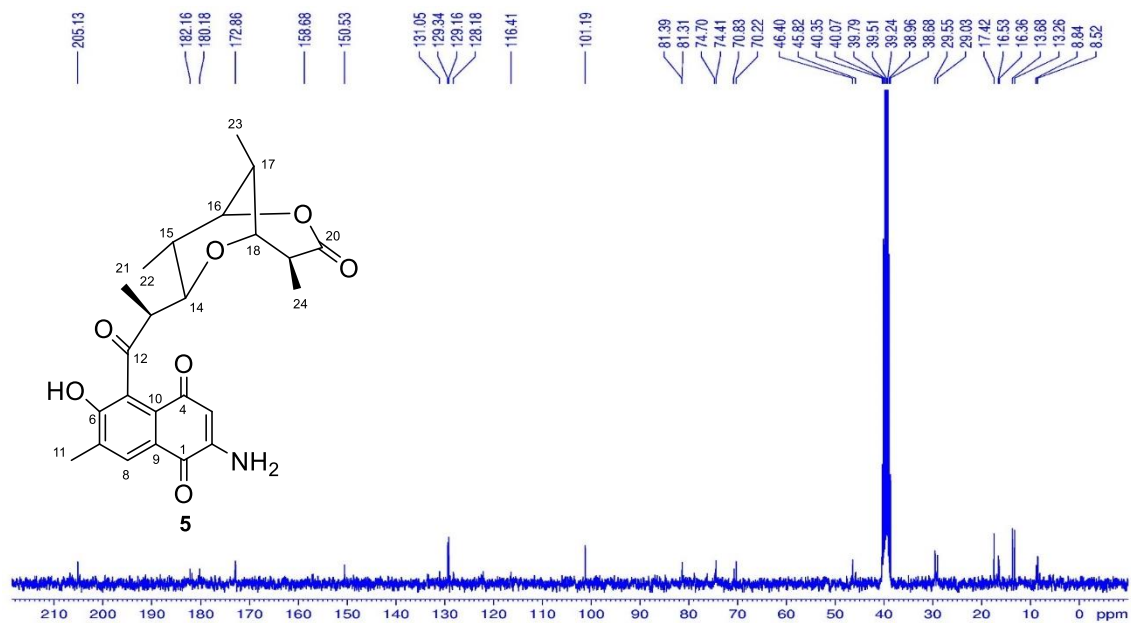
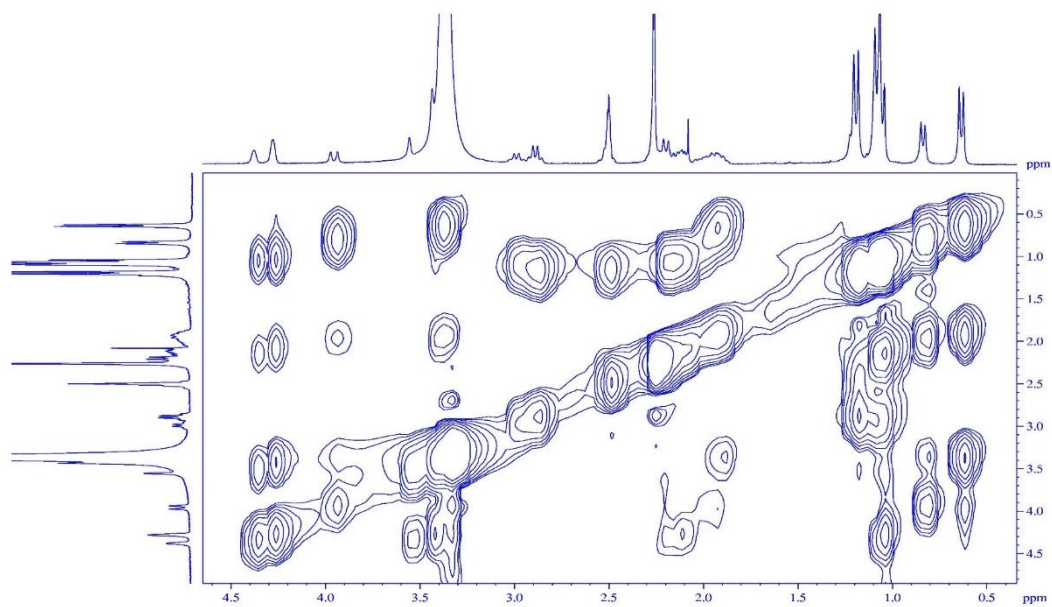
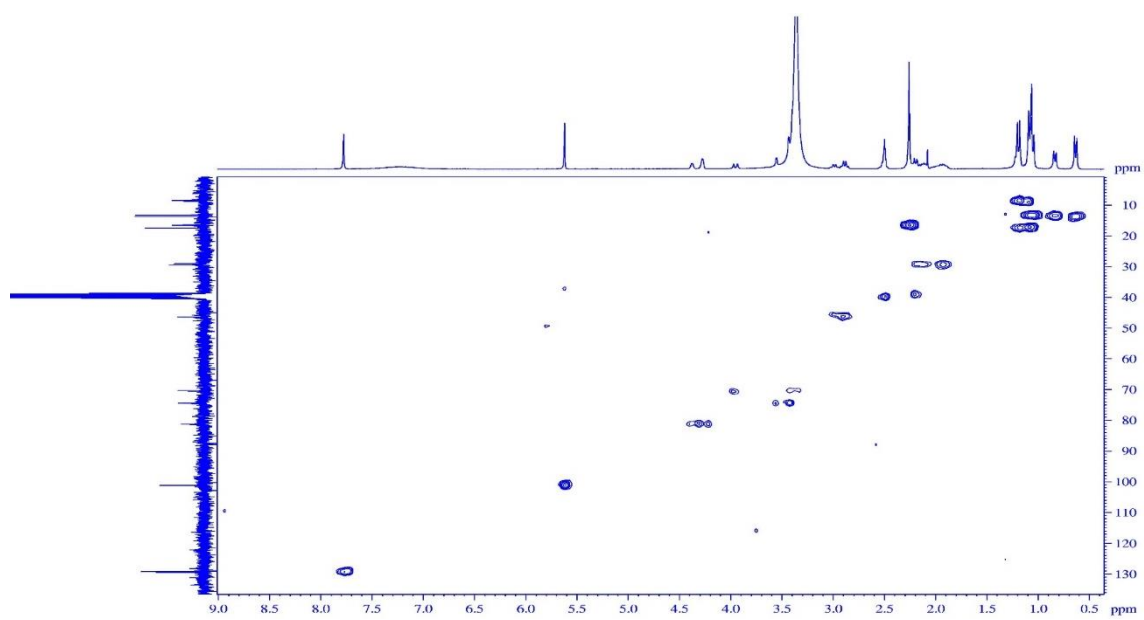


Figure S28.  $^{13}\text{C}$  NMR (75 MHz) spectrum of **5** in  $\text{DMSO-}d_6$ .



**Figure S29.** TOCSY NMR spectrum of **5** in DMSO-*d*<sub>6</sub>.



**Figure S30.** HSQC NMR spectrum of **5** in DMSO-*d*<sub>6</sub>.

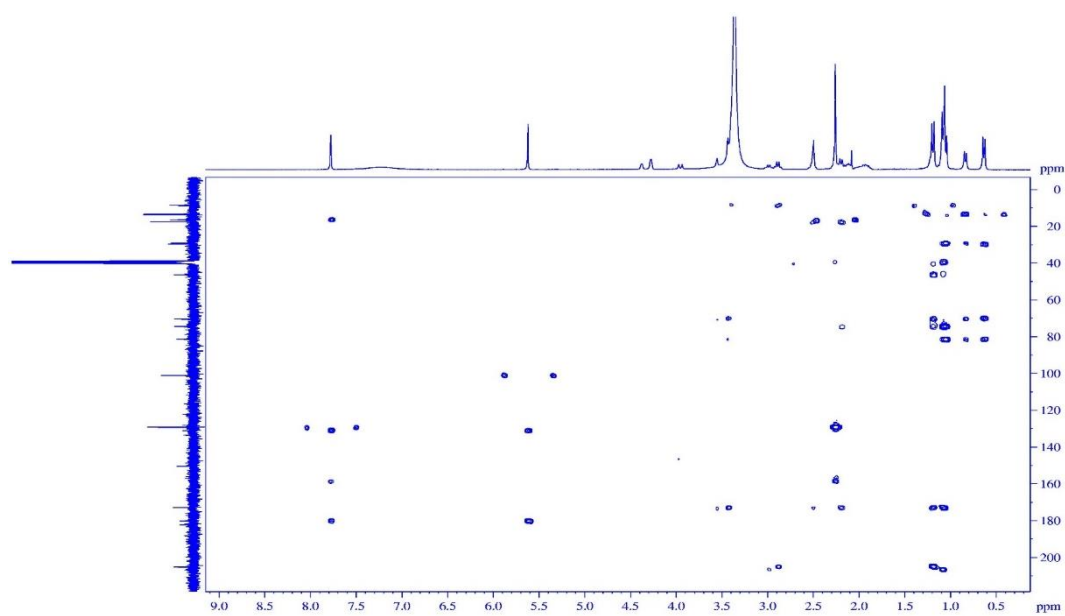


**Figure S31.** HMBC NMR spectrum of **5** in DMSO- $d_6$ .

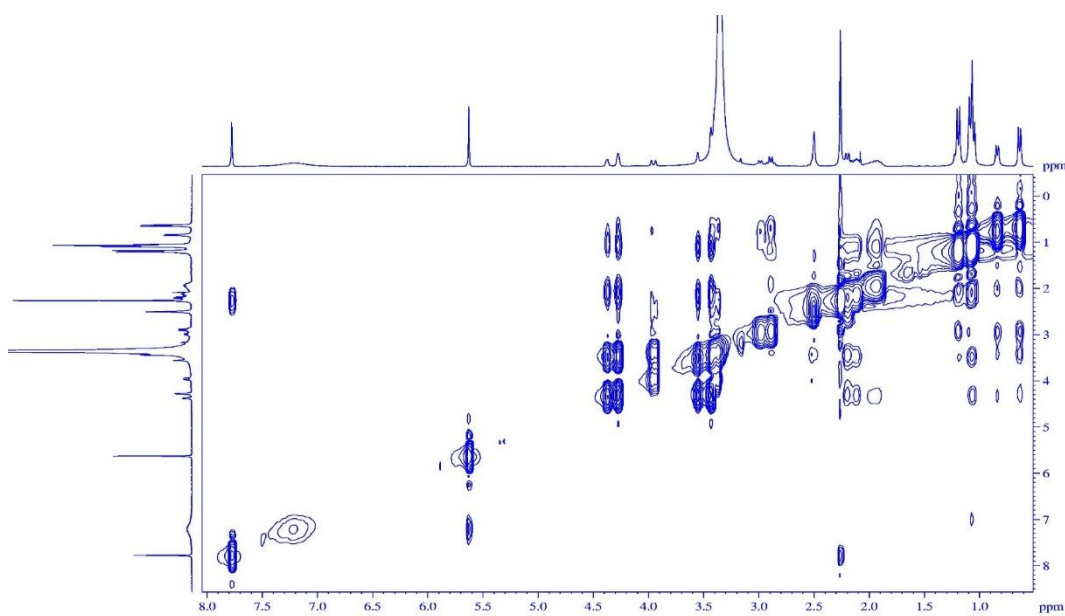


**Figure S32.** NOESY NMR spectrum of **5** in DMSO- $d_6$ .

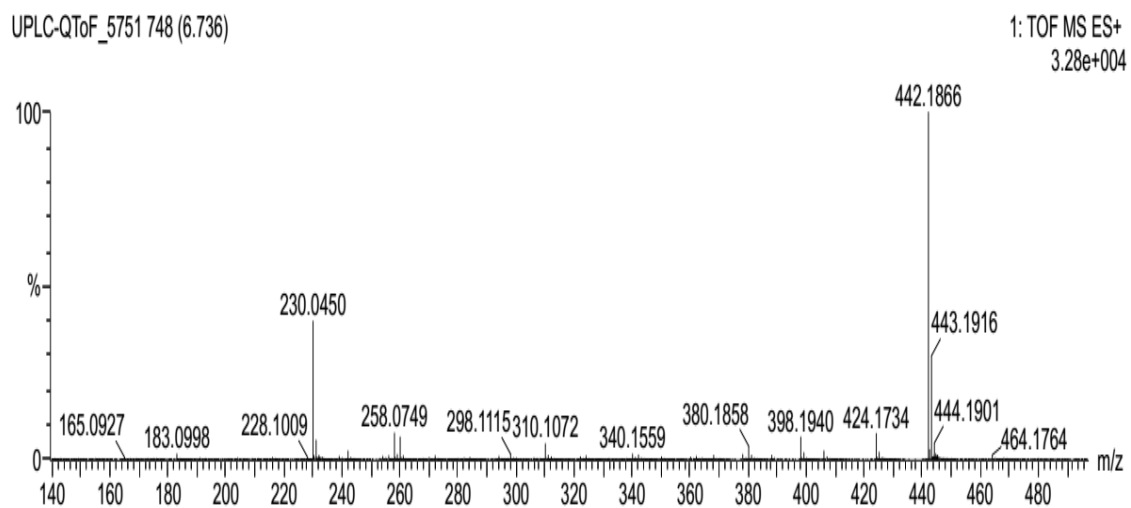


**Figure S33.** HRESIMS spectrum of **5**.

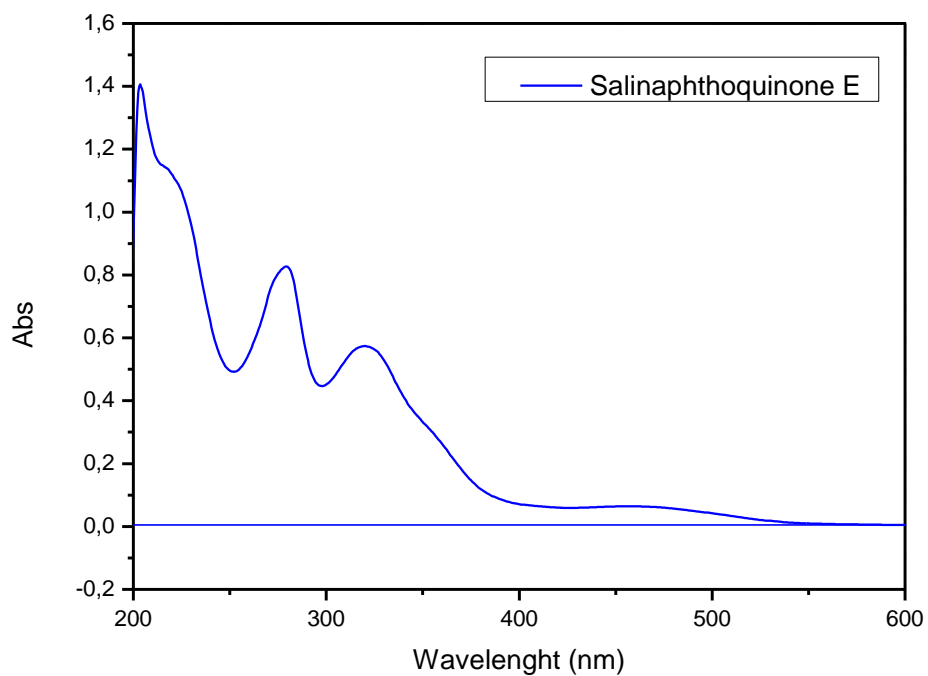


**Figure S34.** UV spectrum of **5**.

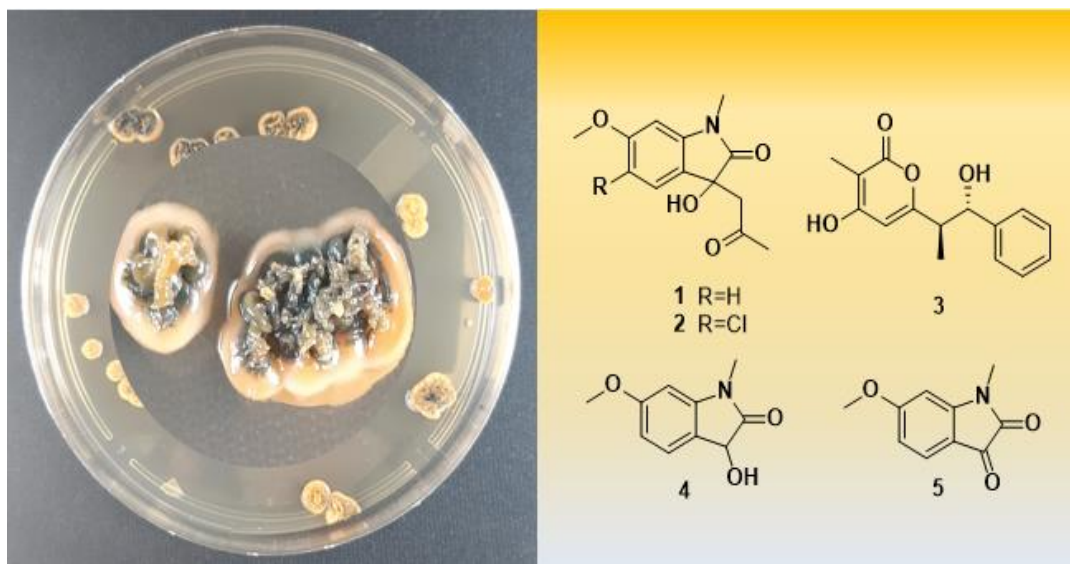
4.2

# Capítulo 2

---

## 4-Hydroxy-pyran-2-one and 3-hydroxy-*N*-methyl-2-oxindole derivatives of *Salinispora arenicola* from Brazilian marine sediments

---



## **4-Hydroxy-pyran-2-one and 3-hydroxy-N-methyl-2-oxindole derivatives of *Salinispora arenicola* from Brazilian marine sediments**

Alison B. da Silva<sup>a</sup>, Francisco C. L. Pinto<sup>a</sup>, Edilberto R. Silveira<sup>a</sup>, Leticia V. Costa-Lotufo<sup>b</sup>, Wendell S. Costa<sup>c</sup>, Alejandro Pedro Ayala<sup>c</sup>, Kirley M. Canuto<sup>d</sup>, Ayslan B. Barros<sup>e</sup>, Ana Jérsia Araújo<sup>e</sup>, José Delano B. Marinho Filho<sup>e</sup>, Otilia Deusdenia L. Pessoa<sup>a,\*</sup>

<sup>a</sup>*Departamento de Química Orgânica e Inorgânica, Universidade Federal do Ceará, 60.021-970, Fortaleza-CE, Brazil*

<sup>b</sup>*Departamento de Farmacologia, Universidade de São Paulo, 05508-900, São Paulo-SP, Brazil*

<sup>c</sup>*Departamento de Física, Universidade Federal do Ceará, 60.440-970, Fortaleza-CE, Brazil*

<sup>d</sup>*Embrapa Agroindústria Tropical, 60.511-110, Fortaleza-CE, Brazil*

<sup>e</sup>*Núcleo de Pesquisa em Biodiversidade e Biotecnologia, Universidade Federal do Piauí, 64202-020, Parnaíba-PI, Brazil*

\*Corresponding author

*E-mail address:* [opessoa@ufc.br](mailto:opessoa@ufc.br) (O.D.L. Pessoa).

## ABSTRACT

Three new 3-hydroxy-*N*-methyl-2-oxindole (**1** and **2**) and 4-hydroxy-pyran-2-one (**3**) derivatives, along with the known 3-hydroxy-*N*-methyl-2-oxindole (**4**) and 6-methoxy-*N*-methylisatin (**5**) were isolated from a marine *Salinispora arenicola* strain from sediments of the St. Peter and St. Paul Archipelago, Brazil. The structures of the new compounds were elucidated by a combination of spectroscopic (1D and 2D NMR and HR-ESIMS) data, including single-crystal X-ray diffraction analysis for **2** and **3**. Compounds **1** to **5** were assayed for their antimicrobial properties, but only **4** and **5** were active against *Enterococcus faecalis* with MIC value of 15.6 µg/mL.

**Keywords:** *Salinispora arenicola*; Marine actinomycete; 4-Hydroxy-pyran-2-one; 3-Hydroxy-*N*-methyl-2-oxindole; X-Ray structure analysis; Antimicrobial activity.

## 1. Introduction

The genus *Salinispora*, formally described in 2005 by Maldonado and co-workers as the first obligate marine actinomycete [1], comprises only the three species: *S. tropica*, *S. pacifica*, and *S. arenicola* [2]. These bacteria are reported as an extraordinary source of unusual bioactive secondary metabolites [3]. In fact, dozens of compounds structurally diverse and unprecedented have been isolated from *Salinispora* species as the salinosporamides [4,5], saliniquinones [6], arenicolides [7], saliniketals [8], arenamides [9], salinipyrones, and pacificanones [10,11]. Interesting and relevant activities such as antibiotic [12,13], anticancer [6,14], antimalarial [15], and immunosuppressant [16] have been reported to the compounds isolated from *Salinispora*.

In the course of our study for bioactive natural compounds from marine microorganisms [17–19], we have investigated the EtOAc extract of *S. arenicola* strain [20] from the sediments of Saint Peter and Saint Paul Archipelago (ASPSA), an outlying group of islets located in the Brazilian Atlantic ocean [21]. Herein the isolation and characterization of novel 4-hydroxy-pyran-2-one and 3-hydroxy-*N*-methyl-2-oxindole derivatives are described. It is worth mentioning that this is the first report on the isolation of 2-oxindole derivatives from *Salinispora* adding one more interesting class of compound to the genus. Natural 3-substituted-3-hydroxy-2-oxindole derivatives have been isolated from various sources, including plants [22,23], microorganisms [24,25], and

marine invertebrates [26]. Anti-cancer, anti-HIV, and neuroprotective properties, including several modes of action has been described for this class of natural compounds inspiring innumerable organic synthesis using 3-hydroxy-2-oxindole frameworks as promising scaffold for new drug discovery [27,28].

## **2. Experimental section**

### **2.1 General procedures**

Optical rotations were measured on a JASCO P-2000 digital polarimeter. IR spectra were recorded on Perkin-Elmer Spectrum 100 FTIR spectrometer NMR spectra were obtained either on a Bruker Avance DRX-500 (500 MHz to  $^1\text{H}$  and 125 MHz to  $^{13}\text{C}$ ) or Avance DPX-300 (300 MHz to  $^1\text{H}$  and 75 MHz to  $^{13}\text{C}$ ) spectrometers. High resolution electrospray ionization mass spectra (HR-ESIMS) were acquired using on an Acquity Xevo UPLC-QTOF-MS system from Waters (Milford, MA). Sephadex LH-20 (Pharmacia) and SPE cartridges C18 (20g/60 mL; Strata, Phenomenex) were used for the chromatographic fractionations. HPLC analyses were carried out using a UFLC (SHIMADZU) system equipped with on an SPD-M20A diode array UV–Vis detector, a Phenomenex C-18 column, 5 $\mu\text{m}$  (10.0 x 250 mm), and a CHIRALCEL OD-H chiral-phase column, 5 $\mu\text{m}$  (4.6 x 150 mm).

### **2.2 Bacterial material**

The bacterial strain BRA-213, identified by Bauermeister et al. [29], was isolated on solid A1 media (18 g of agar, 10 g of starch, 4 g of yeast extract, and 2 g of peptone dissolved in 1 L of artificial seawater) from a marine sediment collected around SPSPA, Pernambuco state-Brazil at a depth of 16 m (N 0°55', W 29°38') in November 2011. NCBI BLAST analysis of the partial 16S rRNA sequence of strain BRA-213 (deposited in GenBank with an accession number MH910695) is identical to *S. arenicola*. A voucher strain BRA-213 is preserved at the Laboratory of Marine Bioprospection and Biotechnology, Universidade Federal do Ceará, Brazil. The license for collection was granted by Biodiversity Authorization and Information, SisGen number AA8F8B8.

### **2.3 Fermentation**

Colonies of the strain BRA-213 were inoculated into Erlenmeyer flasks (2L) containing 500 mL of A1 media (10 g of soluble starch, 4 g of yeast extract, and 2 g of peptone in 1 L of artificial seawater) supplemented with calcium carbonate (0.5 g/L



CaCO<sub>3</sub>), 5 mL of solutions of iron (III) sulfate (8 g/L Fe<sub>2</sub>(SO<sub>4</sub>)<sub>3</sub>) and potassium bromide (20 g/L KBr). On the second day, Sterile Amberlite XAD-16 resin (10 g) was added to each flask, and the cultures were shaken at 200 rpm at 28 °C for 14 days.

#### 2.4 Extraction and isolation

The whole fermentation broth (20 L) was filtered through cheesecloth to separate the Amberlite XAD-16 resin, which was extracted with acetone (3 x 300 mL). The combined acetone fraction was distilled under reduced pressure to yield a residual aqueous layer which was further extracted with EtOAc (3 x 500 mL). The resulting EtOAc fraction was evaporated under reduced pressure to yield a crude organic extract (9 g), which was fractionated on a C-18 SPE (9 x 1.0 g), cartridge and eluted with MeOH/H<sub>2</sub>O (7:3 and 8:2), and MeOH to give three fractions (A-C). Fraction A (5 g) was chromatographed using a C-18 SPE cartridge (5 x 1.0 g) and eluted with MeOH/H<sub>2</sub>O (3:7, 4:6, 5:5, 6:4, 7:3, and 8:2) and MeOH to give seven fractions (AA-AG). Fraction AB (660 mg) was fractionated by a Sephadex LH-20 column, eluted with MeOH to give five subfractions (AB1-AB5). Subfraction AB3 (120 mg) was purified by semipreparative HPLC (MeOH/H<sub>2</sub>O, 40–100%, 20 min, flow rate of 4.72 mL/min) to provide the known compounds **4** (6.8 mg, t<sub>R</sub> = 8.5 min) and **5** (8.1 mg, t<sub>R</sub> = 12.5 min). Subfraction AB4 (32 mg) was also purified by semipreparative HPLC [CH<sub>3</sub>CN/H<sub>2</sub>O (0,1% TFA), 50–100%, 30 min, flow rate of 3.00 mL/min] to provide a mixture AB4P1 (8.0 mg, t<sub>R</sub> = 5.5 min) and compound **3** (3.8 mg, t<sub>R</sub> = 6.6 min). The mixture AB4P1 (8.0 mg) was further purified by semipreparative HPLC [CH<sub>3</sub>CN/H<sub>2</sub>O (0,1% TFA), 40–70%, 30 min, flow rate of 3.00 mL/min] to provide compounds **1** (2. mg, t<sub>R</sub> = 8.2 min) and **2** (1.0 mg, t<sub>R</sub> = 10.5 min).

#### Physical and spectroscopic data of 1–5

*3-Hydroxy-6-methoxy-3-(2-oxopropyl)-N-methyl-2-oxindole (1)*: yellowish oil;  $[\alpha]_D^{22} + 16.3$  (*c* 0.05, MeOH); IR ( $\nu_{\max}$ ) 3369, 2926, 2852, 1710, 1622, 1508, 1458, 1379, 1230, 1091, 833, 802, 717cm<sup>-1</sup>; <sup>1</sup>H and <sup>13</sup>C NMR data, see Table 1; HR-ESIMS *m/z* 272.0905 [M + Na]<sup>+</sup> (calcd for C<sub>13</sub>H<sub>15</sub>NNaO<sub>4</sub>, 272.0899).

*5-Chloro-3-hydroxy-6-methoxy-3-(2-oxopropyl)-N-methyl-2-oxindole (2)*: yellow crystals;  $[\alpha]_D^{22} + 94.1$  (*c* 0.05, MeOH); IR ( $\nu_{\max}$ ) 3338, 2924, 2852, 1714, 1618, 1504, 1456, 1379, 1259, 1103, 1043, 798, 682 cm<sup>-1</sup>; <sup>1</sup>H and <sup>13</sup>C NMR data, see Table 1; HR-ESIMS *m/z* 284.0692 [M + H]<sup>+</sup> (calcd for C<sub>13</sub>H<sub>15</sub>NO<sub>4</sub>Cl, 284.0690).

*4-Hydroxy-6-(2-hydroxy-2-phenyl-1-methylethyl)-3-methyl-2H-pyran-2-one* (**3**): colorless crystals;  $[\alpha]_D^{22} - 7.8$  (*c* 0.10, MeOH); IR ( $\nu_{\max}$ ) 3448, 2931, 2881, 1668, 1581, 1417, 1249, 1203, 1139, 1041, 964, 842, 756  $\text{cm}^{-1}$ ;  $^1\text{H}$  and  $^{13}\text{C}$  NMR data, see Table 1; HR-ESIMS  $m/z$  261.1123  $[\text{M} + \text{H}]^+$  (calcd for  $\text{C}_{15}\text{H}_{17}\text{O}_4$ , 261.1127).

*3-Hydroxy-N-methyl-2-oxindole* (**4**): pale powder;  $[\alpha]_D^{22} + 2.8$  (*c* 0.05, MeOH); IR ( $\nu_{\max}$ ) 3346, 3027, 2927, 2851, 1697, 1627, 1517, 1462, 1380, 1270, 1088, 832  $\text{cm}^{-1}$ ;  $^1\text{H}$  and  $^{13}\text{C}$  NMR data; HR-ESIMS  $m/z$  194.0817  $[\text{M} + \text{H}]^+$  (calcd for  $\text{C}_{10}\text{H}_{12}\text{NO}_3$ , 194.0816).

*6-Methoxy-N-methylisatin* (**5**): bright orange needles; IR ( $\nu_{\max}$ ) 3076, 2926, 2849, 1738, 1720, 1614, 1517, 1482, 1368, 1245, 1096, 841  $\text{cm}^{-1}$ ;  $^1\text{H}$  and  $^{13}\text{C}$  NMR data; HR-ESIMS  $m/z$  192.0659  $[\text{M} + \text{H}]^+$  (calcd for  $\text{C}_{10}\text{H}_{10}\text{NO}_3$ , 192.0661).

## 2.5 X-ray crystallographic analyses of compounds 2 and 3

The single-crystal X-ray intensity data of compounds **2** and **3** were measured on a Bruker D8 Venture equipped with a microfocus Mo generator ( $\lambda K\alpha = 0.71073 \text{ \AA}$ ) and a Photon II CMOS detector. The frames were integrated with the Bruker SAINT software package (v8.34A) using a narrow-frame algorithm. The final cell parameters for each crystal were based upon the refinement of the XYZ-centroids of some reflections. Data were corrected for absorption effects using the Multi-Scan method. The structure was solved using Olex2 [30], with the ShelXT [31] structure solution program using Charge Flipping or Direct Methods and refined with the ShelXL [32] refinement package using Least Squares minimization. Olex2 was also used to prepare the crystallographic information file (CIF). The program ORTEP-III (version 1.0.3) [33] was used to prepare the artwork representations for publication.

*Crystal data of compound 2*: Yellow prism crystals of compound **2** were obtained from an acetone solution after slow evaporation in a refrigerator for 2 weeks.  $\text{C}_{15}\text{H}_{13}\text{NO}_4\text{Cl}$ ,  $M_r = 283.70 \text{ g mol}^{-1}$ ; size  $0.512 \times 0.227 \times 0.081 \text{ mm}$ ; monoclinic, space group  $P2_1/c$ ,  $a = 7.9022(8) \text{ \AA}$ ,  $b = 10.6193(10) \text{ \AA}$ ,  $c = 15.9197(14) \text{ \AA}$ ,  $\alpha = 90^\circ$ ,  $\beta = 95.065(4)^\circ$ ,  $\gamma = 90^\circ$ ;  $V = 1330.7(2) \text{ \AA}^3$ ,  $Z = 4$ ,  $\rho_{\text{calc}} = 1.416 \text{ g cm}^{-3}$ ,  $\mu (\text{Mo } K\alpha) = 0.71073 \text{ cm}^{-1}$ , multi-scan,  $\text{trans}_{\min} = 0.3958$ ,  $\text{trans}_{\max} = 0.7457$ ,  $F(000) = 592.0$ . The total number of reflections were 19 852 ( $-10 \leq h \leq 10$ ,  $-14 \leq k \leq 14$ ,  $-21 \leq l \leq 21$ ) measured in the range  $5.138^\circ \leq 2\Theta \leq 56.308^\circ$ , completeness  $\Theta_{\max} = 100.0\%$ , 3 268 unique ( $R_{\text{int}} = 0.0890$ ,  $R_{\text{sigma}} = 0.0651$ ) which were used in all calculations; Final indices:  $R_{1\text{obs}} = 0.0566$ ,  $wR_{2\text{obs}} =$

0.1293 [ $I \geq 2\sigma(I)$ ];  $R_{1\text{all}} = 0.0881$ ,  $wR_{2\text{all}} = 0.1464$  [all data], GOOF = 1.033, largest difference peak and hole 0.36/-0.27 e  $\text{\AA}^{-3}$ .

*Crystal data of compound 3*: Colorless crystals of compound **3** were obtained from a methanol solution after slow evaporation in a refrigerator for 2 weeks.  $\text{C}_{15}\text{H}_{16}\text{O}_4$ ,  $M_r = 260.28 \text{ g mol}^{-1}$ ; size  $0.344 \times 0.078 \times 0.068 \text{ mm}$ ; orthorhombic, space group  $P2_12_12_1$ ,  $a = 7.1897(6) \text{ \AA}$ ,  $b = 13.5319(10) \text{ \AA}$ ,  $c = 28.297(2) \text{ \AA}$ ,  $\alpha = 90^\circ$ ,  $\beta = 90^\circ$ ,  $\gamma = 90^\circ$ ;  $V = 2753.3(2) \text{ \AA}^3$ ,  $Z = 8$ ,  $\rho_{\text{calc}} = 1.256 \text{ g cm}^{-3}$ ,  $\mu (\text{Mo K}\alpha) = 0.71073 \text{ cm}^{-1}$ , multi-scan,  $\text{trans}_{\text{min}} = 0.6947$ ,  $\text{trans}_{\text{max}} = 0.7471$ ,  $F(000) = 1104.0$ . The total number of reflections were 29 289 ( $-9 \leq h \leq 9$ ,  $-18 \leq k \leq 14$ ,  $-37 \leq l \leq 37$ ) measured in the range  $5.84^\circ \leq 2\theta \leq 56.574^\circ$ , completeness  $\Theta_{\text{max}} = 100\%$ , 6819 unique ( $R_{\text{int}} = 0.0832$ ,  $R_{\text{sigma}} = 0.0585$ ) which were used in all calculations; Final indices:  $R_{1\text{obs}} = 0.0516$ ,  $wR_{2\text{obs}} = 0.1116 [I \geq 2\sigma(I)]$ ;  $R_{1\text{all}} = 0.1015$ ,  $wR_{2\text{all}} = 0.1368$  [all data], GOOF = 1.000, Flack parameter =  $-0.6(8)$ , largest difference peak and hole 0.175/-0.152 e  $\text{\AA}^{-3}$ .

The crystallographic data for compounds **2** and **3** has been deposited to the Cambridge Crystallographic Data Center as supplementary publication no. CCDC 1847811 and 1847809, respectively. Copies of the data are available online free of charge at <http://www.ccdc.cam.ac.uk> (or from CCDC, 12 Union Road, Cambridge CB2 1EZ, e-mail: deposit@ccdc.cam.ac.uk, fax: +44-1223-336033).

## 2.6 Antimicrobial assay

The antibacterial activity of the compounds **1–5** was assayed on four Gram-positive bacteria: *Staphylococcus aureus* (ATCC 29213), Methicillin-Resistant *Staphylococcus aureus* (ATCC 43300, MRSA), *Enterococcus faecalis* (ATCC 29212) and Vancomycin-Resistant *Enterococcus faecalis* (ATCC 51212, VRE), and on the Gram-negative *Escherichia coli* (ATCC 25922). Initially, the strains were previously seeded in Petri dishes containing Mueller Hinton agar (Difco™), which were incubated for 24 hours at temperature of  $35 \pm 2^\circ \text{C}$ , under aerobic conditions. Posteriorly the isolated colonies were collected and suspended in sterile saline solution (NaCl 0.85% (w/v)). This suspension was then used to obtain the bacterial inoculum in Mueller Hinton Broth -MHB (Difco™) with final bacterial concentration of  $5 \times 10^5 \text{ CFU/mL}$ . The method used was broth microdilution in 96-well plate, and the minimum inhibitory concentrations (MICs) of the substances was determined according to Clinical Laboratory Standards Institute [34]. Rifampicin was used as positive control. The microplates were incubated at same

conditions cited above and the MIC was determined after observation of the absence of bacterial growth in the culture medium.

### 3. Results and discussion

Five compounds (**1–5**) were isolated from the EtOAc extract obtained in the fermentation broth of a marine bacterial strain of *S. arenicola*. The structures of compounds **1–5** were established by a combination of their 1D and 2D NMR, HR-ESIMS spectroscopic data, and single-crystal X-ray diffraction analyses, including comparison with previously published data of analogous compounds, as described below (Figure 1).

Compound **1** was isolated as a yellowish oil. Its molecular formula was assigned as C<sub>13</sub>H<sub>15</sub>NO<sub>4</sub> based on the [M + Na]<sup>+</sup> ion peak at *m/z* 272.0905 (calcd *m/z* 272.0899) by HR-ESIMS. The <sup>1</sup>H NMR spectrum exhibited signals at δ<sub>H</sub> 7.26 (d, *J* = 8.1 Hz, H-4), 6.54 (dd, *J* = 8.1, 2.1 Hz, H-5) and 6.42 (d, *J* = 2.1 Hz, H-7), typical of benzene ring AMX system. In addition, it also displayed signals for methylene diastereotopic protons at δ<sub>H</sub> 3.18 (d, *J* = 17.0 Hz, H-8b) and 2.94 (d, *J* = 17.0 Hz, H-8a), and one methyl group at δ<sub>H</sub> 2.18 (s) characteristic of a 2-oxopropyl group, as well as two singlets at δ<sub>H</sub> 3.83 (s) and 3.19 (s) corresponding to one OCH<sub>3</sub> and one NCH<sub>3</sub>, respectively. The <sup>13</sup>C NMR spectrum showed signals to 13 carbon atoms which were classified, from the DEPT and HSQC spectra, as three methyl, one methylene, three sp<sup>2</sup> methines, and six non-hydrogenated carbons, two of which corresponding to the carbonyls at δ<sub>C</sub> 207.8 (C-9) and 176.9 (C-2) (Table 1). These data were consistent with the structure of 3-hydroxy-*N*-methyl-2-oxindole derivative. In fact, except for the 2-oxopropyl moiety the <sup>1</sup>H and <sup>13</sup>C NMR data of **1** were similar to those of 3-hydroxy-6-methoxy-*N*-methyl-2-oxindole (**4**), previously synthesized by Chen and co-workers [35]. The unequivocal position of the 2-oxopropyl substituent at C-3 was inferred by the HMBC correlations of the diastereotopic protons H-8a and H-8b with the carbon signals at δ<sub>C</sub> 176.9 (C-2), 121.9 (C-3a) and 74.1 (C-3) (Figure 2). Based on the aforementioned data, the structure of **1** was established as 3-hydroxy-6-methoxy-3-(2-oxopropyl)-*N*-methyl-2-oxindole. It is interesting to note that natural 3-substituted-3-hydroxy-2-oxindole derivatives bearing an uncommon 2-oxopropyl moiety was previously isolated from the marine Bryozoan *Amanthia convolata* [26].

Compound **2** was isolated as yellow crystals, and its molecular formula of C<sub>13</sub>H<sub>14</sub>NO<sub>4</sub>Cl was defined based on HR-ESIMS whose spectrum displayed a protonated [M + H]<sup>+</sup> molecular ion at *m/z* 284.0692. Its <sup>1</sup>H NMR spectrum exhibited signals for two

*para*-positioned protons at  $\delta_{\text{H}}$  7.37 (s, H-4) and 6.45 (s, H-7), two methylene diastereotopic protons at  $\delta_{\text{H}}$  3.19/2.94 (d,  $J = 17.3$  Hz, 2H-8), and three methyl groups (OCH<sub>3</sub>, NCH<sub>3</sub> and COCH<sub>3</sub>) evidencing a structure similar to that of **1**, but bearing a chlorine atom as substituent at C-5. As expected, the <sup>13</sup>C NMR data of **2** were similar to that observed for **1** (Table 1). The difference in the chemical shifts of **2** when compared to **1** was found to be in the aromatic ring due the replacement of a hydrogen atom by a chlorine atom at C-5 ( $\delta_{\text{C}}$  116.2), corroborating with the observed *para*-positioned protons in the <sup>1</sup>H NMR spectrum. In addition, the complete structure of **2** was confirmed by a single-crystal X-ray diffraction analysis (Figure 3) as 5-chloro-3-hydroxy-6-methoxy-3-(2-oxopropyl)-*N*-methyl-2-oxindole.

Compound **3**, colorless crystals, had its molecular formula C<sub>15</sub>H<sub>16</sub>O<sub>4</sub> deduced through the protonated [M + H]<sup>+</sup> ion at  $m/z$  261.1123 (calcd 261.1127) observed by HR-ESIMS. The <sup>1</sup>H NMR spectrum displayed signals for a monosubstituted benzene ring at  $\delta_{\text{H}}$  7.28-7.33 (m, 5H), an olefinic proton at  $\delta_{\text{H}}$  6.08 (s, H-5), an oxymethine proton at  $\delta_{\text{H}}$  4.76 (d,  $J = 8.7$  Hz, H-8) and a methine 2.87 (dq,  $J = 8.7$  and 7 Hz, H-7), in addition to two methyl groups at  $\delta_{\text{H}}$  1.87 (s, H-15) and 0.96 (d,  $J = 7.0$  Hz, Me-16). The <sup>13</sup>C NMR spectrum exhibited 15 carbon signals defined, through APT spectra, as two methyl, eight methines, and five sp<sup>2</sup> non-hydrogenated carbons, including one extended conjugated lactone carboxyl at  $\delta_{\text{C}}$  168.0 (C-2) and two oxygenated sp<sup>2</sup> carbons at  $\delta_{\text{C}}$  169.3 (C-4) and 166.1 (C-6) (Table 1). These data led to the suggesting of a structure for a 4-hydroxypyran-2-one derivative, similar to a known tetraketide, previously isolated from a mutant strain of *Amycolatopsis mediterranei* [36], but bearing a non-substituted aromatic ring instead of a hydroxylated ring as the above-mentioned tetraketide and confirmed by 2D NMR as showed in figure 2. The dipolar interaction of the methyl protons at  $\delta_{\text{H}}$  0.96 (Me-16) with the oxymethine proton at  $\delta_{\text{H}}$  4.76 (H-8) indicated an *anti*-positioning of both the Me-16 and HO-8, as observed previously for similar compounds [36]. The unequivocal structure of **3** were confirmed by a single-crystal X-ray diffraction analysis (Figure 4). Thus, the structure of **3** was established as 4-hydroxy-6-(2-hydroxy-2-phenyl-1-methylethyl)-3-methyl-2H-pyran-2-one.

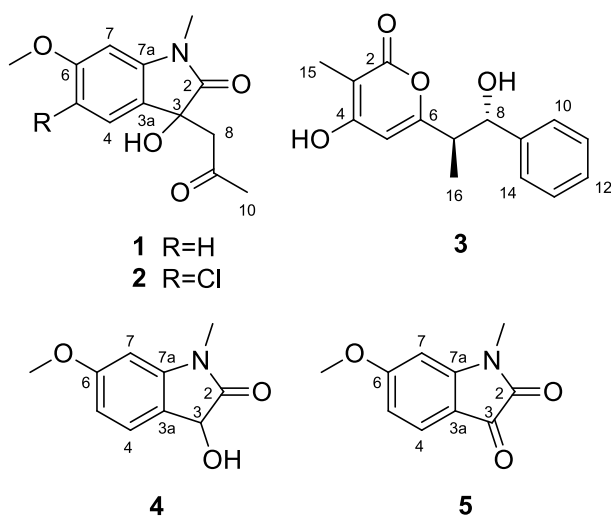


**Figure 1.** Chemical structures of compounds 1–5.

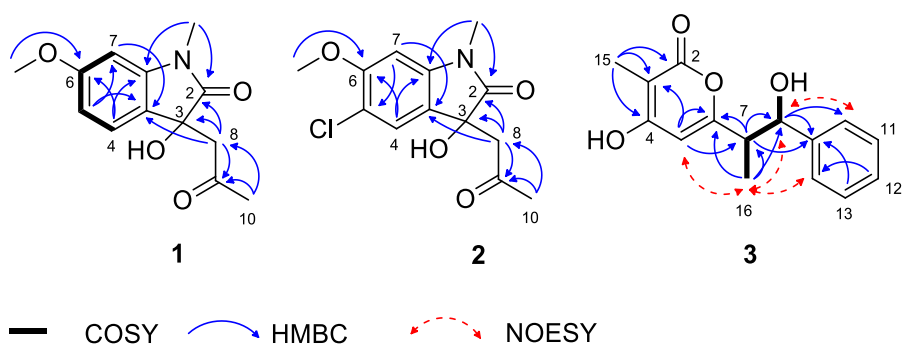


**Figure 2.** Key COSY, HMBC and NOESY correlations of compounds 1–3.

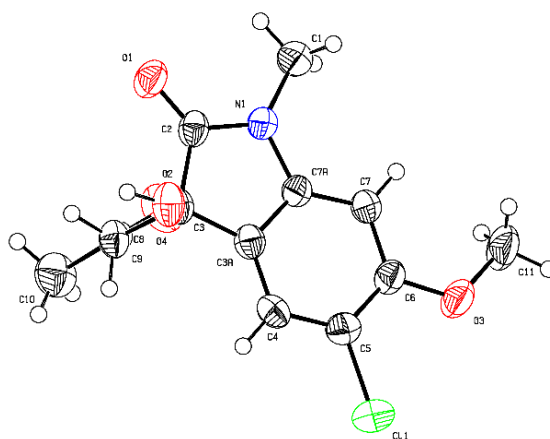


**Figure 3.** Asymmetric unit of the crystalline structure of compound 2.

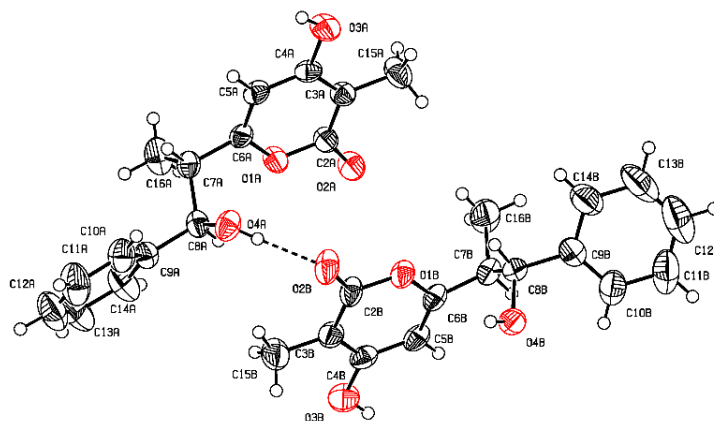


**Figure 4.** Asymmetric unit of the crystalline structure of compound **3**.

**Table 1.**  $^1\text{H}$  and  $^{13}\text{C}$  NMR Data Assignment for Compounds **1–3** ( $\delta$  in ppm).

no.	<u>1<sup>a</sup></u>		<u>2</u>		<u>3<sup>b</sup></u>	
	$\delta_{\text{C}}$ , type	$\delta_{\text{H}}$	$\delta_{\text{C}}$ , type	$\delta_{\text{H}}$	$\delta_{\text{C}}$ , type	$\delta_{\text{H}}$
2	176.9, C		176.0, C		168.0, C	
3	74.1, C		73.9, C		99.4, C	
3a	121.9, C		121.8, C			
4	125.0, CH	7.26 d (8.1)	125.8, CH	7.37 s	169.3, C	
5	106.8, CH	6.54 dd (8.1, 2.1)	116.2, C		102.3, CH	6.08 s
6	161.8, C		156.7, C		166.1, C	
7	97.0, CH	6.42 d (2.1)	94.2, CH	6.46 s	47.4, CH	2.87, dq (8.7, 7.0)
7a	145.2, C		143.7, C			
8	49.2, CH <sub>2</sub>	2.94 d (17.0)	48.7, CH <sub>2</sub>	2.94 d (17.3)	77.1, CH	4.76, d (8.7)
		3.18 d (17.0)		3.19 d (17.3)		

9	207.8, C		207.3, C		143.9, C	
10	31.6, CH <sub>3</sub>	2.18 s	31.1, CH <sub>3</sub>	2.19 s	128.1, CH	7.33, m
11					129.5, CH	7.33, m
12					129.0, CH	7.28, m
15					8.4, CH <sub>3</sub>	1.87, s
16					15.6, CH <sub>3</sub>	0.96, d (7.0)
N-CH <sub>3</sub>	26.5, CH <sub>3</sub>	3.19 s	26.4, CH <sub>3</sub>	3.22 s		
O-CH <sub>3</sub>	55.8, CH <sub>3</sub>	3.83 s	56.4, CH <sub>3</sub>	3.96 s		

<sup>a</sup> Compound **1** (CDCl<sub>3</sub>, 300 MHz).

<sup>a</sup> Compound **2** (CDCl<sub>3</sub>, 600 MHz).

<sup>b</sup> Compound **3** (CD<sub>3</sub>OD, 300 MHz).

<sup>c</sup> Chemical shift deduced from the HSQC and HMBC experiments.

In addition to **1–3**, the known compounds 3-hydroxy-*N*-methyl-2-oxindole (**4**), and 6-methoxy-*N*-methylisatin (**5**) were also isolated. Despite the very simple NMR data suggesting that compound **4** was pure enough, the very low value of its  $[\alpha]_D^{22}$  required a further analysis by HPLC using a chiral-phase column (Fig. S23 in Supplementary material). Indeed, two peaks in a 1:2 ratio were observed, what is in agreement with a scalemic mixture. Compound **4** had been described as a synthetic product [35] and this study is the first report of its isolation as a natural source, while **5** was solely isolated from the plant *Boronella koniambiensis* (Rutaceae) [37].

The antibacterial activity of compounds **1** to **5** were assayed against Gram-positive (*Enterococcus faecalis* and *Staphylococcus aureus*) and Gram-negative (*Escherichia coli*) bacteria strains, but only **4** and **5** were active showing susceptibility on *E. faecalis* with MIC value of 15.6 µg/mL (Table S1 in Supplementary material).



#### 4. Conclusions

One new 4-hydroxy-pyran-2-one and two new 3-hydroxy-*N*-methyl-2-oxindole derivatives were isolated from *S. arenicola*. A similar tetraketide was previously isolated from a marine mutant strain of *Amycolatopsis mediterranei*, the rifamycin producer [36]. On the other hand, isatins are putative compounds produced by higher plants although there are some few examples from marine microorganisms [38,39].

#### Acknowledgments

The authors express gratitude to Secretaria da Comissão Interministerial dos Recursos do Mar (SECIRM) for providing all the logistic support disposed to the scientific expedition, as part of the Program PROARQUIPELAGO. This research was financially supported by CNPq (No. 420454/2016-0 and 309060/2016-8), CAPES/FUNCAP (No. 88887.113263/2015-01) and INCT BioNat (No. 465637/2014-0).

#### Conflict of interest

The authors declare no competing financial interest.

#### Appendix A. Supplementary data

Supplementary material (<sup>1</sup>H and <sup>13</sup>C NMR, COSY, HSQC, HMBC, NOESY and HR-ESIMS) is available free of charge at doi: 10.1016/j.fitote.2019.104357.

#### References

- [1] L.A. Maldonado, W. Fenical, P.R. Jensen, C.A. Kauffman, T.J. Mincer, A.C. Ward, A.T. Bull, M. Goodfellow, *Salinispora arenicola* gen. nov., sp. nov. and *Salinispora tropica* sp. nov., obligate marine actinomycetes belonging to the family Micromonosporaceae, *Int. J. Syst. Evol. Microbiol.* 55 (2005) 1759–1766. doi:10.1099/ijs.0.63625-0.
- [2] P.R. Jensen, P.G. Williams, D.C. Oh, L. Zeigler, W. Fenical, Species-specific secondary metabolite production in marine actinomycetes of the genus *Salinispora*, *Appl. Environ. Microbiol.* 73 (2007) 1146–1152. doi:10.1128/aem.01891-06.
- [3] P.R. Jensen, B.S. Moore, W. Fenical, The marine actinomycete genus *Salinispora*: a model organism for secondary metabolite discovery, *Nat. Prod. Rep.* 32 (2015)

- 738–751. doi:10.1039/c4np00167b.
- [4] R.H. Feling, G.O. Buchanan, T.J. Mincer, C.A. Kauffman, P.R. Jensen, W. Fenical, Salinosporamide A: A highly cytotoxic proteasome inhibitor from a novel microbial source, a marine bacterium of the new genus *Salinospira*, *Angew. Chemie - Int. Ed.* 42 (2003) 355–357. doi:10.1002/anie.200390115.
- [5] K.A. Reed, R.R. Manam, S.S. Mitchell, J. Xu, S. Teisan, T.H. Chao, G. Deyanat-Yazdi, S.T.C. Neuteboom, K.S. Lam, B.C.M. Potts, Salinosporamides D-J from the marine actinomycete *Salinispira tropica*, bromosalinosporamide, and thioester derivatives are potent inhibitors of the 20S proteasome, *J. Nat. Prod.* 70 (2007) 269–276. doi:10.1021/np0603471.
- [6] B.T. Murphy, T. Narendar, C.A. Kauffman, M. Woolery, P.R. Jensen, W. Fenical, Saliniquinones A-F, new members of the highly cytotoxic anthraquinone- $\gamma$ -pyrones from the marine actinomycete *Salinispira arenicola*, *Aust. J. Chem.* 63 (2010) 929–934. doi:10.1071/ch10068.
- [7] P.G. Williams, E.D. Miller, R.N. Asolkar, P.R. Jensen, W. Fenical, Arenicolides A-C, 26-membered ring macrolides from the marine actinomycete *Salinispira arenicola*, *J. Org. Chem.* 72 (2007) 5025–5034. doi:10.1021/jo061878x.
- [8] P.G. Williams, R.N. Asolkar, T. Kondratyuk, J.M. Pezzuto, P. R. Jensen, W. Fenical, Saliniketals A and B, bicyclic polyketides from the marine actinomycete *Salinispira arenicola*, *J. Nat. Prod.* 70 (2007) 83–88. doi:10.1021/np0604580.
- [9] R.N. Asolkar, K.C. Freel, P.R. Jensen, W. Fenical, T. P. Kondratyuk, E. J. Park, J.M. Pezzuto, Arenamides A - C, cytotoxic NF $\kappa$ B inhibitors from the marine actinomycete *Salinispira*, *J. Nat. Prod.* 72 (2009) 396–402. doi:10.1021/np800617a.
- [10] D.C. Oh, E.A. Gontang, C.A. Kauffman, P.R. Jensen, W. Fenical, Salinipyrones and pacificanones, mixed-precursor polyketides from the marine actinomycete *Salinispira pacifica*, *J. Nat. Prod.* 71 (2008) 570–575. doi:10.1021/np0705155.
- [11] T. Awakawa, M. Crüsemann, J. Munguia, N. Ziemert, V. Nizet, W. Fenical, B.S. Moore, Salinipyrene and pacificanone are biosynthetic by-products of the rosamicin polyketide synthase, *ChemBioChem.* 16 (2015) 1443–1447. doi:10.1002/cbic.201500177.
- [12] R.N. Asolkar, T.N. Kirkland, P.R. Jensen, W. Fenical, Arenimycin, an antibiotic effective against rifampin- and methicillin-resistant *Staphylococcus aureus* from the marine actinomycete *Salinispira arenicola*, *J. Antibiot.* 63 (2010) 37–39.

- doi:10.1038/ja.2009.114.
- [13] S. Matsuda, K. Adachi, Y. Matsuo, M. Nukina, Y. Shizuri, Salinisporamycin, a novel metabolite from *Salinispora arenicora*, J. Antibiot. 62 (2009) 519–526. doi:10.1038/ja.2009.75.
- [14] P.G. Williams, G.O. Buchanan, R.H. Felting, C.A. Kauffman, P.R. Jensen, W. Fenical, New cytotoxic salinosporamides from the marine actinomycete *Salinispora tropica*, J. Org. Chem. 70 (2005) 6196–6203. doi:10.1021/jo050511+.
- [15] J. Prudhomme, E. McDaniel, N. Ponts, S. Bertani, W. Fenical, P. Jensen, K. Le Roch, Marine actinomycetes: A new source of compounds against the human malaria parasite, PLoS One. 3 (2008). doi:10.1371/journal.pone.0002335.
- [16] A. Miyanaga, J.E. Janso, L. McDonald, M. He, H. Liu, L. Barbieri, A.S. Eustáquio, E.N. Fielding, G.T. Carter, P.R. Jensen, X. Feng, M. Leighton, F.E. Koehn, B.S. Moore, Discovery and assembly-line biosynthesis of the lymphostin pyrroloquinoline alkaloid family of mtor inhibitors in *Salinispora* bacteria, J. Am. Chem. Soc. 133 (2011) 13311–13313. doi:10.1021/ja205655w.
- [17] E.G. Ferreira, M. D. C.M. Torres, A.B. Da Silva, L.L.F. Colares, K. Pires, T.M.C. Lotufo, E.R. Silveira, O.D.L. Pessoa, L. V. Costa-Lotufo, P.C. Jimenez, Prospecting anticancer compounds in actinomycetes recovered from the sediments of Saint Peter and Saint Paul's Archipelago, Brazil, Chem. Biodivers. 13 (2016) 1149–1157. doi:10.1002/cbdv.201500514.
- [18] A.E.T. Silva, L.A. Guimarães, E.G. Ferreira, M. D. C. M. Torres, A.B. Da Silva, P.C. Branco, F.A.S. Oliveira, G.G.Z. Silva, D. V. Wilke, E.R. Silveira, O.D.L. Pessoa, P.C. Jimenez, L. V. Costa-Lotufo, Bioprospecting anticancer compounds from the marine-derived actinobacteria *Actinomadura* sp. collected at the Saint Peter and Saint Paul Archipelago (Brazil), J. Braz. Chem. Soc. 28 (2017) 465–474. doi:10.21577/0103-5053.20160297.
- [19] T.D.S. Sousa, P.C. Jimenez, E.G. Ferreira, E.R. Silveira, R. Braz-Filho, O.D.L. Pessoa, L. V. Costa-Lotufo, Anthracyclines from *Micromonospora* sp., J. Nat. Prod. 75 (2012) 489–493. doi:10.1021/np200795p.
- [20] A.B. Silva, E.R. Silveira, D. V Wilke, E.G. Ferreira, L. V Costa-lotufo, M. M. C. Torres, A.P. Ayala, W.S. Costa, K.M. Canuto, A. R. Araújo-Nobre, A. J. Araújo, J. D. B. Marinho Filho, O.D.L Pessoa, Antibacterial Salinaphthoquinones from a Strain of the Bacterium *Salinispora arenicola* Recovered from the Marine Sediments of St. Peter and St. Paul Archipelago, Brazil, J. Nat. Prod. 82 (2019)

- 1831–18381. doi:10.1021/acs.jnatprod.9b00062.
- [21] L. M. Vieira, C. M. R. Farrapeira, F. D. Amaral, S. M. A. Lira, Bryozoan biodiversity in Saint Peter and Saint Paul Archipelago, Brazil, *Cah. Biol. Mar.* 53 (2012) 159–167. doi:10.21411/cbm.a.2ce08b6.
- [22] T. Kagata, S. Saito, H. Shigemori, A. Ohsaki, H. Ishiyama, T. Kubota, J. Kobayashi, Paratunamides A-D, oxindole alkaloids from *Cinnamodendron axillare*, *J. Nat. Prod.* 69 (2006) 1517–1521. doi:10.1021/np0602968.
- [23] H. B. Rasmussen, J.K. MacLeod, Total synthesis of donaxaridine, *J. Nat. Prod.* 60 (1997) 1152–1154. doi:10.1021/np970246q.
- [24] J. Peng, T. Lin, W. Wang, Z. Xin, T. Zhu, Q. Gu, D. Li, Antiviral alkaloids produced by the mangrove-derived fungus *Cladosporium* sp. PJX-41, *J. Nat. Prod.* 76 (2013) 1133–1140. doi:10.1021/np400200k.
- [25] W. Balk-Bindseil, E. Helmke, H. Weyland, H. Laatsch, Marine bacteria, VIII. Maremycin A and B, new diketopiperazines from a marine *Streptomyces* sp., *Liebigs Ann.* 1995 (1995) 1291–1294. doi:10.1002/jlac.1995199507171.
- [26] Y. Kamano, H. P. Zhang, Y. Ichihara, H. Kizu, K. Komiyama, G.R. Pettit, Convolutamydine A, a novel bioactive hydroxyoxindole alkaloid from marine bryozoan *Amathia convoluta*, *Tetrahedron Lett.* 36 (1995) 2783–2784. doi:10.1016/0040-4039(95)00395-s.
- [27] S. Peddibhotla, 3-Substituted-3-hydroxy-2-oxindole, an emerging new scaffold for drug discovery with potential anti-cancer and other biological activities, *Curr. Bioact. Compd.* 5 (2009) 20–38. doi:10.2174/157340709787580900.
- [28] M. N. Moghaddam, R. Jalal, Z. Zeraatkar, Synthesis and antiproliferative and apoptosis-inducing activity of novel 3-substituted-3-hydroxy-2-oxindole compounds, *Vitr. Cell. Dev. Biol. - Anim.* 54 (2018) 61–70. doi:10.1007/s11626-017-0204-8.
- [29] A. Bauermeister, K. Velasco-Alzate, T. Dias, H. Macedo, E.G. Ferreira, P.C. Jimenez, T.M.C. Lotufo, N.P. Lopes, S.P. Gaudêncio, L. V. Costa-Lotufo, Metabolomic fingerprinting of *Salinispora* from Atlantic oceanic islands, *Front. Microbiol.* 9 (2018) 3021–3033. doi:10.3389/fmicb.2018.03021.
- [30] O. V. Dolomanov, L.J. Bourhis, R.J. Gildea, J.A.K. Howard, H. Puschmann, OLEX2 : a complete structure solution, refinement and analysis program , *J. Appl. Crystallogr.* 42 (2009) 339–341. doi:10.1107/s0021889808042726.
- [31] G.M. Sheldrick, SHELXT - Integrated space-group and crystal-structure

- determination, *Acta Crystallogr. Sect. A Found. Crystallogr.* 71 (2015) 3–8. doi:10.1107/S2053273314026370.
- [32] G.M. Sheldrick, A short history of SHELX, *Acta Crystallogr. Sect. A Found. Crystallogr.* 64 (2008) 112–122. doi:10.1107/s0108767307043930.
- [33] Burnett, M.N., Johnson, C.K., ORTEP-III: Oak ridge thermal ellipsoid plot program for crystal structure illustrations. United States, **1996**.
- [34] CLSI - Clinical Laboratory Standards Institute (2015) Approved standard M07–A10. Wayne, Pa.
- [35] J. Chen, C. Song, P. Chen, J. Zhu, An intermolecular C–H functionalization method for the synthesis of 3-hydroxy-2-oxindoles, *Org. Biomol. Chem.* 12 (2014) 8390–8393. doi:10.1039/c4ob01643b.
- [36] I. Bułyszko, G. Dräger, A. Klenge, A. Kirschning, Evaluation of the synthetic potential of an AHBA knockout mutant of the rifamycin producer *Amycolatopsis mediterranei*, *Chem. Eur. J.* 21 (2015) 19231–19242. doi:10.1002/chem.201503548.
- [37] R. Grougnet, P. Magiatis, N. Fokialakis, S. Mitaku, A. L. Skaltsounis, F. Tillequin, T. Sévenet, M. Litaudon, Koniamborine, the first pyrano [ 3,2- *b* ] indole alkaloid and other secondary metabolites from *Boronella koniambiensis*, (2005) 1083–1086. doi:10.1021/np050013w.
- [38] C. Wu, C. Du, J. Gubbens, Y.H. Choi, G.P. Van Wezel, Metabolomics-driven discovery of a prenylated isatin antibiotic produced by *Streptomyces* species MBT28, *J. Nat. Prod.* 78 (2015) 2355–2363. doi:10.1021/acs.jnatprod.5b00276.
- [39] K.A. Shaaban, M. Shaaban, V. Nair, I. Schuhmann, H.Y. Win, L. Lei, B. Dittrich, E. Helmke, A. Schüffler, H. Laatsch, Structure elucidation and synthesis of hydroxylated isatins from Streptomycetes, *Z Zeitschrift für Naturforsch. - Sect. B J. Chem. Sci.* 71 (2016) 1191–1198. doi:10.1515/znb-2016-0143.

## SUPPORTING INFORMATION

### Table of Contents

**Table S1.** Antibacterial activity of compounds **1–5** (MIC,  $\mu\text{g/mL}$ ).

**Figure S1.**  $^1\text{H}$  NMR (300 MHz) spectrum of **1** in  $\text{CDCl}_3$

**Figure S2.**  $^{13}\text{C}$  NMR (75 MHz) spectrum of **1** in  $\text{CDCl}_3$

**Figure S3.** DEPT  $135^\circ$  NMR (75 MHz) spectrum of **1** in  $\text{CDCl}_3$

**Figure S4.** COSY NMR spectrum of **1** in  $\text{CDCl}_3$

**Figure S5.** HSQC NMR spectrum of **1** in  $\text{CDCl}_3$

**Figure S6.** HMBC NMR spectrum of **1** in  $\text{CDCl}_3$

**Figure S7.** HR-ESIMS spectrum of **1**

**Figure S8.**  $^1\text{H}$  NMR (600 MHz) spectrum of **2** in  $\text{CDCl}_3$

**Figure S9.** Edited HSQC NMR spectrum of **2** in  $\text{CDCl}_3$

**Figure S10.** HMBC NMR spectrum of **2** in  $\text{CDCl}_3$

**Figure S11.** HR-ESIMS spectrum of **2**

**Figure S12.**  $^1\text{H}$  NMR (300 MHz) spectrum of **3** in  $\text{CD}_3\text{OD}$

**Figure S13.**  $^{13}\text{C}$  NMR (75 MHz) spectrum of **3** in  $\text{CD}_3\text{OD}$

**Figure S14.** APT NMR (75 MHz) spectrum of **3** in  $\text{CD}_3\text{OD}$

**Figure S15.** COSY NMR spectrum of **3** in  $\text{CD}_3\text{OD}$

**Figure S16.** HSQC NMR spectrum of **3** in  $\text{CD}_3\text{OD}$

**Figure S17.** HMBC NMR spectrum of **3** in  $\text{CD}_3\text{OD}$

**Figure S18.** NOESY NMR spectrum of **3** in  $\text{CD}_3\text{OD}$

**Figure S19.** HR-ESIMS spectrum of **3**

**Figure S20.**  $^1\text{H}$  NMR (300 MHz) spectrum of **4** in  $\text{CDCl}_3$

**Figure S21.**  $^{13}\text{C}$  NMR (75 MHz) spectrum of **4** in  $\text{CDCl}_3$

**Figure S22.** DEPT  $135^\circ$  NMR (75 MHz) spectrum of **4** in  $\text{CDCl}_3$

**Figure S23.** Chiral-phase HPLC (isopropanol/n-hexane (5:95), 30 min, flow rate of 1.00 mL/min) analysis of **4**.

**Figure S24.**  $^1\text{H}$  NMR (500 MHz) spectrum of **5** in  $\text{CDCl}_3$

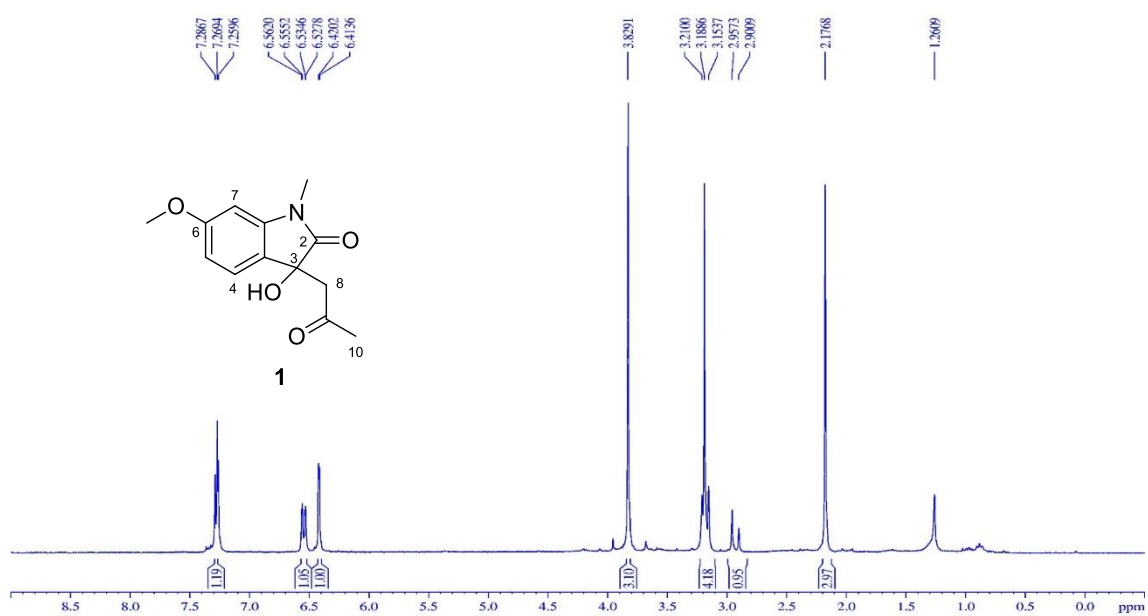
**Figure S25.**  $^{13}\text{C}$  NMR (125 MHz) spectrum of **5** in  $\text{CDCl}_3$

**Figure S26.** DEPT  $135^\circ$  NMR (125 MHz) spectrum of **5** in  $\text{CDCl}_3$

**Table S1.** Antibacterial activity of compounds **1–5** (MIC,  $\mu\text{g/mL}$ ).

Compound	<i>S. aureus</i> (ATCC 29213)	<i>S. aureus</i> (ATCC 43300, MRSA)	<i>E. faecalis</i> (ATCC 29219)	<i>E. faecalis</i> (ATCC 51212, VRE)	<i>Escherichia coli</i> (ATCC 25922)
<b>1</b>	-	-	-	-	*
<b>2</b>	-	-	-	-	-
<b>3</b>	-	-	-	-	*
<b>4</b>	-	-	15.6	-	-
<b>5</b>	-	-	15.6	-	*

No activity in the tested concentrations. Rifampicin showed MIC  $\leq 0.03 \mu\text{g/mL}$  for strains tested.  
\* not evaluated.

**Figure S1.**  $^1\text{H}$  NMR (300 MHz) spectrum of **1** in  $\text{CDCl}_3$ .

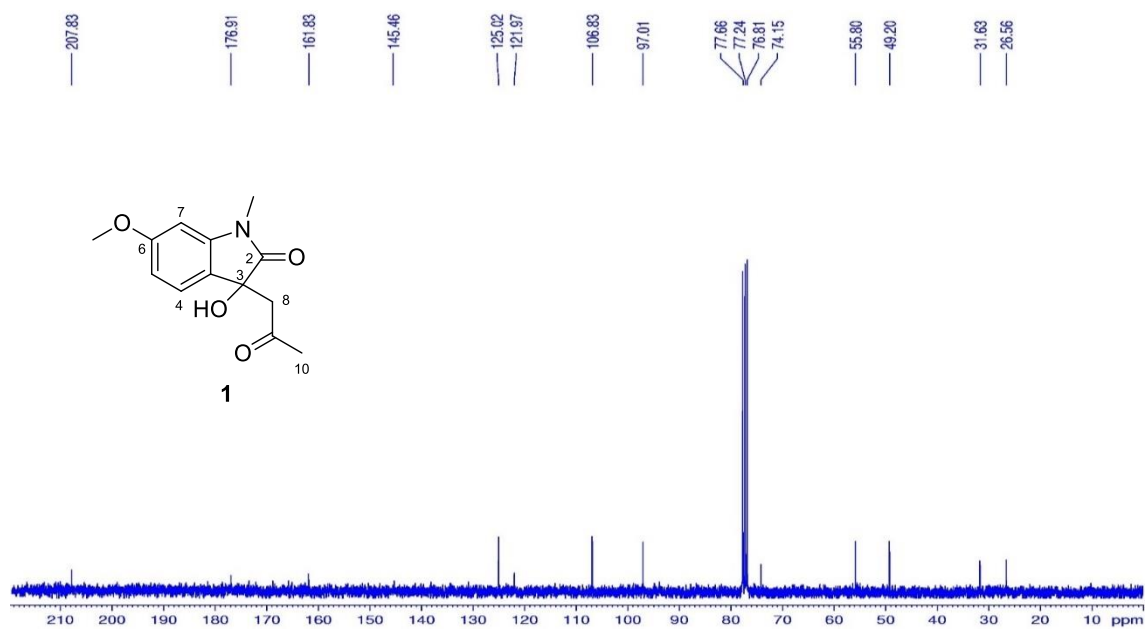


**Figure S2.**  $^{13}\text{C}$  NMR (75 MHz) spectrum of **1** in  $\text{CDCl}_3$ .

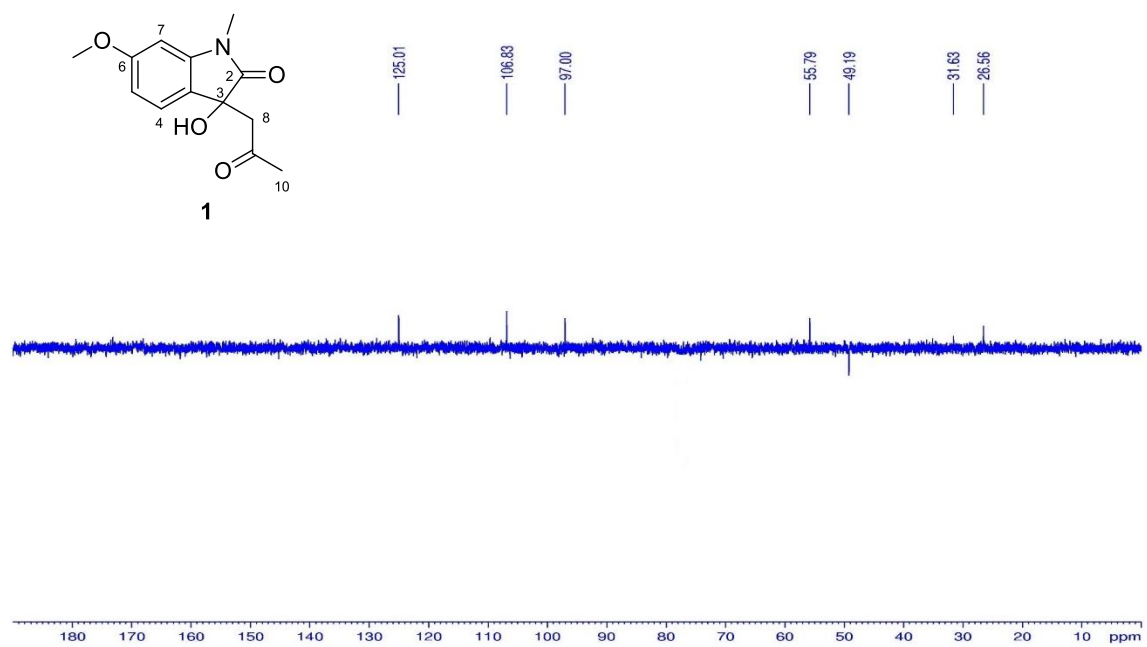


**Figure S3.** DEPT  $135^\circ$  NMR (75 MHz) spectrum of **1** in  $\text{CDCl}_3$ .



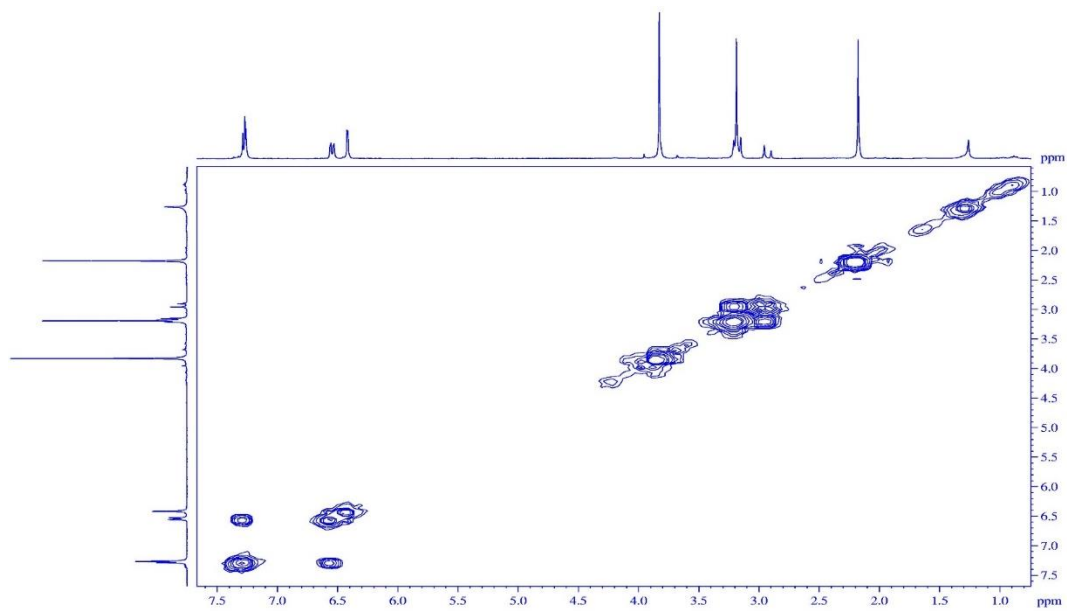


**Figure S4.** COSY NMR spectrum of **1** in  $\text{CDCl}_3$ .

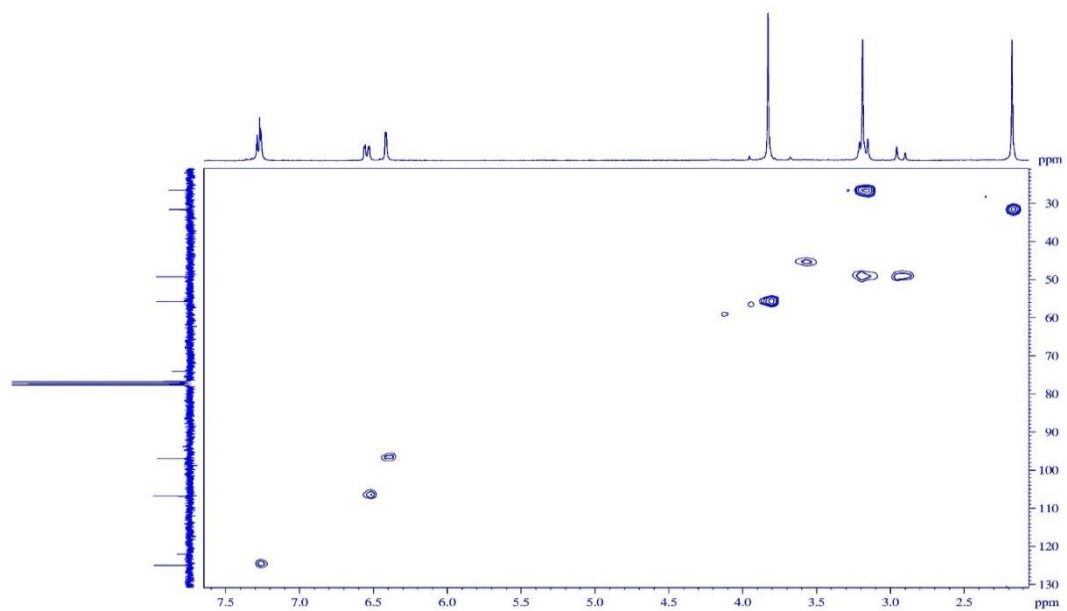


**Figure S5.** HSQC NMR spectrum of **1** in  $\text{CDCl}_3$ .

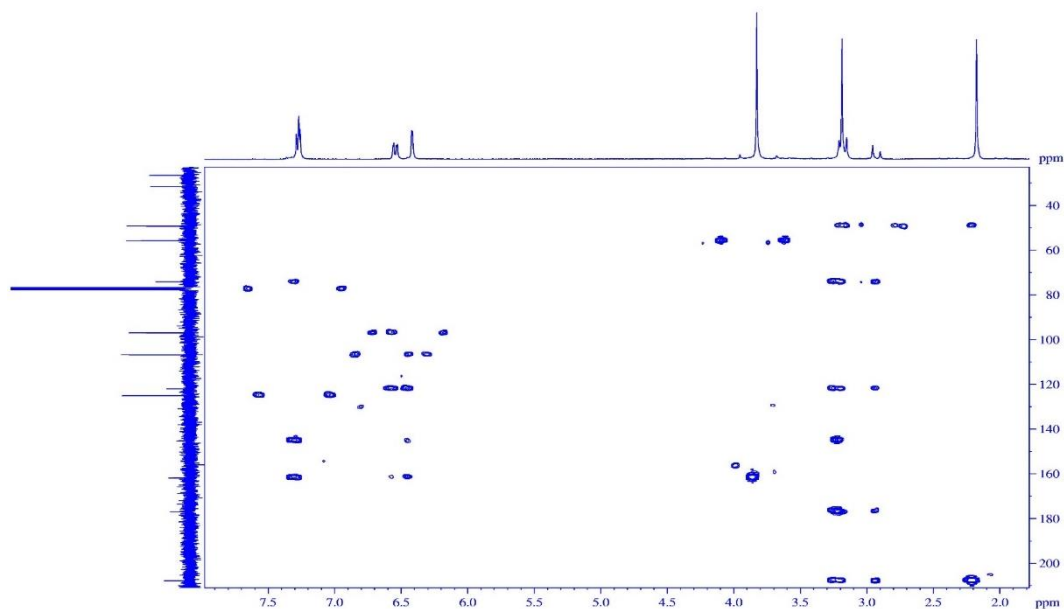
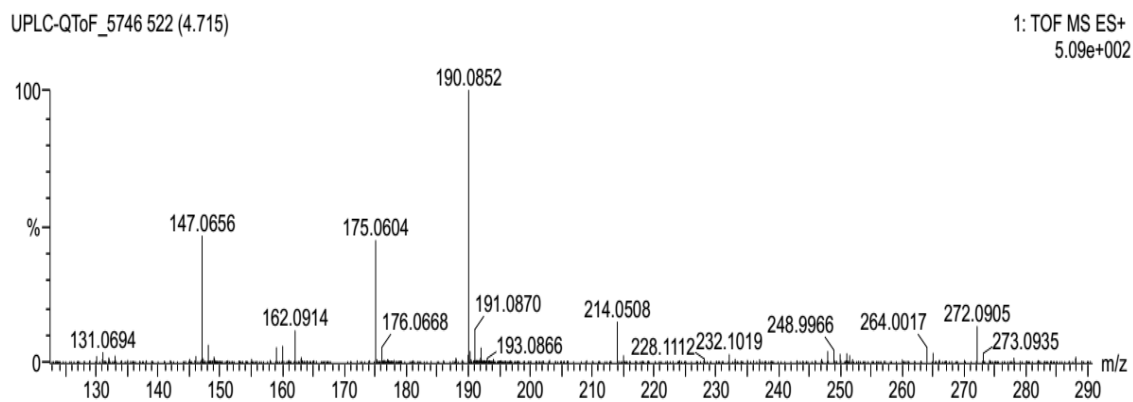


**Figure S6.** HMBC NMR spectrum of **1** in  $\text{CDCl}_3$ .



Minimum: -1.5  
Maximum: 10.0 10.0 50.0

Mass	Calc. Mass	mDa	PPM	DBE	i-FIT	i-FIT (Norm)	Formula
272.0905	272.0899	0.6	2.2	6.5	15.8	0.0	C13 H15 N O4 Na

**Figure S7.** HR-ESIMS spectrum of **1**.

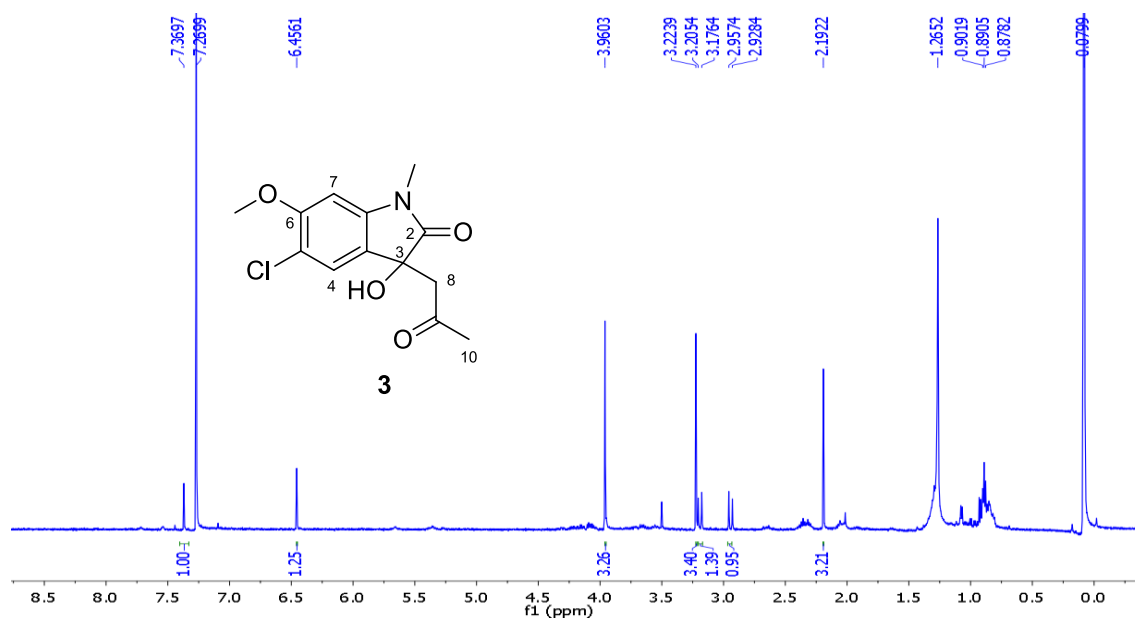


**Figure S8.** <sup>1</sup>H NMR (600 MHz) spectrum of **2** in CDCl<sub>3</sub>.

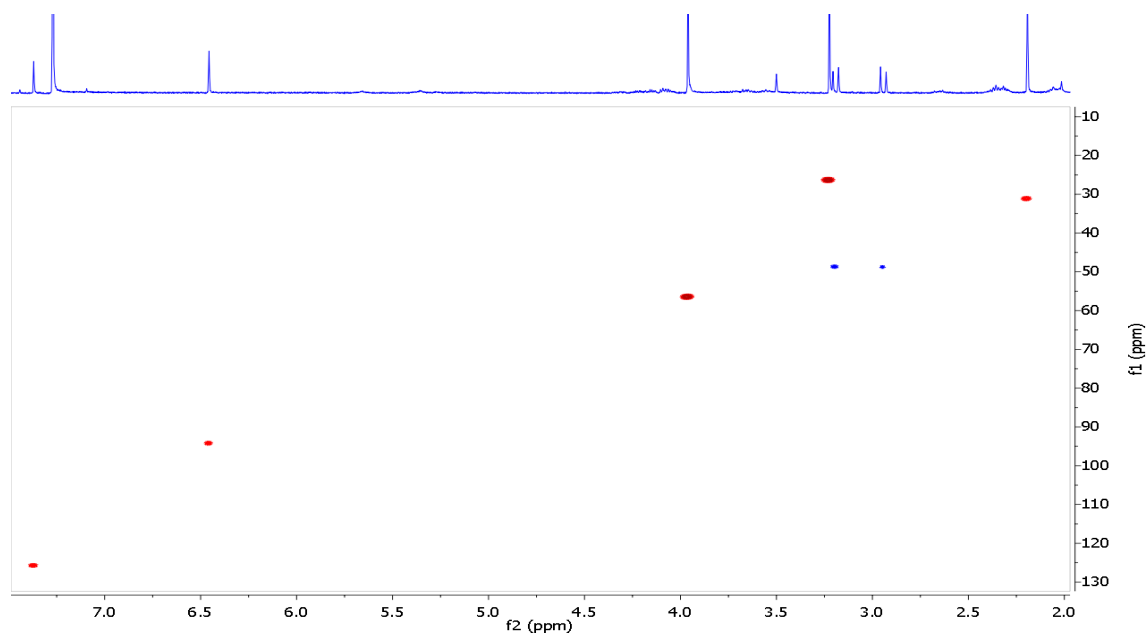


**Figure S9.** Edited HSQC NMR spectrum of **2** in CDCl<sub>3</sub>.

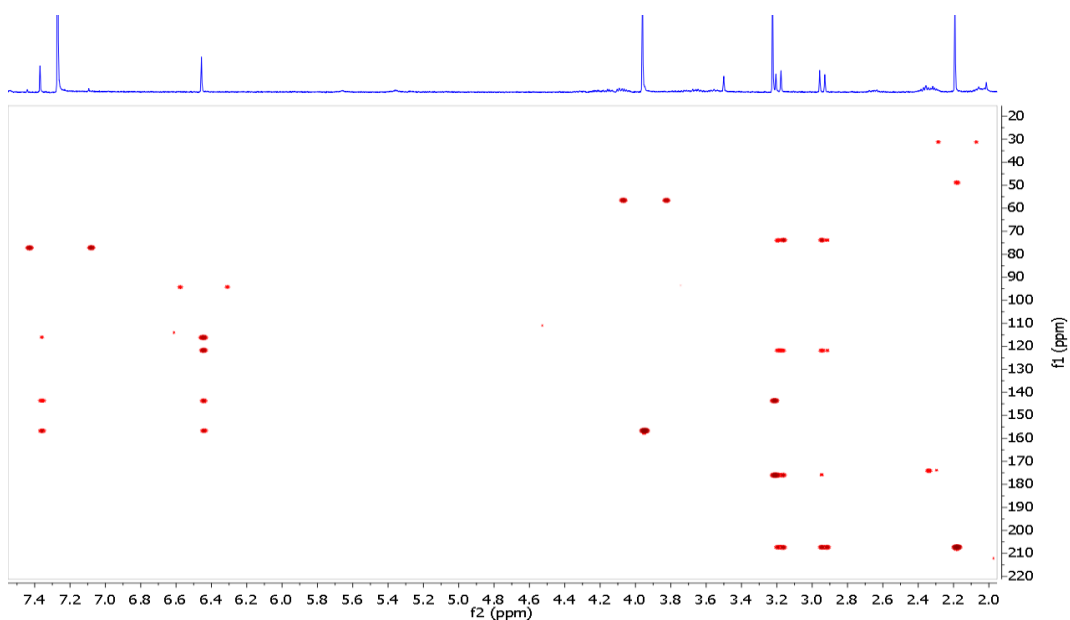
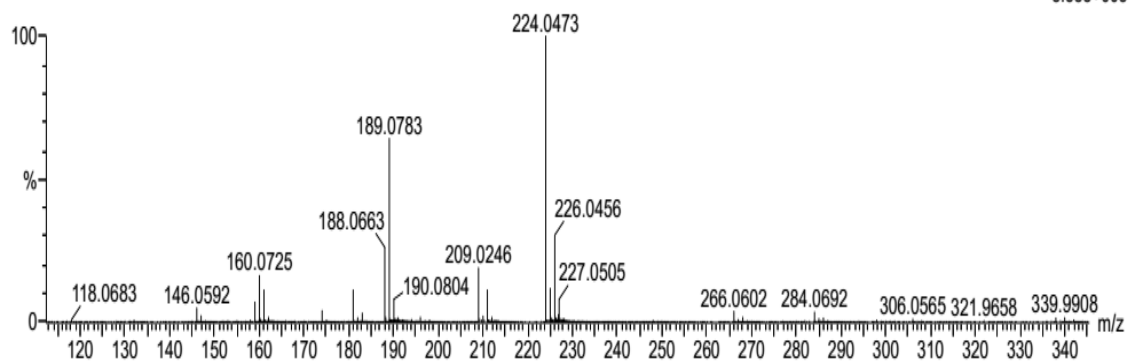


**Figure S10.** HMBC NMR spectrum of **2** in  $\text{CDCl}_3$ .

UPLC-QToF\_5749 577 (5.212)

1: TOF MS ES+  
8.38e+003



Minimum: -1.5

Maximum: 10.0 10.0 50.0

Mass	Calc. Mass	mDa	PPM	DBE	i-FIT	i-FIT (Norm)	Formula
284.0692	284.0690	0.2	0.7	6.5	61.2	0.0	C13 H15 N O4 Cl

**Figure S11.** HR-ESIMS spectrum of **2**.

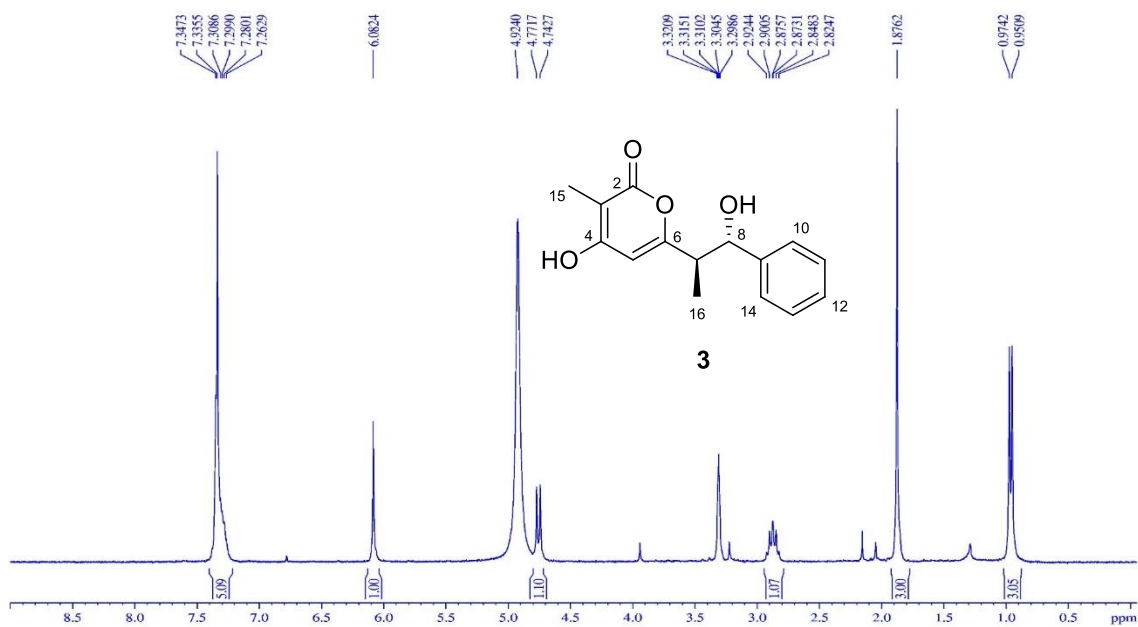


**Figure S12.**  $^1\text{H}$  NMR (300 MHz) spectrum of **3** in  $\text{CD}_3\text{OD}$ .

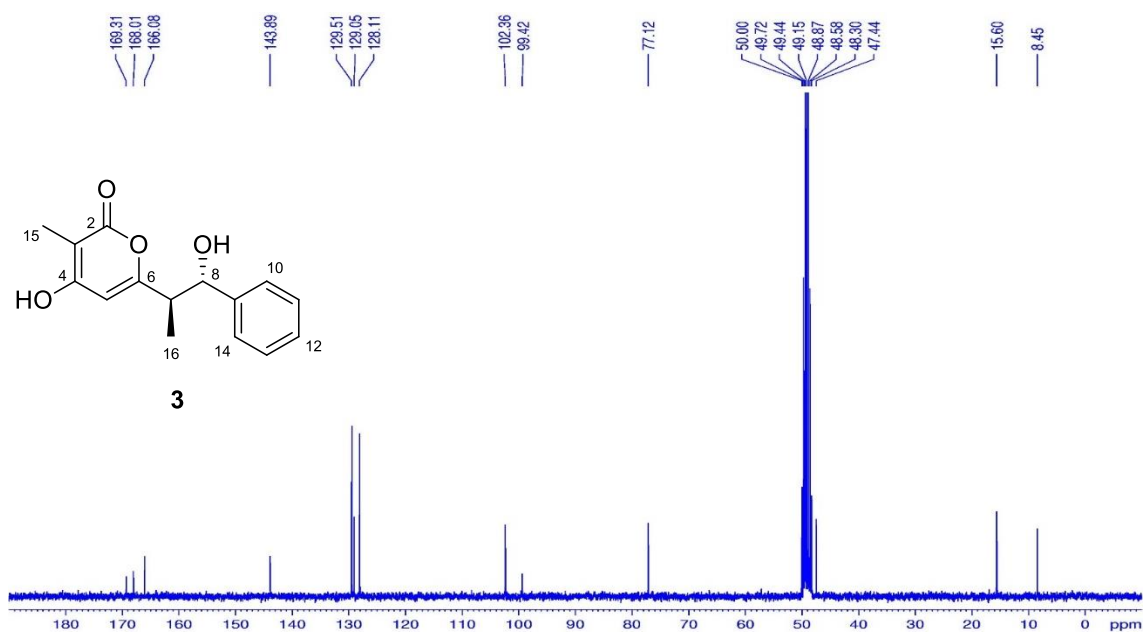


**Figure S13.**  $^{13}\text{C}$  NMR (75 MHz) spectrum of **3** in  $\text{CD}_3\text{OD}$ .

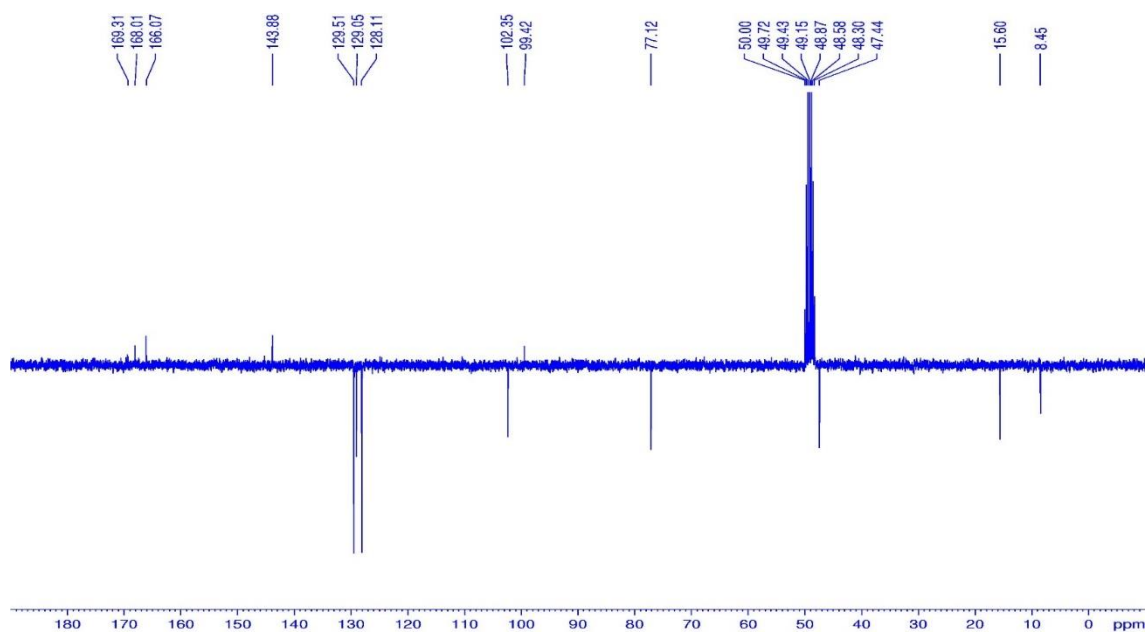


**Figure S14.** APT NMR (75 MHz) spectrum of **3** in CD<sub>3</sub>OD.

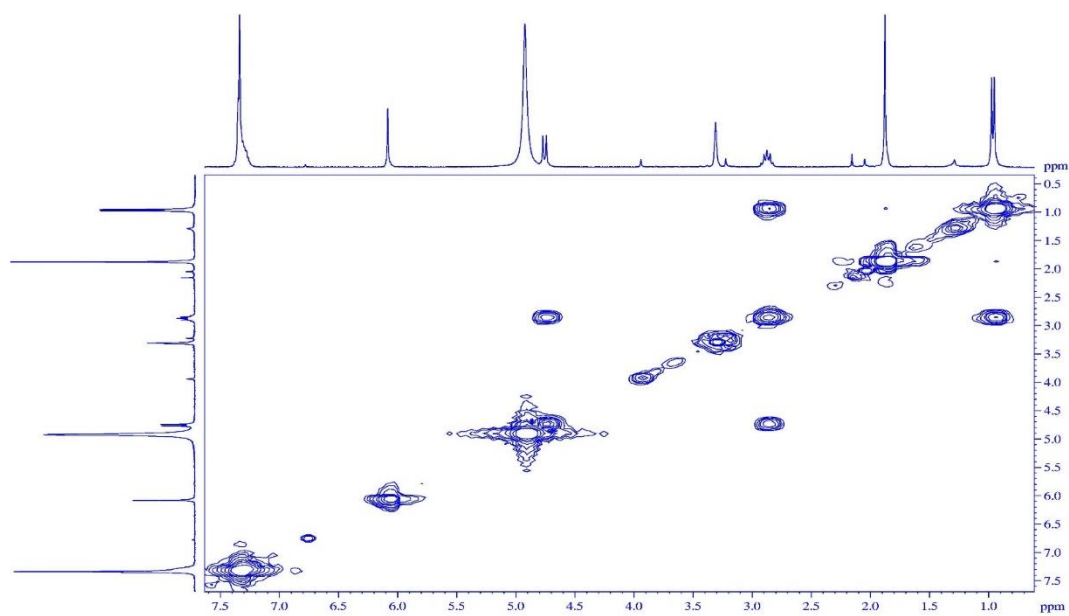


**Figure S15.** COSY NMR spectrum of **3** in CD<sub>3</sub>OD.

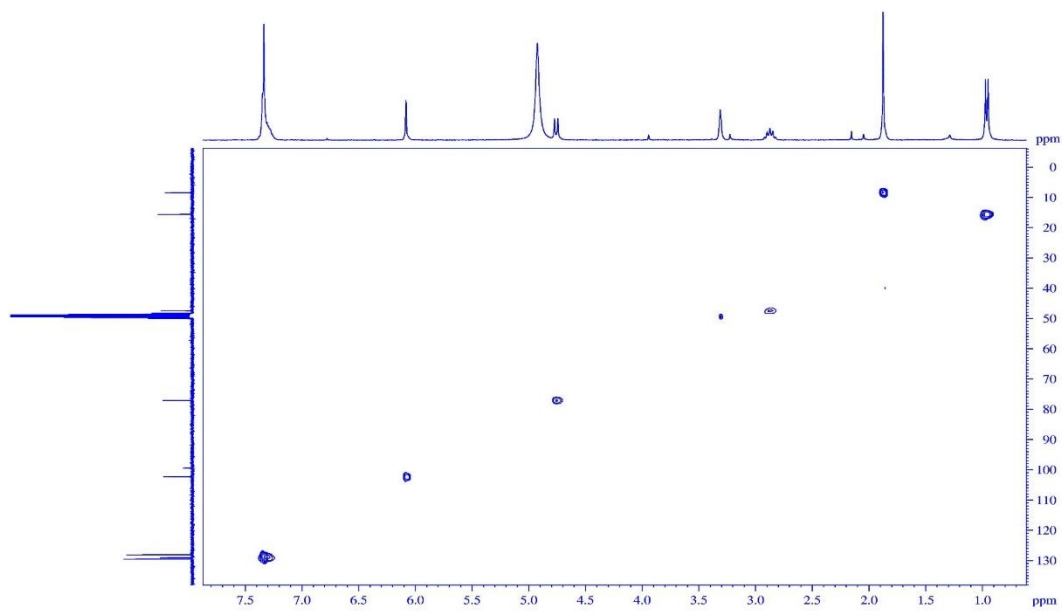


**Figure S16.** HSQC NMR spectrum of **3** in CD<sub>3</sub>OD.

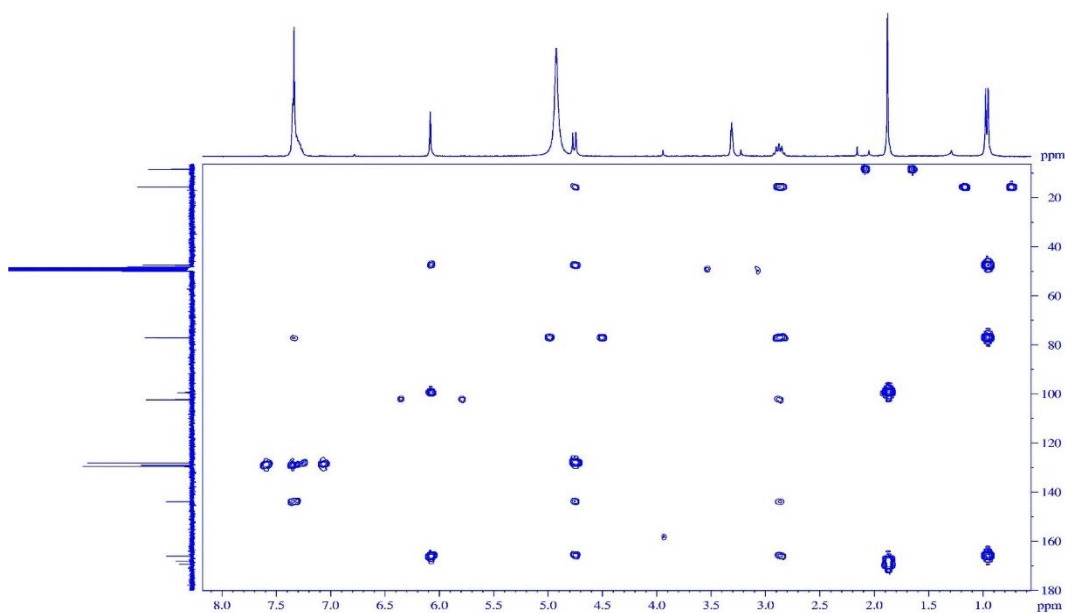


**Figure S17.** HMBC NMR spectrum of **3** in CD<sub>3</sub>OD.

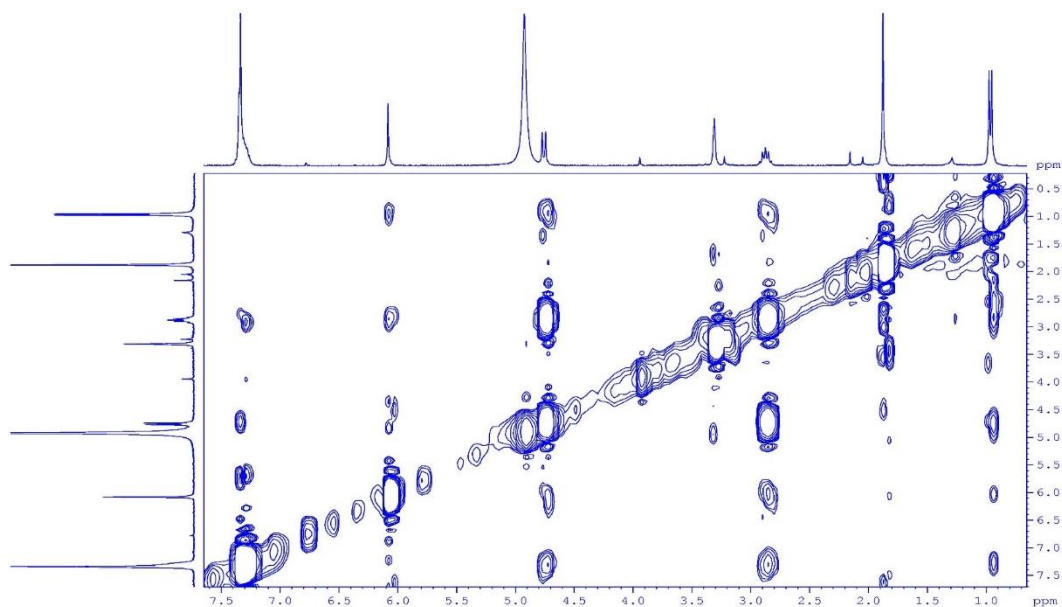


**Figure S18.** NOESY NMR spectrum of **3** in CD<sub>3</sub>OD.

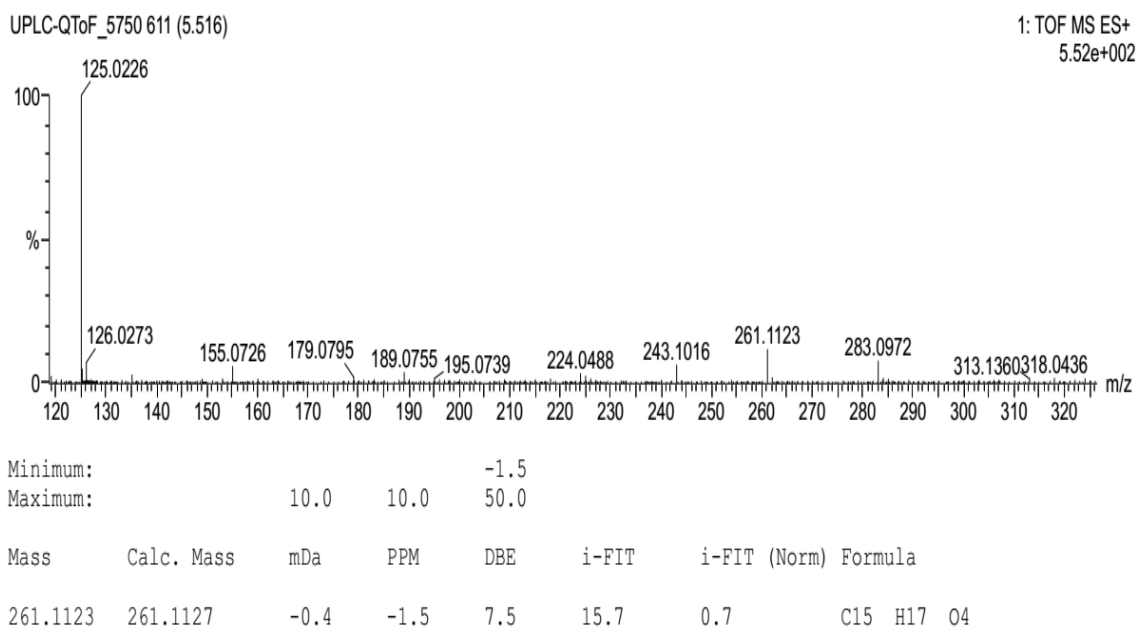


**Figure S19.** HR-ESIMS spectrum of **3**.



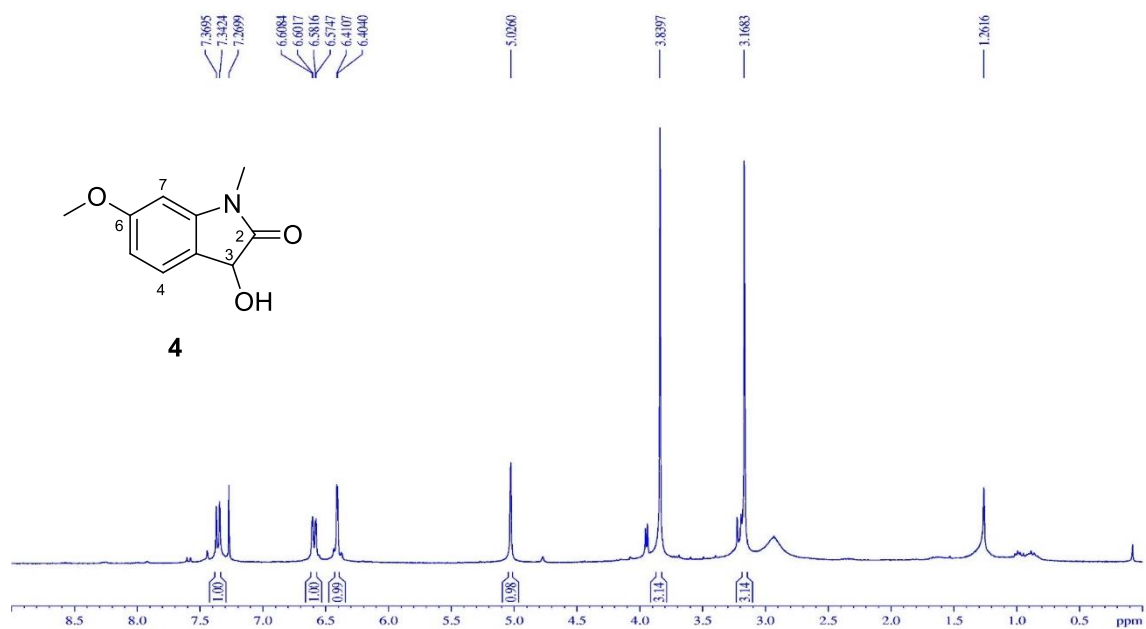


**Figure S20.**  $^1\text{H}$  NMR (300 MHz) spectrum of **4** in  $\text{CDCl}_3$ .

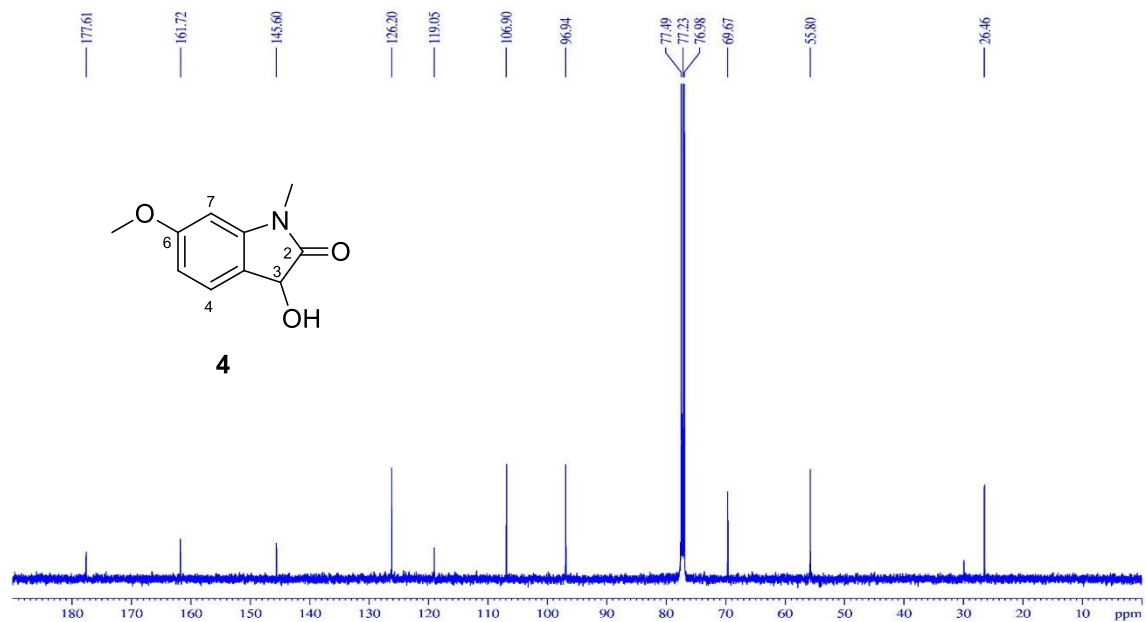


**Figure S21.**  $^{13}\text{C}$  NMR (75 MHz) spectrum of **4** in  $\text{CDCl}_3$ .

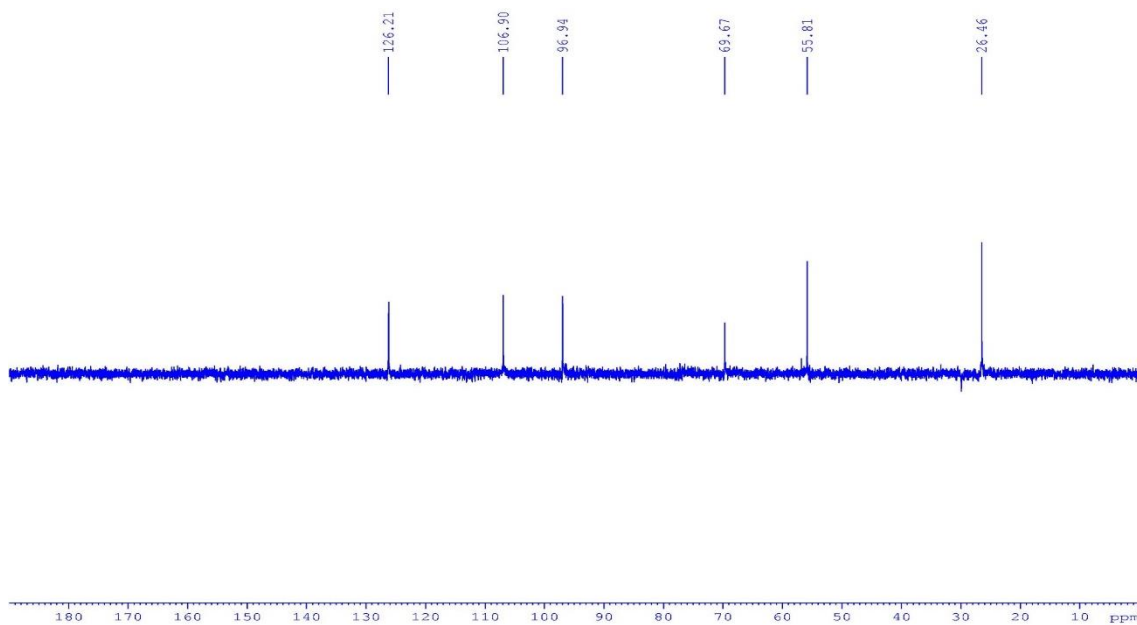


**Figure S22.** DEPT 135° NMR (75 MHz) spectrum of **4** in CDCl<sub>3</sub>.

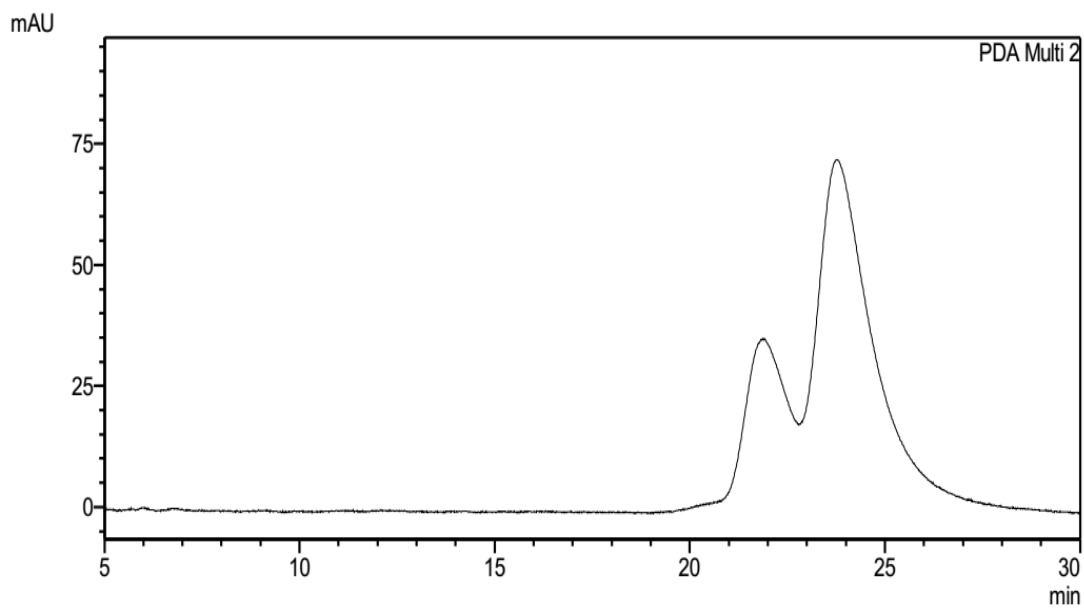


**Figure S23.** Chiral-phase HPLC (isopropanol/n-hexane (5:95), 30 min, flow rate of 1.00 mL/min) analysis of **4**.

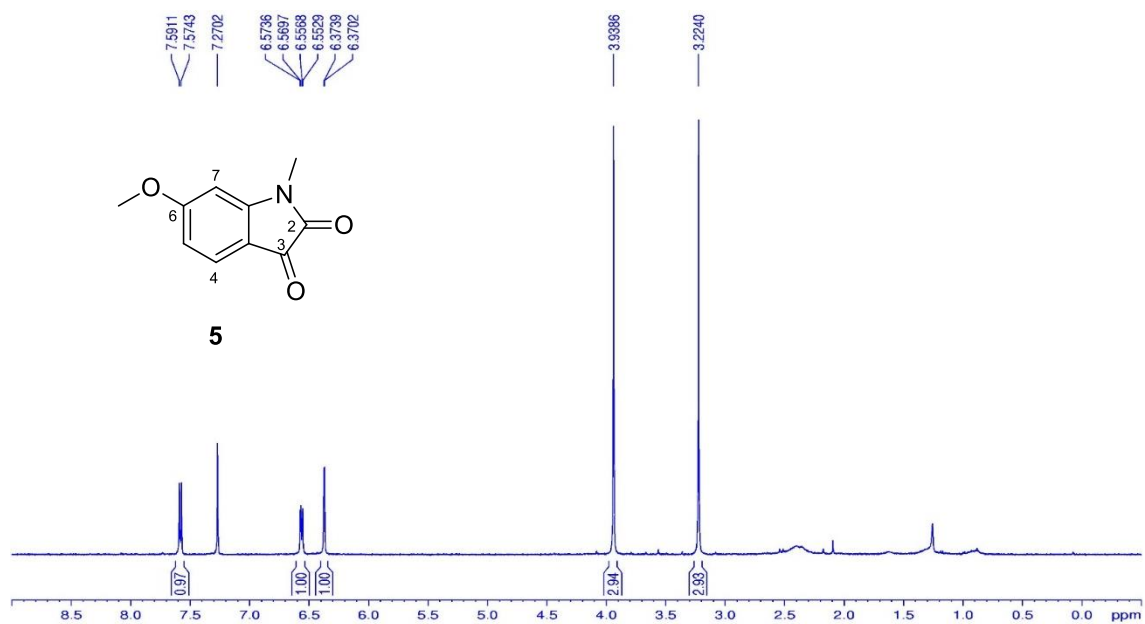


**Figure S24.**  $^1\text{H}$  NMR (500 MHz) spectrum of **5** in  $\text{CDCl}_3$ .

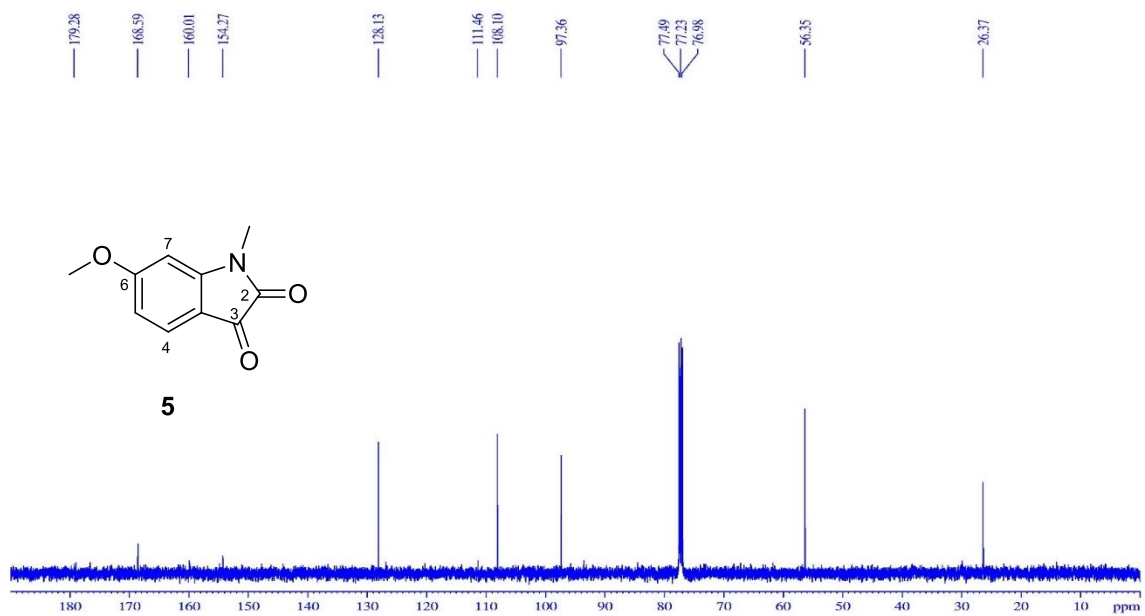


**Figure S25.**  $^{13}\text{C}$  NMR (125 MHz) spectrum of **5** in  $\text{CDCl}_3$ .

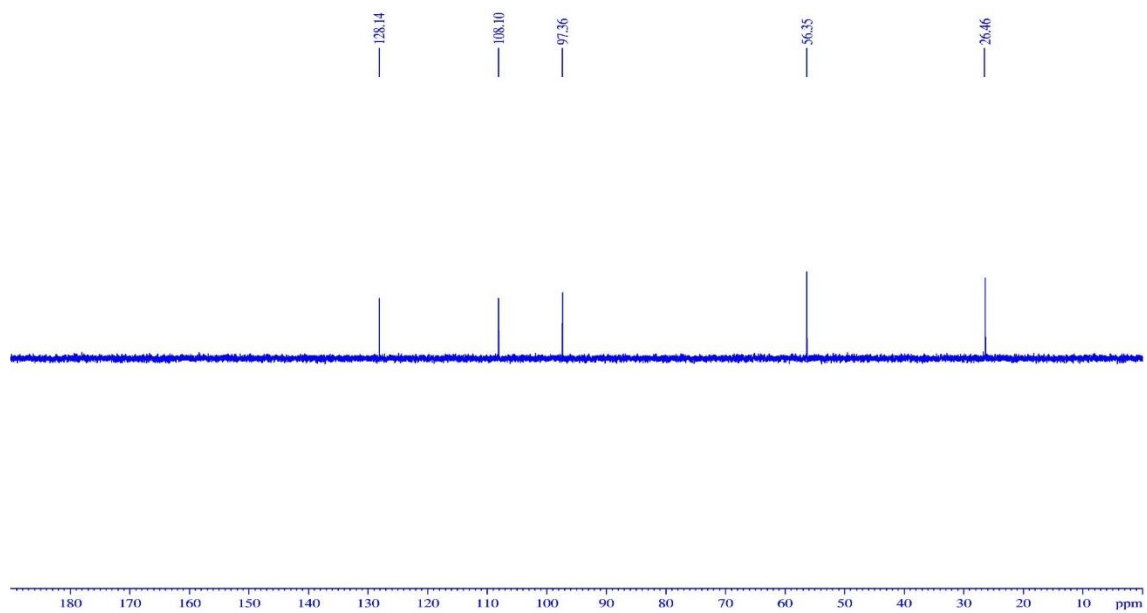


**Figure S26.** DEPT 135 NMR (125 MHz) spectrum of **5** in CDCl<sub>3</sub>.

4.3

# Capítulo 3

---

## Salinirifamycin A, a Natural Pyridine-Rifamycin from the Marine Actinomycete *Salinispora arenicola*

---



## **Salinirifamycin A, a Natural Pyridine-Rifamycin from the Marine Actinomycete *Salinispora arenicola***

Alison B. da Silva,<sup>†</sup> Edilberto R. Silveira,<sup>†</sup> Norberto Kássio. V. Monteiro,<sup>‡</sup> Ayslan B. Barros,<sup>§</sup> Ana Jérsia Araújo,<sup>§</sup> José Delano B. Marinho Filho,<sup>§</sup> Leticia V. Costa-Lotufo,<sup>⊥</sup> and Otilia Deusdenia L. Pessoa<sup>\*,†</sup>

<sup>†</sup>*Departamento de Química Orgânica e Inorgânica, Universidade Federal do Ceará, 60.021-970, Fortaleza-CE, Brazil*

<sup>‡</sup>*Departamento de Química Analítica e Físico-Química – Universidade Federal do Ceará, 60020-181 Fortaleza, CE, Brazil.*

<sup>§</sup>*Laboratório de Cultura de Células do Delta, Universidade Federal do Delta do Parnaíba, 64202-020, Parnaíba-PI, Brazil*

<sup>⊥</sup>*Departamento de Farmacologia, Universidade de São Paulo, 05508-900, São Paulo, SP, Brazil*

\*Phone: +55-85-33669441. E-mail: [otilialoiola@gmail.com](mailto:otilialoiola@gmail.com)

**ABSTRACT:** Salinirifamycin A (**1**), a rifamycin-like compound, bearing an unusual tetracyclic 5/6/6/6 pyridine-fused system, was isolated from *Salinispora arenicola* (BRA-213). Its structure was elucidated using a combination of spectroscopic (1D and 2D NMR, and HRESIMS) data and quantum-chemical calculations. Compound **1** displayed antibacterial activity against *S. aureus* (MIC 0.02  $\mu\text{g/mL}$ ). *In silico* assay using molecular dynamics simulations in lipid bilayers, including ONION calculations, showed that **1** interacts with Gram-positive bacteria in accordance with the *in vitro* assay.

## INTRODUCTION

As widely reported in the literature, actinomycetes represent a wide source of bioactive natural products of economical and biotechnological value.<sup>1</sup> In this context, species of the marine genus *Salinispora* have shown an extraordinary ability to produce novel structural classes of active secondary metabolites highly complex and functionalized as the salinisporamides,<sup>2</sup> saliniketals,<sup>3</sup> arenamides,<sup>4</sup> salinipyrones,<sup>5</sup> and salinaphthoquinones,<sup>6</sup> in addition to the well-known antibiotic rifamycins.<sup>7,8</sup> Since their discovery (1957) until some years ago, the rifamycins, particularly the semisynthetic derivatives such as rifampicin,<sup>9</sup> have been the most prescribed drugs to treat bacterial pathogens like tuberculosis,<sup>10</sup> leprosis,<sup>11</sup> osteoarticular,<sup>12</sup> and AIDS-related mycobacterial infections.<sup>13</sup> Unfortunately, due to their widespread and indiscriminate uses, pathogens, especially *Mycobacterium tuberculosis*, have developed resistance to rifampicin difficulting the effective treatment of diseases related to these pathogens.<sup>14,15</sup> As part of our interest in discovering new marine bioactive compounds from marine bacteria,<sup>16–18</sup> we have given special attention to the study of *Salinispora arenicola* (BRA-213) recovered from the marine sediments of St. Peter and St. Paul Archipelago, Brazil from which we have isolated salinaphthoquinones, a 4-hydroxy-pyran-2-one, and 3-hydroxy-*N*-methyl-2-oxindole derivatives contributing to the chemical knowledge about these amazing actinomycetes.<sup>6,18</sup> Further, special attention was driven to those compounds whose HPLC UV-Vis bands ( $\lambda$  223, 319, and 420 nm) were suggestive of rifamycin derivatives.<sup>19</sup> Herein, an uncommon rifamycin derivative bearing a pyridine-fused system is reported (Figure 1). Additionally, its antibiotic properties including molecular dynamics (MD) simulations in lipid bilayer models are also described.

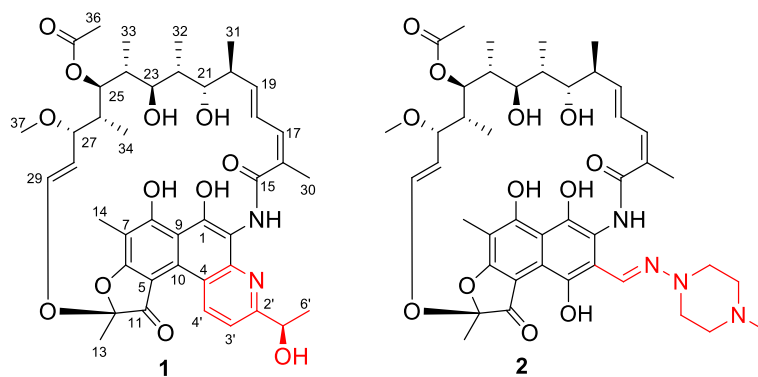


**Figure 1.** Chemical structures of Salinifamycin A (**1**) and Rifampicin (**2**).

## RESULTS AND DISCUSSION

Salinirifamycin A (**1**) was obtained as a red powder with a molecular formula of  $C_{42}H_{52}N_2O_{12}$  based on the protonated molecule  $[M + H]^+$  at  $m/z$  777.3597 (calcd for  $C_{42}H_{53}N_2O_{12}$ , 777.3593) in the HRESIMS spectrum, requiring 18 degrees of unsaturation. Its  $^1H$  NMR spectrum exhibited two deshielded signals at  $\delta_H$  8.50 (H-4') and 8.23 (H-3'), both appearing as a doublet and coupling constant ( $J$ ) value of 8.9 Hz, indicating *ortho*-positioned protons of a pyridine ring,<sup>20</sup> five olefinic protons at  $\delta_H$  6.81 (dd,  $J = 15.3, 11.4$  Hz, H-18), 6.41 (d,  $J = 11.4$  Hz, H-17), 6.19 (d,  $J = 12.6$  Hz, H-29), 6.10 (dd,  $J = 15.3, 7.0$  Hz, H-19), and 4.99 (m, H-18), and five oxygen-bearing methine proton at  $\delta_H$  5.33 (m, H-5'), 4.94 (d,  $J = 11.6$  Hz, H-25), 3.52 (br d,  $J = 9.8$  Hz, H-21), 3.22 (br d,  $J = 7.1$  Hz, H-27), and 2.69 (br t,  $J = 9.1$  Hz, H-23). Additionally, ten methyl groups including a methoxy ( $\delta_H$  2.88) and an acetyl group ( $\delta_H$  1.90) as well as six exchangeable NH or OH protons were assigned (Table 1). Detailed TOCSY, HSQC, and HMBC analyses (Figure 2) showed a polyketide side chain similar to that found in rifamycins.<sup>21</sup> Furthermore, a fully substituted naphthofuranone core, also typical of those compounds<sup>22</sup> was established by the HMBC correlations of the Me-13 ( $\delta_H$  1.83) with the carbons at  $\delta_C$  188.9 (C-11) and 108.2 (C-12); Me-14 ( $\delta_H$  2.09) with the carbons at  $\delta_C$  182.1 (C-8), 171.3 (C-6), and 105.9 (C-7), and a chelated hydroxy proton at  $\delta_H$  18.02 (OH-1) with  $\delta_C$  157.9 (C-1), 111.0 (C-2), and 116.3 (C-9). The connection between the naphthofuranone and the polyketide moieties was established by the HMBC correlations of both amide  $\delta_H$  9.42 and olefinic  $\delta_H$  6.41 (H-17) protons with the carboxyl at  $\delta_C$  167.8 (C-15), as well as of the olefinic proton  $\delta_H$  6.19 (H-29) with the ketal carbon  $\delta_C$  108.2 (C-12), leading to a partial structure similar to rifamycin SV.<sup>22</sup> Additional proton and carbon signals at  $\delta_C/\delta_H$  156.5,



138.7/8.50, 120.3/8.23, 66.0/5.33, and 22.6/1.59 along with the three remaining degrees of unsaturation were compatible with a fused pyridine ring substituted by a 1-hydroxyethyl group. The presence of the vicinal coupled protons H-3' ( $\delta_{\text{H}}$  8.23)/H-4' ( $\delta_{\text{H}}$  8.50) both exhibiting  $J = 8.9$  Hz, together with the HMBC correlation of H-4' to  $\delta_{\text{C}}$  110.5 (C-10) were crucial to determining the unequivocal position of the pyridine ring at C-3/C-4 of the naphthofuranone core (Figure 2). Similarly, HMBC correlations of H-4' ( $\delta_{\text{H}}$  8.50), Me-6' ( $\delta_{\text{H}}$  1.59), and HO-5' ( $\delta_{\text{H}}$  6.46) to  $\delta_{\text{C}}$  156.5 (C-2') ensured the 1-hydroxyethyl group position at C-2'. Except for the configuration of C-5', the NOESY spectrum enabled the definition of the relative configuration of the polyketide chain of **1** which corresponds to the stereochemistry of the known rifamycins S and SV.<sup>21,22</sup>

**Table 1.**  $^1\text{H}$  and  $^{13}\text{C}$  NMR spectroscopic data of compound **1** in DMSO- $d_6$ .

no.	<b>1</b>	
	$\delta_{\text{C}}^{\text{a}}$	$\delta_{\text{H}}$
1	157.9, C	
2	111.0, C	
3	129.1, C	
4	127.2, C	
5	nd <sup>b</sup>	
6	171.3, C	
7	105.9, C	
8	182.1, C	
9	116.3, C	
10	110.5, C	
11	188.9, C	
12	108.2, C	
13	21.1, CH <sub>3</sub>	1.83 s
14	7.3, CH <sub>3</sub>	2.09 s
15	167.8, C	
16	132.7, C	
17	131.6, CH	6.41 d (11.4)
18	125.3, CH	6.81 dd (15.3, 11.4)
19	138.8, CH	6.10 dd (15.3, 7.0)
20	37.6, CH	2.26 m <sup>c</sup>
21	71.9, CH	3.52 br d (9.8)
22	32.2, CH	1.55 m
23	75.2, CH	2.69 br t (9.1)
24	37.5, CH	0.86 m

25	71.7, CH	4.94 d (11.6)
26	39.3, CH	0.43 m
27	75.5, CH	3.22 br d (7.1)
28	118.3, CH	4.99 m
29	141.6, CH	6.19 d (12.6)
30	19.9, CH <sub>3</sub>	2.01 s
31	17.7, CH <sub>3</sub>	0.84 d (7.6)
32	10.7, CH <sub>3</sub>	0.86 d (7.5)
33	8.0, CH <sub>3</sub>	-0.11 d (6.7)
34	7.9, CH <sub>3</sub>	-0.69 d (6.8)
35	169.0, C	
36	20.7, CH <sub>3</sub>	1.90 s
37	55.6, CH <sub>3</sub>	2.88 s
2'	156.5, C	
3'	120.3, CH	8.23 d (8.9)
4'	138.7, CH	8.50 d (8.9)
5'	66.0, CH	5.33 m
6'	22.6, CH <sub>3</sub>	1.59 d (6.6)
HN-2		9.42 s
HO-1		18.02 s
HO-8		18.87 s
HO-21		4.95 br s
HO-23		3.96 d (8.8)
HO-5'		6.46 d (3.2)

<sup>a</sup>Chemical shift deduced from the HSQC and HMBC experiments; <sup>b</sup> nd: not detected;

<sup>c</sup>“m” means overlapped or multiplet with other signals.

Regarding the configuration of C-5', theoretical calculation methods were performed to accurately assign it as *S*\* (**1a**) or *R*\* (**1b**). Thus, for both epimers, **1a** and **1b**, were calculated their optimized geometries (Figure 3), <sup>13</sup>C isotropic magnetic shielding ( $\delta_{\text{C calcd}}$ ) values using GIAO-mPW1PW91/6-31G(d,p) level of theory, and DP4+ probability analysis<sup>23,24</sup>. As a result, the C-5'*R*\* relative configuration was suggested based on the correlation coefficient ( $R^2 = 0.9838$ ) between experimental and calculated <sup>13</sup>C NMR data (Figure 4) and DP4+ probability analysis of 92.27 % for isomer **1b** (Table 2).

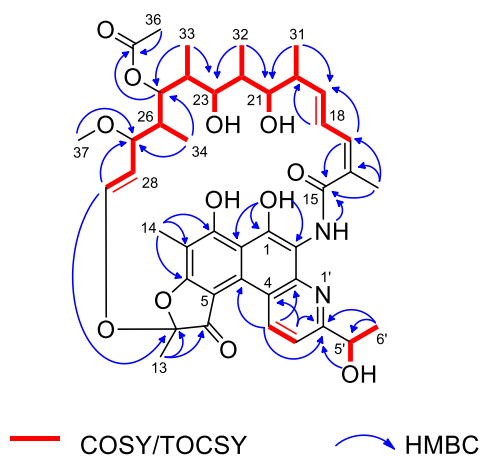


**Figure 2.** Key COSY, TOCSY, and HMBC correlations of salinirifamycin A (**1**).

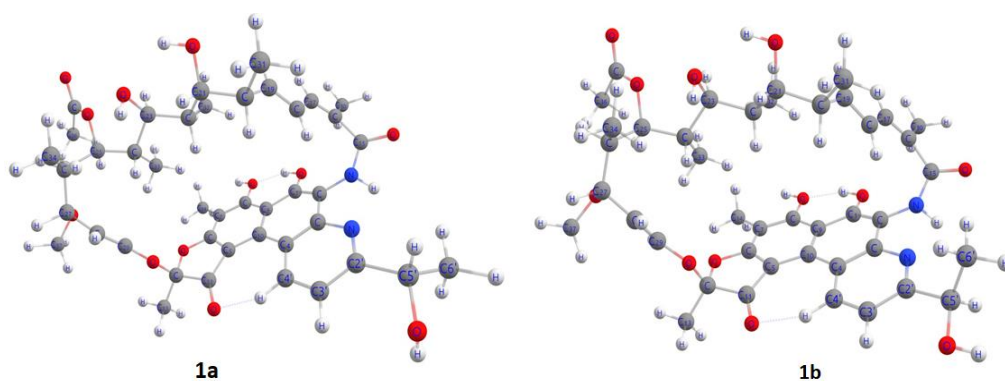


**Figure 3.** Optimized geometries of **1a** (C-5'*S*\*) and **1b** (C-5'*R*\*) epimers using mPW1PW91/6-31G(d,p) level of theory.

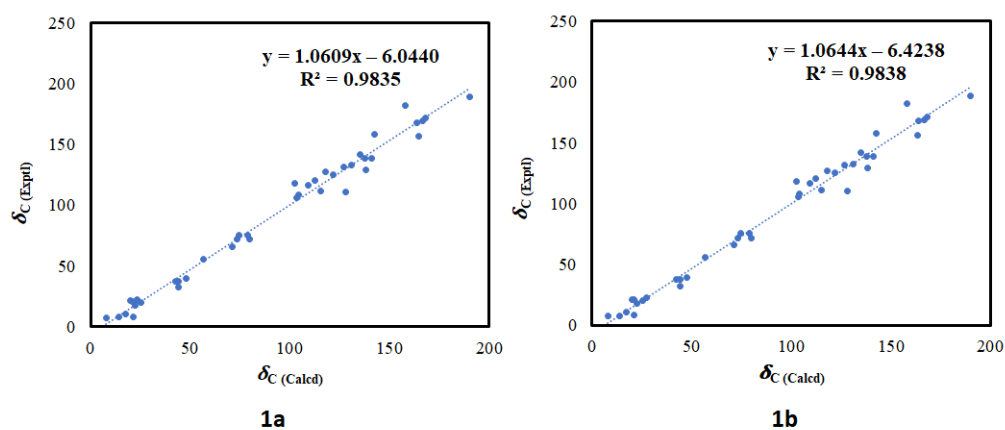


**Figure 4.** Linear correlation between the experimental chemical shift ( $\delta_{\text{C (exptl)}}$ ) versus calculated magnetic isotropic shielding ( $\delta_{\text{C (calcd)}}$ ) for **1a** (C-5'*S*\*) and **1b** (C-5'*R*\*)).

The identification of rifamycins in the genus *Salinispora* has been well-documented,<sup>25–27</sup> but, to our knowledge, salinirifamycin A (**1**) is the first example of a new rifamycin, bearing a natural tetracyclic 5/6/6/6 pyridine-fused system isolated from this genus. Ever since the discovery of its biosynthetic gene clusters, the biosynthesis of rifamycins has been extensively studied,<sup>28–30</sup> providing support to suggest a plausible biogenetic pathway to **1** (Scheme 1). Biosynthetically, the rifamycins are derived from the aromatic starter unit 3-amino-5-hydroxybenzoic acid (AHBA), which is progressively extended through two malonyl-CoA plus eight methyl malonyl-CoA on a type I polyketide synthase. After the PKS naphthalene ring building,<sup>31</sup> the terminal polyketide side chain is cyclized by an amide synthase to give the macrolactam proansamycin X, which is later transformed to rifamycin S.<sup>32</sup> Nucleophilic addition of a diketoacetyl-CoA unit to rifamycin S followed by a sequence of typical biosynthetic reactions as hydrolysis, decarboxylation, reduction, dehydration, and oxidation gives intermediate **i**. A classic ammonia-ketone condensation<sup>33</sup> to **i** provides the gem-hydroxyamine intermediate **ii** which via an aza-Michael addition to the  $\alpha,\beta$ -conjugated ketone portion of the naphthalene ring produces **iii**, that after aromatization reaction yields compound **1**.

**Table 2.** <sup>13</sup>C NMR experimental data ( $\delta_{\text{C exptl}}$ ) and calculated <sup>13</sup>C nuclear magnetic shielding ( $\delta_{\text{C calcd}}$ ) for **1a** (5'S\*) and **1b** (5'R\*).

no.	$\delta_{\text{C exptl}}$	$\delta_{\text{C calcd}}$ ( <b>1a</b> )	$\Delta\delta$ ( <b>1a</b> )	$\delta_{\text{C calcd}}$ ( <b>1b</b> )	$\Delta\delta$ ( <b>1b</b> )
1	157.9	142.5886	15.3114	142.5422	15.3578
2	111.0	115.4118	-4.4118	115.1495	-4.1495
3	129.1	138.3854	-9.2854	138.1537	-9.0537
4	127.2	117.7873	9.4127	117.8482	9.3518
5	nd	-	-	-	-
6	171.3	168.2997	3.0003	168.2443	3.0557
7	105.9	103.6815	2.2185	103.6378	2.2622
8	182.1	157.9520	24.1480	157.9598	24.1402
9	116.3	109.2273	7.0727	109.1878	7.1122
10	110.5	128.1875	-17.6875	128.3154	-17.8154
11	188.9	190.0921	-1.1921	190.0719	-1.1719
12	108.2	104.1925	4.0075	104.1761	4.0239
13	21.1	20.0570	1.0430	20.0990	1.0010
14	7.3	7.8577	-0.5577	7.8602	-0.5602
15	167.8	163.7707	4.0293	163.8171	3.9829

16	132.7	131.1034	1.5966	131.1489	1.5511
17	131.6	126.8719	4.7281	126.7755	4.8245
18	125.3	121.8738	3.4262	121.8873	3.4127
19	138.8	141.2072	-2.4072	141.1205	-2.3205
20	37.6	44.1410	-6.5410	44.1241	-6.5241
21	71.9	73.4087	-1.5087	73.4107	-1.5107
22	32.2	44.1481	-11.9481	44.1855	-11.9855
23	75.2	74.5264	0.6736	74.5338	0.6662
24	37.5	42.5451	-5.0451	42.5483	-5.0483
25	71.7	79.7098	-8.0098	79.7191	-8.0191
26	39.3	47.7568	-8.4568	47.7437	-8.4437
27	75.5	78.7877	-3.2877	78.7901	-3.2901
28	118.3	102.6434	15.6566	102.6327	15.6673
29	141.6	135.1437	6.4563	135.1455	6.4545
30	19.9	25.2716	-5.3716	25.2510	-5.3510
31	17.7	22.3006	-4.6006	22.2930	-4.5930
32	10.7	17.3261	-6.6261	17.3594	-6.6594
33	8.0	21.2384	-13.2384	21.2213	-13.2213
34	7.9	14.0584	-6.1584	14.0649	-6.1649
35	169.0	166.7889	2.2111	166.7985	2.2015
36	20.7	20.9629	-0.2629	20.9730	-0.2730
37	55.6	56.8716	-1.2716	56.8518	-1.2518
2'	156.5	164.6222	-8.1222	163.6117	-7.1117
3'	120.3	112.5915	7.7085	112.3692	7.9308
4'	138.7	137.8709	0.8291	137.8958	0.8042
5'	66.0	71.3223	-5.3223	71.4808	-5.4808
6'	22.6	23.4928	-0.8928	27.2876	-4.6876
uDP4+		50.00 %		50.00 %	
sDP4+		7.73 %		<b>92.27 %</b>	
DP4+		7.73 %		<b>92.27 %</b>	

The antibacterial activity of salinirifamycin A (**1**) was evaluated against both Gram-positive ( $G^+$ ) *Staphylococcus aureus* and *Enterococcus faecalis*, and the Gram-negative ( $G^-$ ) *Escherichia coli* bacterial strains (Table 3). Compound **1** was weakly active against *E. coli* (MIC 100.0  $\mu\text{g/mL}$ ) but highly active against *S. aureus* (MIC 0.02  $\mu\text{g/mL}$ ), and *E. faecalis* (MIC 0.2  $\mu\text{g/mL}$ ). It is worth mentioning that **1** displayed antibacterial activity against *S. aureus* similarly to the positive control rifampicin (**2**) (MIC 0.03  $\mu\text{g/mL}$ ).

**Scheme 1.** Plausible Biogenetic Pathways for Salinirifamycin A (**1**).

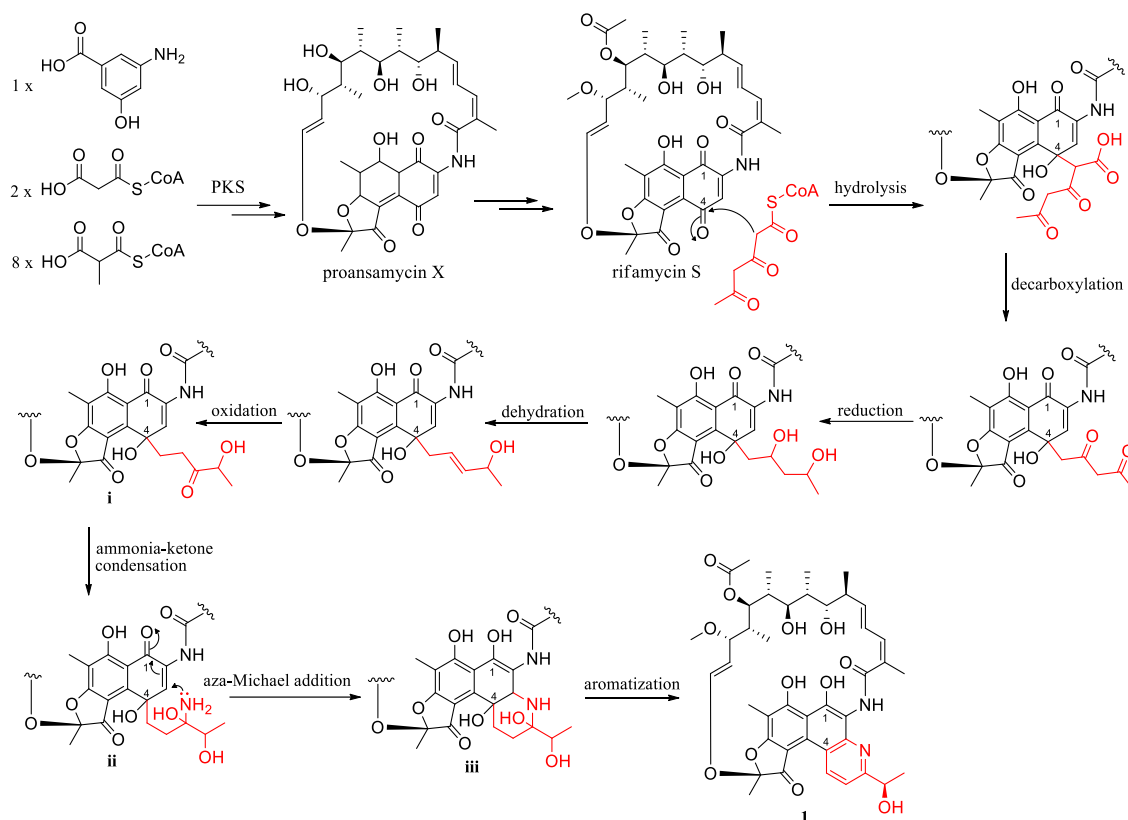


**Table 3.** Antibacterial activity of compound **1** (MIC,  $\mu\text{g/mL}$ ).

Bacteria				
<i>S. aureus</i>	<i>S. aureus</i> (MRSA)	<i>E. faecalis</i>	<i>E. faecalis</i> (VRE)	<i>E. coli</i>
0.02	0.02	0.2	3.1	100.0

Positive control: Rifampicin, MIC 0.03  $\mu\text{g/mL}$ .

Encouraged by the antibacterial activity of **1**, molecular dynamics (MD) simulations in lipid bilayer models were performed to **1** and **2** to compare the antibacterial potential of this uncommon natural product. The root means square deviation (RMSD) of the systems reached a constant value around  $\sim 5.6$  nm (Figure 5) indicating a structural equilibrium after around  $\sim 300$  ns of simulation, hence, the interaction potential energy (IPE) analysis was performed in the last 300 ns for the systems. Based on the results, **1** showed a higher negative IPE in the *in silico* analysis for  $G^-$  lipid bilayer ( $-82.32$  kcal  $\text{mol}^{-1}$ ) indicating a stronger intermolecular interaction when compared with  $G^+$  lipid

bilayer ( $-17.74 \text{ kcal mol}^{-1}$ ), while **2** showed an IPE of  $-83.05$  and  $-82.42 \text{ kcal mol}^{-1}$  for  $G^-$  and  $G^+$  lipid bilayers, respectively (Figure 6).

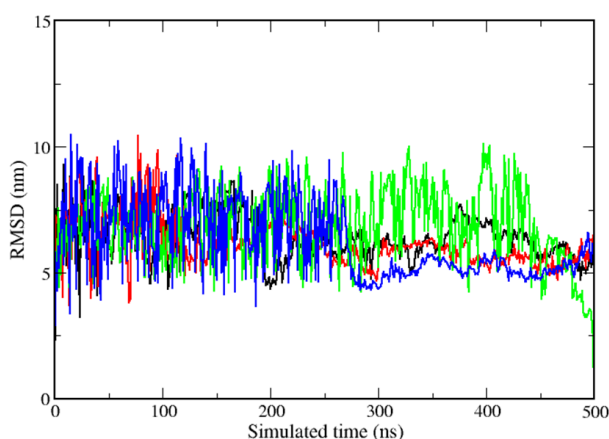


**Figure 5.** RMSD profile for systems over 500 ns from MD simulations. Compounds **1** (black) and **2** (red) simulated in  $G^-$  lipid bilayer. Compounds **1** (green) and **2** (blue) simulated in  $G^+$  lipid bilayer.

The results suggest that **1** can exhibit the highest *in vitro* antimicrobial activity on  $G^-$  bacteria due to the highest IPE value, diverging of the *in vitro* assays that show the highest antimicrobial activity on  $G^+$  bacteria strains. Therefore, more accurate analysis of interaction was necessary to evaluate the *in silico* antibacterial activity of **1**. From the ligand-lipid bilayer complexes obtained in the molecular dynamics simulations, ONIOM calculations (Figure 7) were performed for the systems containing compounds **1** and **2** in  $G^-$  and  $G^+$  lipid bilayers within  $3.0 \text{ \AA}$  radius. ONIOM calculations showed that **1** has a higher negative electronic energy of interaction ( $\Delta E_{EEI}$ ) for  $G^+$  lipids bilayer ( $\Delta E_{EEI} = -11.96 \text{ kcal mol}^{-1}$ ) when compared with  $G^-$  ( $\Delta E_{EEI} = -4.63 \text{ kcal mol}^{-1}$ ), indicating a stronger intermolecular interaction for compound **1**, while **2** showed an  $\Delta E_{EEI}$  of  $-7.82$  and  $-13.25 \text{ kcal mol}^{-1}$  for  $G^-$  and  $G^+$  lipids, respectively. Based on these results, **1** should have higher antibacterial activity for  $G^+$  bacteria due to the more negative  $\Delta E_{EEI}$  value ( $-11.96 \text{ kcal mol}^{-1}$ ) compared to  $G^-$  lipid bilayer ( $-4.63 \text{ kcal mol}^{-1}$ ). Furthermore, compound **1** showed an  $\Delta E_{EEI}$  value close to that of **2** (**1**,  $-11.96 \text{ kcal mol}^{-1}$ ; **2**,  $-13.25 \text{ kcal mol}^{-1}$ ), suggesting that **1** exhibits an antimicrobial activity similar to **2** for  $G^+$  bacteria. In front of the results, the computational data performed through the ONIOM (QM/QM) calculations at the B3LYP/6-31G(d,p) level of theory (high layer) and semi-empirical method AM1 (low layer), showed a good match with the experimental data.

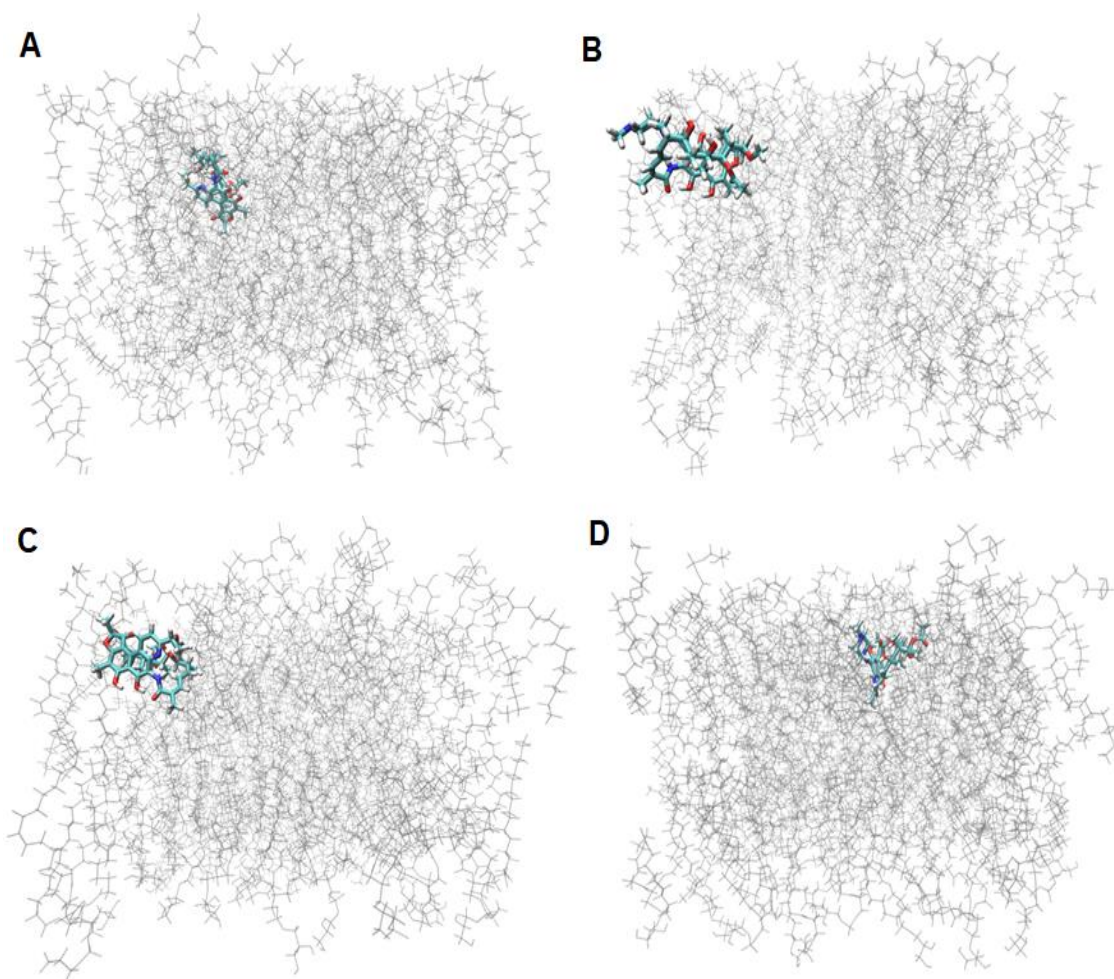


**Figure 6.** Schematic views of MD simulation systems on  $G^-$  and  $G^+$  lipid bilayers bacteria mimicked. XZ plane representations of systems presenting their final simulated perspective: (A) Compounds **1** and (B) **2** simulated in  $G^-$  lipid bilayer. (C) Compounds **1** and (D) **2** simulated in  $G^+$  lipid bilayer. Lipid molecules are represented in lines. Water molecules were removed for better viewing.

In conclusion, the identification of rifamycins from *S. arenicola* has been previously reported,<sup>25,26</sup> but, so far, little attention was driven to the isolation of new rifamycins. In this study, salinirifamycin A (**1**), a new and unusual 5/6/6/6 tetracyclic pyridine-rifamycin was isolated, which, in preliminary *in vitro* and *in silico* studies, showed potent antibacterial activity against *S. aureus* similar to the standard rifampicin (**2**), a well-known antibiotic currently used to treat infectious diseases.



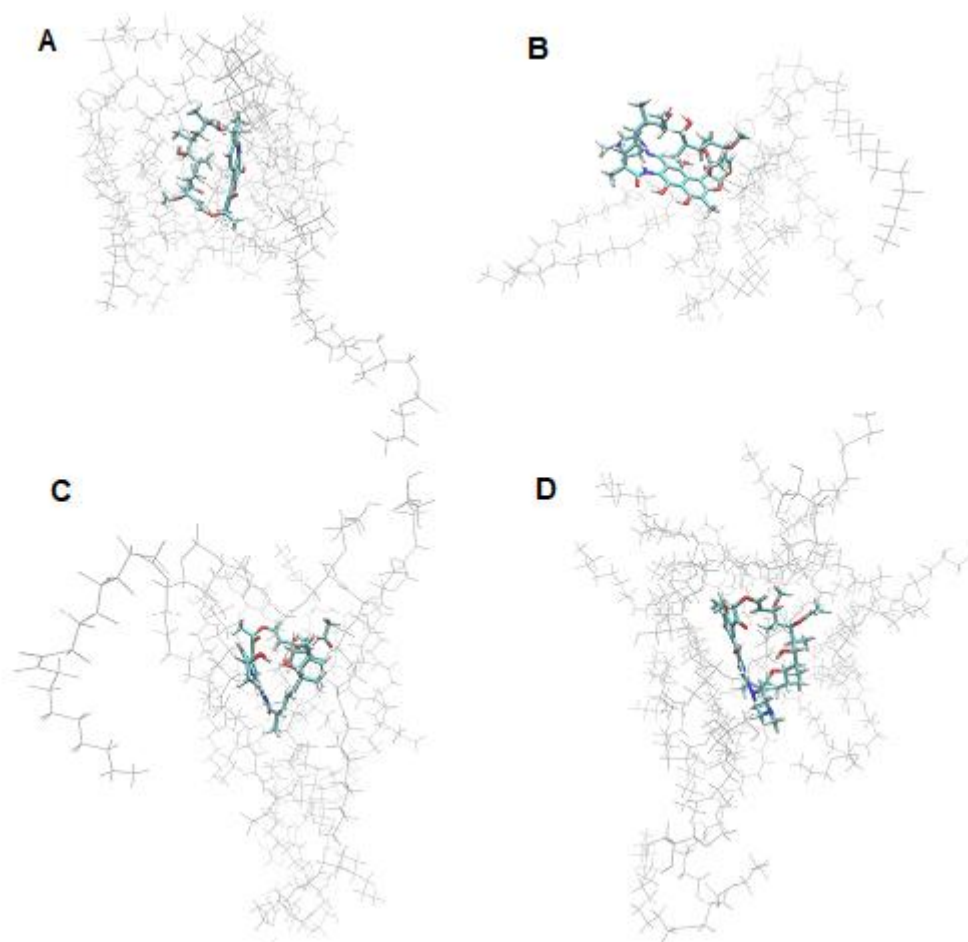


**Figure 7.** Schematic views of the structural systems submitted to ONIOM calculations. (A) Compounds **1** and (B) **2** (in ball-and-stick, treated with B3LYP/6-31G(d,p) level of theory) surrounding  $G^-$  POPE and POGE lipids (in gray lines, treated at the AM1 semi-empirical method). (C) Compounds **1** and (D) **2** surrounding  $G^+$  POPE and POGE lipids.

## EXPERIMENTAL SECTION

### General Experimental Procedures.

Optical rotation was measured using a JASCO P-2000 digital polarimeter. UV and IR spectra were acquired on a Shimadzu 2600 UV/vis spectrophotometer and a Perkin-Elmer Spectrum 100 FTIR spectrophotometer, respectively. NMR spectra were obtained on a Bruker Avance DRX-500 (500 MHz to  $^1\text{H}$  and 125 MHz to  $^{13}\text{C}$ ). High-resolution electrospray ionization mass spectrum (HRESIMS) was acquired using an Acquity Xevo UPLC-QTOF-MS system from Waters (Milford, MA). Sephadex LH-20 (Pharmacia) and SPE cartridges C18 (20 g/ 60 mL; Strata, Phenomenex) were used for the chromatographic fractionations. HPLC analyses were carried out using a UFLC

(SHIMADZU) system equipped with an SPD-M20A diode array UV/vis detector and a Phenomenex silica column 5  $\mu\text{m}$  (10.0 x 250 mm).

### **Bacterial Material and Fermentation.**

The strain *Salinispora arenicola* (BRA-213) was isolated from marine sediment collected around St. Peter and St. Paul Archipelago, Brazil, at a depth of 16 m (N 0°55', W 29°38') and identified by Bauermeister et al.,<sup>34</sup> (GenBank No. MH910695). The license for the collection was granted by the Conselho de Gestão do Patrimônio Genético (CGEN) (SisGen No. AA8F8B8). The strain is preserved at the Laboratório de Bioprospecção e Biotecnologia Marinha (LaBBMar), Universidade Federal do Ceará, Brazil. Colonies of this strain were inoculated into Erlenmeyer flasks (2 L) containing 500 mL of A1 media (10 g soluble starch, 4 g yeast extract, and 2 g peptone) supplemented with calcium carbonate (0.5 g/L  $\text{CaCO}_3$ ), solutions of iron (III) sulfate (5 g/L  $\text{Fe}_2(\text{SO}_4)_3$ ) and potassium bromide (5 g/L KBr). Steril Amberlite XAD-16 resin (10 g) was added to each flask on day 2 and the culture flasks were shaken at 200 rpm at 28 °C for 14 days.

### **Extraction and Isolation.**

After 14 days, the whole fermentation broth (20 L) was filtered to separate the resin from the supernatant. The resin was then extracted with acetone (2 L), which was posteriorly removed under-vacuum, while the residual aqueous phase was extracted with ethyl acetate (3 x 500 mL). The EtOAc fraction was vacuum dried and yielded an organic extract (9 x 1g), which was fractionated on a C18 cartridge by elution with MeOH/H<sub>2</sub>O (7:3; 4:1, and 1:0) to give three fractions (A–C). Fraction B (1.1 g) was chromatographed over a Sephadex LH-20 column, using MeOH as eluent, to give six fractions (B1-B6). Subfraction B2 (55.0 mg) was directly purified by semipreparative HPLC (hexane/acetone, 30-100 %, 20 min, flow rate of 3.0 mL/min) to give compound **1** (1.5 mg,  $t_R = 10.3$  min).

### **Physical and spectroscopic data of 1.**

*Salinirifamycin A* (**1**): red powder;  $[\alpha]_D^{22} + 23.1$  ( $c$  0.10, MeOH); UV (MeOH)  $\lambda_{\text{max}}$  (log  $\epsilon$ ) 223 (4.00), 246 (4.01), 294 (3.72), 319 (3.67), 382 (3.25), 420 (3.17), 505 (3.09) nm; IR ( $\nu_{\text{max}}$ ) 3410, 3238, 2925, 2855, 1735, 1643, 1592, 1526, 1456, 1373, 1258, 1238, 1160,

1087, 1062, 1048, 1024, 974, 803, 723  $\text{cm}^{-1}$ ;  $^1\text{H}$  and  $^{13}\text{C}$  NMR data, see Table 1; HRESIMS  $m/z$  777.3597  $[\text{M} + \text{H}]^+$  (calcd for  $\text{C}_{42}\text{H}_{53}\text{N}_2\text{O}_{12}$ , 777.3593).

### Computational NMR Chemical Shift Calculation and DP4+ Analyses.

To determine the relative stereochemistry of **1**, focusing on the C-5' stereocenter, two possible epimeric structures were built and denominated **1a** (C-5'S\*) and **1b** (C-5'R\*). The geometries of the studied structures were optimized by using standard techniques.<sup>35</sup> Optimization calculations were performed by using the Density Functional Theory<sup>36</sup> (DFT) method at mPW1PW91 functional<sup>37</sup> along with a 6-31G(d,p) basis set implemented in Gaussian 16 package.<sup>38</sup> Vibrational modes of the optimized geometries were calculated to determine whether the resulting geometries are true minima or transition states. All optimization calculations were performed in solution by using the Polarizable Continuum Model (PCM)<sup>39</sup> with the Integral Equation Formalism (IEF)<sup>40</sup> using DMSO as a solvent.

The NMR isotropic shielding constants were determined from the optimized geometries for **1a** and **1b** with mPW1PW91/6-31G(d,p) level of theory based on the Gauge Independent Atomic Orbitals (GIAO) proposal,<sup>41</sup> implemented in the Gaussian 16. The IEF-PCM solvation method was performed using DMSO as an implicit solvent to simulate the medium on the chemical shifts of isomers **1a** and **1b**. To correlate the theoretically calculated chemical shifts with the experimental one, the theoretical isotropic shielding constants ( $\sigma_{\text{calcd}}$ ) of carbon atoms were compared with the calculated isotropic shielding constants ( $\sigma_{\text{TMS}}$ ) using tetramethylsilane (TMS) as reference:  $\delta_{\text{C(calcd)}} = \sigma_{\text{C(TMS)}} - \sigma_{\text{calcd}}$ , where the  $\sigma_{\text{C(TMS)}} = 196.7782$  ppm. To elucidate the most likely structure for both the epimers, a supplemental analysis DP4+<sup>42</sup> that uses Quantum Chemical Calculated NMR parameters combined with refined statistical data was performed.

### Antimicrobial Assay.

Compound **1** was assayed against the Gram-positive bacteria ( $G^+$ ): *Staphylococcus aureus* (ATCC 29213), methicillin-resistant *S. aureus* (ATCC 43300, MRSA), *Enterococcus faecalis* (ATCC 29212), and vancomycin-resistant *Enterococcus faecalis* (ATCC 51212, VRE), and the Gram-negative ( $G^-$ ): *Escherichia coli* (ATCC 25922). Initially, the strains were previously seeded in Petri dishes containing Mueller Hinton agar (Difco), which were incubated for 24 hours at 35 °C, under aerobic

conditions. Further, the isolated colonies were collected and suspended in a sterile saline solution of NaCl 0.85% (w/v) which was used to obtain the bacterial inoculum in Mueller Hinton broth (Difco) in the concentration of  $5 \times 10^5$  CFU/mL. The method used was the broth microdilution in a 96-well plate, and the minimum inhibitory concentrations (MICs) were determined according to Clinical Laboratory Standards Institute (2015).<sup>43</sup> Rifampicin (**2**) was used as a positive control. The microplate was incubated at the same condition cited above and the MIC value was determined after the observation of the absence of bacterial growth in the culture medium.

### **Molecular Dynamics Simulations.**

The lipid bilayer models were build to simulating the  $G^-$  and  $G^+$  membrane bacteria for the theoretical study. To building the  $G^-$  bacteria membrane has used a mixture of 1:3 molar ratio of anionic 1-palmitoyl-2-oleoyl-sn-glycerol-3-phosphoethanolamine (POPE), while to the  $G^+$  bacteria membrane<sup>44</sup> a 3:1 molar ratio POPG/POPE was used. The CHARMM-GUI<sup>45</sup> Membrane Builder was used for the construction of lipid bilayers. The initial geometries of **1** and **2** were simulated separately and optimized with mPW1PW91/6-31G(d,p) level of theory implemented in the Gaussian 16 package. For each simulation, the molecule (**1** or **2**) was placed in the upper region of the membrane ( $G^-$  or  $G^+$ ) at approximately 10 nm above the lipid bilayer surface, with the initial position being the same for both molecules. The lipid bilayers used for  $G^-$  and  $G^+$  membrane simulations, were positioned in the  $xy$  plane of the box and were composed of 120 lipids between POPE and POPG molecules. A  $\sim 40$  Å thick layer of water ( $z$ -axis) was always maintained on both sides of the lipid bilayers. All molecular dynamics (MD) simulations were performed using the GROMACS 2018.4<sup>46</sup> package implemented with the CHARMM36 force field.<sup>47</sup> The Transferable Intramolecular Potential with 3 points (TIP3P)<sup>48</sup> water molecules were used to solvate the simulated systems. The systems neutralization was achieved through the addition of counterions. The Leap-Frog algorithm<sup>49</sup> was applied to integrate the motion equation with a time step of 2.0 fs. The long-range interactions were modeled using particle-mesh Ewald sum (PME)<sup>50</sup> with a cut-off of 1.2 nm. The van der Waals interactions were also calculated using the same threshold. Bonds involving hydrogen atoms were restrained using the LINCS algorithm.<sup>51</sup> The Nosé–Hoover thermostat<sup>52</sup> was used to fix the system temperature (310 K) in all production simulations, while the system pressure was controlled using a Parrinello–Rahman barostat<sup>53</sup> in the NPT simulations. The geometry of the systems was minimized

by the steepest descent algorithm<sup>54</sup> for 10000 steps with a tolerance of 10 kJ mol<sup>-1</sup> nm<sup>-1</sup> followed by conjugate gradient algorithm<sup>55</sup> for 10000 steps with a tolerance of 5.0 kJ mol<sup>-1</sup> nm<sup>-1</sup>. Two shorts 200 ps equilibrium dynamics with NVT and NPT ensembles were performed. Finally, 500 ns production MD simulation using NVT ensemble was performed for each system to determine the molecules **1** and **2** adsorptions with lipid bilayers.

To analyze the interaction between **1**, or **2**, with the lipid bilayer was used the Interaction Potential Energy (*IPE*)<sup>56</sup>, which can be defined as the total interaction energy between two groups, (the sum of van der Waals and electrostatic contributions), and it was calculated according to the equation (1):

$$IPE_{i,j} = \sum_i^{N_i} \sum_{j \neq i}^{N_j} V_{vdW}(r_{ij}) + V_{elec}(r_{ij}) \quad (1)$$

where  $IPE_{i,j}$  is the interaction energy between a group of atoms  $i$  and a group of atoms  $j$ , and  $N_i$  and  $N_j$  is the total number of atoms on groups  $i$  and  $j$ ,  $V_{elec}$  and  $V_{vdW}$  are the terms corresponding to electrostatic and van der Waals contribution, respectively. This parameter is often used to evaluate interaction energies in protein-ligand and protein-protein systems<sup>57</sup>, but can also be applied to quantify the interaction between specific ligand and the lipid bilayers<sup>58</sup>. For *IPE* calculations, all atoms of **1** and **2** were considered in the calculation. For the lipid bilayer group, only the hydrophilic head atoms of POPE and POPG were considered.

### ONIOM Calculations.

Quantum mechanics/quantum mechanics (QM/QM) calculations, specifically the ONIOM (Our own N-layered Integrated molecular Orbital and Molecular Mechanics) method<sup>59</sup> was used to accurately elucidate the electronic and energetic effects. The equilibrium structures from 500 ns molecular dynamics simulations were chosen as a starting point for the ONIOM calculations. Water molecules and counterions were removed to reduce the system size. Only lipids within a 3.0 Å radius from the ligands **1** or **2** were considered for the calculations.

The ONIOM calculations were performed with two QM regions. One with a more accurate calculation method: Becke, 3-parameter, Lee-Yang-Parr (B3LYP)<sup>60,61</sup> with 6-31g(d,p) basis set, used for ligands **1** or **2**. For lipids within the 3.0 Å radius, was used semiempirical molecular orbital method, namely Austin Model (AM1)<sup>62</sup>. Single-

point energies were performed for all systems to determine the electronic energy of interaction between **1** or **2** with the lipid bilayers. The electronic energy of interaction ( $\Delta E_{EEI}$ ) is expressed as:

$$\Delta E_{EEI} = E_{LIG+LIP} - (E_{LIG} + E_{LIP}) \quad (2)$$

where  $E_{LIG+LIP}$  is the electronic energy of the ligand and lipids complex (entire system), and  $E_{LIG}$  and  $E_{LIP}$  are the electronic energies ligand and lipids, respectively. ONIOM calculations were done using Gaussian 16 package<sup>38</sup>.

## ASSOCIATED CONTENT

### Supporting Information

The supporting information is available free of charge on the ACS publications website at DOI:

Experimental details, IR, UV, ECD, HRESIMS, and NMR data of **1** (PDF)

### Notes

The authors declare no competing financial interest.

## ACKNOWLEDGMENTS

The authors are grateful to Secretaria da Comissão Interministerial dos Recursos do Mar (SECIRM) for providing all the logistic support to the scientific expedition, as part of the PROARQUIPELAGO Program, Núcleo de Processamento de Alto Desempenho (NPAD) at the Universidade Federal do Rio Grande do Norte (UFRN) and Centro Nacional de Processamento de Alto Desempenho (CENAPAD) at the Universidade Federal do Ceará (UFC) for providing computational resources. This work was financially supported in part by the Coordenação de Aperfeiçoamento de Pessoal de Nível Superior - Brazil (CAPES) - Finance Code 001, CNPq (No. 420454/2016-0 and 309060/2016-8), and INCT BioNat (No. 465637/2014-0).

## REFERENCES

- (1) Subramani, R.; Sipkema, D. *Mar. Drugs*. **2019**, *17*, 249–288.
- (2) Feling, R. H.; Buchanan, G. O.; Mincer, T. J.; Kauffman, C. A.; Jensen, P. R.; Fenical, W. *Angew. Chem. Int. Ed.* **2003**, *42*, 355–357.
- (3) Williams, P. G.; Asolkar, R. N.; Kondratyuk, T.; Pezzuto, J. M.; Jensen, P. R.; Fenical, W. *J. Nat. Prod.* **2007**, *70*, 83–88.

- (4) Asolkar, R. N.; Freel, K. C.; Jensen, P. R.; Fenical, W.; Kondratyuk, P.; Park, E. J.; Pezzuto, J. M. *J. Nat. Prod.* **2009**, *72*, 396–402.
- (5) Oh, D. C.; Gontang, E. A.; Kauffman, C. A.; Jensen, P. R.; Fenical, W. *J. Nat. Prod.* **2008**, *71*, 570–575.
- (6) Da Silva, A. B.; Silveira, E. R.; Wilke, D. V.; Ferreira, E. G.; Costa-Lotufo, L. V.; Torres, M. C. M.; Ayala, A. P.; Costa, W. S.; Canuto, K. M.; de Araújo-Nobre, A. R.; Araújo, A. J.; Marinho Filho, J. D. B.; Pessoa, O. D. L. *J. Nat. Prod.* **2019**, *82*, 1831–1838.
- (7) Bose, U.; Hewavitharana, A. K.; Ng, Y. K.; Shaw, P. N.; Fuerst, J. A.; Hodson, M. *P. Mar. Drugs.* **2015**, *13*, 249–266.
- (8) Duncan, K. R.; Crüsemann, M.; Lechner, A.; Sarkar, A.; Li, J.; Ziemert, N.; Wang, M.; Bandeira, N.; Moore, B. S.; Dorrestein, P. C.; Jensen, P. R. *Chem. Biol.* **2015**, *22*, 460–471.
- (9) Czerwonka, D.; Domagalska, J.; Pyta, K.; Kubicka, M. M.; Pecyna, P.; Gajecka, M.; Przybylski, P. *Eur. J. Med. Chem.* **2016**, *116*, 216–221.
- (10) Aristoff, P. A.; Garcia, G. A.; Kirchhoff, P. D.; Showalter, H. D. H. *Tuberculosis* **2010**, *90*, 94–118.
- (11) Ramos-e-Silva, M.; Rebello, P. F. B. *Am. J. Clin. Dermatol.* **2001**, *2*, 203–211.
- (12) Marsot, A.; Ménard, A.; Dupouey, J.; Allanioux, L.; Blin, O.; Guilhaumou, R. *Br. J. Clin. Pharmacol.* **2020**, *86*, 2319–2324.
- (13) Sepkowitz, K. A.; Raffalli, J.; Riley, L.; Kiehn, T. E.; Armstrong, D. *Clin. Microbiol. Rev.* **1995**, *8*, 180–199.
- (14) Goldstein, B. P. *J. Antibiot.* **2014**, *67*, 625–630.
- (15) Peek, J.; Xu, J.; Wang, H.; Suryavanshi, S.; Zimmerman, M.; Russo, R.; Park, S.; Perlin, D. S.; Brady, S. F. *ACS Infect. Dis.* **2020**, *6*, 2431–2440.
- (16) Pinto, F. C. L.; Silveira, E. R.; Vasconcelos, A. C. L.; Florêncio, K. G. D.; Oliveira, F. A. S.; Sahm, B. B.; Costa-lotufo, L. V.; Bauermeister, A.; Lopes, N. P.; Wilke, D. V.; Pessoa, O. D. L. *J. Braz. Chem. Soc.* **2020**, *31*, 143–152.
- (17) Sousa, T. D. S.; Jimenez, P. C.; Ferreira, E. G.; Silveira, E. R.; Braz-Filho, R.; Pessoa, O. D. L.; Costa-Lotufo, L. V. *J. Nat. Prod.* **2012**, *75*, 489–493.
- (18) Da Silva, A. B.; Pinto, F. C. L.; Silveira, E. R.; Costa-Lotufo, L. V.; Costa, W. S.; Ayala, A. P.; Canuto, K. M.; Barros, A. B.; Araújo, A. J.; Marinho Filho, J. D. B.; Pessoa, O. D. L. *Fitoterapia* **2019**, *138*, 104357–104361.
- (19) Stratmann, A.; Schupp, T.; Toupet, C.; Schilling, W.; Oberer, L.; Traber, R. *J.*

- Antibiot.* **2002**, *55*, 396–406.
- (20) Silverstein, R. M.; Webster, F. X.; Kiemle, D. J. *Spectrometric Identification of Organic Compounds*, 7th ed.; Wiley: UK, 2005.
- (21) Chen, M.; Roush, W. R. *J. Org. Chem.* **2013**, *78*, 3–8.
- (22) Hewavitharana, A. K.; Shaw, P. N.; Kim, T. K.; Fuerst, J. A. *J. Chromatogr. B.* **2007**, *852*, 362–366.
- (23) Grimblat, N.; Zanardi, M. M.; Sarotti, A. M. *J. Org. Chem.* **2015**, *80*, 12526–12534.
- (24) Smith, S. G.; Goodman, J. M. *J. Am. Chem. Soc.* **2010**, *132*, 12946–12959.
- (25) Jensen, P. R.; Moore, B. S.; Fenical, W. *Nat. Prod. Rep.* **2015**, *32*, 738–751.
- (26) Kim, H.; Kim, S.; Kim, M.; Lee, C.; Yang, I.; Nam, S. J. *Arch. Pharm. Res.* **2020**, *43*, 1230–1258.
- (27) Wilson, M. C.; Gulder, T. A. M.; Mahmud, T.; Moore, B. S. *J. Am. Chem. Soc.* **2010**, *132*, 12757–12765.
- (28) Kang, Q.; Shen, Y.; Bai, L. *Nat. Prod. Rep.* **2012**, *29*, 243–263.
- (29) Qi, F.; Lei, C.; Li, F.; Zhang, X.; Wang, J.; Zhang, W.; Fan, Z.; Li, W.; Tang, G. L.; Xiao, Y.; Zhao, G.; Li, S. *Nat. Commun.* **2018**, *9*, 2342–2350.
- (30) August, P. R.; Tang, L.; Yoon, Y. J.; Ning, S.; Muller, R.; Yu, T.-W.; Taylor, M.; Hoffmann, D.; Kim, C.-G.; Zhang, X.; Hutchinson, C. R.; Floss, H. G. *Chem. Biol.* **1998**, *5*, 69–79.
- (31) Buyszko, I.; Drager, G.; Klenge, A.; Kirschning, A. *Chem. Eur. J.* **2015**, *21*, 19231–19242.
- (32) Xu, J.; Mahmud, T.; Floss, H. G. *Arch. Biochem. Biophys.* **2003**, *411*, 277–288.
- (33) Tian, J.; Han, C.; Guo, W. H.; Yin, Y.; Wang, X. B.; Sun, H. Bin; Yao, H. Q.; Yang, Y.; Wang, C.; Liu, C.; Yang, M. H.; Kong, L. Y. *Org. Lett.* **2017**, *19*, 6348–6351.
- (34) Bauermeister, A.; Velasco-Alzate, K.; Dias, T.; Macedo, H.; Ferreira, E. G.; Jimenez, P. C.; Lotufo, T. M. C.; Lopes, N. P.; Gaudêncio, S. P.; Costa-Lotufo, L. V. *Front. Microbiol.* **2018**, *9*, 1–13.
- (35) Chambers, L. G.; Fletcher, R. *Math. Gaz.* **2001**, *85*, 562–563.
- (36) Zinola, C. F. *Electrocatalysis: Computational, Experimental, and Industrial Aspects*; 1st ed.; CRC Press: US, 2010.



- (37) Perdew, J. P.; Burke, K.; Ernzerhof, M. Generalized Gradient Approximation Made Simple. *Phys. Rev. Lett.* **1996**, *77*, 3865–3868.
- (38) Frisch, M. J.; Trucks, G. W.; Schlegel, H. B.; Scuseria, G. E.; Robb, M. A.; Cheeseman, J. R.; Scalmani, G.; Barone, V.; Petersson, G. A.; Nakatsuji, H.; Li, X.; Caricato, M.; Marenich, A. V.; Bloino, J.; Janesko, B. G.; Gomperts, R.; Mennucci, B.; Hratchian, H. P.; Ortiz, J. V.; Izmaylov, A. F.; Sonnenberg, J. L.; Williams, Y. D.; Ding, F.; Lipparini, F.; Egidi, F.; Goings, J.; Peng, B.; Petrone, A.; Henderson, T.; Ranasinghe, D.; Zakrzewski, V. G.; Gao, J.; Rega, N.; Zheng, G.; Liang, W.; Hada, M.; Ehara, M.; Toyota, K.; Fukuda, R.; Hasegawa, J.; Ishida, M.; Nakajima, T.; Honda, Y.; Kitao, O.; Nakai, H.; Vreven, T.; Throssell, K.; Montgomery, J. A. Jr.; Peralta, J. E.; Ogliaro, F.; Bearpark, M. J.; Heyd, J. J.; Brothers, E. N.; Kudin, K. N.; Staroverov, V. N.; Keith, T. A.; Kobayashi, R.; Normand, J.; Raghavachari, K.; Rendell, A. P.; Burant, J. C.; Iyengar, S. S.; Tomasi, J.; Cossi, M.; Millam, J. M.; Klene, M.; Adamo, C.; Cammi, R.; Ochterski, J. W.; Martin, R. L.; Morokuma, K.; Farkas, O.; Foresman, J. B.; Fox, D. J.; Gaussian 16, Rev. C.01. Wallingford CT, New York: Gaussian, Inc.; 2016.
- (39) Mennucci, B. *WIREs Comput. Mol. Sci.* **2012**, *2*, 386–404.
- (40) Mennucci, B.; Cancès, E.; Tomasi, J. *J. Phys. Chem. B* **1997**, *101*, 10506–10517.
- (41) Wolinski, K.; Hinton, J. F.; Pulay, P. *J. Am. Chem. Soc.* **1990**, *112*, 8251–8260.
- (42) Smith, S. G.; Goodman, J. M. *J. Am. Chem. Soc.* **2010**, *132*, 12946–12959.
- (43) CLSI - Clinical Laboratory Standards Institute Approved standard M07-A10; Wayne, PA, 2015.
- (44) Mukherjee, S.; Kar, R. K.; Nanga, R. P. R.; Mroue, K. H.; Ramamoorthy, A.; Bhunia, A. *Phys. Chem. Chem. Phys.* **2017**, *19*, 19289–19299.
- (45) Wu, E. L.; Cheng, X.; Jo, S.; Rui, H.; Song, K. C.; Dávila-Contreras, E. M.; Qi,

- Y.; Lee, J.; Monje-Galvan, V.; Venable, R. M.; Klauda, J. B.; Im, W. *J. Comput. Chem.* **2014**, *35*, 1997–2004.
- (46) Van Der Spoel, D.; Lindahl, E.; Hess, B.; Groenhof, G.; Mark, A. E.; Berendsen, H. J. C. *J. Comput. Chem.* **2005**, *26*, 1701–1718.
- (47) Huang, J.; MacKerell Jr, A. D. *J. Comput. Chem.* **2013**, *34*, 2135–2145.
- (48) Jorgensen, W. L.; Chandrasekhar, J.; Madura, J. D.; Impey, R. W.; Klein, M. L. *J. Chem. Phys.* **1983**, *79*, 926–935.
- (49) Van Gunsteren, W. F.; Berendsen, H. J. C. *Mol. Simul.* **1988**, *1*, 173–185.
- (50) Darden, T.; York, D.; Pedersen, L. *J. Chem. Phys.* **1993**, *98*, 10089–10092.
- (51) Hess, B.; Bekker, H.; Berendsen, H. J. C.; Fraaije, J. G. E. M. *J. Comput. Chem.* **1997**, *18*, 1463–1472.
- (52) Hoover, W. G. *Phys. Rev. A* **1985**, *31*, 1695–1697.
- (53) Nosé, S.; Klein, M. L. *Mol. Phys.* **1983**, *50*, 1055–1076.
- (54) Arfken, G. B.; Weber, H. J.; Harris, F. E. *Mathematical Methods for Physicists*; 7th ed.; Elsevier Inc., 2013.
- (55) Hestenes, M. R.; Stiefel, E. *J. Res. Natl. Bur. Stand.* **1952**, *49*, 409–436.
- (56) Amorim-Carmo, B.; Daniele-Silva, A.; Parente, A. M. S.; Furtado, A. A.; Carvalho, E.; Oliveira, J. W. F.; Santos, E. C. G.; Silva, M. S.; Silva, S. R. B.; Silva-Júnior, A. A.; Monteiro, N. K.; Fernandes-Pedrosa, M. F. *Int. J. Mol. Sci.* **2019**, *20*, 623–643.
- (57) Ribeiro, L. F.; Tullman, J.; Nicholes, N.; Silva, S. R. B.; Vieira, D. S.; Ostermeier, M.; Ward, R. J. *Biotechnol. Biofuels* **2016**, *9*, 119–130.
- (58) Riccardi, L.; Genna, V.; De Vivo, M. *Nat. Rev. Chem.* **2018**, *2*, 100–112.
- (59) Rega, N.; Iyengar, S. S.; Voth, G. A.; Schlegel, H. B.; Vreven, T.; Frisch, M. J. *J. Phys. Chem. B* **2004**, *108*, 4210–4220.

- (60) Kim, K.; Jordan, K. D. *J. Phys. Chem.* **1994**, *98*, 10089–10094.
- (61) Becke, A. D. *Phys. Rev. A* **1988**, *38*, 3098–3100.
- (62) Dewar, M. J. S.; Zoebisch, E. G.; Healy, E. F.; Stewart, J. J. P. *J. Am. Chem. Soc.* **1985**, *107*, 3902–3909.

**SUPPORTING INFORMATION****Table of Contents**

- Figure S1.**  $^1\text{H}$  NMR (500 MHz) spectrum of **1** in  $\text{DMSO-}d_6$
- Figure S2.** Expanded  $^1\text{H}$  NMR (500 MHz) spectrum of **1** in  $\text{DMSO-}d_6$
- Figure S3.** Expanded  $^1\text{H}$  NMR (500 MHz) spectrum of **1** in  $\text{DMSO-}d_6$
- Figure S4.** COSY NMR spectrum of **1** in  $\text{DMSO-}d_6$
- Figure S5.** TOCSY NMR spectrum of **1** in  $\text{DMSO-}d_6$
- Figure S6.** HSQC NMR spectrum of **1** in  $\text{DMSO-}d_6$
- Figure S7.** HMBC NMR spectrum of **1** in  $\text{DMSO-}d_6$
- Figure S8.** HMBC NMR spectrum of **1** in  $\text{DMSO-}d_6$
- Figure S9.** NOESY NMR spectrum of **1** in  $\text{DMSO-}d_6$
- Figure S10.** HRESIMS spectrum of **1**
- Figure S11.** IR spectrum of **1**
- Figure S12.** UV spectrum of **1** in MeOH

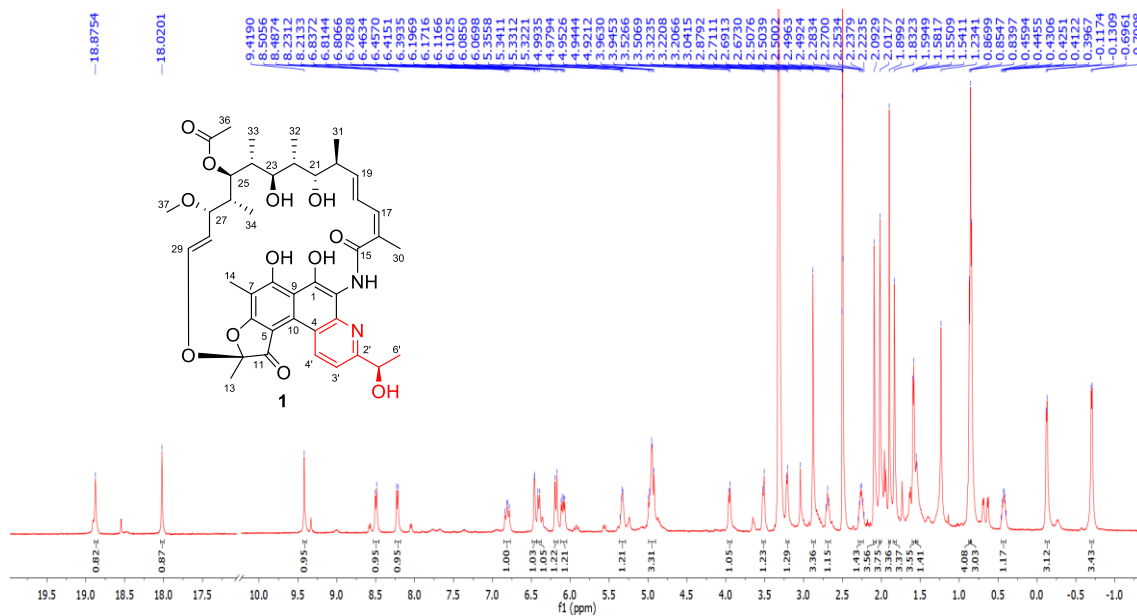


Figure S1.  $^1\text{H}$  NMR (500 MHz) spectrum of **1** in  $\text{DMSO-}d_6$ .

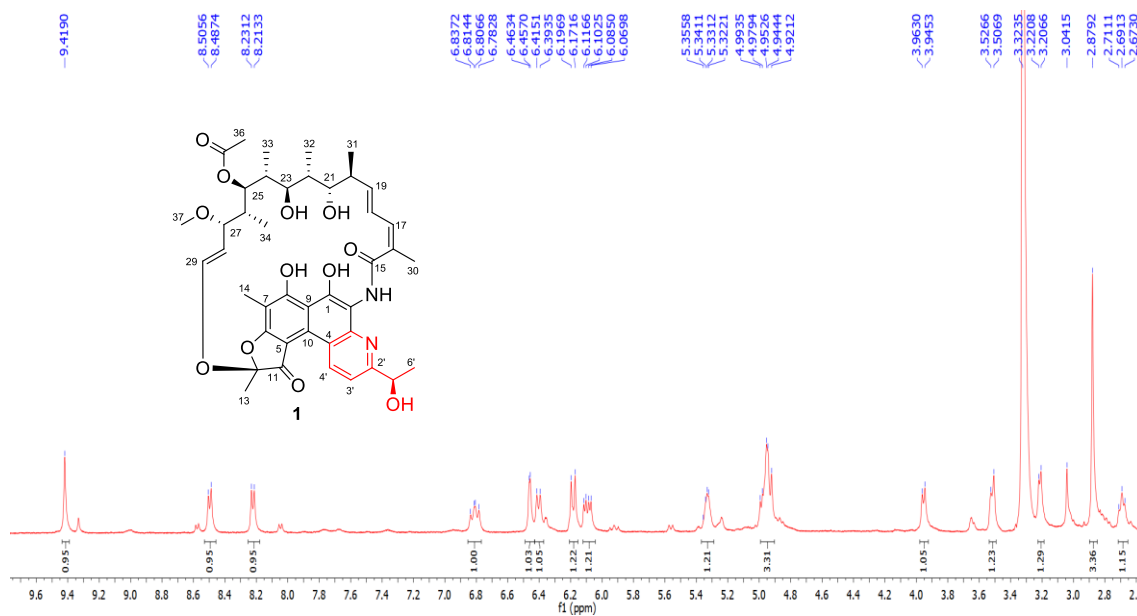
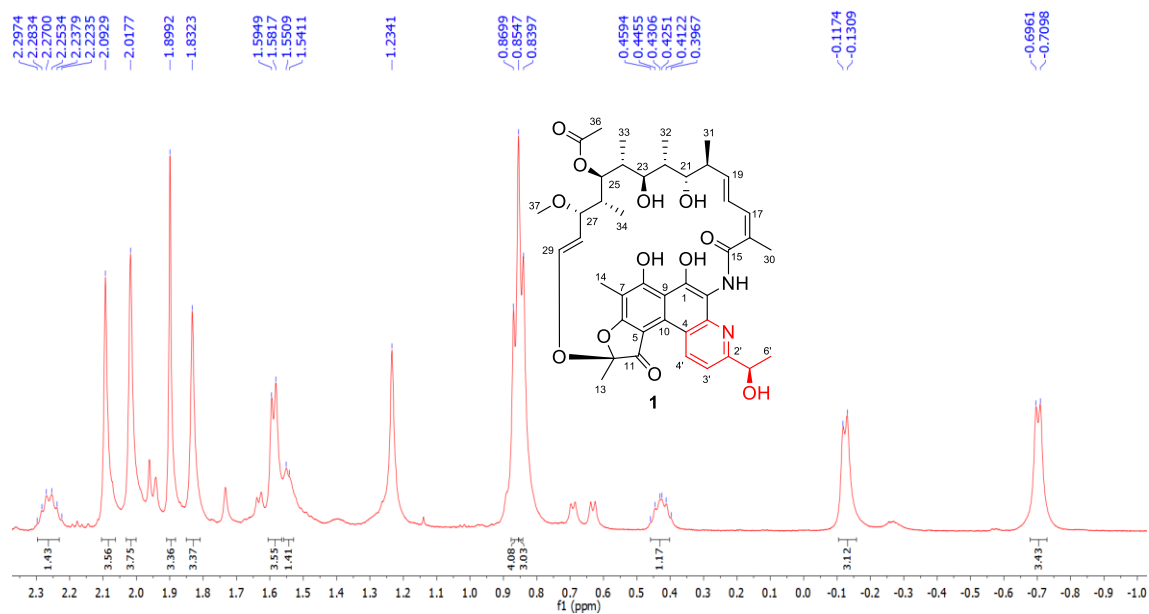
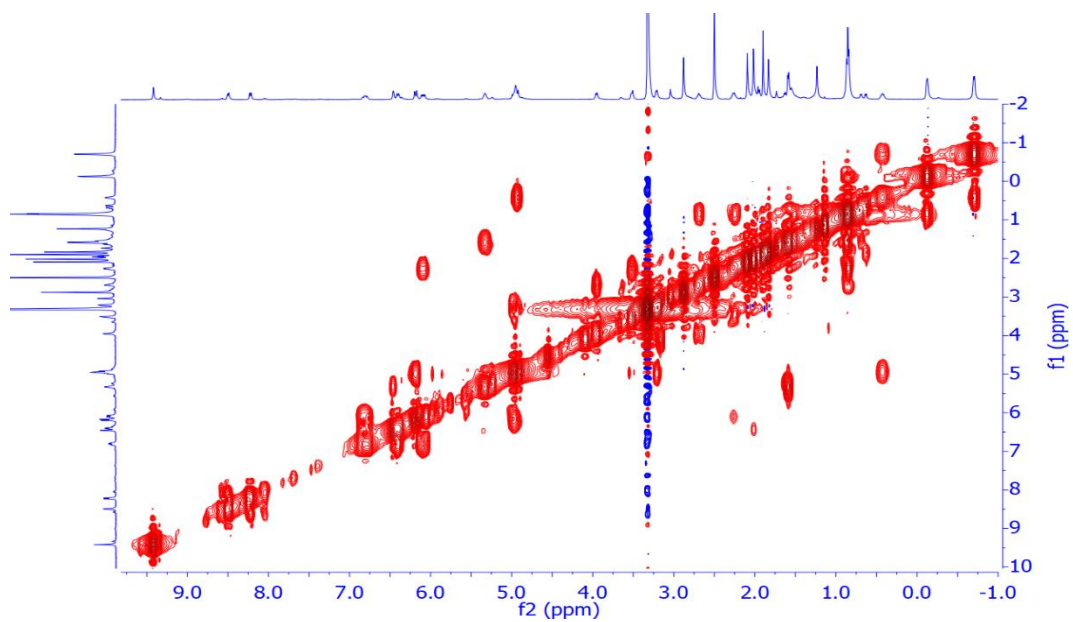


Figure S2. Expanded  $^1\text{H}$  NMR (500 MHz) spectrum of **1** in  $\text{DMSO-}d_6$ .



**Figure S3.** Expanded  $^1\text{H}$  NMR (500 MHz) spectrum of **1** in  $\text{DMSO-}d_6$ .



**Figure S4.** COSY NMR spectrum of **1** in  $\text{DMSO-}d_6$ .

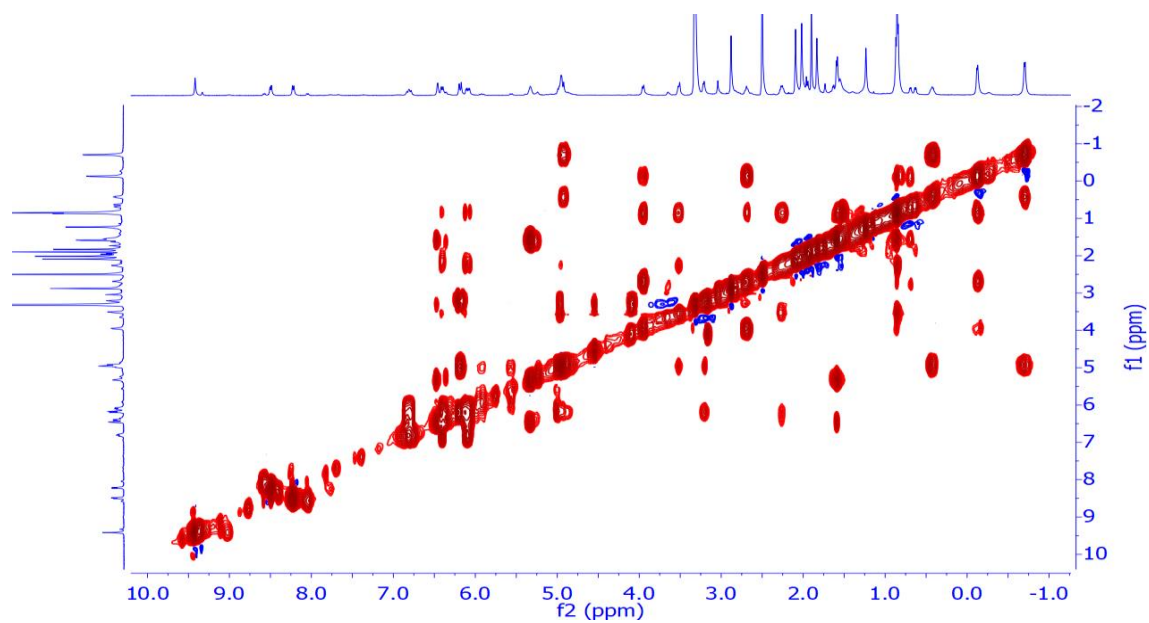


**Figure S5.** TOCSY NMR spectrum of **1** in DMSO- $d_6$ .

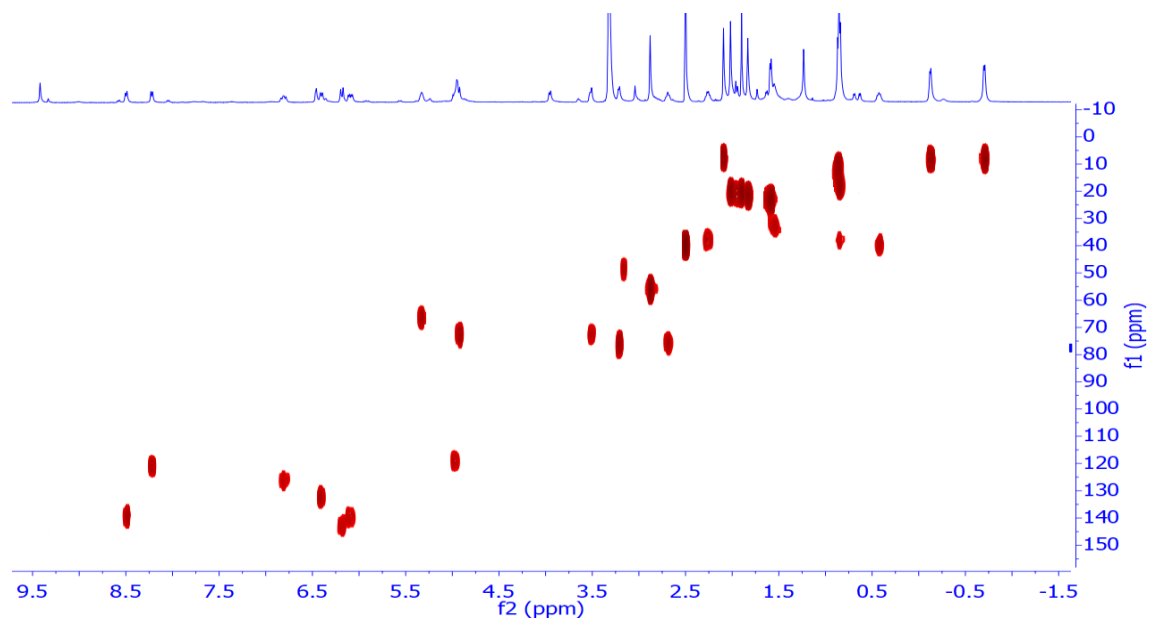


**Figure S6.** HSQC NMR spectrum of **1** in DMSO- $d_6$ .

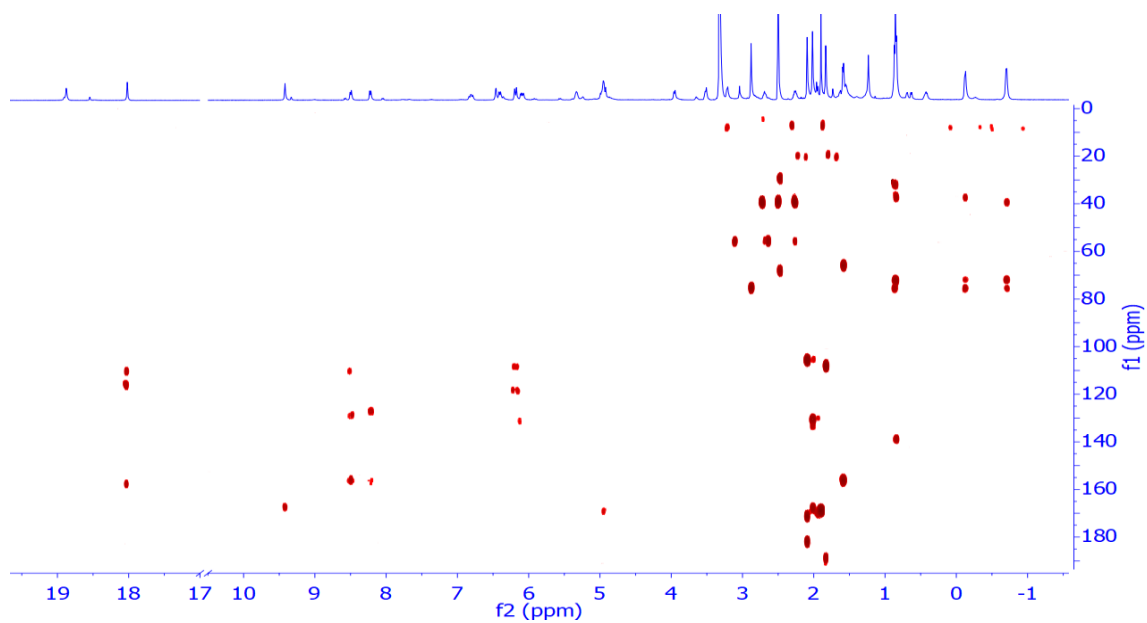


**Figure S7.** HMBC NMR spectrum of **1** in DMSO-*d*<sub>6</sub>.

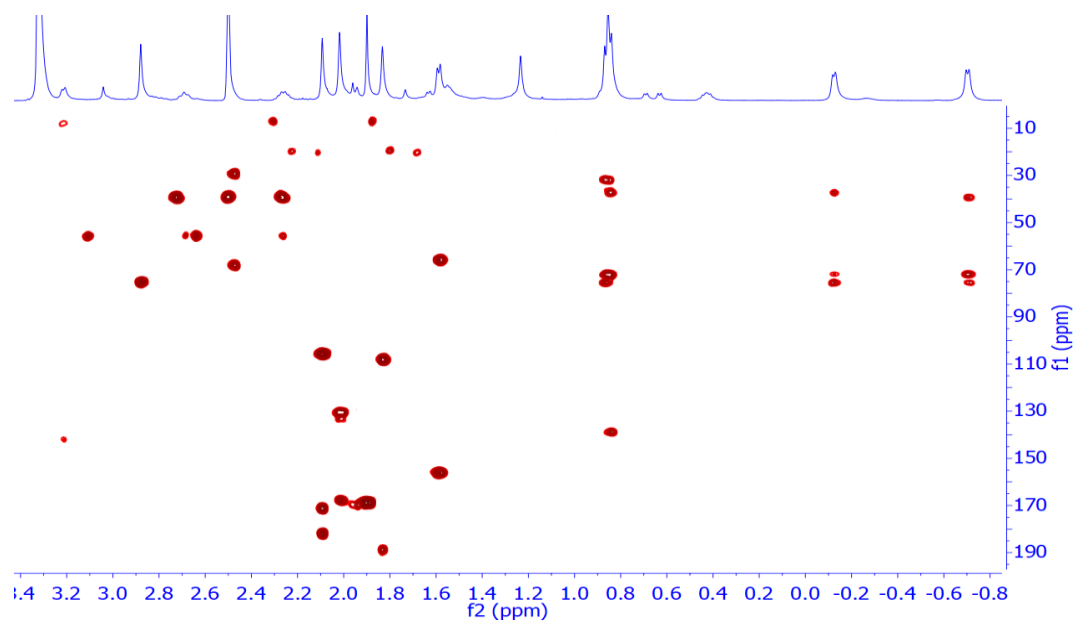


**Figure S8.** HMBC NMR spectrum of **1** in DMSO-*d*<sub>6</sub>.



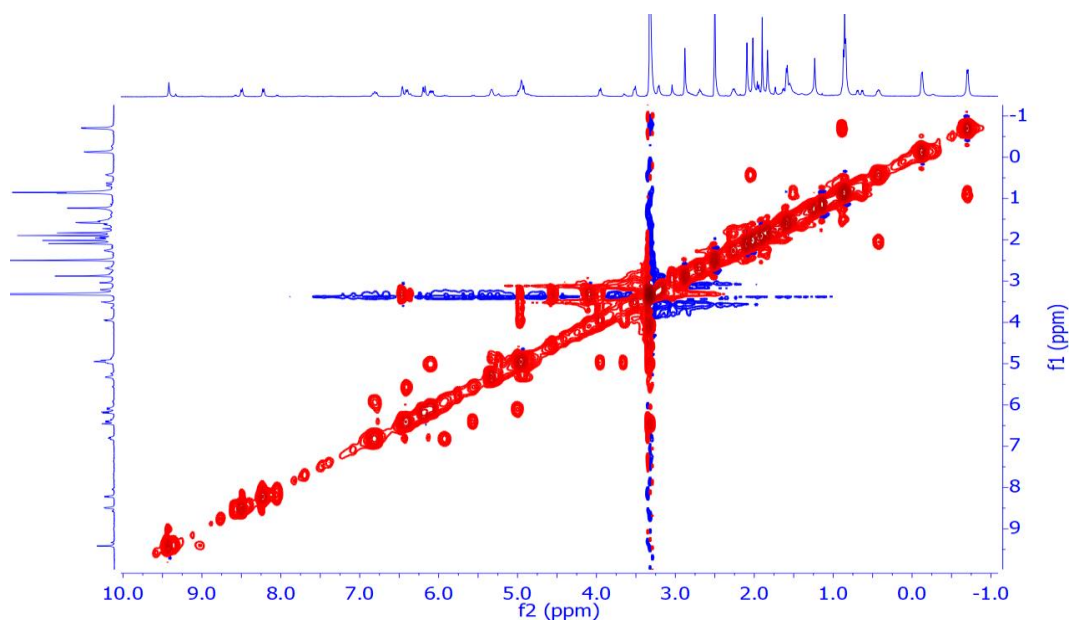


**Figure S9.** NOESY NMR spectrum of **1** in DMSO-*d*<sub>6</sub>.

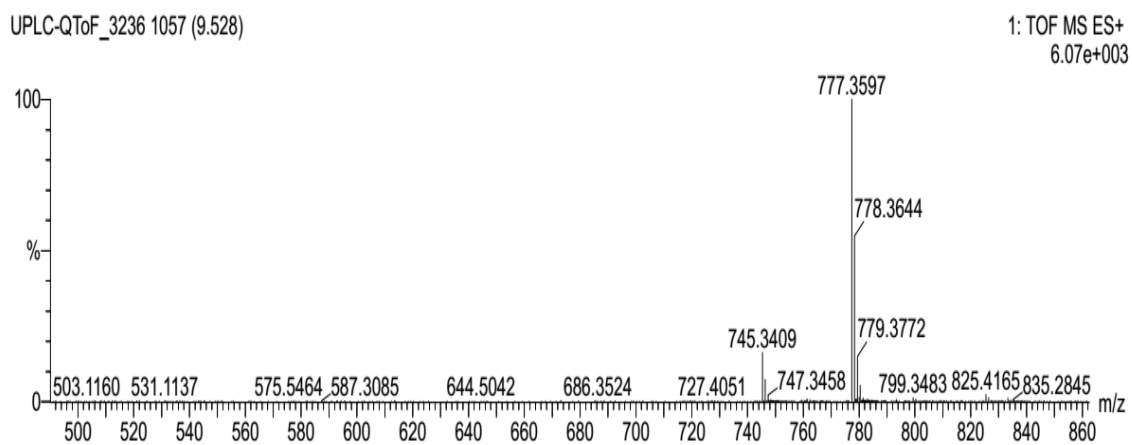


**Figure S10.** HRESIMS spectrum of **1**.

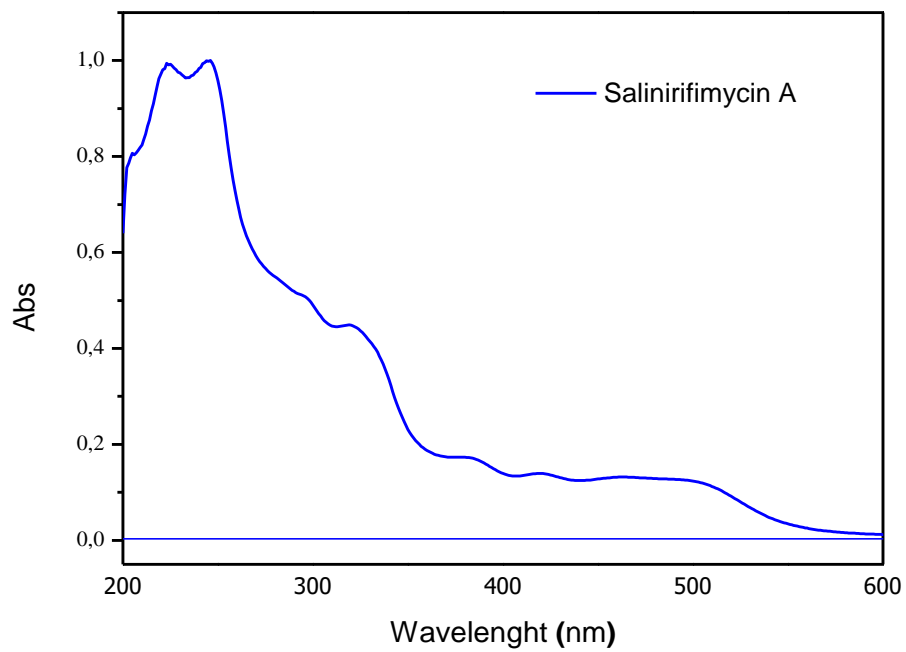


**Figure S12.** UV spectrum of **1** in MeOH.

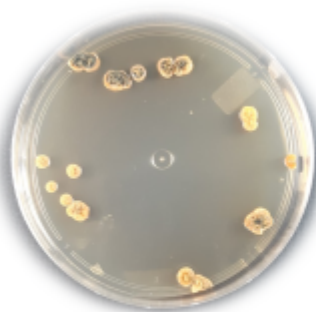
4.4

# Capítulo 4

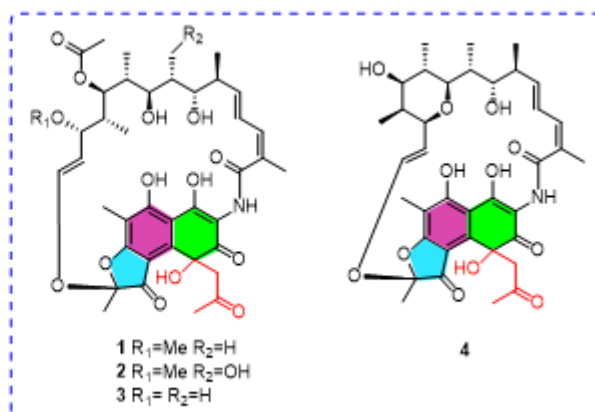
---

## Salinirifamycins B–E: Further Rifamycin S Derivatives from the Brazilian Marine Actinomycete *Salinispora arenicola*

---



*Salinispora arenicola*  
(BRA-213)



## **Salinirifamycins B–E: Further Rifamycin S Derivatives from the Brazilian Marine Actinomycete *Salinispora arenicola***

Alison B. da Silva,<sup>†</sup> Francisco C. L. Pinto,<sup>†</sup> Edilberto R. Silveira,<sup>†</sup> Diego V. Wilke,<sup>‡</sup> Elhton G. Ferreira,<sup>‡</sup> Leticia V. Costa-Lotufo,<sup>§</sup> Kirley M. Canuto,<sup>⊥</sup> José Delano B. Marinho Filho,<sup>||</sup> and Otilia Deusdenia L. Pessoa<sup>\*†</sup>

<sup>†</sup>*Departamento de Química Orgânica e Inorgânica, Universidade Federal do Ceará, 60.021-970, Fortaleza-CE, Brazil*

<sup>‡</sup>*Núcleo de Pesquisa e Desenvolvimento de Medicamentos, Universidade Federal do Ceará, 60.430-275, Fortaleza-CE, Brazil*

<sup>§</sup>*Departamento de Farmacologia, Universidade de São Paulo, 05508-900, São Paulo-SP, Brazil*

<sup>⊥</sup>*Embrapa Agroindústria Tropical, 60.511-110, Fortaleza-CE Brazil*

<sup>||</sup>*Núcleo de Pesquisa em Biodiversidade e Biotecnologia, Universidade Federal do Piauí, 64202-020, Parnaíba-PI, Brazil*

\*Phone: +55-85-33669441. E-mail: otialoiola@gmail.com

**ABSTRACT:** Four rifamycin S derivatives, named salinirifamycins B–E (**1–4**), were isolated from a fermented extract of a marine *Salinispora arenicola* (BRA-213). Their structures were elucidated using a combination of spectroscopic techniques (NMR, IR, UV, and, HRMS). Compounds **1**, **2**, and **4** displayed antibacterial activity against *Staphylococcus aureus* and *Enterococcus faecalis* with MIC values of 2.0 to 125.0 µg/mL. A plausible biosynthetic pathway for **1–4** is proposed.

## INTRODUCTION

Marine bacteria, particularly actinomycetes, represent an extraordinary source of natural products that possess unusual structural features and a wide variety of biological activity.<sup>1</sup> Among the various genera of the actinomycetes, *Salinispora* is a prolific source of novel natural products and has become model organisms in the development of methods for new secondary metabolites discovery.<sup>2</sup> The *Salinispora* genus was formally described in 2005 as the first group of exclusively marine actinomycetes comprised of three species (*S. tropica*, *S. arenicola*, and *S. pacifica*); however, recently six new species have been reported for this genus.<sup>3,4</sup> These bacteria are reported as a source of unusual bioactive compounds, among which over 50 natural products structurally diverse and unprecedented have been isolated as salinosporamides,<sup>5</sup> saliniquinones,<sup>6</sup> arenicolides,<sup>7</sup> saliniketals,<sup>8</sup> arenamides,<sup>9</sup> and the important class well-known antibiotics rifamycins are also reported.<sup>10</sup> Rifamycins of the ansamycin family, first isolated in 1957 from *Amycolatopsis mediterranei* S699.<sup>11</sup> Semisynthetic rifamycin derivatives (e.g., rifampicin) have been widely used in clinical settings and still are the principal chemotherapeutic agents for combating tuberculosis, leprosy, and AIDS-related mycobacterial infections.<sup>12-14</sup> In continuation of our study for bioactive natural compounds from marine bacteria,<sup>15-16</sup> we have investigated the EtOAc extract of *S. arenicola* (BRA-213) strain recovered from the sediments of the Saint Peter and Saint Paul Archipelago-Brazil, (ASPSP), an outlying group of islets located in the Atlantic

Ocean. Herein, are describe the isolation, characterization of four novel rifamycin S derivatives, and their antibacterial activity against Gram-positive bacteria.

## RESULTS AND DISCUSSION

LC-MS analysis of the AcOEt extract of *S. arenicola* showed the presence of several compounds with a similar UV profile ( $\lambda$  268, 378, and 429 nm) and high molecular weight ( $[M - H]^-$  at  $m/z$  600-800). This extract was subjected to chromatographic procedures (cartridge C-18, Sephadex LH-20, and reverse-phase HPLC) leading to the isolation of four new rifamycin S derivatives (Figure 1), named salinirifamycins B–E (1–4).

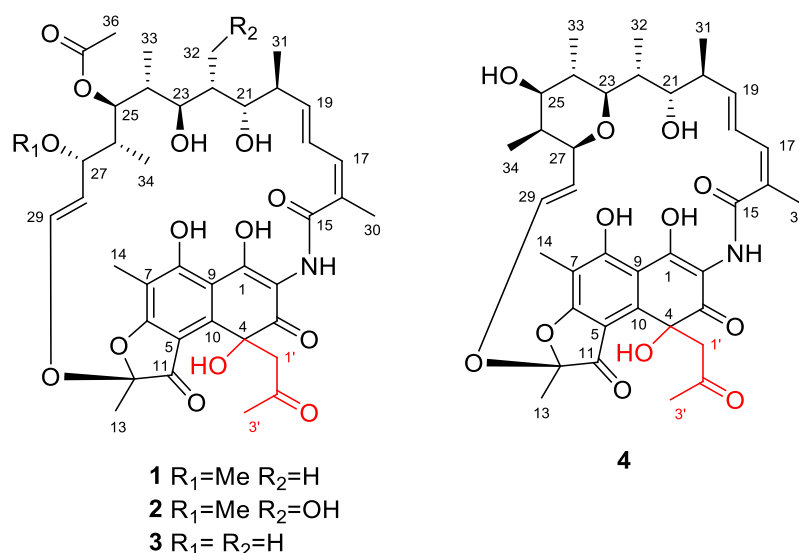


**Figure 1.** Chemical structures of Salinirifamycins B–E (1–5).

Salinirifamycin B (**1**) was isolated as a yellowish solid. Its molecular formula was determined as  $C_{40}H_{51}NO_{14}$  by HRESIMS data ( $m/z$  768.3240  $[M - H]^-$ , calcd for  $C_{40}H_{50}NO_{14}$ , 768.3237), with corresponding degrees of hydrogen deficiency of 16. Its  $^1H$  and HSQC NMR spectra showed five exchangeable protons ( $\delta_H$  19.15, 8.00, 6.09, 5.00, and 4.00) assigned to NH or OH groups, five olefinic protons at  $\delta_H$  7.07 (dd,  $J = 15.9, 10.7$  Hz, H-18), 6.28 (d,  $J = 12.9$  Hz,

H-29), 6.09 (d,  $J = 10.7$  Hz, H-17), 5.93 (dd,  $J = 15.9, 7.6$  Hz, H-19), and 4.90 (dd,  $J = 12.9, 8.6$  Hz, H-28), and four oxymethine protons at  $\delta_{\text{H}} 5.07$  (d,  $J = 10.6$  Hz, H-25), 3.86 (br d,  $J = 8.9$  Hz, H-21), 3.26 (d,  $J = 8.6$  Hz, H-27), and 2.82 (m, H-23). In addition, were observed ten methyl groups including a methoxy ( $\delta_{\text{H}} 2.87$ ), a methyl ketone ( $\delta_{\text{H}} 2.16$ ), and an acetyl group ( $\delta_{\text{H}} 1.97$ ) as well as signals for one pair of diastereotopic methylene protons at  $\delta_{\text{H}} 2.81$  (d,  $J = 11.9$  Hz, H<sub>2</sub>-1'b) and 2.72 (d,  $J = 11.9$  Hz, H<sub>2</sub>-1'a). The <sup>13</sup>C-APT NMR displayed resonances for 40 carbons (Table 1), which were characterized as 10 methyls, one methylene, 13 methines (five olefinic and four oxygenated), and 16 non-hydrogenated carbons (five carbonyls). The chemical shifts of methyl ketone ( $\delta_{\text{H}}/\delta_{\text{C}} 2.16/32.7$ , Me-3'), methylene group ( $\delta_{\text{H}}/\delta_{\text{C}} 2.81$  and  $2.73/32.7$ , C-1'), and carbonyl carbon at  $\delta_{\text{C}} 205.0$  (C-2'), along with the HMBC correlations of the methyl protons and methylene protons with C-2', suggested the presence of the 2'-oxo-propyl group. Detailed analysis of the <sup>1</sup>H and <sup>13</sup>C NMR spectroscopic data (Table 1), along with the COSY, HSQC, and HMBC correlations of **1** (Figure 1) showed the same polyketide chain from the C-15 ( $\delta_{\text{C}} 167.7$ ) to C-29 ( $\delta_{\text{C}} 143.2$ ) present in rifamycins.<sup>17</sup> The presence of the fully substituted naphthofuranone core was indicated by the HMBC correlations of the Me-13 ( $\delta_{\text{H}} 1.60$ ) with the carbons at  $\delta_{\text{C}} 193.6$  (C-11) and 107.6 (C-12); Me-14 ( $\delta_{\text{H}} 1.96$ ) with  $\delta_{\text{C}} 175.6$  (C-6), 169.2 (C-8), and 105.9 (C-7), and the hydroxy proton at  $\delta_{\text{H}} 19.15$  (OH-1) with  $\delta_{\text{C}} 172.8$  (C-1), 106.0 (C-2), and 109.4 (C-9). The polyketide chain was attached to the naphthofuranone moiety in C-2 and C-12 based on the HMBC correlations of amide proton at  $\delta_{\text{H}} 8.00$  with the carbons at  $\delta_{\text{C}} 188.3$  (C-3), 167.7 (C-15), and 106.0 (C-2) as well as of the olefinic proton  $\delta_{\text{H}} 6.28$  (H-29) with the ketal carbon  $\delta_{\text{C}} 107.6$  (C-12). Finally, the unequivocal position of the 2'-oxo-propyl group located at C-4 was established by HMBC correlations of methylene protons with the carbons at  $\delta_{\text{C}} 188.3$  (C-3), 145.1 (C-10), and 76.5 (C-4). The relative configuration of polyketide of **1** was assigned to be the same as the of rifamycin S based on the NOESY spectrum and biosynthetic logic.<sup>18</sup> However, due to the lack of NOESY correlation of the hydroxy proton HO-4 ( $\delta_{\text{H}} 6.09$ ), it was not possible to

assign the relative configuration of C-4. Thus, the structure of **1** was proposed as a new 4-(2'-oxopropyl)-3-oxorifamycin S derivative.

Salinirifamycin C (**2**) was isolated as a yellowish solid. Its molecular formula of  $C_{40}H_{51}NO_{14}$  was defined based on HRESIMS whose spectrum displayed an ion peak at  $m/z$  784.3193.  $[M - H]^-$ . Analyses of the  $^1H$  and  $^{13}C$  NMR data of **2** (Table 1) showed the presence of the rifamycin S derivative bearing the 2'-oxo-propyl group at C-4 similar to **1**. The major difference observed was the replacement of the methyl group ( $\delta_H/\delta_C$  0.91/10.7, Me-32) in **1** by a hydroxymethyl group ( $\delta_H$  3.64, dd,  $J = 10.8, 4.6$  Hz, H-32b, 3.53, dd,  $J = 10.8, 8.5$  Hz, H-32a;  $\delta_C$  57.2, C-32) in **2**. The position of the hydroxymethyl group in C-32 was supported by the HMBC correlation of H<sub>2</sub>-32 ( $\delta_H$  3.53) with the carbon at  $\delta_C$  71.1 (C-23) support the structure of **2** as a new 32-hydroxy-4-(2'-oxopropyl)-3-oxorifamycin S derivative.

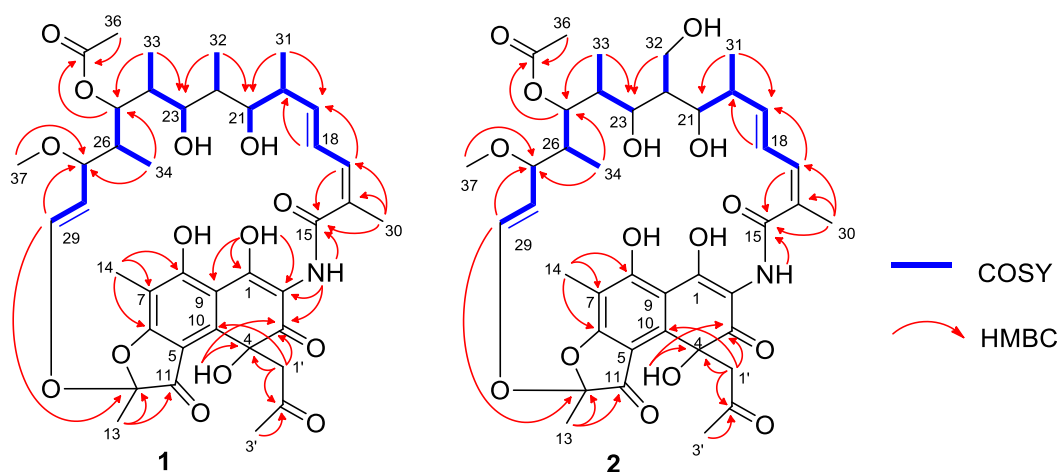


**Figure 2.** Key COSY and HMBC correlations of compounds **1** and **2**.

Salinirifamycin D (**3**) was isolated as a yellowish solid, had its molecular formula assigned as  $C_{39}H_{49}NO_{14}$  based on the  $[M - H]^-$  ion peak at  $m/z$  754.3074 (calcd  $m/z$  754.3080) observed by HRESIMS. The NMR spectroscopic data of **3** were similar to those of **1**, except by replacement of the OMe substituent at C-27 in **1** with OH substituent in **3**. Thus, compound **3**



was determined to be 27-demethoxy-27-hydroxy-4(2'-oxopropyl)-3-oxorifamycin S, a further new rifamycin S derivative.

Salinirifamycin E (**4**) was isolated as a yellowish solid. Its molecular formula was determined as  $C_{37}H_{45}NO_{12}$  by HRESIMS data ( $m/z$  694.2872  $[M - H]^-$ , calcd for  $C_{37}H_{44}NO_{12}$ , 694.2869), which was indicative of sixteen degrees indices of hydrogen deficiency. Analyses of the  $^1H$  and  $^{13}C$  NMR data of **4** (Table 2) showed also the presence of the rifamycin S derivative bearing the 2'-oxo-propyl group at C-4 similar to **1**. The major difference observed in **4** was the absence of the acetyl and methoxy groups found in **1**. The sequence of scalar couplings for the spins systems Me-33(C-24)–H-23, Me-34(C-26)–HO-25, and H-29–H-27 observed in the COSY spectrum, along with the HMBC correlations of the Me-33 ( $\delta_H$  0.54, d,  $J = 6.7$  Hz) with the carbons at  $\delta_C$  76.1 (C-23) and 69.5 (C-25) and Me-34 ( $\delta_H$  -0.22, d,  $J = 6.6$  Hz) with  $\delta_C$  69.5 (C-25) and 65.4 (C-27) support the presence of the ether group (C-23/O/C-27) as depicted in Figure 3. Thus, compound **4** was determined as a new 4-(2'-oxopropyl)-3-oxorifamycin S derivative.

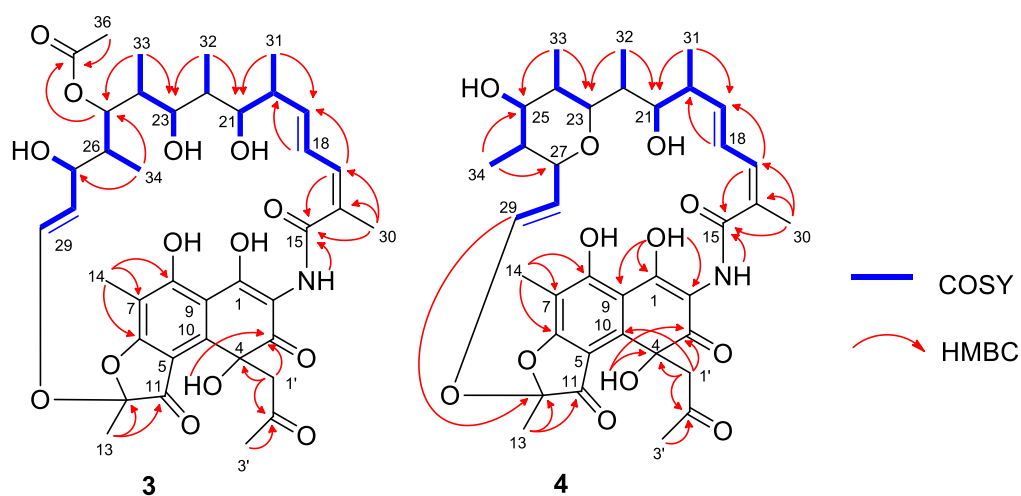


**Figure 3.** Key COSY and HMBC correlations of compounds **3** and **4**.

**Table 1.**  $^1\text{H}$  (600 MHz) and  $^{13}\text{C}$  (150 MHz) NMR Spectroscopic Data for Compounds **1** and **2** ( $\delta$  in ppm,  $J$  in Hz) in  $\text{DMSO-}d_6$ .

no.	<b>1</b>		<b>2</b>	
	$\delta_{\text{C}}$ , type	$\delta_{\text{H}}$	$\delta_{\text{C}}$ , type	$\delta_{\text{H}}$
1	172.8, C		173.0, C	
2	106.0, C		106.0, C	
3	188.3, C		188.1, C <sup>a</sup>	
4	76.5, C		76.4, C <sup>a</sup>	
5	105.7, C		105.7, C	
6	175.6, C		175.5, C	
7	106.4, C		106.5, C	
8	169.2, C		169.3, C	
9	109.4, C		109.4, C	
10	145.1, C		145.2, C	
11	193.6, C		193.6, C	
12	107.6, C		107.5, C	
13	22.2, CH <sub>3</sub>	1.60 s	22.1, CH <sub>3</sub>	1.60 s
14	7.1, CH <sub>3</sub>	1.96 s	7.0, CH <sub>3</sub>	1.96 s
15	167.7, C		167.8, C	
16	132.6, C		132.2, C <sup>a</sup>	
17	131.2, CH	6.09 d (10.7)	131.2, CH	6.09 d (10.9)
18	127.5, CH	7.07 dd (15.9, 10.7)	127.6, CH	7.08 dd (16.2, 10.9)
19	137.5, CH	5.93 dd (15.9, 7.6)	137.8, CH	5.94 dd (16.2, 7.7)
20	37.3, CH	2.20 m	37.3, CH	2.38 m
21	72.7, CH	3.86 br d (8.9)	73.1, CH	3.84 br d (10.1)
22	32.3, CH	1.72 m	41.2, CH	1.65 m
23	76.2, CH	2.82 m	71.1, CH	3.24 br t (8.8)
24	39.2, CH	1.46 m	39.9, CH	1.47 m
25	73.7, CH	5.07 d (10.6)	73.8, CH	5.07 d (10.9)
26	38.6, CH	1.44 m	38.3, CH	1.42 m
27	76.3, CH	3.26 d (8.6)	76.4, CH	3.27 d (8.7)
28	117.9, CH	4.90 dd (12.9, 8.6)	117.9, CH	4.91 dd (12.9, 8.5)
29	143.2, CH	6.28 d (12.9)	143.1, CH	6.27 d (12.9)
30	20.3, CH <sub>3</sub>	1.87 s	20.2, CH <sub>3</sub>	1.85 s
31	18.3, CH <sub>3</sub>	0.85 d (6.7)	18.5, CH <sub>3</sub>	0.93 d (6.8)
32a	10.7, CH <sub>3</sub>	0.91 d (7.0)	57.2, CH <sub>2</sub>	3.53 dd (10.8, 8.5)
32b				3.64 dd (10.8, 4.6)
33	9.6, CH <sub>3</sub>	0.65 d (6.7)	9.5, CH <sub>3</sub>	0.62 d (6.8)
34	9.5, CH <sub>3</sub>	-0.08 d (6.6)	9.5, CH <sub>3</sub>	-0.07 d (6.7)
35	169.3, C		169.3, C	
36	20.7, CH <sub>3</sub>	1.97 s	20.7, CH <sub>3</sub>	1.97 s
37	55.6, CH <sub>3</sub>	2.87 s	55.6, CH <sub>3</sub>	2.88 s
1'a	54.9, CH <sub>2</sub>	2.73 d (11.9)	55.1, CH <sub>2</sub>	2.75 d (12.0)
1'b		2.81 d (11.9)		2.80 d (12.0)
2'	205.0, C		205.0, C	
3'	32.7, CH <sub>3</sub>	2.16 s	32.7, CH <sub>3</sub>	2.16 s

HN-2	8.00 s	7.92 s
HO-1	19.15 s	19.11 br s
HO-4	6.09 s	6.10 s
HO-21	5.00 d (3.4)	4.94 br s
HO-23	4.00 d (8.9)	4.03 d (8.7)
HO-32		4.24 br s

<sup>a</sup>The <sup>13</sup>C chemical shifts were determined by analysis of the HMBC spectrum.

**Table 2.** <sup>1</sup>H and <sup>13</sup>C NMR Spectroscopic Data for Compounds **3** and **4** ( $\delta$  in ppm,  $J$  in Hz) in DMSO-*d*<sub>6</sub>.

no.	<b>3<sup>a</sup></b>		<b>4<sup>b</sup></b>	
	$\delta_C$ , type <sup>c</sup>	$\delta_H$	$\delta_C$ , type <sup>c</sup>	$\delta_H$
1	nd <sup>d</sup>		173.0, C	
2	nd		105.6, C	
3	188.6, C		188.2, C	
4	76.2, C		76.4, C	
5	nd		nd	
6	175.4, C		175.1, C	
7	105.7, C		105.5, C	
8	169.6, C		169.8, C	
9	nd		109.3, C	
10	nd		145.2, C	
11	194.0, C		194.2, C	
12	107.6, C		107.0, C	
13	21.9, CH <sub>3</sub>	1.58 s	21.3, CH <sub>3</sub>	1.57 s
14	7.0, CH <sub>3</sub>	1.97 s	6.9, CH <sub>3</sub>	1.96 s
15	167.7, C		167.5, C	
16	132.1, C		131.3, C	
17	131.2, CH	6.09 d (11.0)	131.1, CH	6.09 d (10.7)
18	127.5, CH	7.06 dd (16.1, 11.0)	127.1, CH	7.02 dd (16.0, 10.7)
19	137.6, CH	5.93 dd (16.1, 7.6)	137.8, CH	5.93 dd (16.0, 7.7)
20	37.4, CH	2.22 m	37.3, CH	2.22 m
21	73.1, CH	3.85 br d (9.7)	72.7, CH	3.90 br d (9.3)
22	32.4, CH	1.72 m	32.3, CH	1.74 m
23	76.3, CH	2.86 br t (8.7)	76.1, CH	3.21 br t (9.7)
24	38.9, CH	1.45 m	38.6, CH	1.32 m
25	74.4, CH	5.02 d (11.0)	69.5, CH	3.53 dd (10.3, 6.4)
26	39.4, CH	1.37 m	40.2, CH	1.11 m
27	66.0, CH	3.77 m	65.4, CH	4.30 br t (8.6)
28	123.0, CH	5.08 dd (12.6, 7.5)	124.5, CH	5.13 dd (12.7, 6.5)
29	140.8, CH	6.16 d (12.6)	139.3, CH	6.07 d (12.7)
30	20.4, CH <sub>3</sub>	1.85 s	20.2, CH <sub>3</sub>	1.85 s
31	18.3, CH <sub>3</sub>	0.86 d (6.5)	18.1, CH <sub>3</sub>	0.86 d (6.7)
32	10.9, CH <sub>3</sub>	0.91 d (7.0)	10.7, CH <sub>3</sub>	0.93 d (7.0)
33	9.5, CH <sub>3</sub>	0.65 d (6.7)	8.5, CH <sub>3</sub>	0.54 d (6.7)

34	9.2, CH <sub>3</sub>	-0.11 d (6.5)	9.0, CH <sub>3</sub>	-0.22 d (6.6)
35	170.2, C			
36	20.9, CH <sub>3</sub>	1.95 s		
1'a	55.0, CH <sub>2</sub>	2.73 d (12.0)	55.1, CH <sub>2</sub>	2.73 d (11.9)
1'b		2.81 d (12.0)		2.80 d (11.9)
2'	205.2, C		205.1, C	
3'	32.9, CH <sub>3</sub>	2.16 s	32.4, CH <sub>3</sub>	2.16 s
HN-2		8.01 s		7.94 s
HO-1				19.10 s
HO-4		6.07 s		6.00 s
HO-21		5.00 br s		4.90 d (3.7)
HO-23		4.03 d (8.5)		
HO-25				3.99 d (4.1)
HO-27		3.99 d (4.0)		

<sup>a</sup>500 MHz (<sup>1</sup>H) and 125 MHz (<sup>13</sup>C); <sup>b</sup>600 MHz (<sup>1</sup>H) and 150 MHz (<sup>13</sup>C); <sup>c</sup>The <sup>13</sup>C chemical shifts were determined by analysis of 2D spectra; <sup>d</sup>nd: not detected.

Plausible biogenetic pathways for compounds **1–4** were proposed based on well-described biosyntheses of rifamycins <sup>19-21</sup> (Scheme 1). Rifamycin S (**5**), identified in the *S. arenicola* <sup>22</sup>, was considered as the biosynthetic precursor of compounds **1–4**. Intermediate **i** could be obtained from **5** by oxidation and keto-enol tautomerization of the hydroxy group at C-3 of 3-hydroxy-rifamycin S (**6**). Nucleophilic addition of acetoacetyl-CoA, which is obtained by a Claisen condensation reaction between acetyl-CoA and malonyl-CoA, with intermediate **i** followed by hydrolysis and decarboxylation give **1**. Compounds **2–4** could be easily obtained from **1** through a series of typical reactions such as oxidation, demethylation, cyclization, and hydrolysis as showed in Scheme 1.

The antibacterial activity of compounds **1**, **2**, and **4** was evaluated against *Staphylococcus aureus* and *Enterococcus* (Table 3) bacterial strains. Compound **1** showed good activity against *S. aureus* and *E. faecalis* with MICs values of 31.2 to 2.0 µg/ mL. Compound **4** were susceptible only against *S. aureus*, with MIC value of 62.5 µg/ mL, whereas compound **2** showed moderate activity against *S. aureus* and *E. faecalis* with MICs values of 125.0 to 15.6 µg/ mL.

In summary, four rifamycin S derivatives called Salinifamycins B–E (**1–4**) were isolated from the *S. arenicola*. Salinifamycins B–E (**1–4**) represent new rifamycins with the unusual 2-oxo-propyl group as a substituent. The discovery of these compounds enriches the structural diversity reported for the *Salinispora* enabling the development of new therapeutic agents used to treat infectious diseases.

**Table 3. Antibacterial activity of compounds 1, 2, and 4 (MIC,  $\mu\text{g/mL}$ ).**

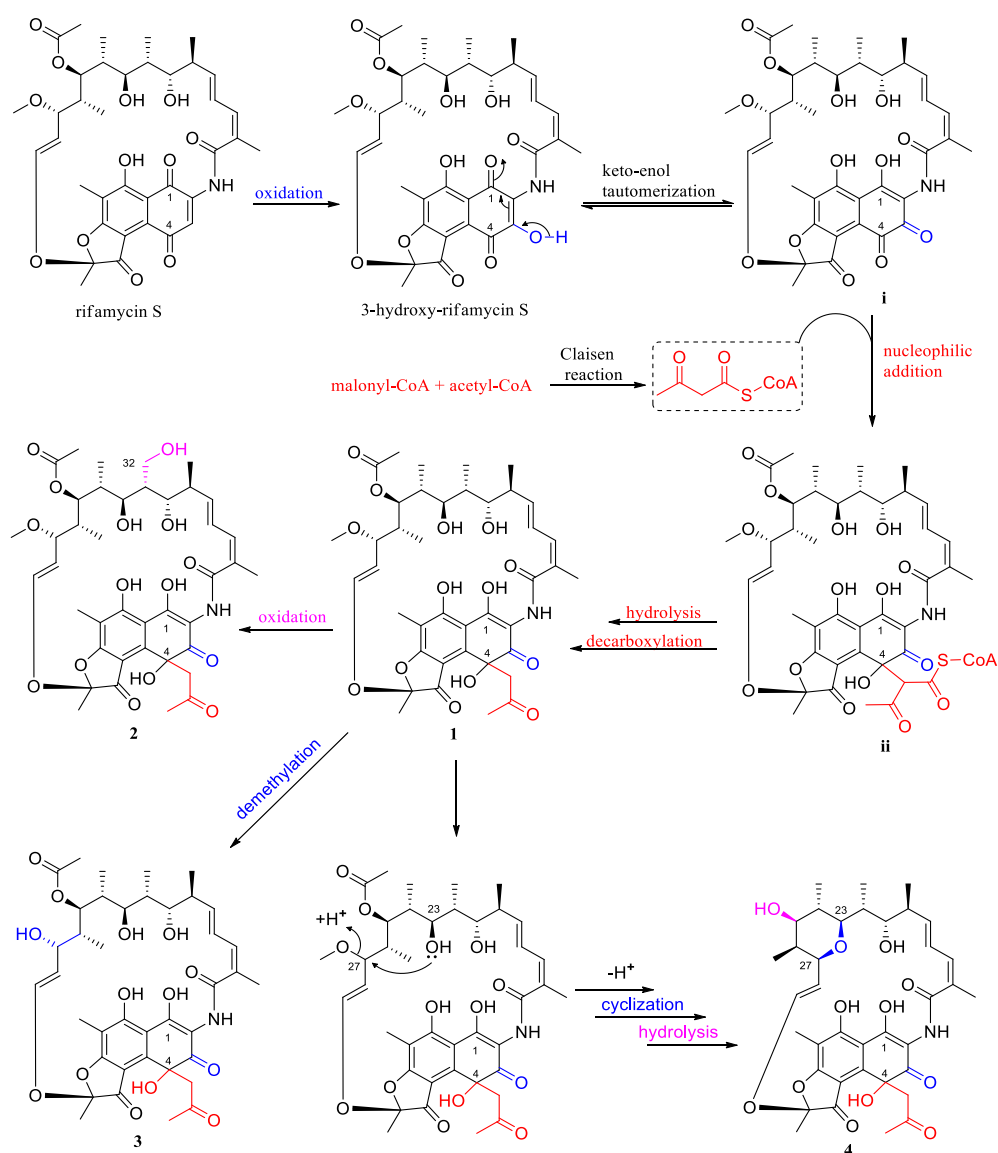
Compound	<i>S. aureus</i> (ATCC 29213)	<i>S. aureus</i> (ATCC 43300, MRSA)	<i>E. faecalis</i> (ATCC 29219)	<i>E. faecalis</i> (ATCC 51212, VRE)
<b>1</b>	3.9	2.0	15.6	31.2
<b>2</b>	62.5	31.2	15.6	125.0
<b>4</b>	62.5	62.5	<sup>a</sup>	<sup>a</sup>

<sup>a</sup> No activity in the tested concentrations. Rifampicin showed MIC  $\leq 0.03 \mu\text{g/mL}$ .

## EXPERIMENTAL SECTION

### General Experimental Procedures.

Optical rotations were measured using a JASCO P-2000 digital polarimeter. IR spectra were recorded using a Perkin-Elmer Spectrum 100 FTIR spectrometer equipped with a universal attenuated total reflectance accessory (UATR) in the range from 4000 to 650  $\text{cm}^{-1}$ . NMR spectra were obtained either on a Bruker Avance DRX-500 (500 MHz to  $^1\text{H}$  and 125 MHz to  $^{13}\text{C}$ ) or Agilent DD2- 600 spectrometers (600 MHz to  $^1\text{H}$  and 150 MHz to  $^{13}\text{C}$ ). High-resolution electrospray ionization mass spectra (HRESIMS) were acquired using an Acquity Xevo UPLC-QTOF-MS system from Waters (Milford, MA). Sephadex LH-20 (Pharmacia) and SPE cartridges C18 (20g/60 mL; Strata, Phenomenex) were used for the chromatographic fractionations. HPLC analyses were carried out using a UFLC (SHIMADZU) system equipped with an SPD-M20A diode array UV–Vis detector, a Phenomenex C-18 column, 5 $\mu\text{m}$  (10.0 x 250 mm).

**Scheme 1.** Plausible Biogenetic Pathways for Salinirifamycins B–E (1–4).**Bacterial Material.**

The bacterial strain BRA-213 was identified as *Salinispora arenicola* by Bauermeister et al.<sup>23</sup> (deposited in GenBank with an accession number MH910695). The bacteria strain was isolated on solid A1 media [18 g agar, 10 g starch, 4 g yeast extract, and 2 g peptone dissolved in 1 L of artificial seawater Red Sea Fish Pharm Ltd (40.0 g/L)] from marine sediment collected around SPSPA, Pernambuco, Brazil at a depth of 16 m (N 0°55', W 29°38') in

November 2011. A voucher strain is preserved at the Laboratório de Bioprospecção e Biotecnologia Marinha (LaBBMar), Universidade Federal do Ceará, Brazil. The license for the collection was granted by the Conselho de Gestão do Patrimônio Genético (CGEN) (SisGen No. AA8F8B8).

### **Fermentation.**

Colonies of the strain BRA-213 were inoculated into Erlenmeyer flasks (2L) containing 500 mL of A1 media (10 g soluble starch, 4 g yeast extract, and 2 g peptone) supplemented with calcium carbonate (0.5 g/L  $\text{CaCO}_3$ ), solutions of iron (III) sulfate (5 g/L  $\text{Fe}_2(\text{SO}_4)_3$ ) and potassium bromide (5 g/L KBr). Steril Amberlite XAD-16 resin (10 g) was added to each flask on day 2. The culture flasks were shaken at 200 rpm at 28 °C for 14 days.

### **Extraction and Isolation.**

The whole fermentation broth (20 L) was filtered through cloth to separate the resin from the supernatant. The resin was then extracted with acetone (2 L), which was posteriorly removed under vacuum, while the residual aqueous phase was extracted with ethyl acetate (3 x 500 mL). The resulting EtOAc fraction was vacuum dried and yielding an organic extract (9.0 g), which was fractionated on a C18 cartridge by elution with MeOH/ $\text{H}_2\text{O}$  (7:3; 4:1, and 1:0) to give three fractions (A-C). Fraction A (5.0 g) was chromatographed using a C18 cartridge and elution with MeOH/ $\text{H}_2\text{O}$  (3:7; 2:3; 1:1; 3:2; 7:3; 4:1, and 1:0) to give seven fractions (AA-AG). The fraction AB (660 mg) was chromatographed over a Sephadex LH-20 column, using also MeOH as eluent, to give five subfractions (AB1-AB5). Subfraction AB3 (120.7 mg) was purified by semipreparative HPLC (MeCN/ $\text{H}_2\text{O}$ , 50-80 %, 30 min, flow rate of 3.0 mL/min) to give compounds **2** (3.0 mg,  $t_R = 9.2$  min), **3** (0.6 mg,  $t_R = 10.6$  min), and **4** (2.5 mg,  $t_R = 12.3$  min). Fraction AD (910 mg) was chromatographed over a Sephadex LH-20 column, using also MeOH as eluent, to give five subfractions (AD1-AD5). Subfraction AD2 (118.0 mg) was directly

purified by semipreparative HPLC using the method MeCN/H<sub>2</sub>O, 50-80 %, 30 min, flow rate of 3.0 mL/min, to give compound **1** (15.0 mg,  $t_R = 14.3$  min)

### Physical and spectroscopic data of **1**.

*Salinirifamycin B (1)*: yellowish solid;  $[\alpha]_D^{22} + 65.9$  ( $c$  0.13, MeOH); UV (MeOH)  $\lambda_{\max}$  (log  $\epsilon$ ) 232 (3.96), 269 (3.73), 318 (3.69), 417 (3.00) nm; IR ( $\nu_{\max}$ ) 3375, 2968, 2933, 1701, 1607, 1540, 1418, 1368, 1241, 1165, 1083, 972, 814, 761  $\text{cm}^{-1}$ ;  $^1\text{H}$  and  $^{13}\text{C}$  NMR data, see Table 1; HRESIMS  $m/z$  768.3240  $[\text{M} - \text{H}]^-$  (calcd for  $\text{C}_{40}\text{H}_{50}\text{NO}_{14}$ , 768.3237).

*Salinirifamycin C (2)*: yellowish solid;  $[\alpha]_D^{22} + 66.1$  ( $c$  0.10, MeOH); UV (MeOH)  $\lambda_{\max}$  (log  $\epsilon$ ) 233 (3.87), 271 (3.65), 318 (3.60), 413 (2.88) nm; IR ( $\nu_{\max}$ ) 3342, 3242, 2976, 2884, 1670, 1606, 1542, 1427, 1358, 1262, 1190, 1076, 973, 801, 721  $\text{cm}^{-1}$ ;  $^1\text{H}$  and  $^{13}\text{C}$  NMR data, see Table 1; HRESIMS  $m/z$  784.3193  $[\text{M} - \text{H}]^-$  (calcd for  $\text{C}_{40}\text{H}_{50}\text{NO}_{15}$ , 784.3186).

*Salinirifamycin D (3)*: yellowish solid;  $[\alpha]_D^{22} + 60.5$  ( $c$  0.10, MeOH); UV (MeOH)  $\lambda_{\max}$  (log  $\epsilon$ ) 232 (3.61), 269 (3.63), 320 (3.37), 405 (2.70) nm; IR ( $\nu_{\max}$ ) 3364, 2970, 2924, 1716, 1638, 1603, 1544, 1466, 1371, 1242, 1175, 1064, 964, 808, 729  $\text{cm}^{-1}$ ;  $^1\text{H}$  and  $^{13}\text{C}$  NMR data, see Table 2; HRESIMS  $m/z$  754.3074  $[\text{M} - \text{H}]^-$  (calcd for  $\text{C}_{39}\text{H}_{48}\text{NO}_{14}$ , 754.3080).

*Salinirifamycin E (4)*: yellowish solid;  $[\alpha]_D^{22} + 70.8$  ( $c$  0.13, MeOH); UV (MeOH)  $\lambda_{\max}$  (log  $\epsilon$ ) 227 (3.60), 268 (3.43), 323 (3.12), 420 (2.34) nm; IR ( $\nu_{\max}$ ) 3350, 2924, 2852, 1707, 1674, 1608, 1543, 1433, 1348, 1236, 1163, 1070, 974, 804, 721  $\text{cm}^{-1}$ ;  $^1\text{H}$  and  $^{13}\text{C}$  NMR data, see Table 2; HRESIMS  $m/z$  694.2872  $[\text{M} - \text{H}]^-$  (calcd for  $\text{C}_{37}\text{H}_{44}\text{NO}_{12}$ , 694.2869).

### Antimicrobial Assay

The antibacterial activity of the compounds **1**, **2**, and **4** was assayed on four Gram-positive bacteria: *Staphylococcus aureus* (ATCC 29213), methicillin-resistant *Staphylococcus aureus* (ATCC 43300, MRSA), *Enterococcus faecalis* (ATCC 29212), and vancomycin-resistant



*Enterococcus faecalis* (ATCC 51212, VRE). Initially, the strains were previously seeded in Petri dishes containing Mueller Hinton agar (Difco™), which were incubated for 24 hours at a temperature of  $35\pm 2$  °C, under aerobic conditions. Posteriorly the isolated colonies were collected and suspended in sterile saline solution (NaCl 0.85% (w/v)). This suspension was then used to obtain the bacterial inoculum in Mueller Hinton Broth -MHB (Difco™) with a final bacterial concentration of  $5 \times 10^5$  CFU/mL. The method used was broth microdilution in a 96-well plate and the minimum inhibitory concentrations (MICs) of the substances were determined according to Clinical Laboratory Standards Institute (2015).<sup>24</sup> Rifampicin was used as a positive control and the microplates were incubated at the same conditions cited above. The MIC value was determined after the observation of the absence of bacterial growth in the culture medium.

#### ASSOCIATED CONTENT

##### **Supporting Information**

The Supporting Information is available free of charge on the ACS publications website at DOI: HRESIMS, UV, and NMR data of **1–4** (PDF)

#### AUTHOR INFORMATION

##### **Corresponding Author**

E-mail: otialoiola@gmail.com

##### **ORCID**

Alison B. da Silva: 0000-0002-8453-8160

Otília Deusdenia L. Pessoa: 0000-0002-1617-7586

Diego V. Wilke: 0000-0001-9481-6702

Leticia V. Costa-Lotufo; 0000-0003-1861-5153

##### **Notes**

The authors declare no competing financial interest.

## ACKNOWLEDGMENTS

The authors are grateful to Secretaria da Comissão Interministerial dos Recursos do Mar (SECIRM) for providing all the logistic support disposed to the scientific expedition, as part of the Program PROARQUIPELAGO. This work was financially supported by CNPq (No. 420454/2016-0 and 309060/2016-8), CAPES/FUNCAP (No. 88887.113263/2015-01) and INCT BioNat (No. 465637/2014-0).

## REFERENCES

- (1) Manivasagan, P.; Kang, K. H.; Sivakumar, K.; Li-Chan, E. C. Y.; Oh, H. M.; Kim, S. K. *Environ. Toxicol. Phar.* **2014**, *38*, 172–188.
- (2) Jensen, P. R.; Moore, B. S.; Fenical, W. *Nat. Prod. Rep.* **2015**, *32*, 738–751.
- (3) Maldonado, L. A.; Fenical, W.; Jensen, P. R.; Kauffman, C. A.; Mincer, T. J.; Ward, A. C.; Bull, A. T.; Goodfellow, M. *Int. J. Syst. Evol. Microbiol.* **2005**, *55*, 1759–1766.
- (4) Román-Ponce, B.; Millán-Aguiñaga, N.; Guillen-Matus, D.; Chase, A. B.; Ginigini, J. G. M.; Soapi, K.; Feussner, K. D.; Jensen, P. R.; Trujillo, M. E. *Int. J. Syst. Evol. Microbiol.* **2020**, *70*, 4668–4682.
- (5) Feling, R. H.; Buchanan, G. O.; Mincer, T. J.; Kauffman, C. A.; Jensen, P. R.; Fenical, W. *Angew. Chem. Int. Ed.* **2003**, *42*, 355–357.
- (6) Murphy, B. T.; Narender, T.; Kauffman, C. A.; Woolery, M.; Jensen, P. R.; Fenical, W. *Aust. J. Chem.* **2010**, *63*, 929–934.
- (7) Williams, P.G.; Miller, E. D.; Asolkar, R. N.; Jensen, P. R.; Fenical, W. *J. Org. Chem.* **2007**, *72*, 5025–5034.
- (8) Williams, P. G.; Asolkar, R. N.; Kondratyuk, T.; Pezzuto, J. M.; Jensen, P. R.; Fenical, W. *J. Nat. Prod.* **2007**, *70*, 83–88.
- (9) Asolkar, R. N.; Freel, K. C.; Jensen, P. R.; Fenical, W.; Kondratyuk, P.; Park, E. J.; Pezzuto, J. M. *J. Nat. Prod.* **2009**, *72*, 396–402.
- (10) Duncan, K. R.; Crüsemann, M.; Lechner, A.; Sarkar, A.; Li, J.; Ziemert, N.; Wang, M.;

- Bandeira, N.; Moore, B. S.; Dorrestein, P. C.; Jensen, P. R. *Chem. Biol.* **2015**, *22*, 460–471.
- (11) Sensi, P. *Boll. Chim. Farm.* **1957**, *96*, 437–457.
- (12) Aristoff, P. A.; Garcia, G. A.; Kirchoff, P. D.; Showalter, H. D. H. *Tuberculosis* **2010**, *90*, 94–118.
- (13) Ramos-e-Silva, M.; Rebello, P. F. B. *Am. J. Clin. Dermatol.* **2001**, *2*, 203–211.
- (14) Sepkowitz, K. A.; Raffalli, J.; Riley, L.; Kiehn, T. E.; Armstrong, D. *Clin. Microbiol. Rev.* **1995**, *8*, 180–199.
- (15) Pinto, F. C. L.; Silveira, E. R.; Vasconcelos, A. C. L.; Florêncio, K. G. D.; Oliveira, F. A. S.; Sahm, B. B.; Costa-lotufo, L. V.; Bauermeister, A.; Lopes, N. P.; Wilke, D. V.; Pessoa, O. D. L. *J. Braz. Chem. Soc.* **2020**, *31*, 143–152.
- (16) Sousa, T. D. S.; Jimenez, P. C.; Ferreira, E. G.; Silveira, E. R.; Braz-Filho, R.; Pessoa, O. D. L.; Costa-Lotufo, L. V. *J. Nat. Prod.* **2012**, *75*, 489–493.
- (17) Chen, M.; Roush, W. R. *J. Org. Chem.* **2013**, *78*, 3–8.
- (18) August, P. R.; Tang, L.; Yoon, Y. J.; Ning, S.; Muller, R.; Yu, T. W.; Taylor, M.; Hoffmann, D.; Kim, C. G.; Zhang, X.; Hutchinson, C. R.; Floss, H. G. *Chem. Biol.* **1998**, *5*, 69–79.
- (19) Kang, Q.; Shen, Y.; Bai, L. *Nat. Prod. Rep.* **2012**, *29*, 243–263.
- (20) Qi, F.; Lei, C.; Li, F.; Zhang, X.; Wang, J.; Zhang, W.; Fan, Z.; Li, W.; Tang, G. L.; Xiao, Y.; Zhao, G.; Li, S. *Nat. Commun.* **2018**, *9*, 2342–2350.
- (21) August, P. R.; Tang, L.; Yoon, Y. J.; Ning, S.; Muller, R.; Yu, T.-W.; Taylor, M.; Hoffmann, D.; Kim, C.-G.; Zhang, X.; Hutchinson, C. R.; Floss, H. G. *Chem. Biol.* **1998**, *5*, 69–79.
- (22) Bose, U.; Hewavitharana, A. K.; Ng, Y. K.; Shaw, P. N.; Fuerst, J. A.; Hodson, M. P. *Mar. Drugs.* **2015**, *13*, 249–266.

- (23) Bauermeister, A.; Velasco-Alzate, K.; Dias, T.; Macedo, H.; Ferreira, E. G.; Jimenez, P. C.; Lotufo, T. M. C.; Lopes, N. P.; Gaudêncio, S. P.; Costa-Lotufo, L. V. *Front. Microbiol.* **2018**, *9*, 1–13.
- (24) CLSI - Clinical Laboratory Standards Institute **Approved standard M07-A10; Wayne, PA, 2015.**

## SUPPORTING INFORMATION

### Table of Contents

- Figure S1.**  $^1\text{H}$  NMR (600 MHz) spectrum of **1** in  $\text{DMSO-}d_6$
- Figure S2.** Expanded  $^1\text{H}$  NMR (600 MHz) spectrum of **1** in  $\text{DMSO-}d_6$
- Figure S3.** Expanded  $^1\text{H}$  NMR (600 MHz) spectrum of **1** in  $\text{DMSO-}d_6$
- Figure S4.**  $^{13}\text{C}$ -APT NMR (150 MHz) spectrum of **1** in  $\text{DMSO-}d_6$
- Figure S5.** COSY NMR spectrum of **1** in  $\text{DMSO-}d_6$
- Figure S6.** Edited HSQC NMR spectrum of **1** in  $\text{DMSO-}d_6$
- Figure S7.** HMBC NMR spectrum of **1** in  $\text{DMSO-}d_6$
- Figure S8.** Expanded HMBC NMR spectrum of **1** in  $\text{DMSO-}d_6$
- Figure S9.** ROESY NMR spectrum of **1** in  $\text{DMSO-}d_6$
- Figure S10.** HRESIMS spectrum of **1**
- Figure S11.** UV spectrum of **1** in MeOH
- Figure S12.**  $^1\text{H}$  NMR (600 MHz) spectrum of **2** in  $\text{DMSO-}d_6$
- Figure S13.** Expanded  $^1\text{H}$  NMR (600 MHz) spectrum of **2** in  $\text{DMSO-}d_6$
- Figure S14.** Expanded  $^1\text{H}$  NMR (600 MHz) spectrum of **2** in  $\text{DMSO-}d_6$
- Figure S15.**  $^{13}\text{C}$  NMR (150 MHz) spectrum of **2** in  $\text{DMSO-}d_6$
- Figure S16.** COSY NMR spectrum of **2** in  $\text{DMSO-}d_6$
- Figure S17.** Edited HSQC NMR spectrum of **2** in  $\text{DMSO-}d_6$
- Figure S18.** HMBC NMR spectrum of **2** in  $\text{DMSO-}d_6$
- Figure S19.** Expanded HMBC NMR spectrum of **2** in  $\text{DMSO-}d_6$
- Figure S20.** NOESY NMR spectrum of **2** in  $\text{DMSO-}d_6$
- Figure S21.** HRESIMS spectrum of **2**
- Figure S22.** UV spectrum of **2** in MeOH
- Figure S23.**  $^1\text{H}$  NMR (500 MHz) spectrum of **3** in  $\text{DMSO-}d_6$
- Figure S24.** Expanded  $^1\text{H}$  NMR (500 MHz) spectrum of **3** in  $\text{DMSO-}d_6$
- Figure S25.** Expanded  $^1\text{H}$  NMR (500 MHz) spectrum of **3** in  $\text{DMSO-}d_6$

**Figure S26.** COSY NMR spectrum of **3** in DMSO- $d_6$

**Figure S27.** HSQC NMR spectrum of **3** in DMSO- $d_6$

**Figure S28.** HMBC NMR spectrum of **3** in DMSO- $d_6$

**Figure S29.** Expanded HMBC NMR spectrum of **3** in DMSO- $d_6$

**Figure S30.** NOESY NMR spectrum of **3** in DMSO- $d_6$

**Figure S31.** HRESIMS spectrum of **3**

**Figure S32.** UV spectrum of **3** in MeOH

**Figure S33.**  $^1\text{H}$  NMR (600 MHz) spectrum of **4** in DMSO- $d_6$

**Figure S34.** Expanded  $^1\text{H}$  NMR (600 MHz) spectrum of **4** in DMSO- $d_6$

**Figure S35.** Expanded  $^1\text{H}$  NMR (600 MHz) spectrum of **4** in DMSO- $d_6$

**Figure S36.** COSY NMR spectrum of **4** in DMSO- $d_6$

**Figure S37.** Edited HSQC NMR spectrum of **4** in DMSO- $d_6$

**Figure S38.** HMBC NMR spectrum of **4** in DMSO- $d_6$

**Figure S39.** Expanded HMBC NMR spectrum of **4** in DMSO- $d_6$

**Figure S40.** NOESY NMR spectrum of **4** in DMSO- $d_6$

**Figure S41.** HRESIMS spectrum of **4**

**Figure S42.** UV spectrum of **4** in MeOH.



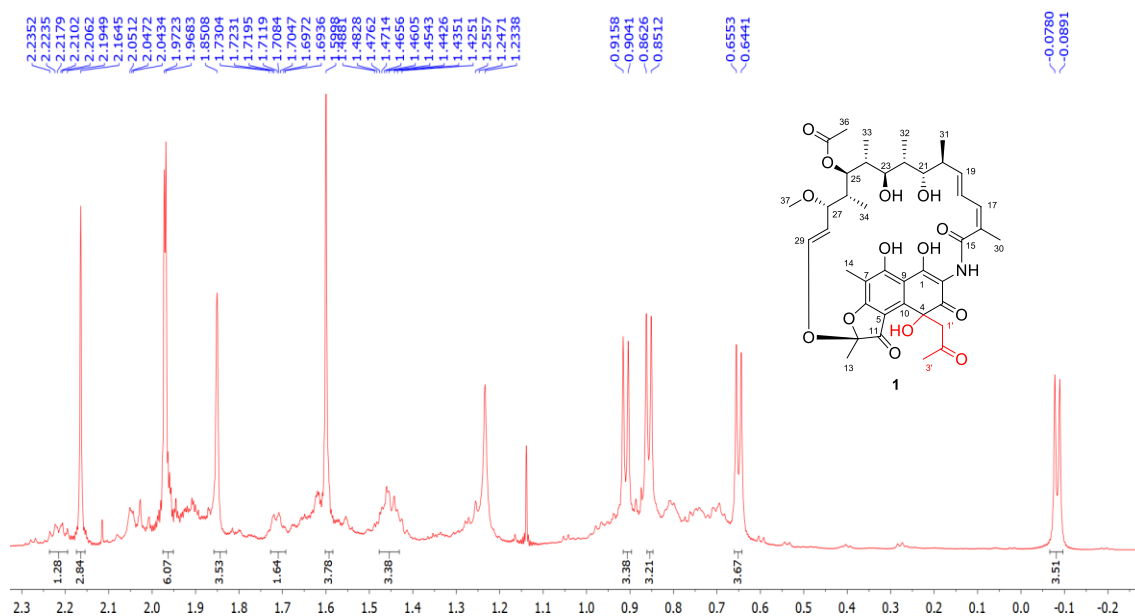


**Figure S3.** Expanded  $^1\text{H}$  NMR (600 MHz) spectrum of **1** in  $\text{DMSO-}d_6$ .

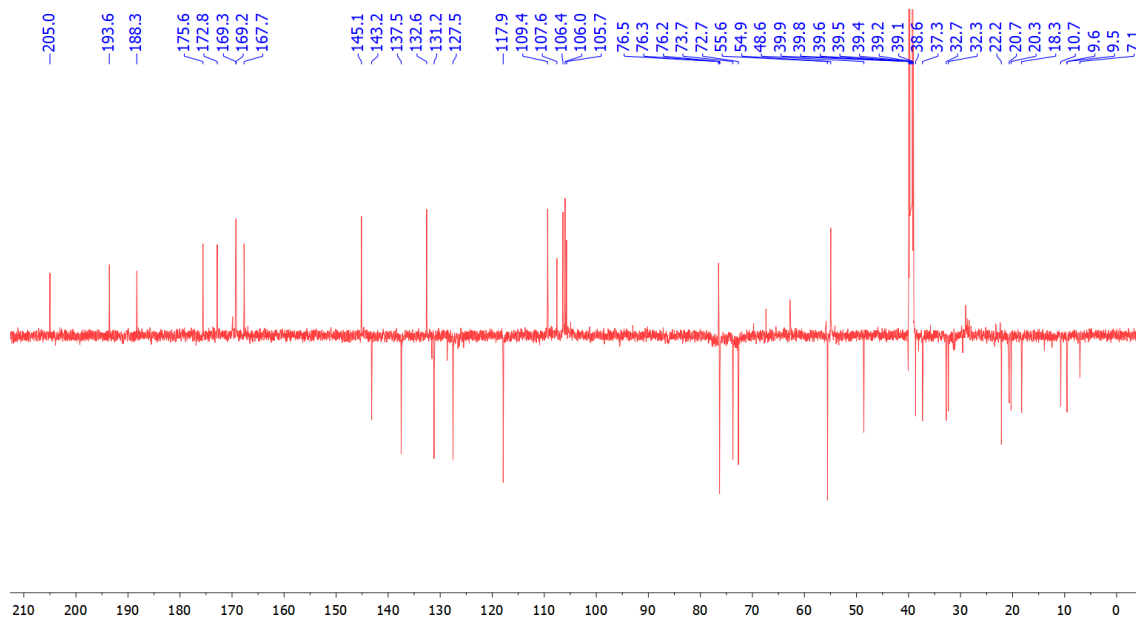


**Figure S4.**  $^{13}\text{C}$ -APT NMR (150 MHz) spectrum of **1** in  $\text{DMSO-}d_6$ .



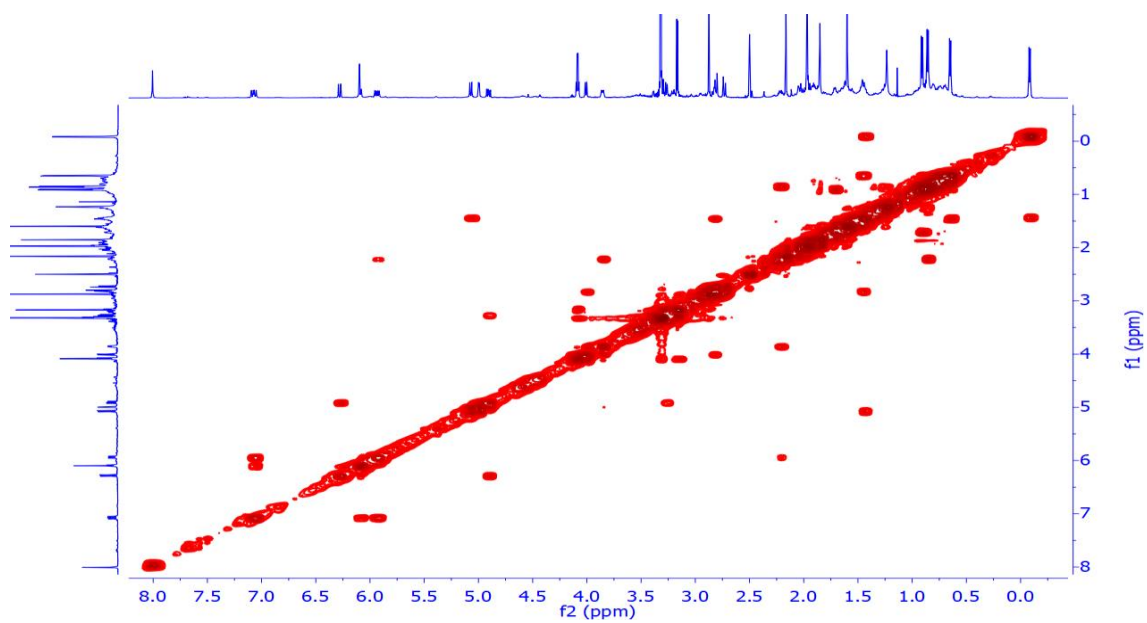


**Figure S5.** COSY NMR spectrum of **1** in DMSO- $d_6$ .

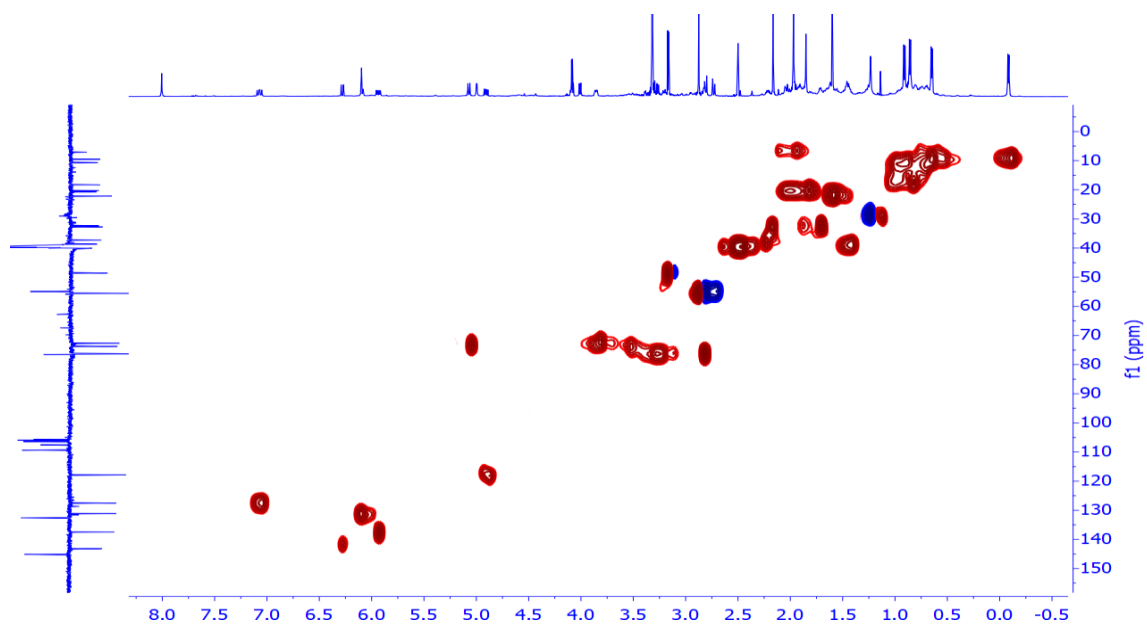


**Figure S6.** Edited HSQC NMR spectrum of **1** in DMSO- $d_6$ .

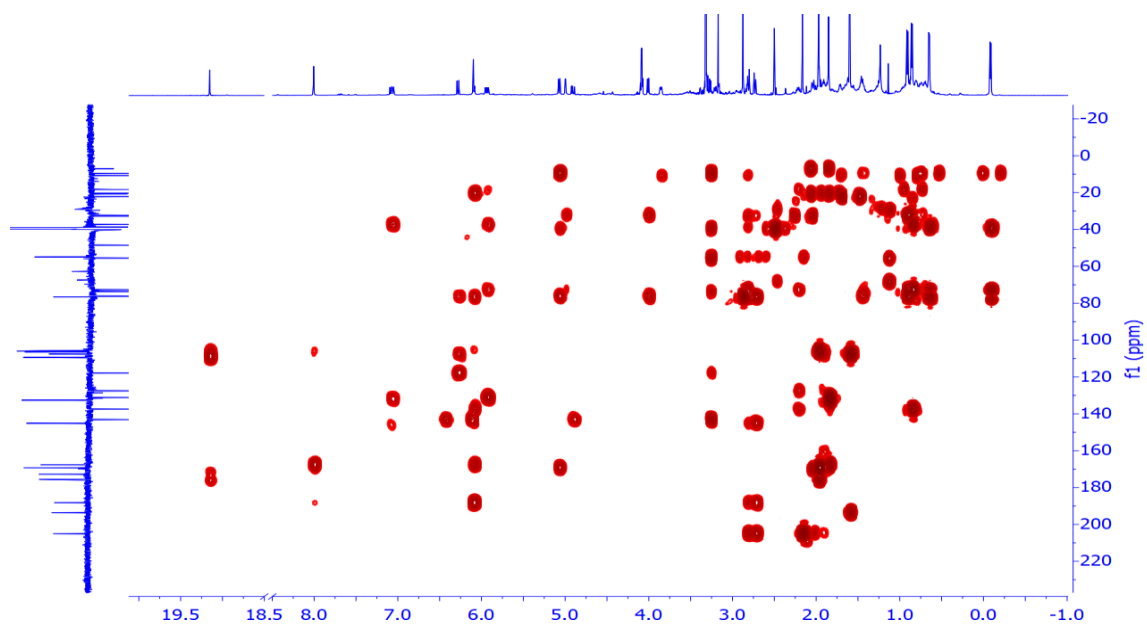


**Figure S7.** HMBC NMR spectrum of **1** in DMSO- $d_6$ .

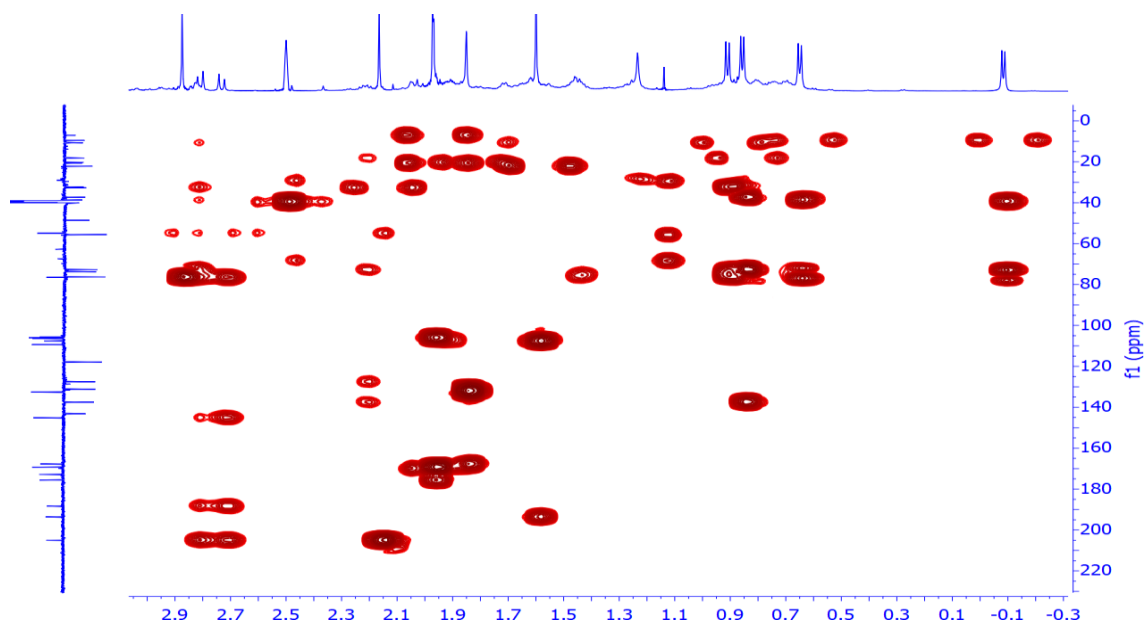


**Figure S8.** Expanded HMBC NMR spectrum of **1** in DMSO- $d_6$ .

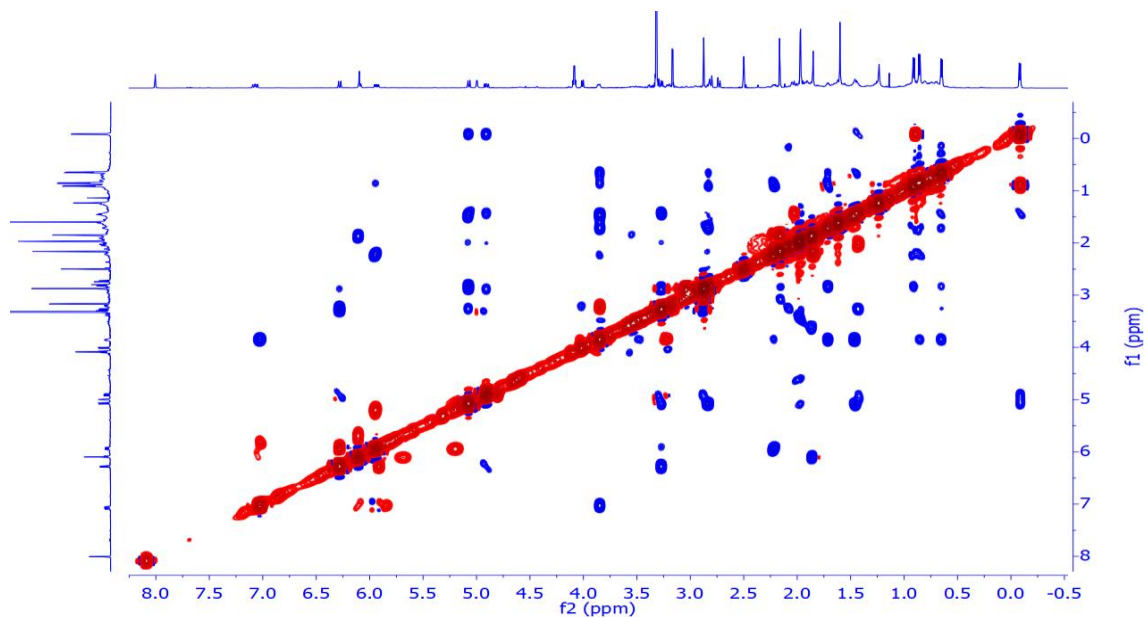


**Figure S9.** ROESY NMR spectrum of **1** in DMSO- $d_6$ .

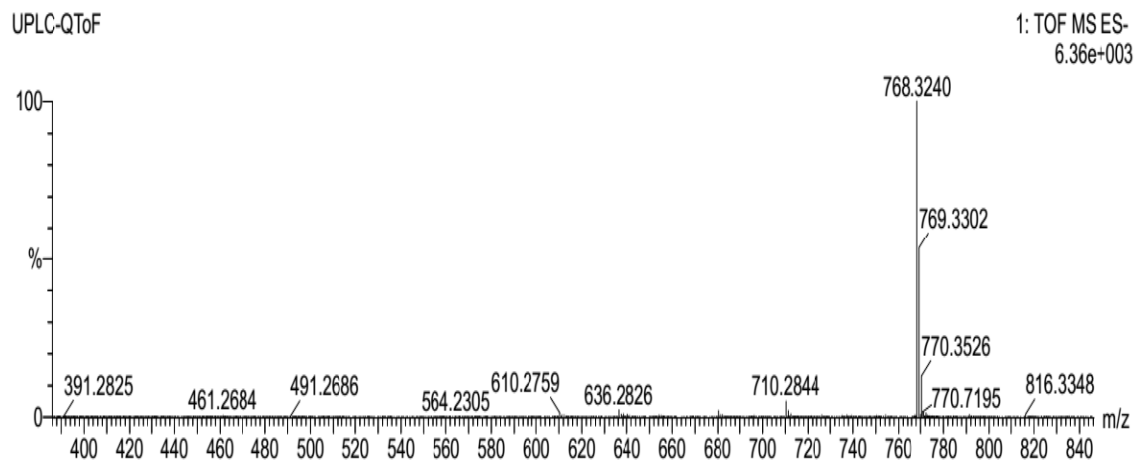


**Figure S10.** HRESIMS spectrum of **1**.

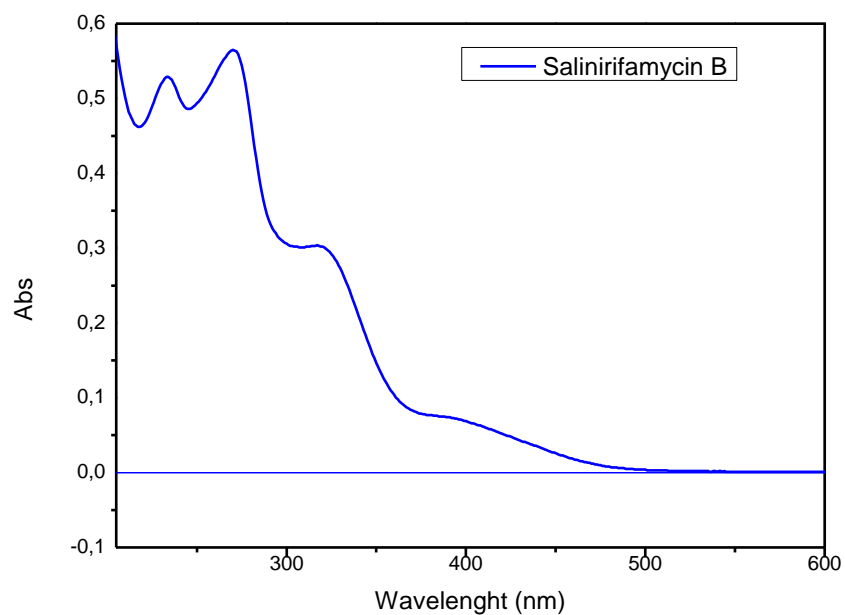


Figure S11. UV spectrum of **1** in MeOH.

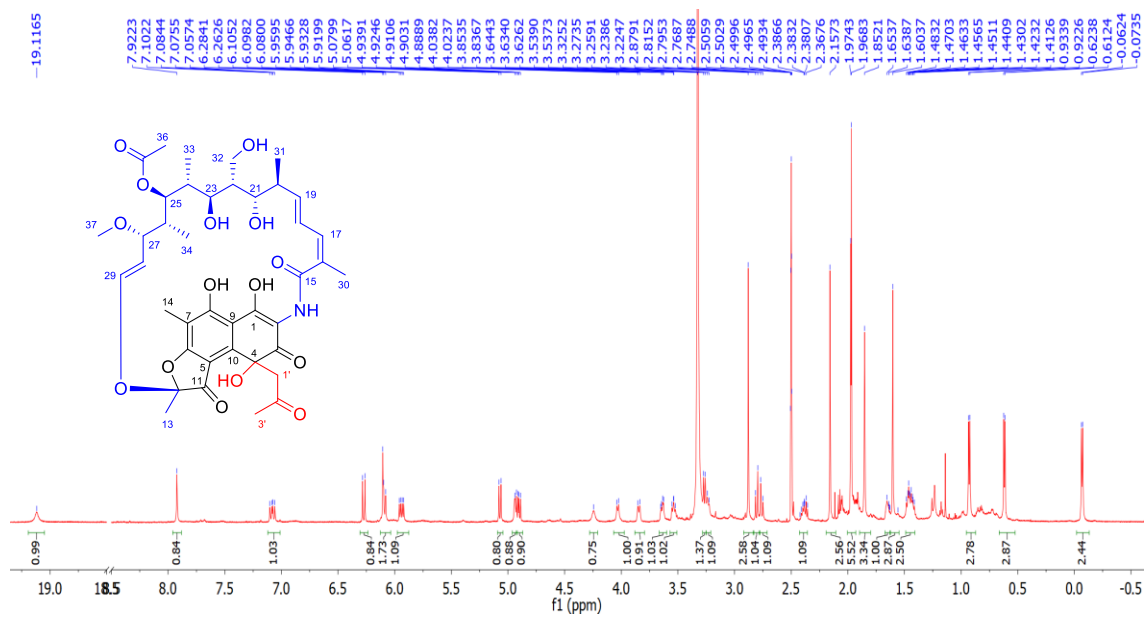
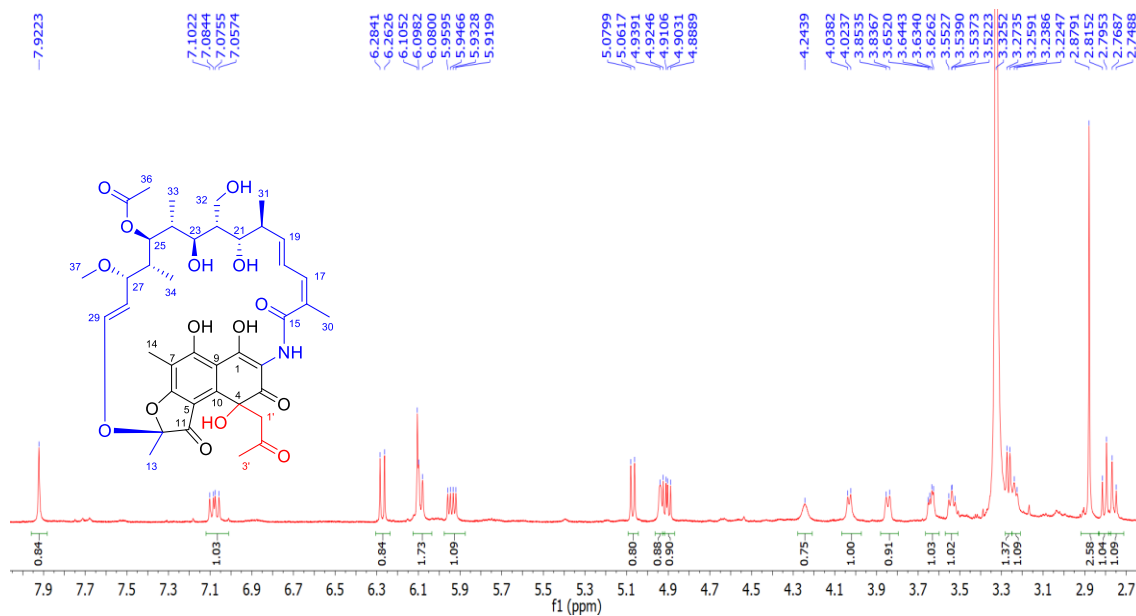
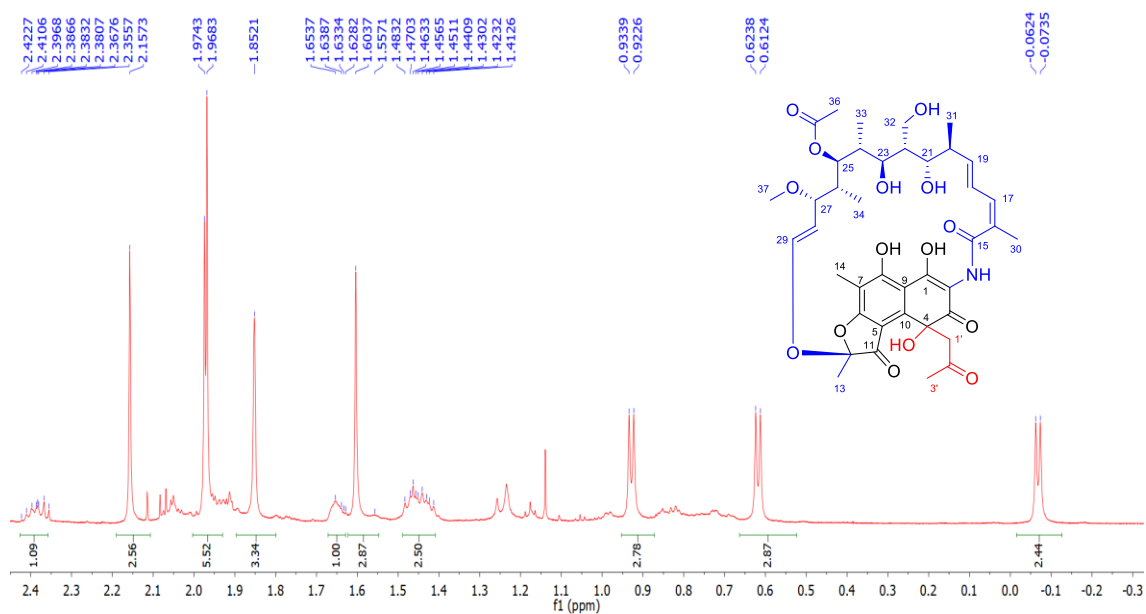


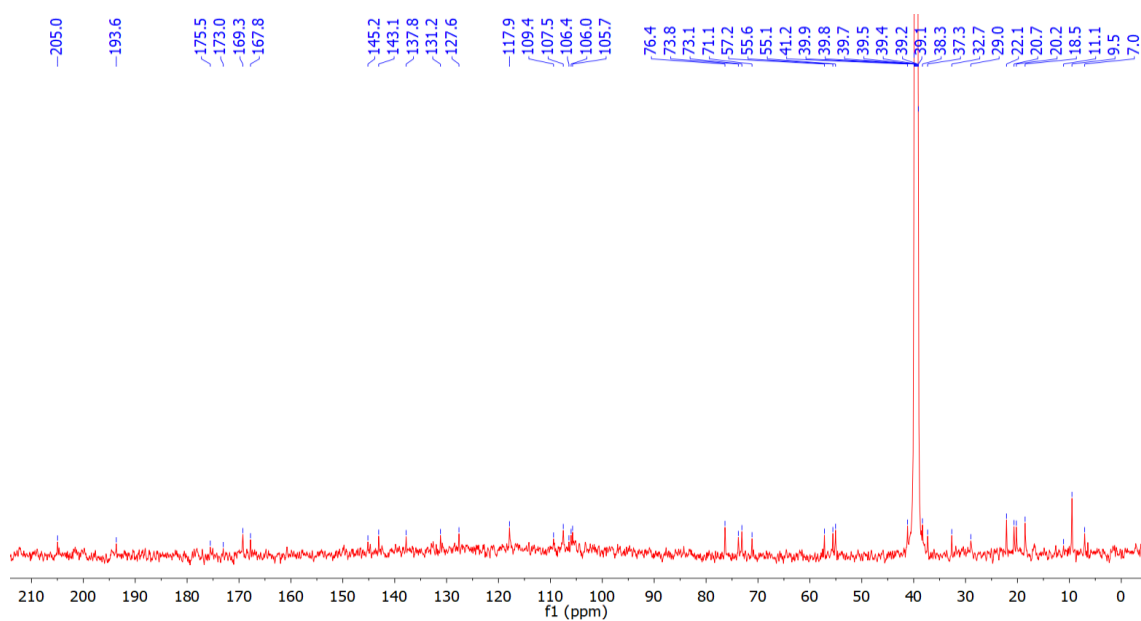
Figure S12. <sup>1</sup>H NMR (600 MHz) spectrum of **2** in DMSO-*d*<sub>6</sub>.



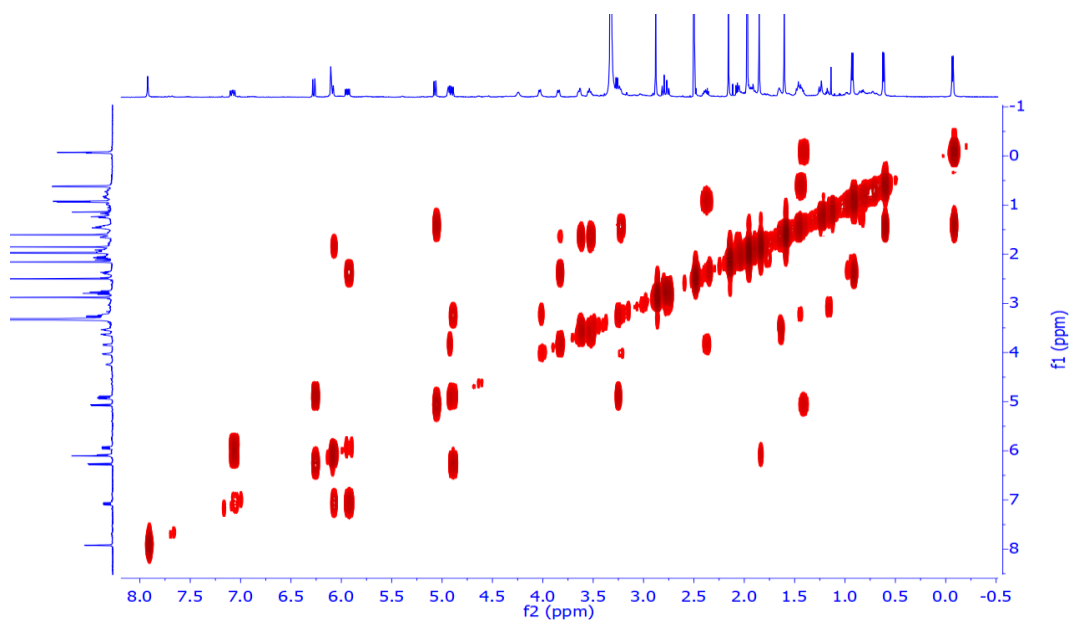
**Figure S13.** Expanded  $^1\text{H}$  NMR (600 MHz) spectrum of **2** in  $\text{DMSO-}d_6$ .



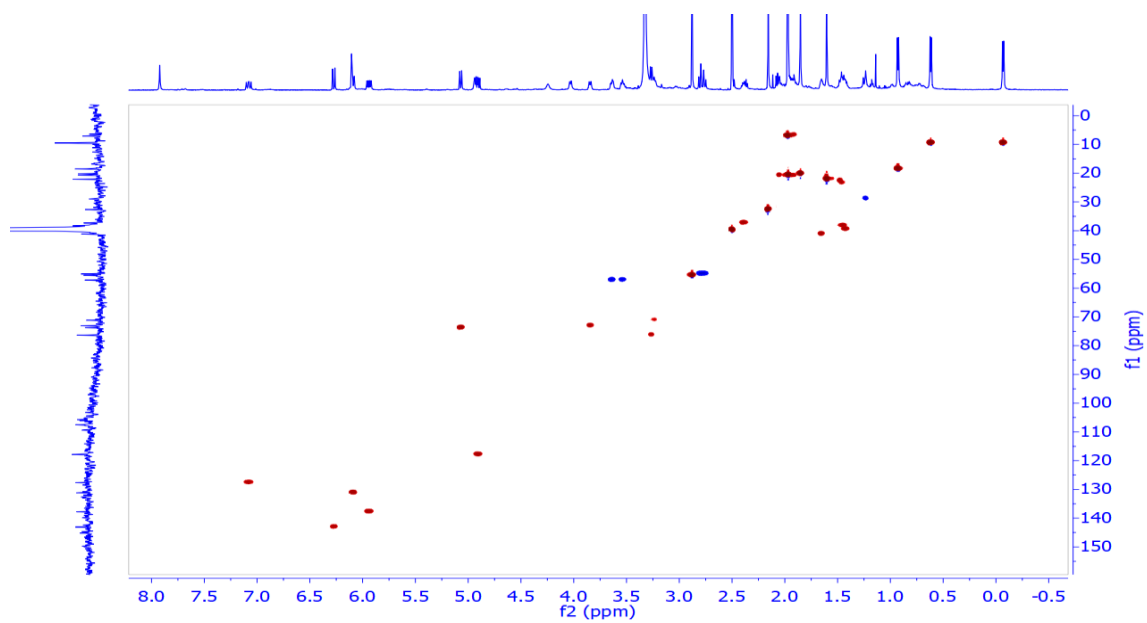
**Figure S14.** Expanded  $^1\text{H}$  NMR (600 MHz) spectrum of **2** in  $\text{DMSO-}d_6$ .



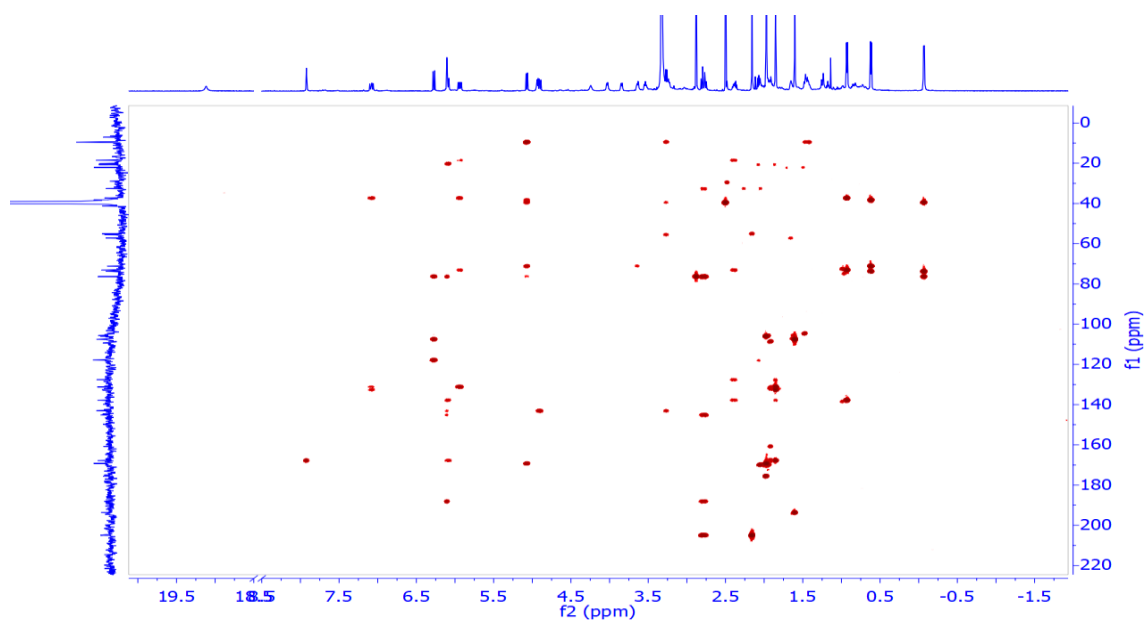
**Figure S15.**  $^{13}\text{C}$  NMR (150 MHz) spectrum of **2** in  $\text{DMSO-}d_6$ .



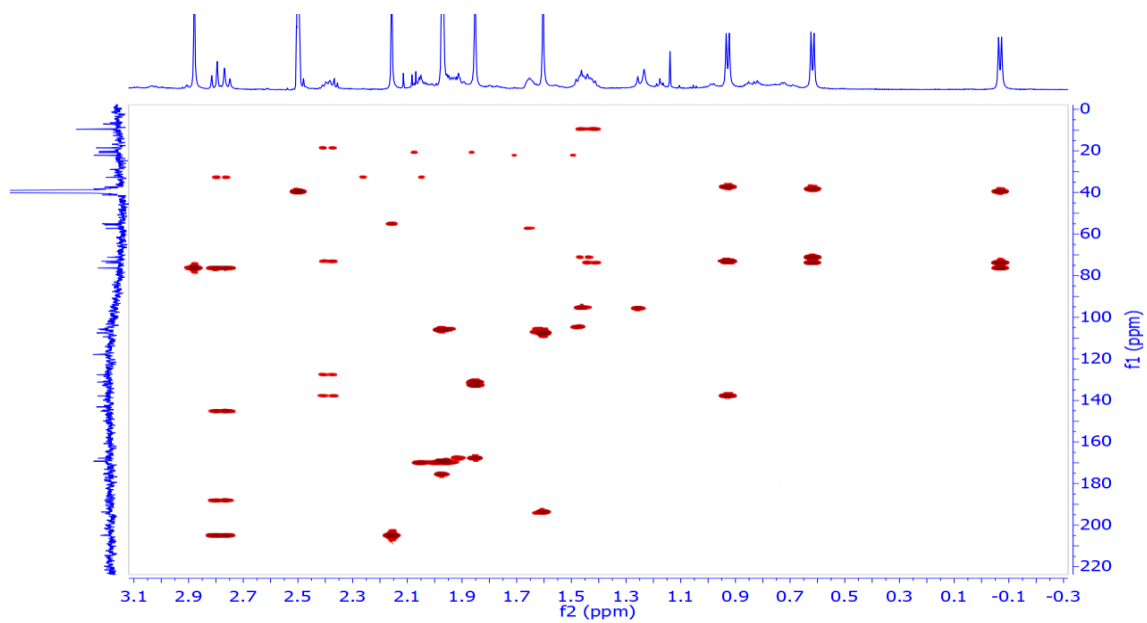
**Figure S16.** COSY NMR spectrum of **2** in  $\text{DMSO-}d_6$ .



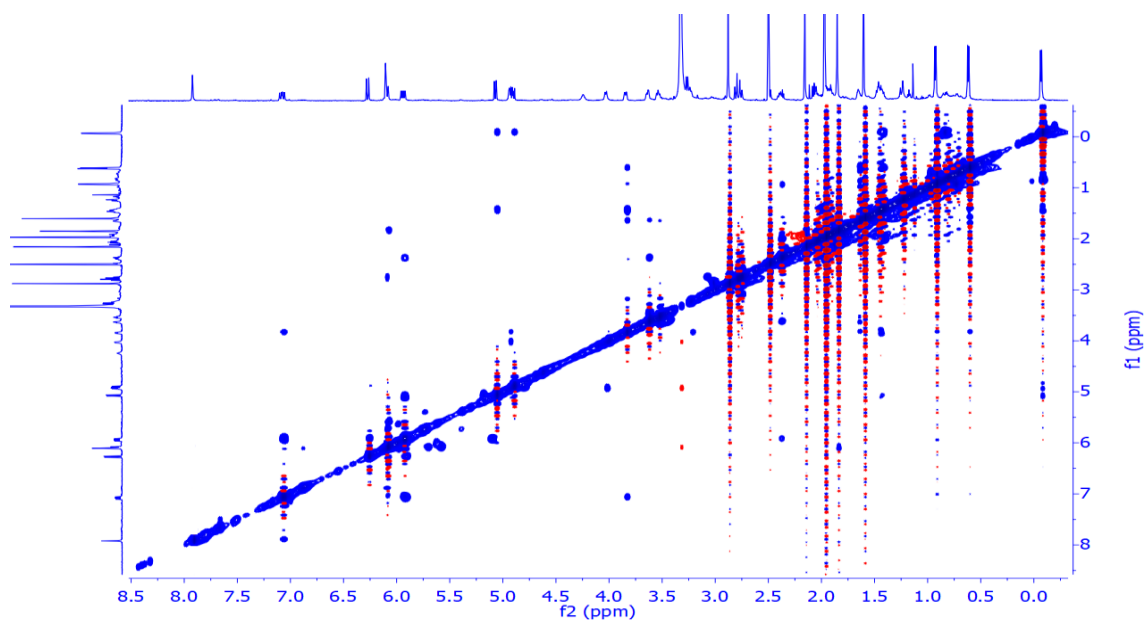
**Figure S17.** Edited HSQC NMR spectrum of **2** in DMSO- $d_6$ .



**Figure S18.** HMBC NMR spectrum of **2** in DMSO- $d_6$ .

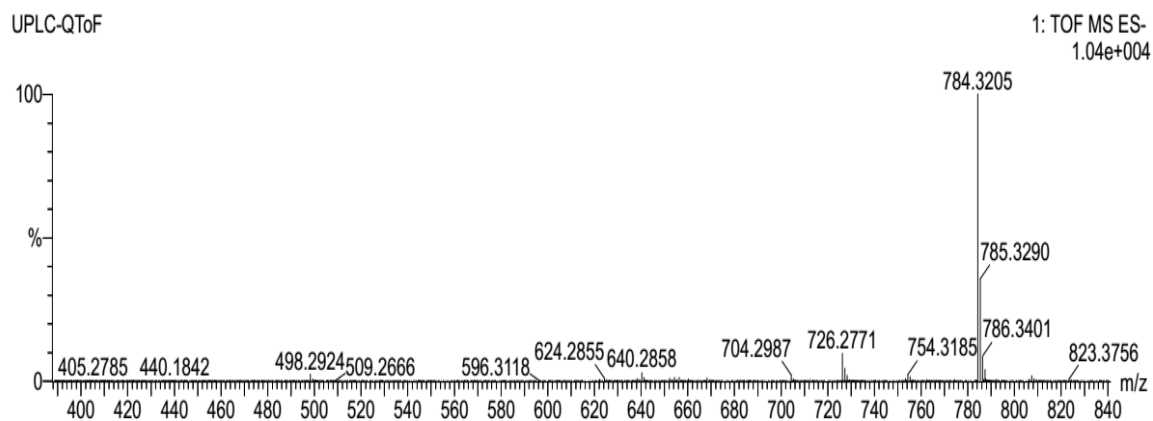


**Figure S19.** Expanded HMBC NMR spectrum of **2** in DMSO- $d_6$ .

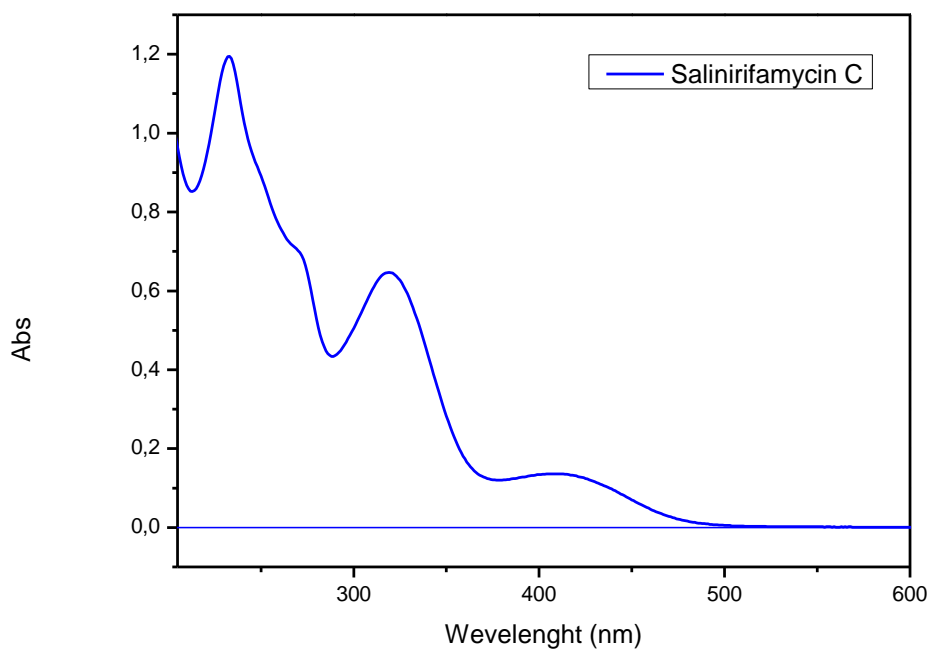


**Figure S20.** NOESY NMR spectrum of **2** in DMSO- $d_6$ .

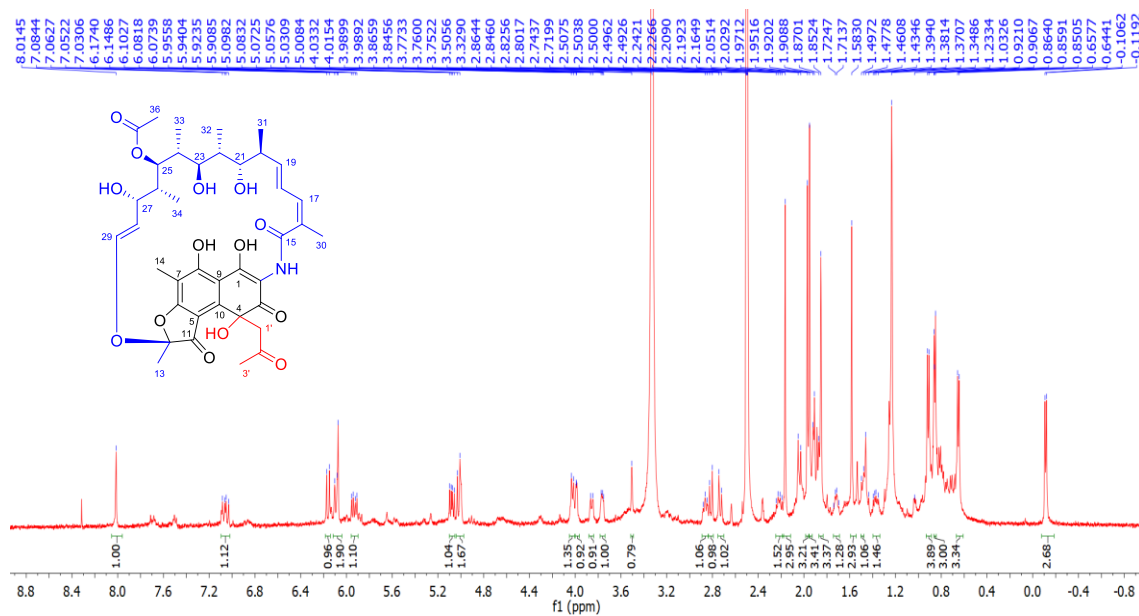




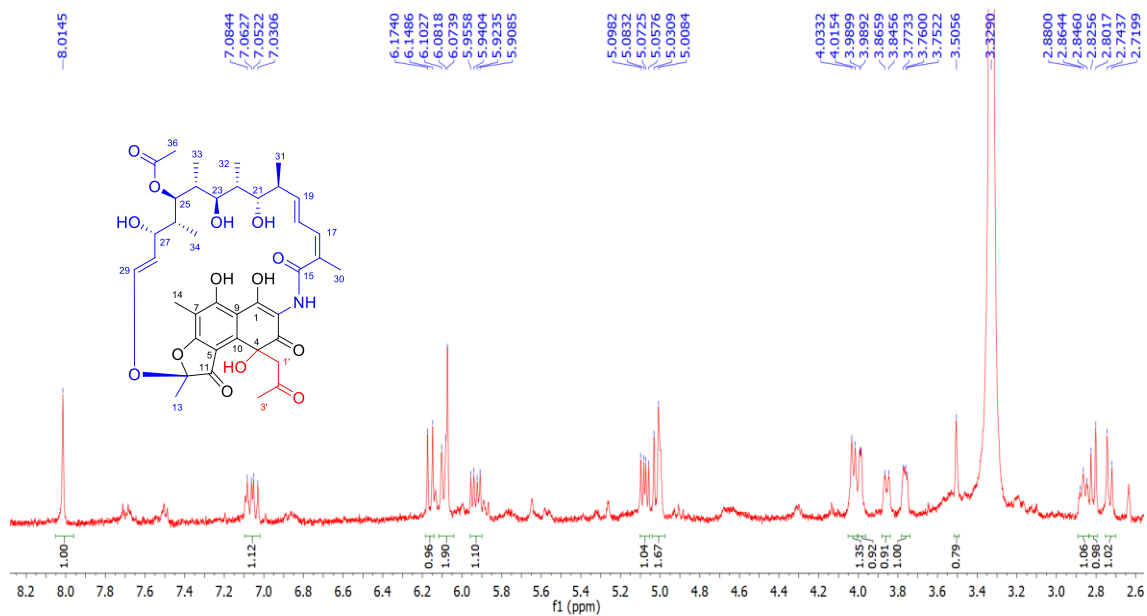
**Figure S21.** HRESIMS spectrum of **2**.



**Figure S22.** UV spectrum of **2** in MeOH.



**Figure S23.**  $^1\text{H}$  NMR (500 MHz) spectrum of **3** in  $\text{DMSO-}d_6$ .



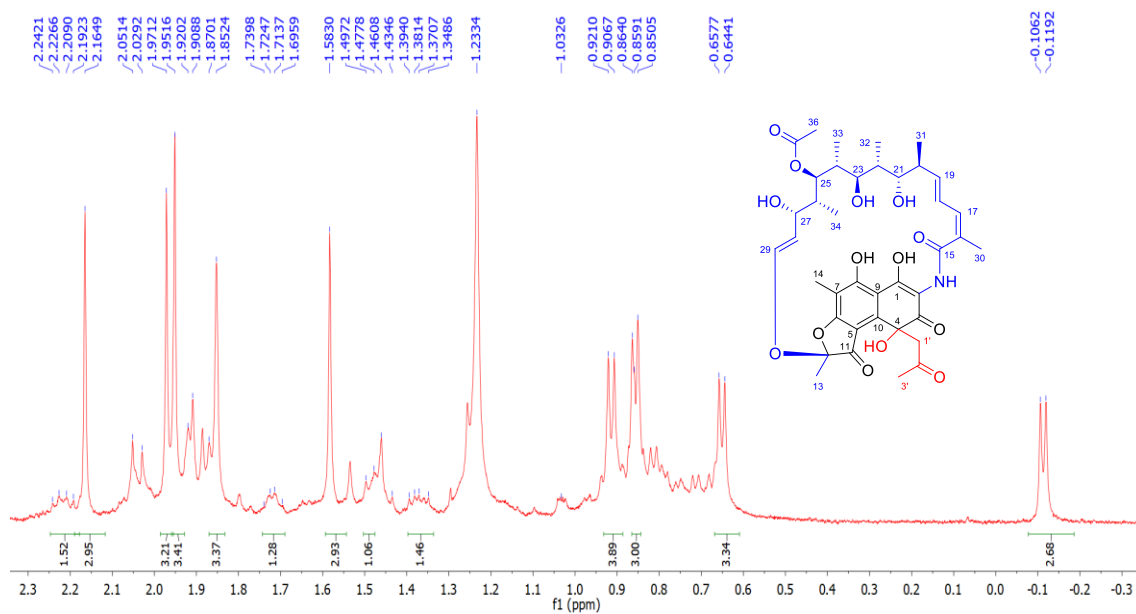


**Figure S25.** Expanded  $^1\text{H}$  NMR (500 MHz) spectrum of **3** in  $\text{DMSO-}d_6$ .

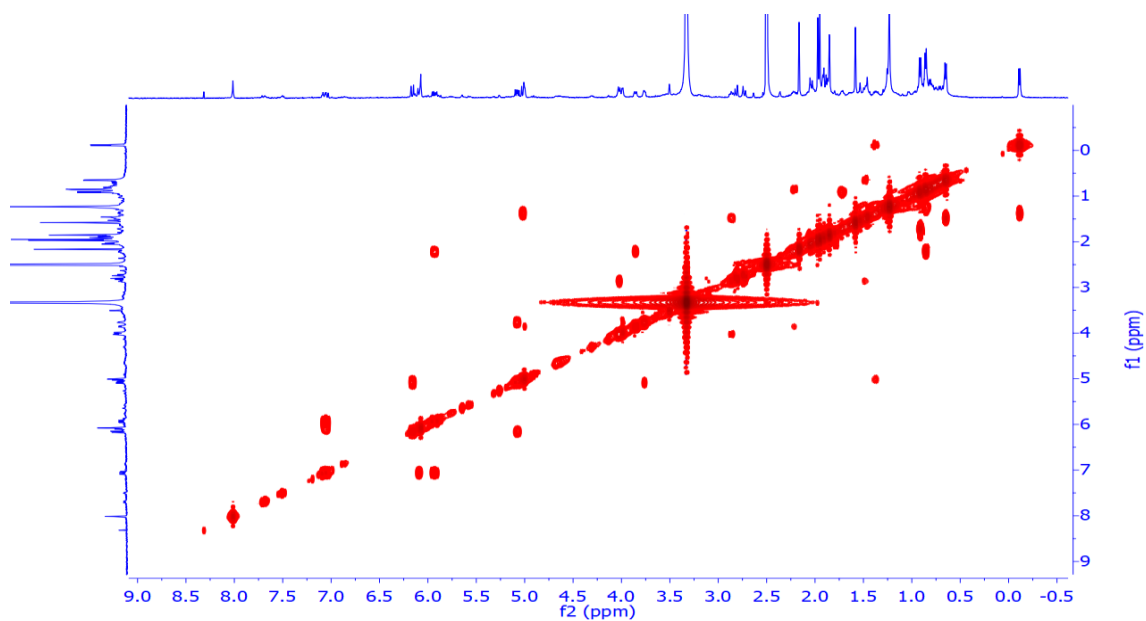


**Figure S26.** COSY NMR spectrum of **3** in  $\text{DMSO-}d_6$ .

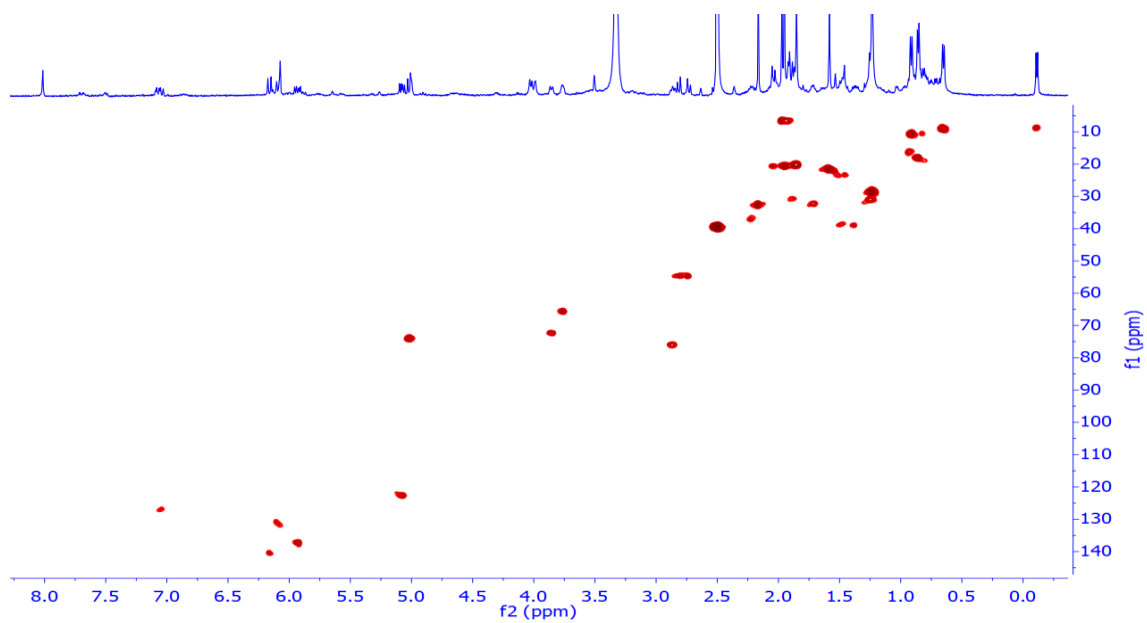


**Figure S27.** HSQC NMR spectrum of **3** in DMSO- $d_6$ .

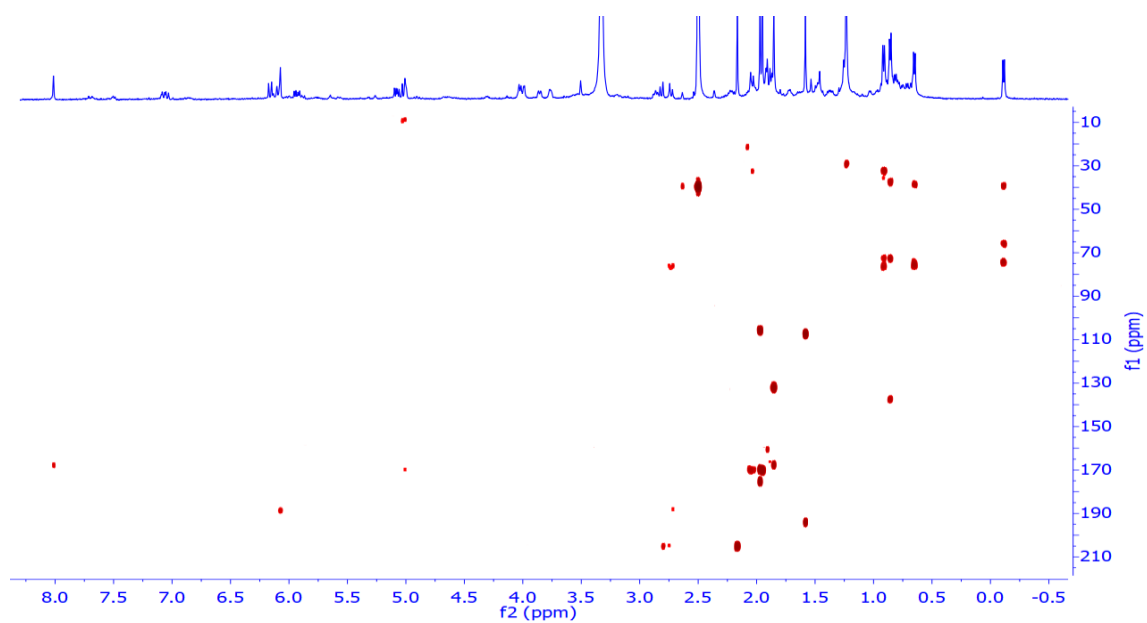


**Figure S28.** HMBC NMR spectrum of **3** in DMSO- $d_6$ .

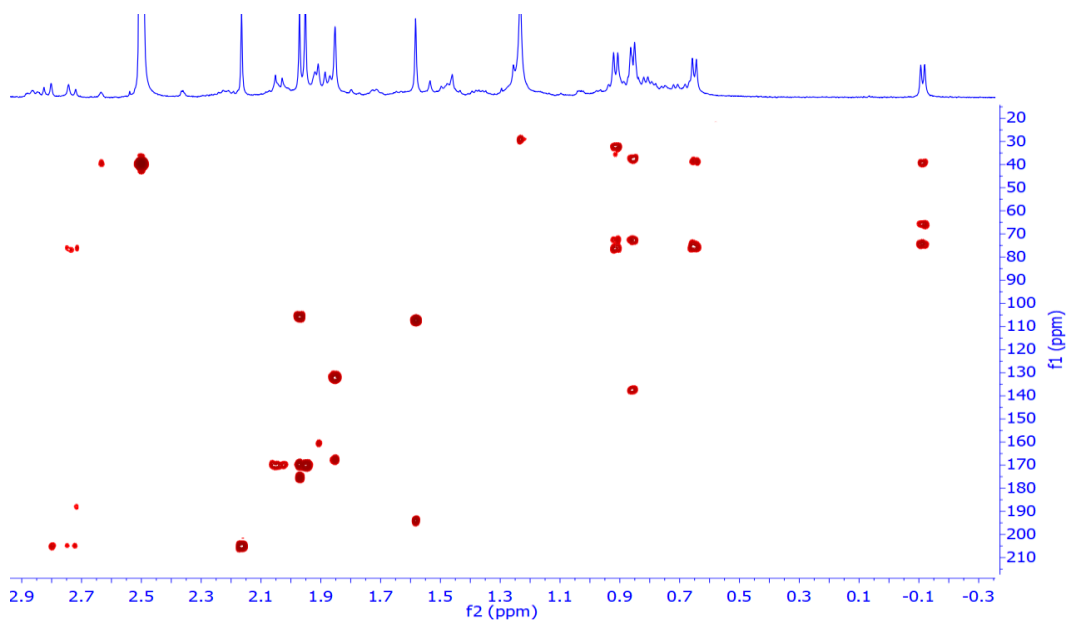


**Figure S29.** Expanded HMBC NMR spectrum of **3** in DMSO- $d_6$ .

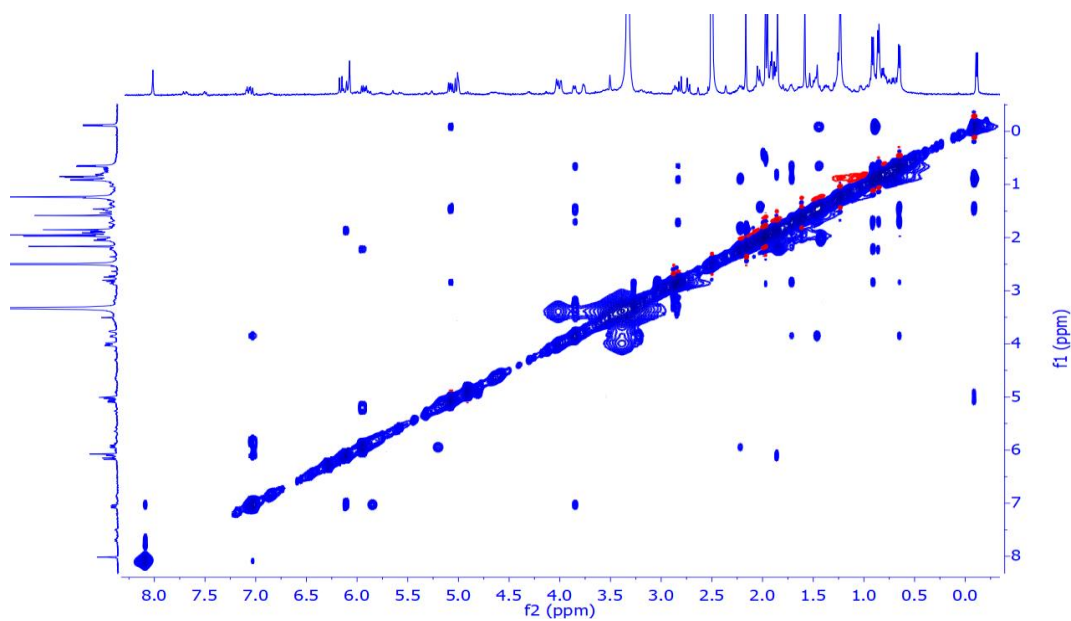


**Figure S30.** NOESY NMR spectrum of **3** in DMSO- $d_6$ .

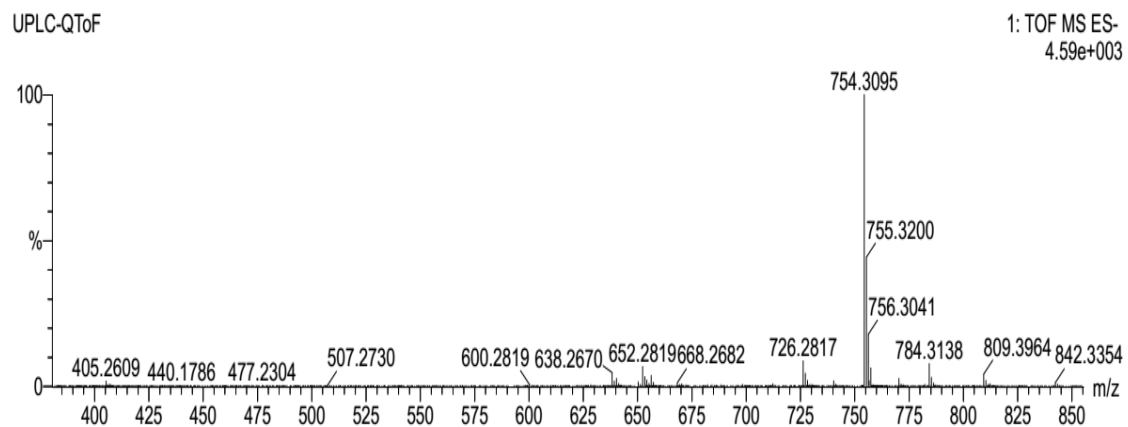


**Figure S31.** HRESIMS spectrum of **3**.

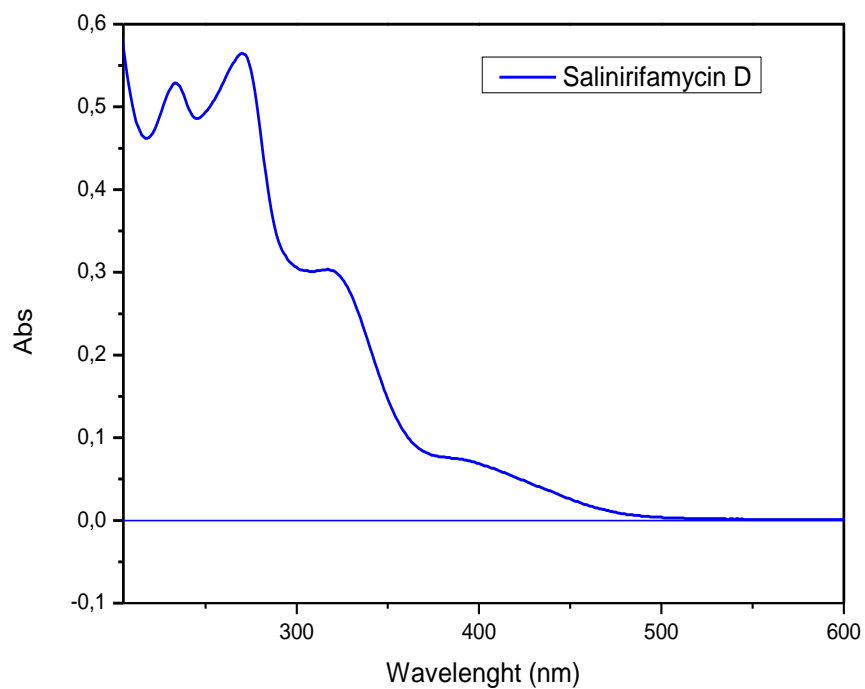


**Figure S32.** UV spectrum of **3** in MeOH.

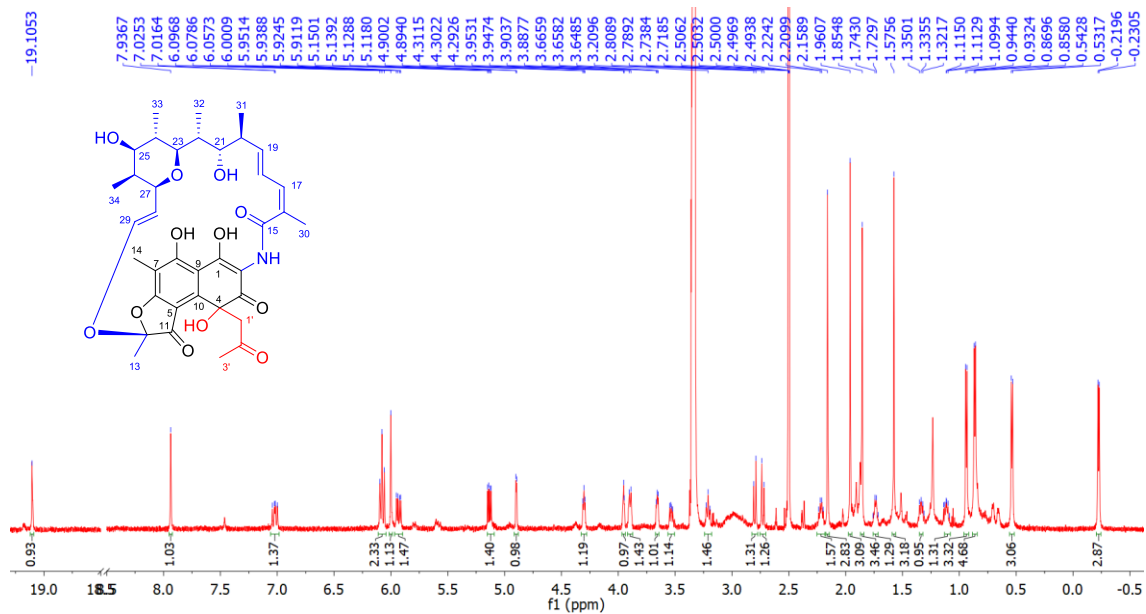


Figure S33.  $^1\text{H}$  NMR (600 MHz) spectrum of **4** in  $\text{DMSO}-d_6$ .

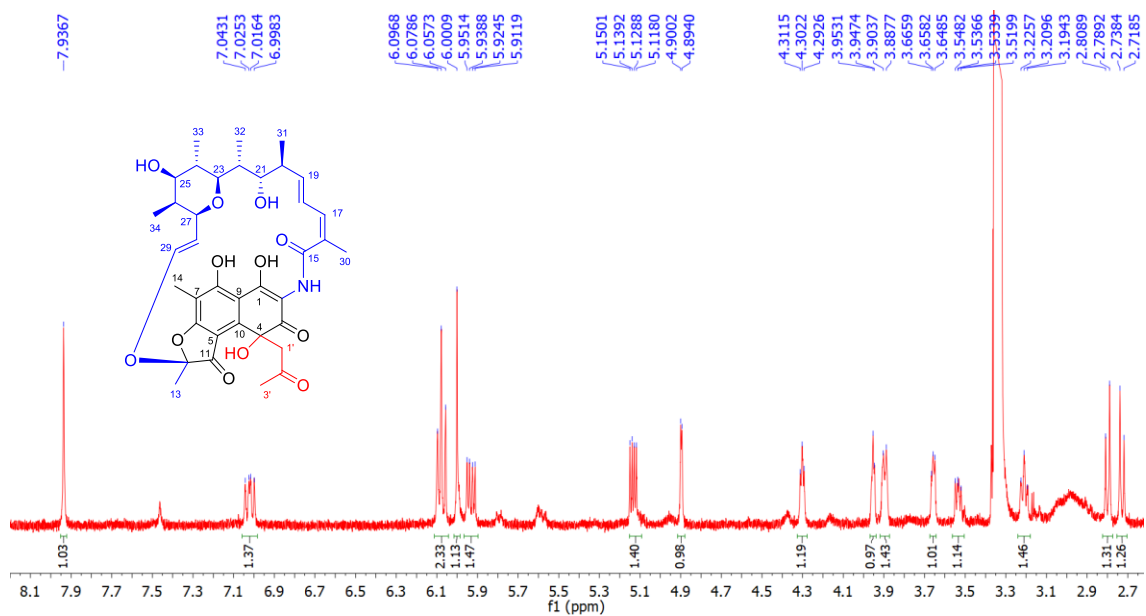
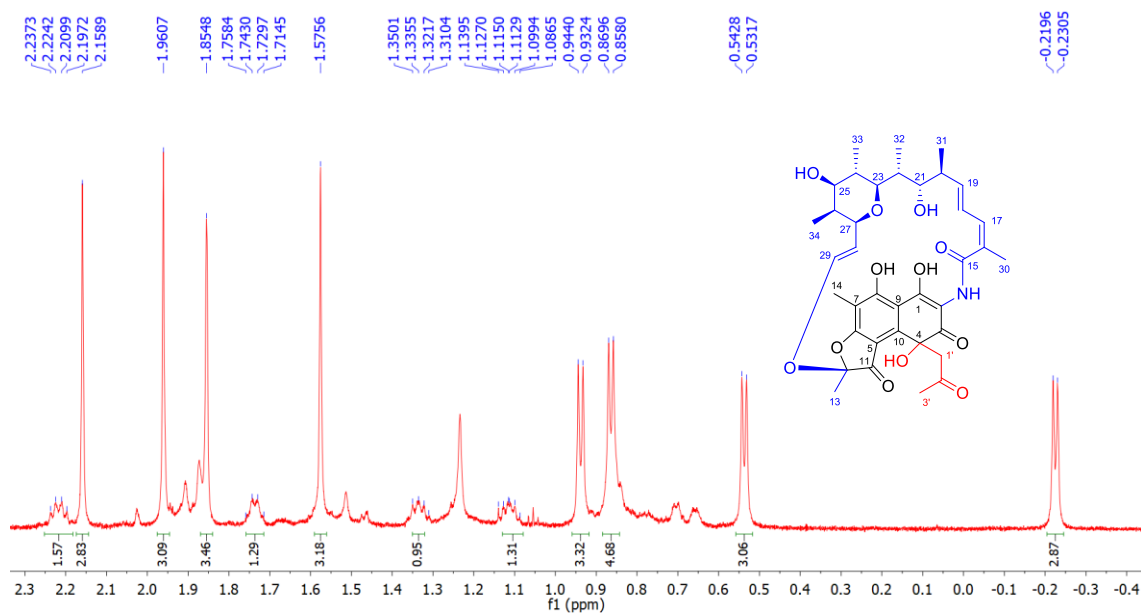
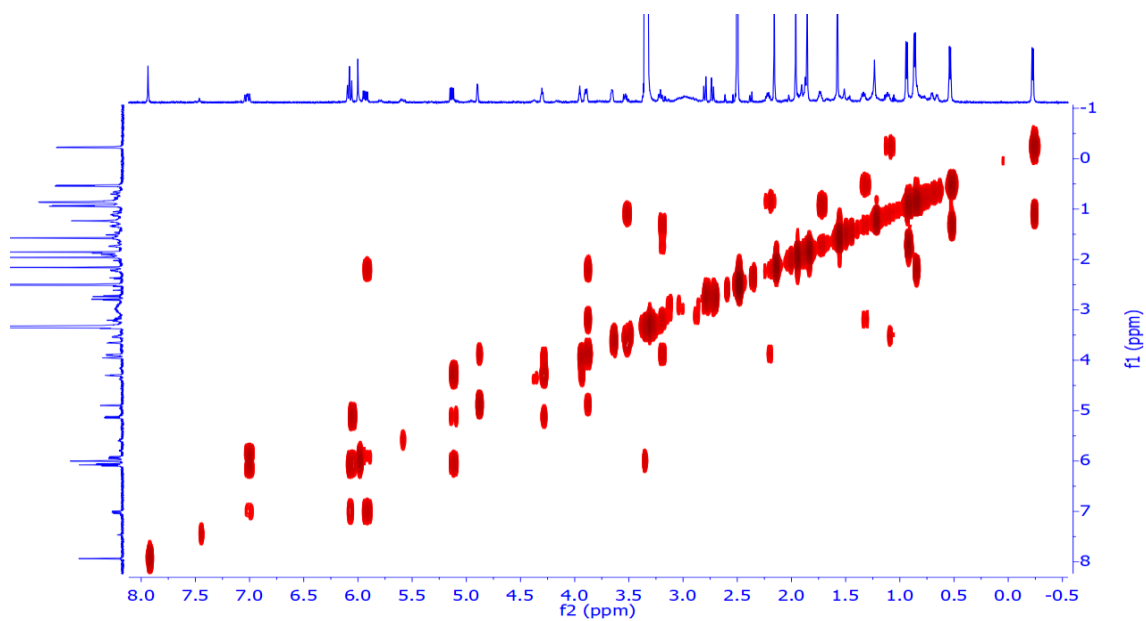


Figure S34. Expanded  $^1\text{H}$  NMR (600 MHz) spectrum of **4** in  $\text{DMSO}-d_6$ .



**Figure S35.** Expanded  $^1\text{H}$  NMR (600 MHz) spectrum of **4** in  $\text{DMSO-}d_6$ .



**Figure S36.** COSY NMR spectrum of **4** in  $\text{DMSO-}d_6$ .



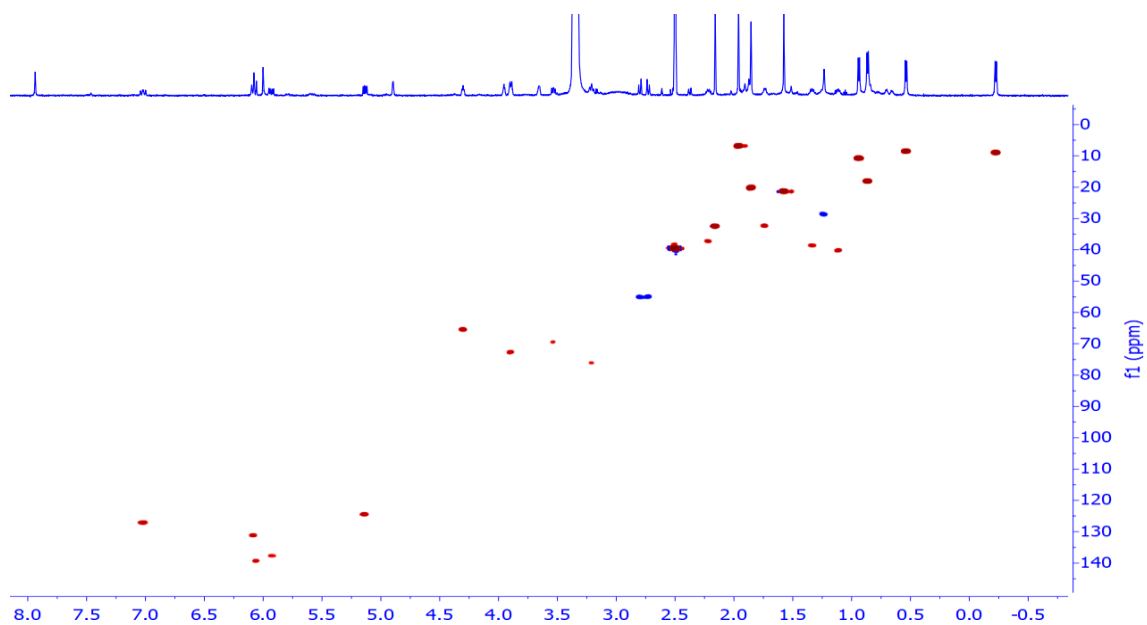


**Figure S37.** Edited HSQC NMR spectrum of **4** in DMSO- $d_6$ .

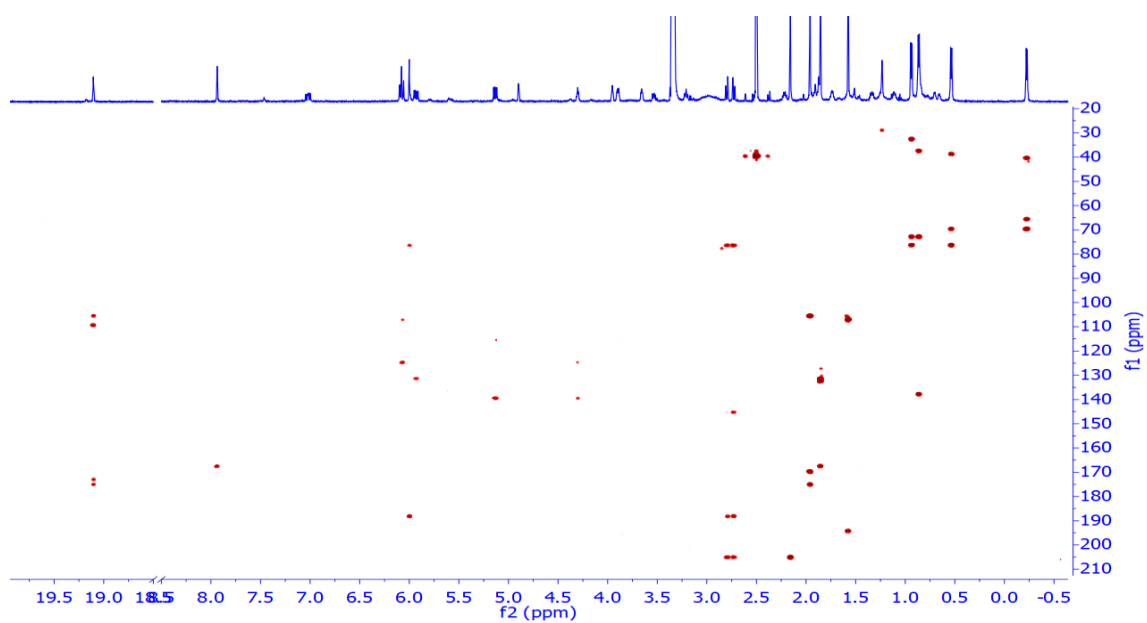


**Figure S38.** HMBC NMR spectrum of **4** in DMSO- $d_6$ .

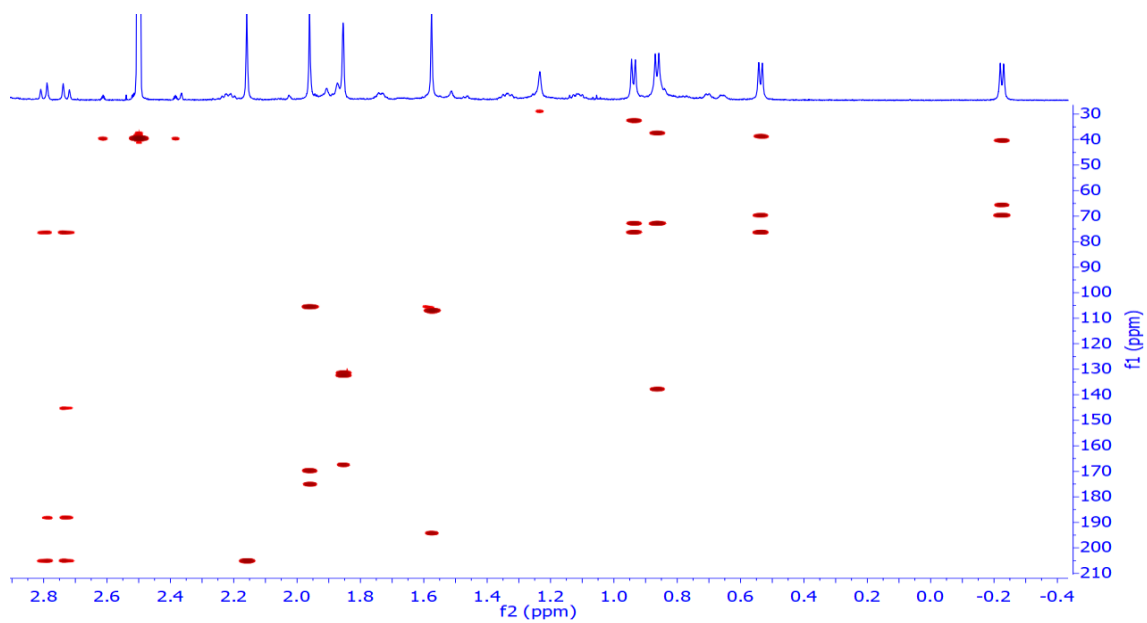


**Figure S39.** Expanded HMBC NMR spectrum of **4** in DMSO-*d*<sub>6</sub>.

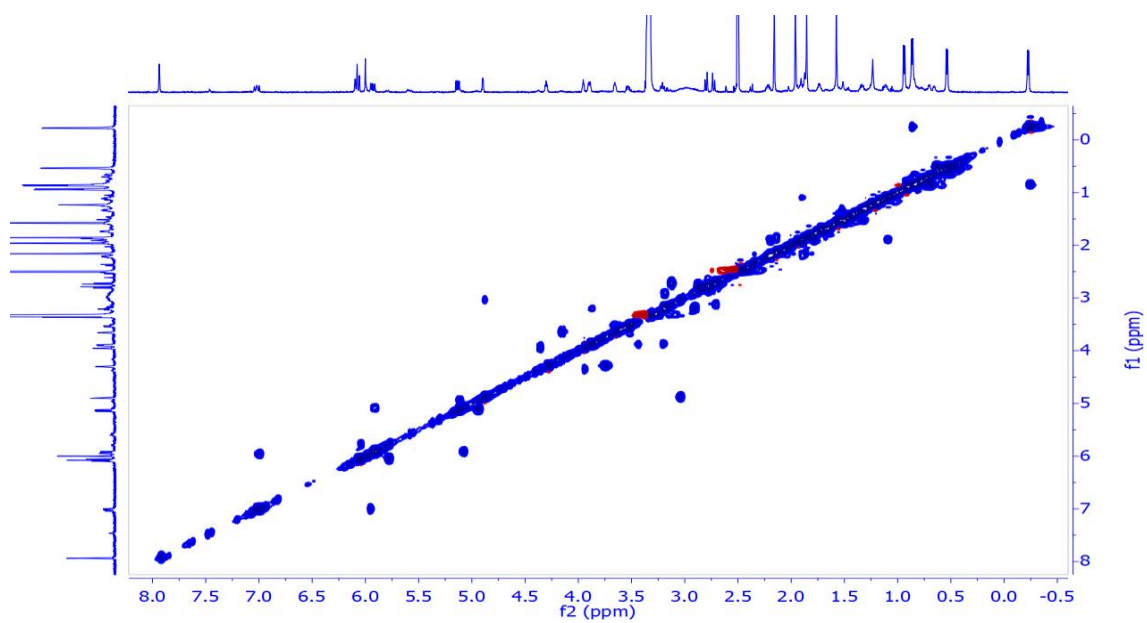


**Figure S40.** NOESY NMR spectrum of **4** in DMSO-*d*<sub>6</sub>.

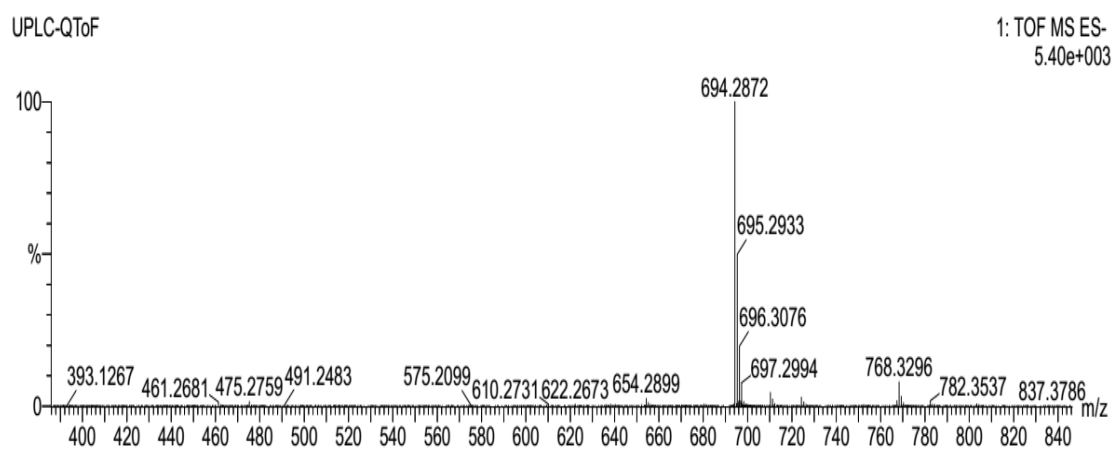


**Figure S41.** HRESIMS spectrum of **4**.

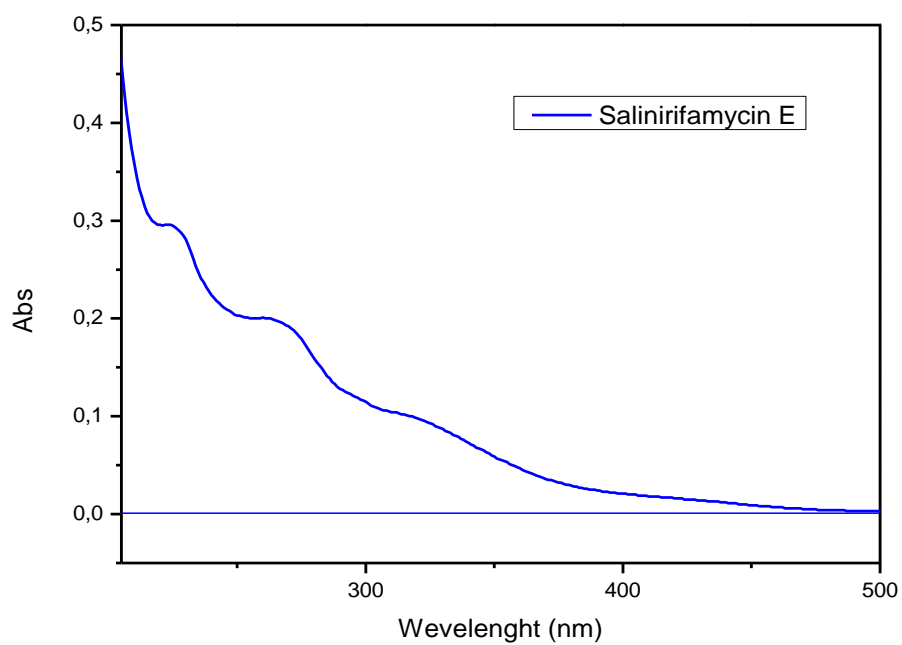


**Figure S42.** UV spectrum of **4** in MeOH.

## 5 CONSIDERAÇÕES FINAIS

Neste trabalho foi relatado o estudo químico e farmacológico da bactéria *Salinispora arenicola* isolada a partir de sedimentos marinhos coletados no Arquipélago de São Pedro e São Paulo, litoral do estado de Pernambuco. Este estudo resultou no isolamento de treze novos compostos pertencentes a classe das aminonafquinonas (SA-1–SA-5), *N*-metil-2-oxindóis (SA-6 e SA-7), derivados de 4-hidroxi-2-onas (SA-8), e rifamicinas (SA-9–SA-13).

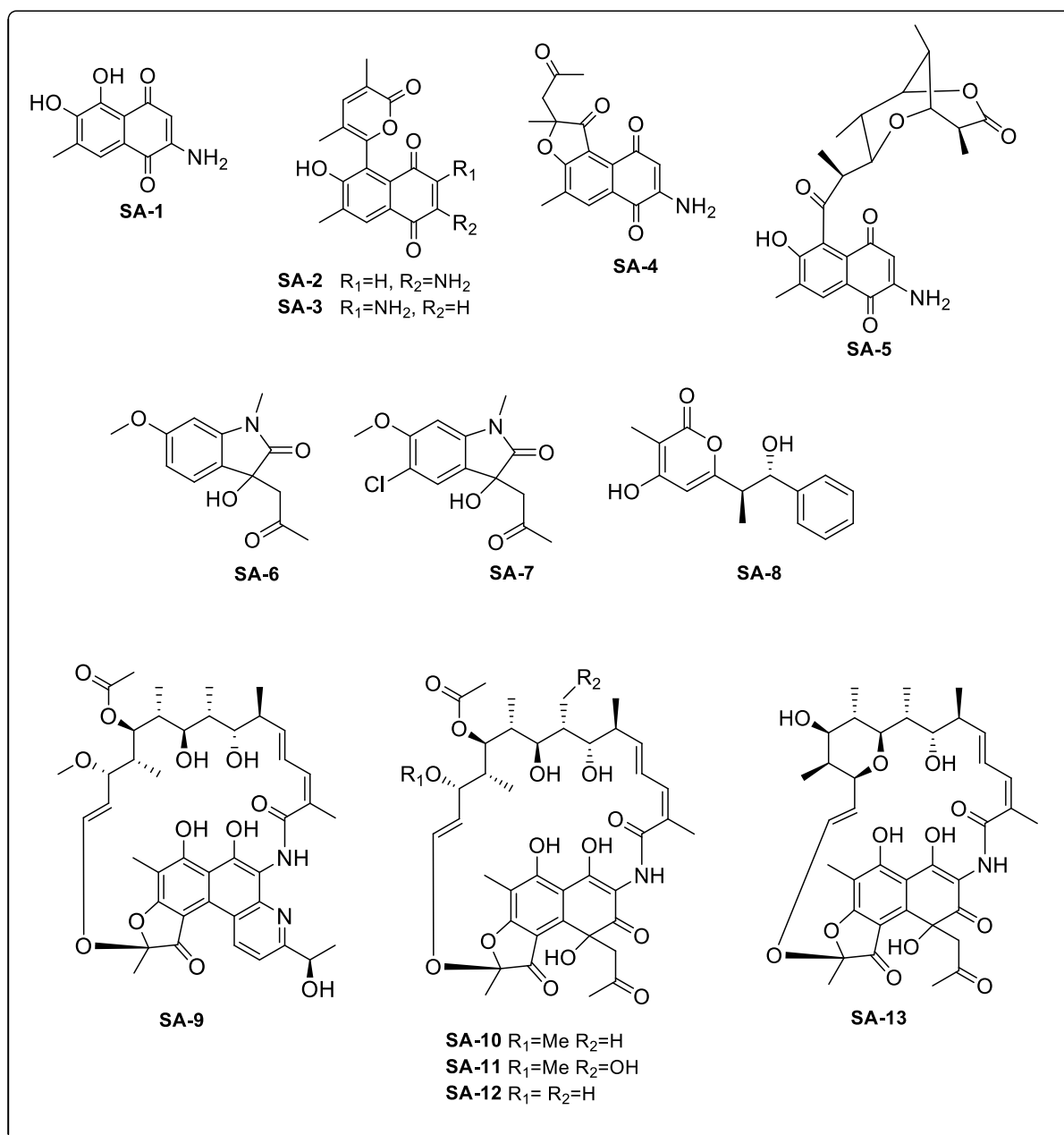
Naftoquinonas são uma grande classe de compostos naturais produzidos por plantas, bactérias e fungos. Vale mencionar que aminonaftoquinonas constituem uma unidade estrutural essencial de vários macrolídeos naturais de importância biológica como as rifamicinas.

Quanto às rifamicinas, já existem relatos de identificação destas a partir do gênero *Salinispora*, porém, apesar da grande contribuição na área de antibióticos, pouca atenção tem sido dada a esses compostos em espécies de *Salinispora*, sendo estes apenas identificados. Este trabalho mostra o primeiro isolamento de novas rifamicinas de *Salinispora*, contribuindo para o reconhecimento desse gênero como modelo para descoberta de novos metabólitos secundários.

Vale ressaltar que derivados naturais 3-hidroxi-2-oxindóis foram isolados de várias fontes naturais, incluindo plantas, microrganismos e invertebrados marinhos. Entretanto, este é o primeiro relato desta classe de *Salinispora*, adicionando ao gênero, mais uma classe de interesse farmacológica já que propriedades anticâncer, anti-HIV e neuroprotetoras, são descritas para esta classe de compostos naturais os quais que tem inspirado inúmeras sínteses orgânicas com vistas a descoberta de novas.

Baseando-se nos diversos estudos precedentes, e nos resultados gerados a partir do presente trabalho, fica claro que os microrganismos são uma fonte única e promissora para a descoberta de novos metabólitos secundários bioativos com potencial uso médico.

**Figura 14-** Estruturas dos metabólitos isolados do extrato em AcOEt produzido por *S. arenicola*.



## REFERÊNCIAS

- ARISTOFF, P. A.; GARCIA, G. A.; KIRCHHOFF, P. D.; SHOWALTER, H. D. Rifamycins-Obstacles and opportunities. **Tuberculosis**, [s. i.], v. 90, p. 94–118, 2010.
- ASOLKAR, R. N.; FREEL, K. C.; JENSEN, P. R.; FENICAL, W.; KONDRATYUK, T. P.; PARK, E. J.; PEZZUTO, J. M. Arenamides A - C, cytotoxic NF $\kappa$ B inhibitors from the marine actinomycete *Salinispora*, **Journal of Natural Products**, Estados Unidos, v. 72, p. 396–402, 2009.
- ASOLKAR, R. N.; KIRKLAND, T. N.; JENSEN, P. R.; FENICAL, W. Arenimycin, an antibiotic effective against rifampin- and methicillin-resistant *Staphylococcus aureus* from the marine actinomycete *Salinispora arenicola*, **Journal of Antibiotics**, Japão, v. 63, p. 37–39, 2010.
- ABDELMOHSEN, U. R.; BALASUBRAMANIAN, S.; OELSCHLAEGER, T. A.; GRKOVIC, T.; PHAM, N. B.; QUINN, R. J.; HENTSCHEL, U. Potential of marine natural products against drug-resistant fungal, viral, and parasitic infections. **The Lancet Infectious Diseases** [s. i.], v. 17, p. 30–40, 2017.
- BABULA, P.; ADAM, V.; HAVEL, L.; KIZEK, R. Secondary metabolites naphthoquinones-their occurrence, pharmacological properties and analysis. **Current Pharmaceutical Analysis**, [s. i.], v. 5, p. 47–68, 2009.
- BADHAN, R. K. S.; GITTINS, R.; AL ZABIT, D. The optimization of methadone dosing whilst treating with rifampicin: A pharmacokinetic modeling study. **Drug and Alcohol Dependence**, [s. i.], v. 200, p. 168–180, 2019.
- BAUERMEISTER, A.; VELASCO-ALZATE, K.; DIAS, T.; MACEDO, H.; FERREIRA, E. G.; JIMENEZ, P. C.; LOTUFO, T. M. C.; LOPES, N. P.; GAUDÊNCIO, S. P.; COSTA-LOTUFO, L. V. Metabolomic fingerprinting of *Salinispora* from Atlantic oceanic islands, **Frontiers Microbiology**, [s. i.], v. 9, p. 3021–3033, 2018.
- BOSE, U.; HEWAVITHARANA, A. K.; NG, Y. K.; SHAW, P. N.; FUERST, J. A.; HODSON, M. P. LC-MS-based metabolomics study of marine bacterial secondary metabolite and antibiotic production in *Salinispora arenicola*. **Marine Drugs**, Itália, v. 13, p. 249–266, 2015.
- CHIN, Y. W.; BALUNAS, M. J.; CHAI, H. B.; KINGHORN, A. D. Drug discovery from natural sources. **The AAPS Journal**, [s. i.], v. 8, p. 239–249, 2006.
- EUSTÁQUIO, A. S.; NAM, S.; PENN, K.; LECHNER, A.; WILSON, M. C.; FENICAL, W.; JENSEN, P. R.; MOORE, B. S. The discovery of salinosporamide K from the marine bacterium “*Salinispora pacifica*” by genome mining gives insight into pathway evolution. **ChemBioChem- Chemistry Europe**, [s. i.], v. 12, p. 61–64, 2011.
- FELING, R. H.; BUCHANAN, G. O.; MINCER, T. J.; KAUFFMAN, C. A.; JENSEN, P. R.; FENICAL, W. Salinosporamide A: A highly cytotoxic proteasome inhibitor from a novel microbial source, a marine bacterium of the new genus *Salinispora*, **Angew. Chemie – International Edition**, Alemanha, v. 42, p. 355–357, 2003.

FENICAL, W.; JENSEN, P. R. Developing a new resource for drug discovery: marine actinomycete bacteria. **Nature Chemical Biology**, [s. i.], v. 2, p. 666–673, 2006.

FERREIRA, E. G.; TORRES, M. D. C. M.; DA SILVA, A. B.; COLARES, L. L. F.; PIRES, K.; LOTUFO, T. M. C.; SILVEIRA, E. R.; PESSOA, O. D. L.; COSTA-LOTUFO, L. V.; JIMENEZ, P. C. Prospecting anticancer compounds in actinomycetes recovered from the sediments of Saint Peter and Saint Paul's Archipelago, Brazil. **Chemistry & Biodiversity**, [s. i.], v. 13, p. 1149–1157, 2016.

FREEL, K. C.; NAM, S.; FENICAL, W.; JENSEN, P. R. Evolution of secondary metabolite genes in three closely related marine actinomycete species. **Applied and Environmental Microbiology**, [s. i.], v. 77, p. 7261–7270, 2011

HE, H.; DING, W.; BERNAN, V. S.; RICHARDSON, A. D.; IRELAND, C. M.; GREENSTEIN, M.; ELLESTAD, G. A.; CARTER, G. T. Lomaiviticins A and B, potent antitumor antibiotics from *Micromonospora lomai Witiensis*. **Journal of the American Chemical Society**, Estados Unidos, v.123, p. 5362–5363, 2001.

JENSEN, P. R.; GONTANG, E.; MAFNAS, C.; MINCER, T. J.; FENICAL, W. Culturable marine actinomycete diversity from tropical Pacific Ocean sediments. **Environmental Microbiology**, [s. i.], v. 73, p. 1146–1152, 2005.

JENSEN, P. R.; MOORE, B. S.; FENICAL, W. The marine actinomycete genus *Salinispora*: a model organism for secondary metabolite discovery. **Natural Product Reports**, Inglaterra, v. 32, p. 738–751, 2015.

JENSEN, P. R.; WIGHT, R. D.; FENICAL, W. Distribution of actinomycetes in near-shore marine sediments. **Applied and Environmental Microbiology**, [s. i.], v. 57, p. 1102–1108, 1991.

JENSEN, P. R.; WILLIAMS, P. G.; OH, D. C.; Zeigler, L.; Fenical, W. Species-specific secondary metabolite production in marine actinomycetes of the genus *Salinispora*. **Applied and Environmental Microbiology**, [s. i.], v. 73, p. 1146–1152, 2007.

JIMÉNEZ, C. Marine Natural Products in Medicinal Chemistry. **ACS Medicinal Chemistry Letters**, Estados Unidos, v. 9, p. 959–961, 2018.

KAGATA, T.; SAITO, S.; SHIGEMORI, H.; OHSAKI, A.; ISHIYAMA, H.; KUBOTA, T.; KOBAYASHI, J. Paratunamides A-D, oxindole alkaloids from *Cinnamodendron axillare*, **Journal of Natural Products**, Estados Unidos, v. 69, p. 1517–1521, 2006.

KAMANO, Y.; ZHANG, H. P.; ICHIHARA, Y.; KIZU, H.; KOMIYAMA, K.; PETTIT, G. R. Convolutamydine A, a novel bioactive hydroxyoxindole alkaloid from marine bryozoan *Amathia convoluta*, **Tetrahedron Letters**, [s. i.], v. 36, p. 2783–2784, 1995.

KERSTEN, R. D.; LANE, A. L.; NETT, M.; RICHTER, T. K. S.; DUGGAN, B. M.; DORRESTEIN, P. C, MOORE, B. S. Bioactivity-guided genome mining reveals the

lomaiviticin biosynthetic gene cluster in *Salinispora tropica*. **ChemBioChem- Chemistry Europe**, [s. i.], v. 14, p. 955–962, 2013.

KIM, T. K.; HEWAVITHARANA, A. K.; SHAW, P. N.; FUERST, J. A. Discovery of a new source of rifamycin antibiotics in marine sponge actinobacteria by phylogenetic prediction. **Applied and Environmental Microbiology**, [s. i.], v. 72, p. 2112–2125, 2006.

KIM, H.; KIM, S.; KIM, M.; LEE, C.; YANG, I.; NAM, S. Bioactive natural products from the genus *Salinispora*: a review. **Archives of Pharmacal Research**, [s. i.], v. 23, p. 1230–1258, 2020.

LUPI, A.; FERRARI, P. G. Action of rifamycin SV for topical use on bone callus. (Experimental research). **Gazzetta Internazionale di Medicina e Chirurgia**, Itália, v. 66, p. 2981–2995, 1962.

MA, L.; DIAO, A. Marizomib, a potent second generation proteasome inhibitor from natural origin. **Anti-Cancer Agents in Medicinal Chemistry**, [s. i.], v. 15, p. 298–306, 2015.

MALDONADO, L. A.; FENICAL, W.; JENSEN, P. R.; KAUFFMAN, C. A.; MINCER, T. J.; WARD, A. C.; BULL, A. T.; GOODFELLOW, M. Diversity of cultivable actinobacteria in geographically widespread marine sediments. **Antonie Van Leeuwenhoek**, Holanda, v. 87, p. 11–18, 2005.

MANAM, R. R.; MACHERL, V. R.; TSUENG, G.; DRING, C. W.; WEISS, J.; NEUTEBOOM, S. T. C.; LAM, K. S.; POTTS, B. C. Antiprotealide is a natural product. **Journal of Natural Products**, Estados Unidos, v. 72, p. 295–297, 2009.

MATSUDA, S.; ADACHI, K.; MATSUO, Y.; NUKINA, M.; SHIZURI, Y. Salinisporamycin, a novel metabolite from *Salinispora arenicora*. **Journal of Antibiotics**, Japão, v. 62, p. 519–526, 2009.

MEREDITH, H. R.; SRIMANI, J. K.; LEE, A. J.; LOPATKIN, A. J.; YOU, L. Collective antibiotic tolerance: mechanisms, dynamics and intervention. **Nature Chemical Biology**, [s. i.], v. 11, p. 182–188, 2015.

MINCER, T. J.; JENSEN, P. R.; KAUFFMAN, C. A.; FENICAL, W.. Widespread and persistent populations of a major new marine actinomycete taxon in ocean sediments. **Applied and Environmental Microbiology**, [s. i.], v. 68, p. 5005–5011, 2002.

MIYANAGA, A.; JANSO, J. E.; MCDONALD, L.; HE, M.; LIU, H.; BARBIERI, L.; EUSTÁQUIO, A. S.; FIELDING, E. N.; CARTER, G. T.; JENSEN, P. R.; FENG, X.; LEIGHTON, M.; KOEHN, F. E.; MOORE, B. S. Discovery and assembly-line biosynthesis of the lymphostin pyrroloquinoline alkaloid family of mtor inhibitors in *Salinispora* bacteria. **Journal of the American Chemical Society**, Estados Unidos, v. 133, p. 13311–13313, 2011.

MOGHADDAM, M. N.; JALAL, R.; ZERAATKAR, Z. Synthesis and antiproliferative and apoptosis-inducing activity of novel 3-substituted-3-hydroxy-2-oxindole compounds. **In Vitro Cellular Developmental & Biology- Animal**, [s. i.], v. 54, p. 61–70, 2018.



- MOLINSKI, T. F.; DALISAY, D. S.; LIEVENS, S. L.; SALUDES, J. P. Drug development from marine natural products. **Nature Reviews Drug Discovery**, [s. i.], v. 8, p. 69–85, 2009.
- MOLONEY, M. G. Natural products as a source for novel antibiotics. **Trends in Pharmacological Sciences**, [s. i.], v. 37, p. 689–701, 2016.
- MOSEY, R. A., FLOREANCIG, P. E. Isolation, biological activity, synthesis, and medicinal chemistry of the pederin/mycalamide family of natural products. **Natural Product Reports**, Inglaterra, v. 29, p. 980–995, 2012.
- MURPHY, B. T.; NARENDER, T.; KAUFFMAN, C. A.; WOOLERY, M.; JENSEN, P. R.; FENICAL, W. Saliniquinones A-F, new members of the highly cytotoxic anthraquinone- $\gamma$ -pyrones from the marine actinomycete *Salinispora arenicola*. **Australian Journal of Chemistry**, Austrália, v. 63, p. 929–934, 2010.
- NEWMAN, D. J.; CRAGG, G. M. Natural products as sources of new drugs over the nearly four decades from 01/1981 to 09/2019. **Journal of Natural Products**, Estados Unidos, v. 83, p. 770-803, 2020.
- NEWMAN, D. J.; CRAGG, G. M. Natural Products as Sources of New Drugs from 1981 to 2014. **Journal of Natural Products**, Estados Unidos, v. 79, p. 629-661, 2016.
- NETT, M.; GULDER, T. A. M.; KALE, A. J.; HUGHES, C. C.; MOORE, B. M. Function-oriented biosynthesis of  $\beta$ -lactone proteasome inhibitors in *Salinispora tropica*. **Journal of Medicinal Chemistry**, Estados Unidos, v. 52, p. 6163–6167, 2009.
- OH, D. C.; GONTANG, E. A.; KAUFFMAN, C. A.; JENSEN, P. R.; FENICAL, W. Salinipyrones and pacificanones, mixed-precursor polyketides from the marine actinomycete *Salinispora pacifica*. **Journal of Natural Products**, Estados Unidos, v. 71, p. 570–575, 2008.
- ÖZAKIN, S.; Ince, E. Genome and metabolome mining of marine obligate *Salinispora* strains to discover new natural products. **Turkish Journal Biology**, Turquia, v. 43, p. 28–36, 2019.
- PATRIDGE, E.; GAREISS, P.; KINCH, M. S.; HOYER, D. An analysis of FDA-approved drugs: natural products and their derivatives. **Drug Discovery Today**, [s. i.], v. 21, p. 204–207, 2016.
- PEDDIBHOTLA, S. 3-Substituted-3-hydroxy-2-oxindole, an emerging new scaffold for drug discovery with potential anti-cancer and other biological activities, **Current Bioactive Compounds**, [s. i.], v. 5, p. 20–38, 2009.
- PENG, J.; LIN, T.; WANG, W.; XIN, Z.; ZHU, T.; GU, Q.; LI, D. Antiviral alkaloids produced by the mangrove-derived fungus *Cladosporium* sp. PJX-41. **Journal of Natural Products**, Estados Unidos, v. 76, p. 1133–1140, 2013.
- PEREIRA, R. B.; EVDOKIMOV, N. M.; LEFRANC, F.; VALENTÃO, P.; KORNIENKO, A.; PEREIRA, D. M.; ANDRADE, P. B.; GOMES, N. G. M. Marine-derived anticancer agents: clinical benefits, innovative mechanisms, and new targets. **Marine Drugs**, Itália, v. 17, p. 329–349, 2019.

PRUDHOMME, J.; MCDANIEL, E.; PONTS, N.; BERTANI, S.; FENICAL, W.; JENSEN, P.; ROCH, L. K. Marine actinomycetes: A new source of compounds against the human malaria parasite, **PLoS One**, Estados Unidos, v. 3, p. 2235–2242, 2008.

POLONIK, N. S.; POLONIK, S. G.; DENISENKO, V. A.; MOISEENKO, O. P. Reaction of dichloronaphthazarins with sodium nitrite as a route to natural pigments echinamines A and B and related aminonaphthazarins. **Synthesis**, [s. i.], v. 20, p. 3350–3358, 2011.

QIU, H. Y.; WANG, P. F.; LIN, H. Y.; TANG, C. Y.; ZHU, H. L.; YANG, Y. H. Naphthoquinones: a continuing source for discovery of therapeutic antineoplastic agents. **Chemical Biology & Drug Design**, [s. i.], v. 91, p. 681–690, 2018.

ROMÁN-PONCE, B.; MILLÁN-AGUIÑAGA, N.; GUILLEN-MATUS, D.; CHASE, A. B.; GINIGINI, J. G. M.; SOAPI, K.; FEUSSNER, K. D.; JENSEN, P. R.; TRUJILLO, M. E. Six novel species of the obligate marine actinobacterium *Salinispora*, *Salinispora cortesiana* sp. nov., *Salinispora fenicalii* sp. nov., *Salinispora goodfellowii* sp. nov., *Salinispora mooreana* sp. nov., *Salinispora oceanensis* sp. nov. and *Salinispora vitie*. **International Journal of Systematic and Evolutionary Microbiology**, [s. i.], v. 70, p. 4668–4682, 2020.

RAO, T.; TAN, Z.; PENG, J.; GUO, Y.; CHEN, Y.; ZHOU, H.; OUYANG, D. The pharmacogenetics of natural products: a pharmacokinetic and pharmacodynamic perspective. **Pharmacological Research**, [s. i.], v. 146, p. 104283–104299, 2019.

SILVA, A. E. T.; GUIMARÃES, L. A.; FERREIRA, E. G.; TORRES, M. D. C. M.; DA SILVA, A. B.; BRANCO, P. C.; OLIVEIRA, F. A. S.; SILVA, G. G. Z.; WILKE, D. V.; SILVEIRA, E. R.; PESSOA, O. D. L.; JIMENEZ, P. C.; COSTA-LOTUFO, L. V. Bioprospecting anticancer compounds from the marine-derived actinobacteria *Actinomadura* sp. collected at the Saint Peter and Saint Paul Archipelago (Brazil). **Journal of the Brazilian Chemical Society**, Brasil, v. 28, p. 465–474, 2017.

SINGH, S.; PRASAD, P.; SUBRAMANI, R.; AALBERSBERG, W. Production and purification of a bioactive substance against multi-drug resistant human pathogens from the marine-sponge-derived *Salinispora* sp. **Asian Pacific Journal of Tropical Biomedicine**, [s. i.], v. 4, p. 825–831, 2014.

SCHLAWIS, C.; KERN, S.; KUDO, Y.; GRUNENBERG, J.; MOORE, B. M.; SCHULZ, S. Structural elucidation of trace components combining GC/MS, GC/IR, DFT-calculation and synthesis—salinilactones, unprecedented bicyclic lactones from *Salinispora* bacteria. **Angew. Chemie – International Edition**, Alemanha, v. 57, p. 14921–14925, 2018.

SCHULTZ, A. W.; OH, D. C.; CARNEY, J. R.; WILLIAMSON, R. T.; UDWARAY, D. W.; JENSEN, P. R.; GOULD, S. J.; FENICAL, W.; MOORE, B. S. Biosynthesis and structures of cyclomarins and cyclomarazines, prenylated cyclic peptides of marine actinobacterial origin. **Journal of the American Chemical Society**, Estados Unidos, v. 130, p. 4507–4516, 2008.

TONRA, J. R.; LLOYD, G. K.; MOHANLAL, R.; HUANG, L.; Plinabulin ameliorates neutropenia induced by multiple chemotherapies through a mechanism distinct from G-CSF therapies. **Cancer Chemotherapy Pharmacology**, [s. i.], v. 85, p. 461–468, 2020.

VASKE-JR, T.; LESSA, R. P.; DE NÓBREGA, M. F.; DO AMARAL, F. M. D.; O'BRIEN, S. R. M.; DA COSTA, F. A. P. Arquipélago de São Pedro e São Paulo: Histórico e recursos naturais. **NAVE/LABOMAR-UFC**, Basil, p. 242. 2007.

WAITES, M. J.; MORGAN, N. L.; ROCKEY, J. S, HIGTON, G. *Industrial Microbiology: An Introduction*. **Oxford, UK: Blackwell Science**, Inglaterra, 2001.

WHO. World Health Organization. **The top 10 causes of death**, [s. i.], Disponível em <https://www.who.int/news-room/fact-sheets/detail/the-top-10-causes-of-death>. Acesso em: 20 de junho, 2021.

WILLIAMS, D. E.; DALISAY, D. S.; CHEN, J.; POLISHCHUCK, E. A.; PATRICK, B. O.; NARULA, G.; KO, M.; AV-GAY, Y.; LI, H.; MAGARVEY, N.; ANDERSEN, R. J. Aminorifamycins and sporolactams produced in culture by a *Micromonospora* sp. isolated from a Northeastern-Pacific marine sediment are potent antibiotic. **Organic Letters**, Estados Unidos, v. 19, p. 766–769, 2017.

WILLIAMS, P. G.; ASOLKAR, R. N.; KONDRATYUK, T.; PEZZUTO, J. M.; JENSEN, P. R.; FENICAL, W. Saliniketals A and B, bicyclic polyketides from the marine actinomycete *Salinispora arenicola*. **Journal of Natural Products**, Estados Unidos, v. 70, p. 83–88, 2007.

WILLIAMS, P. G.; BUCHANAN, G. O.; FELING, R. H.; KAUFFMAN, C. A.; JENSEN, P. R.; FENICAL, W. New cytotoxic salinosporamides from the marine actinomycete *Salinispora tropica*. **The Journal Organic Chemistry**, Estados Unidos, v. 70, p. 6196–6203, 2005.

WILSON, M. C.; GULDER, T. A. M.; MAHMUD, T.; MOORE, B. S. Shared biosynthesis of the saliniketals AND rifamycins in *Salinispora arenicola* is controlled by the sare1259-encoded cytochrome P450. **Journal of The American Chemical Society**, Estados Unidos, v. 132, p. 12757–12765, 2010.

WOO, C. M.; BEIZER, N. E.; JANSO, J. E.; HERZON, S. B. Isolation of lomaiviticins C–E, transformation of lomaiviticin C to lomaiviticin A, complete structure elucidation of lomaiviticin A, and structure–activity analyses. **Journal of The American Chemical Society**, Estados Unidos, v. 134, p. 15285–15288, 2012.

ZHANG, J.; LI, S.; WU, X.; GUO, Z.; LU, C.; SHEN, Y. Nam7 hydroxylase is responsible for the formation of the naphthalenic ring in the biosynthesis of neoansamycins. **Organic Letters**, Estados Unidos, v. 19, p. 2442–2445, 2017,